

Injectable Hydrogels of Cartilaginous Matrix Mimics

Liliana Moreira Teixeira

2011

Members of the Graduation Committee

Chairman:

Prof. Dr. G. van der Steenhoven

Promoter:

Prof. Dr. C.A. van Blitterswijk (University of Twente)

Co-promoter:

Dr. M. Karperien (University of Twente)

Members:

Dr. João Mano (Universidade do Minho, Portugal)

Prof. Dr. F. Luyten (Katholieke Universiteit Leuven, Belgium)

Prof. Dr. P.R. van Weeren (Utrecht University)

Prof. Dr. L. Terstappen (University of Twente)

Dr. Ir. P. Jonkheijm (University of Twente)

Prof. Dr. P.J. Dijkstra (University of Twente)

Prof. Dr. J. Feijen (University of Twente)

Injectable Hydrogels of Cartilaginous Matrix Mimics

Liliana Moreira Teixeira

PhD Thesis, University of Twente, Enschede, The Netherlands

The research described in this thesis was supported by the DPTE (Dutch Program for Tissue Engineering)

This publication was supported by NBTE (Nederlandse vereniging voor Biomaterialen en Tissue Engineering)

ISBN: 978-94-6191-081-3

Copyright: L.S. Moreira Teixeira, 2011, Enschede, The Netherlands. Neither this thesis nor its parts may be reproduced without written permission of the author.

Cover design: L. Moreira Teixeira. The cover shows microscopy images collected throughout the research described in this thesis. Overall, the images focus on cartilage matrix, chondrocytes and Dextran-based hydrogel scaffolds. The background was adapted from the University of Twente most recent image concept, as reflection of dynamic and innovative technologies, incorporated with elements of this thesis concept, such as injectable devices, polymeric structures and cartilaginous matrix components.

INJECTABLE HYDROGELS OF CARTILAGINOUS MATRIX MIMICS

DISSERTATION

to obtain
the doctor's degree at the University of Twente,
on the authority of the rector magnificus,
Prof. Dr. H. Brinksma
on account of the decision of the graduation committee,
to be publicly defended
on Wednesday, December 7th, 2011, at 12.45 hrs

by

Liliana Moreira Teixeira

Born on April 10th, 1982
in Matosinhos, Portugal

Promoter:

Prof. Dr. C.A. van Blitterswijk (University of Twente)

Co-promoter:

Dr. M. Karperien (University of Twente)

Summary

This thesis describes the *in vitro* biological evaluation of a recently developed technology platform of enzymatically crosslinkable hydrogels of natural polymers. *In situ* forming hydrogels scaffolds were tailored for the treatment of local cartilage defects and degenerative cartilage diseases, such as osteoarthritis, by acting as healing plasters. The success of a repair strategy in the management of cartilage defects relies on the following requirements: i) application by simple and minimally invasive procedures, such as an arthroscopy or a single injection; ii) immobilization at the defect site, while coping with normal wear of the joint; iii) be biodegradable and biocompatible and finally, iv) allow cartilaginous matrix deposition and remodeling. Hydrogels consisting of natural polymers are likely to fulfill all these requirements. Dextran was the polysaccharide of choice to form the backbone of the hydrogels described in this thesis. Dextran was selected due to its stability, biocompatibility and structural resemblance to extracellular matrix components. Several strategies described in this thesis aimed at improving the biological properties of these dextran-based hydrogels, such as the incorporation of bioactive compounds and mimicry of the cartilaginous matrix.

Chapter 2 contains a literature review that focuses on emerging strategies to improve cartilage repair. Primarily such strategies attempt to incorporate fundamental knowledge of developmental and cell biology in the design of optimized strategies for cell delivery at the defect site and to locally stimulate cartilage repair responses. Chapter 3 offers description review of enzyme-based crosslinking methods to form hydrogels. Enzymatic crosslinking is a mild and effective method to obtain injectable hydrogels of natural polymers, such as dextran. In chapter 4, *in situ* forming dextran-based enzymatically crosslinkable hydrogels are described. Hydroxyphenyl groups were introduced on dextran backbone by linking tyramine (TA) residues via a urethane bond, denoted as Dex-TA. *In situ* gelation is rapidly induced by covalent crosslinking of the hydroxyphenyl groups. The reaction is catalyzed by the enzyme horseradish peroxidase and low non-toxic concentrations of H_2O_2 . Dex-TA is mechanical stable, however, its biological performance is limited. Three strategies were selected to improve the biological performance of Dex-TA: i) engraftment with hyaluronic acid (HA), ii) mixing with heparin, and iii) incorporation of platelet lysate. Hyaluronic acid is one of the main components of cartilaginous ECM and interacts with chondrocytes by surface receptors such as CD44. The incorporation of HA enabled the modulation of cell activity by contributing to cell proliferation and

migration. For these reasons, HA was engrafted in Dex-TA, denoted as HA-g-Dex-TA and described in chapter 5. These biomimetic hydrogels induced an enhanced cell proliferation and matrix deposition/remodeling, compared to Dex-TA hydrogels. In an alternative approach, heparin was selected to further improve the bioactivity of dextran-based hydrogels, as described in chapter 6. This approach is based on relatively simple chemistry to introduce tyramine residues in the selected model molecule, in this case heparin and resulted in a product referred to as Hep-TA. Heparin's resemblance to heparan sulphate, a natural component of the ECM, significantly improved cell proliferation and the *de novo* formation of a cartilaginous matrix. Interestingly, increasing ratios of Hep-TA in Dex-TA hydrogels also induce cell migration, as described in chapter 7, suggesting that this system can likely be developed into a cell-free system for cartilage repair. In chapter 9, we explored whether the incorporation of autologous platelet-rich lysate could improve the regenerative potential of Dex-TA hydrogels, alternatively for the engraftment of hyaluronic acid or heparin. The Dex-TA/platelet-rich lysate hydrogels showed high potential as an off-the-shelf cell-free product for cartilage repair strategies by combining scaffold-guided regenerative medicine with an autologous source of growth factors.

Inappropriate integration of the tissue engineered constructs with the host tissue can ultimately result in failure. Creating a stabile interface between scaffolds and mechanically challenging tissues, such as the cartilage in the joints is particularly challenging. The TA-functionalized polymers described in this thesis are able to covalently bind to collagen fibers, allowing a stable interface between the construct and the cartilaginous matrix. In chapter 7, we described the self-attachment of Dex-TA hydrogels during the enzymatic crosslinking reaction to predominantly collagen residues in the cartilaginous matrix.

The repair strategies described in this thesis aimed at mimicking the structure and composition of native ECM. Nevertheless, cells play an equally important role when using cell-laden constructs. In chapter 8, we show that seeding hydrogels with micro-aggregated chondrocytes instead of with single cells may be an effective strategy to boost neo-cartilage formation. Moreover, high-throughput formation of micro-aggregates prior to implantation may be an efficient approach to accelerate hyaline cartilage formation during current autologous chondrocyte implantation procedures.

Finally, chapter 10 summarizes and discusses the overall results presented in this thesis and suggests future developments and applications of dextran-based hydrogels.

Samenvatting

Deze thesis beschrijft de *in vitro* biologische evaluatie van een recent ontwikkelt technologie platform gebaseerd op enzymatisch crosslinkende hydrogelen van natuurlijke polymeren. *In situ* vormende hydrogel constructen werden aangepast voor de behandeling van locale kraakbeen defecten en degeneratieve kraakbeen aandoeningen, zoals osteoartritis en osteoartrose, door functioneren als een helende pleister. Het succes van kraakbeen defect reparatie strategien hangt af van de volgende voorwaarden: i) applicatie van door simpele en minimaal invasieve procedures zoals een athroscopie of een enkele injectie; ii) immobilisatie van het materiaal in het defect, onderwijl het niet mag leiden onder de stress van het dagelijks gebruik van het gewricht; iii) het zijn van biologisch afbreekbaar en biologisch verenigbaar; iv) het toelaten van opbouw van een hermoduleerbare kraakbeen matrix. Het is waarschijnlijk dat hydrogelen bestaande uit natuurlijke polymeren aan al deze voorwaarden voldoen. Het polysacharide molecuul dextran was gekozen als basis bouwsteen voor de hydrogelen die beschreven zijn in deze thesis. Dextran is stabiel biologisch verenigbaar en lijkt op moleculen die aanwezig zijn in de natuurlijke matrix van kraakbeen. In deze thesis staan verscheidene strategien beschreven die kunnen bijdragen aan het verbeteren van de biologische eigenschappen van dextraan gebaseerde hydrogelen, zoals de incorporatie van verschillende biologisch actieve en kraakbeen matrix nabootsende elementen.

De literatuur beschouwing in hoofdstuk 2 focuseert op opkomende strategien die trachten het kraakbeen reparatie proces te verbeteren. Dit is gebruikelijk gebaseerd op fundamentele kennis van ontwikkelings- en cel-biologie die word toegepast in het ontwerp van aanbrengen van cellen in het defect of het lokaal stimuleren van de kraakbeen reparatie. Hoofdstuk 3 beschrijft een literatuur overzicht van de bestaande crosslinkende methoden die mogelijk gebruikt kunnen worden voor het vormen van hydrogel netwerken. Enzymatische crosslinking is een milde en effectieve methode voor het vormen van injecteerbare hydrogelen van natuurlijke polymeren zoals dextran. In hoofdstuk 4 beschrijft *in situ* vormende dextraan gebaseerde enzymatische crosslinkende hydrogelen. Hydroxyphenyl groepen zijn aangebracht op de dextran basisbouwstenen door ze te linken met een tyramine (TA) residu via een uretaan binding. Het eindproduct wordt beschreven als Dex-TA. *In situ* gelatie is snel genduceerd door covalente crosslinking van de hydroxyphenyl groepen. Dit proces werd gekatalyseerd door het enzyme horseradish peroxidase en lage niet giftige hoeveelheden van waterstofperoxide. Dex-TA is mechanisch stabiel, maar heeft weinig biologische inter-

acties. Drie strategieën werden ontworpen om de biologische interacties van Dex-TA te verbeteren: i) hyaluronzuur werd ingebouwd; ii) heparine werd ingebonden; iii) bloedplaatjes lysaat werd ingemengd. Hyaluronzuur is een van de hoofdcomponenten van de kraakbeen matrix en gaat interacties aan met kraakbeen cellen (chondrocyten) door bindingen aan te gaan met oppervlakte receptoren zoals CD44. Deze interactie maakt de modulatie van cel activiteit zoals proliferatie en migratie mogelijk. Voor deze redenen werd hyaluronzuur ingebouwd in Dex-TA en werd HA-g-Dex-TA genaamd. Deze biomimetiserende hydrogelen induceerden een verhoogde cell proliferatie en matrix depositie/remodulatie ten opzichte van Dex-TA hydrogelen. In hoofdstuk 6 een alternatieve strategie gebaseerd op heparine was gebruikt om de biologische interacties van de dextran hydrogelen te verbeteren. Deze strategie was gebaseerd op relatief simpele chemische reacties die TA residues aanbrachten in heparine. Dit product werd Hep-TA genoemd. Heparine lijkt sterk op heparaan sulfaat, een belangrijk component van de kraakbeen matrix. Dit resulteerde in verbeterde cel proliferatie en *de novo* formatie van kraakbeen matrix. Zoals beschreven in hoofdstuk 7, toenemende relatieve hoeveelheden van Hep-TA in Dex-TA hydrogelen stimuleerde cel migratie. Dit is van belang, aangezien het suggereert dat dit kan leiden tot een cel-vrije strategie voor kraakbeen reparatie. In hoofdstuk 9 exploreerden we mogelijkheid of incorporatie van autoloog bloedplaatjes lysaat een alternatief kon bieden voor hyaluronzuur en heparine voor de bevordering van het regeneratieve potentiaal van Dex-TA hydrogelen. De Dex-TA/ autoloog bloedplaatjes-rijk lysaat demonstreerde grote potentie voor een off-the-shelf cell-vrij product voor kraakbeen reparatie door construct gestuurde regeneratieve therapie te combineren met een autologe bron van groeifactoren.

Onjuiste integratie van het nieuw gevormde weefsel met de kraakbeen matrix zal uiteindelijk leiden tot het falen van de behandeling. Het bewerkstelligen van een stabiele connectie tussen een construct en een mechanisch belast weefsel zoals kraakbeen is bijzonder uitdagend. In hoofdstuk 7 beschrijven we dat de TA-gefunctionaliseerde polymeren covalent binden aan collageen fibrillen. Dit zorgt voor een stabiele integratie tussen de hydrogel constructen en de kraakbeen matrix.

Deze thesis bevat voornamelijk strategieën gefocuseerd op het nabootsen en structuur en samenstelling van de kraakbeen matrix. Desalniettemin, cellen hebben een even belangrijke rol in cel-geladen constructen. In hoofdstuk 8 demonstreren we dat hydrogelen met micro-aggregaten meer kraakbeen vormen dan hydrogelen met een gelijke hoeveelheid losse cellen. Om dit te bewerkstelligen was een high-through put platform ontwikkeld dat op een simpele en effectieve manier voldoende hoeveelheden van micro-aggregaten kan vormen. Deze procedure is compatible met huidige klinisch behandel methoden en heeft de potentie om op goedkope en eenvoudige wijze de therapeutische resultaten te verbeteren.

Afsluitend, hoofdstuk 10 geeft een bediscussieerde samenvatting van de belangrijkste bevindingen in deze thesis en geeft suggesties voor toekomstige ontwikkelingen en applicaties van dextran gebaseerde hydrogelen.

Table of Contents

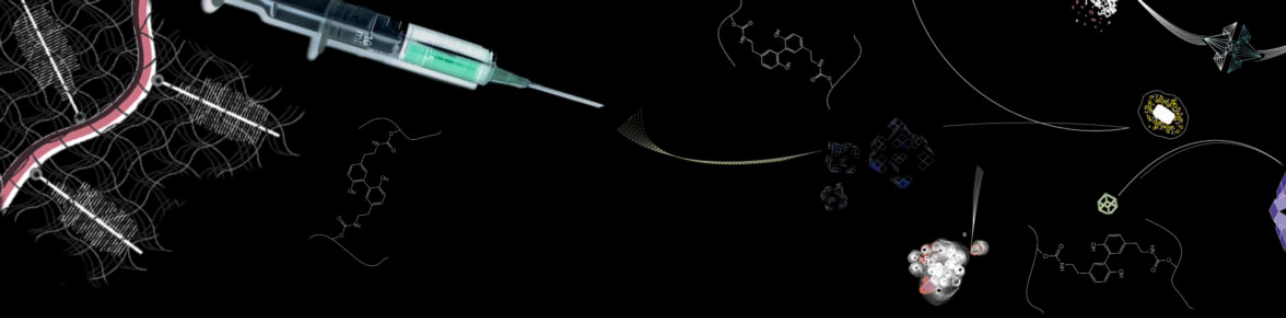
| | | |
|----------|---|-----------|
| 1 | General introduction | 1 |
| 1.1 | Gelation time and crosslinking density | 3 |
| 1.2 | Degradation and mechanical properties | 4 |
| 1.3 | Bioactivity and biomimicry | 6 |
| 1.4 | Cell incorporation and seeding density | 7 |
| 1.5 | Biological integration/adhesive properties | 8 |
| 1.6 | Off-the-shelf approaches and clinical relevance | 9 |
| 1.7 | Aim and outline of this thesis | 9 |
| 2 | Cartilage tissue engineering | 15 |
| 2.1 | Introduction | 15 |
| 2.2 | Development of cartilage | 16 |
| 2.2.1 | Joint formation | 16 |
| 2.2.2 | Growth plate cartilage | 17 |
| 2.2.3 | Articular cartilage | 17 |
| 2.3 | History of clinical applications in cartilage repair | 18 |
| 2.4 | Cell sources for cartilage engineering | 19 |
| 2.5 | Biomaterials for cartilage repair | 21 |
| 2.5.1 | Chondro-conducting scaffolds: natural and synthetic biomaterials | 23 |
| 2.5.2 | Emerging "smart" biomaterials | 24 |
| 2.6 | Future of cartilage tissue engineering | 26 |
| 3 | Enzymatically crosslinked hydrogels | 31 |
| 3.1 | Introduction | 32 |
| 3.2 | Enzymatically crosslinked hydrogels | 33 |
| 3.2.1 | Transglutaminase | 33 |
| 3.2.2 | Tyrosinase | 35 |
| 3.2.3 | Phosphopantetheinyl transferase | 36 |
| 3.2.4 | Lysyl oxidase and plasma amine oxidase | 38 |
| 3.2.5 | Phosphatase, thermolysin, β -lactamase and phosphatase/kinase | 38 |
| 3.2.6 | Peroxidases | 41 |
| 3.2.7 | Horseradish peroxidase mimetic enzymes | 42 |
| 3.3 | Conclusions and future perspectives | 44 |

| | | |
|----------|---|-----------|
| 4 | Enzymatically Crosslinked Dextran-tyramine Hydrogels | 53 |
| 4.1 | Introduction | 54 |
| 4.2 | Materials and methods | 55 |
| 4.2.1 | Materials | 55 |
| 4.2.2 | Hydrogel formation and characterization | 55 |
| 4.2.3 | Nutrient transport | 56 |
| 4.2.4 | Rheological analysis | 56 |
| 4.2.5 | <i>In situ</i> chondrocyte incorporation | 57 |
| 4.2.6 | Cytotoxicity assay | 57 |
| 4.2.7 | Chondrocyte morphology | 58 |
| 4.2.8 | Histology and immunofluorescent staining | 58 |
| 4.2.9 | Biochemical analysis | 58 |
| 4.3 | Results and discussion | 59 |
| 4.3.1 | Hydrogel formation and gelation time | 59 |
| 4.3.2 | Hydrogel characterization | 60 |
| 4.3.3 | Cell viability of chondrocytes in Dex-TA hydrogels | 63 |
| 4.3.4 | Chondrocyte morphology and matrix production | 63 |
| 4.4 | Conclusions | 70 |
| 5 | Biomimetic Dextran-Hyaluronic Acid Injectable Hydrogels | 75 |
| 5.1 | Introduction | 76 |
| 5.2 | Materials and methods | 78 |
| 5.2.1 | Materials | 78 |
| 5.2.2 | Synthesis of amine-terminated dextran-tyramine conjugates . . | 78 |
| 5.2.3 | Synthesis of hyaluronic acid grafted with Dex-TA | 79 |
| 5.2.4 | Polymer characterization | 79 |
| 5.2.5 | Hydrogel formation and gelation time | 79 |
| 5.2.6 | Swelling and enzymatic degradation | 80 |
| 5.2.7 | Rheological analysis | 80 |
| 5.2.8 | Chondrocyte isolation and incorporation | 80 |
| 5.2.9 | Cell viability and SEM | 81 |
| 5.2.10 | Matrix production | 81 |
| 5.2.11 | Statistical analysis | 82 |
| 5.3 | Results and discussion | 82 |
| 5.3.1 | Synthesis and characterization of HA-g-Dex-TA copolymer . . | 82 |
| 5.3.2 | Hydrogel formation and gelation time | 85 |
| 5.3.3 | Hydrogel characterization | 86 |
| 5.3.4 | Enzymatic degradation | 87 |
| 5.3.5 | Cytotoxicity | 89 |
| 5.3.6 | Chondrocyte morphology | 89 |
| 5.3.7 | Swelling and degradation of hydrogels in the presence of cells . | 90 |
| 5.3.8 | Cell proliferation and matrix production | 91 |
| 5.4 | Conclusions | 94 |
| 6 | Injectable Enzymatically Crosslinked Heparin/Dextran Hydrogels | 99 |

| | | |
|----------|--|------------|
| 6.1 | Introduction | 99 |
| 6.2 | Materials and methods | 101 |
| 6.2.1 | Materials | 101 |
| 6.2.2 | Synthesis and characterization of heparin-tyramine conjugates | 101 |
| 6.2.3 | Hydrogel formation and gelation time | 102 |
| 6.2.4 | Hydrogel characterization | 102 |
| 6.2.5 | Chondrocyte isolation and incorporation | 103 |
| 6.2.6 | Cell viability and proliferation | 103 |
| 6.2.7 | Swelling in the presence of chondrocytes | 103 |
| 6.2.8 | Histological staining | 104 |
| 6.2.9 | Matrix production | 104 |
| 6.2.10 | Statistical analysis | 105 |
| 6.3 | Results and discussion | 105 |
| 6.3.1 | Hydrogel formation and gelation time | 105 |
| 6.3.2 | Hydrogel characterization | 107 |
| 6.3.3 | Cell viability and proliferation | 109 |
| 6.3.4 | Matrix production | 110 |
| 6.4 | Conclusions | 116 |
| 7 | Self-attaching and Cell-attracting Hydrogels | 121 |
| 7.1 | Introduction | 122 |
| 7.2 | Materials and Methods | 123 |
| 7.2.1 | Synthesis of Dextran-Tyramine conjugates (Dex-TA) | 123 |
| 7.2.2 | Cell culture | 124 |
| 7.2.3 | Articular cartilage in contact with Dex-TA: SEM and histological analysis | 124 |
| 7.2.4 | Mechanical testing | 125 |
| 7.2.5 | Micro-Raman spectroscopy | 125 |
| 7.2.6 | Crosslinking of fluorescent labeled tyramide with components in the ECM of articular cartilage | 125 |
| 7.2.7 | Cell adhesion and cell migration assay | 126 |
| 7.3 | Results | 126 |
| 7.3.1 | Higher number of hydroxyphenyl groups enabled stronger adhesion to the host tissue | 126 |
| 7.3.2 | Analysis of the hydrogel - cartilage interface showed evidence for gel-tissue integration | 128 |
| 7.3.3 | Bonding of the polymers to collagen fibrils in the cartilaginous matrix | 128 |
| 7.3.4 | Formation of new C-C and C-O-C bonds suggestive of covalent bond formation | 131 |
| 7.3.5 | HRP enabled covalent crosslinking of tyramide residues to cartilage matrix | 131 |
| 7.3.6 | Covalent bonding of hydrogels to collagen-rich tissues other than cartilage | 133 |

| | | |
|----------|---|------------|
| 7.3.7 | Incorporation of Hep-TA enabled cell adhesion and triggered cell homing in Dex-TA hydrogels | 134 |
| 7.4 | Discussion | 136 |
| 7.5 | Conclusion | 141 |
| 8 | Chondrocyte clustering stimulates cartilage matrix deposition | 145 |
| 8.1 | Introduction | 146 |
| 8.2 | Materials and Methods | 147 |
| 8.2.1 | Tissue source and preparation | 147 |
| 8.2.2 | Mold design and micro-aggregate formation | 147 |
| 8.2.3 | Dextran-Tyramine hydrogels (Dex-TA) | 147 |
| 8.2.4 | Metabolic activity and chondrocyte viability | 148 |
| 8.2.5 | <i>In vivo</i> implantation | 148 |
| 8.2.6 | Histological analysis | 148 |
| 8.2.7 | Gene expression analysis | 149 |
| 8.2.8 | Statistical analysis | 149 |
| 8.3 | Results | 149 |
| 8.3.1 | High-throughput generated chondrocyte micro-aggregates resemble chondrocyte clusters in OA | 149 |
| 8.3.2 | Micro-aggregation stimulates cartilage matrix formation | 151 |
| 8.3.3 | Micro-aggregated cell clusters remain viable after embedding in a hydrogel | 152 |
| 8.3.4 | Cell cluster formation enhances cartilage matrix deposition | 152 |
| 8.4 | Discussion | 158 |
| 8.5 | Conclusion | 160 |
| 9 | Autologous growth factor supplemented dextran-based hydrogel | 163 |
| 9.1 | Introduction | 164 |
| 9.2 | Materials and Methods | 165 |
| 9.2.1 | Platelet collection and cell sources | 165 |
| 9.2.2 | Mechanical properties | 165 |
| 9.2.3 | Cell migration assay | 166 |
| 9.2.4 | DNA quantification | 166 |
| 9.2.5 | Scanning Electron Microscopy analyses | 167 |
| 9.2.6 | Multi-lineage differentiation | 167 |
| 9.2.7 | Histological evaluation | 167 |
| 9.2.8 | Gene expression analysis | 168 |
| 9.2.9 | Chorioallantoic membrane (CAM) model | 168 |
| 9.2.10 | Growth factor release profiles | 168 |
| 9.2.11 | Analysis of interface morphology | 169 |
| 9.2.12 | Statistical analysis | 169 |
| 9.3 | Results | 169 |
| 9.3.1 | Platelet lysate does not affect mechanical properties of Dex-TA hydrogels | 169 |
| 9.3.2 | Platelet lysate induced cell migration into Dex-TA hydrogels | 170 |

| | | |
|-----------|--|------------|
| 9.3.3 | Cell adhesion is enhanced by the addition of platelet lysate . . | 171 |
| 9.3.4 | Platelet lysate induces chondrogenic but not osteogenic nor adi- pogenic differentiation | 172 |
| 9.3.5 | Chondro-inductive effect stimulated by addition of platelet lysate | 173 |
| 9.3.6 | Effective adhesion onto OA-affected cartilage | 176 |
| 9.4 | Discussion | 177 |
| 9.5 | Conclusion | 182 |
| 10 | General discussion | 187 |
| 10.1 | Dextran-based <i>in situ</i> forming hydrogels as a potential off-the-shelf injectable system | 188 |
| 10.2 | Bioactivity and biomimicry to improve biological performance | 189 |
| 10.3 | Integrate to repair | 191 |
| 10.4 | Boosting up cartilaginous ECM deposition | 193 |
| 10.5 | Concluding remarks and future perspectives | 193 |
| | Acknowledgements | 197 |
| | Curriculum Vitae | 199 |
| | List of Publications | 201 |
| | List of Figures | 205 |
| | List of Tables | 217 |



Chapter 1

General introduction and thesis outline

Hydrogels tailored to stimulate cartilage repair

Cartilage damage typically arises as a focal defect, usually caused by trauma. If left untreated, these defects can lead to osteoarthritis. Osteoarthritis is a prevalent degenerative cartilage disease, involving the erosion of articulating joint surfaces, as depicted in figure 1.1. Although current medical and surgical therapies for treatment of focal cartilage defects have improved dramatically, further major developments in the therapies and technologies available remain paramount. Current therapies to correct joint articular cartilage defects include mosaicplasty, micro-fracture, partial or total joint arthroplasty and autologous chondrocyte transplantation. Each of these procedures have inherent drawbacks such as sub-optimal long-term outcome due to structural failure, donor site morbidity, possibility of disease transmission in the case of allografting, risk of infection and demand of invasive surgical procedures [1,2]. Additionally, cartilage is aneural, alymphatic and avascular, which severely impairs spontaneous self-repair. Thus, the development of functional articular cartilage replacements is urgent and of key importance. Tissue engineering approaches have demonstrated increasing potential for cartilage tissue repair by the improving current technologies and the development of less invasive alternative treatments. The standard tissue engineering approach consists of isolation of appropriate autologous

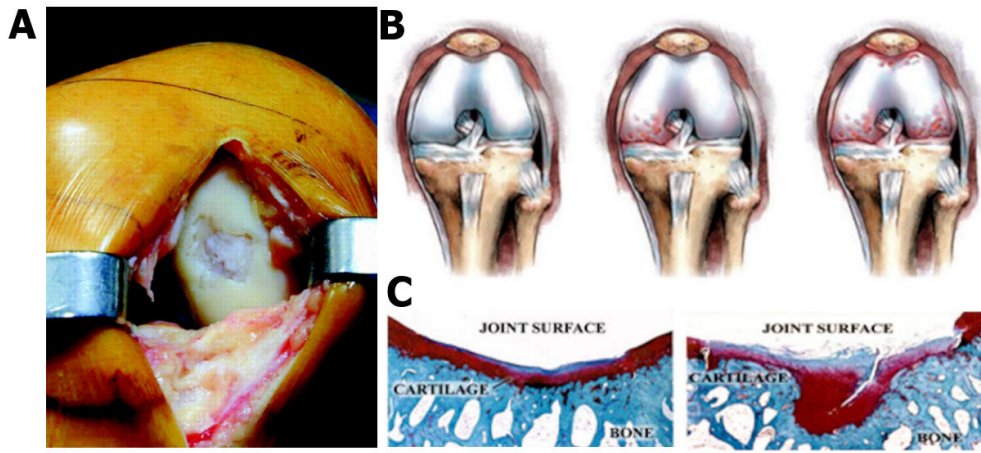


Figure 1.1: Osteoarthritic cartilage. A) Image of a focal cartilage defect. B) From left to right, healthy knee cartilage, partial arthritis and complete arthritis. C) Photo-micrographs of healthy cartilage, in the left, and arthritic cartilage, in the right.

cell sources, cell expansion usually in a 2-D and finally cell seeding on a 3-D scaffold, designed to recreate the native host tissue. Preferably, these scaffolds mimic normal tissue physiology and/or provide molecular cues facilitating de novo tissue formation (figure 1.2). The scaffolds can be designed solely as temporary structures providing support in the initial phases of de novo tissue formation. Such scaffolds often provide cues to the cells in a passive way. Other strategies in scaffold design focus on providing biological cues within the scaffold aiming at actively guiding cells and tissue growth [3]. These scaffolds can be obtained from natural or synthetic biomaterials. Natural biomaterials can be further distinguished into protein-based, which include collagen and fibrin, or into polysaccharide-based scaffolds, such as alginate, chitosan, cellulose, dextran and hyaluronic acid. Polylactic acid (PLA), polyethylene glycol (PEG) and poly(lactic-co-glycolic acid) are examples of synthetic biomaterials frequently used making hydrogels. A growing body of published biomaterials has been used to build scaffolds for cartilage regeneration. Hydrogels are a very interesting class of materials highly suitable for this application, since they consist of 3-D hydrophilic networks with high water up-take capacity. They are water insoluble, and can be tailored to have tissue-like elastic properties, which makes them excellent mimetics of the native tissue. Besides, hydrogels allow efficient transportation of nutrients and waste products, which is crucial for cell growth. A multitude of variables must be considered when designing hydrogels for cartilage repair, ranging from the type of polymer to be used, the design of the network morphology, hydrogel degradability, and the incorporation of biofunctionality and biomimicry. Additional factors of major importance to be considered are whether to include cells or develop a cell-free system, to combine the hydrogels with sustained drug release strategies and to address the integration of

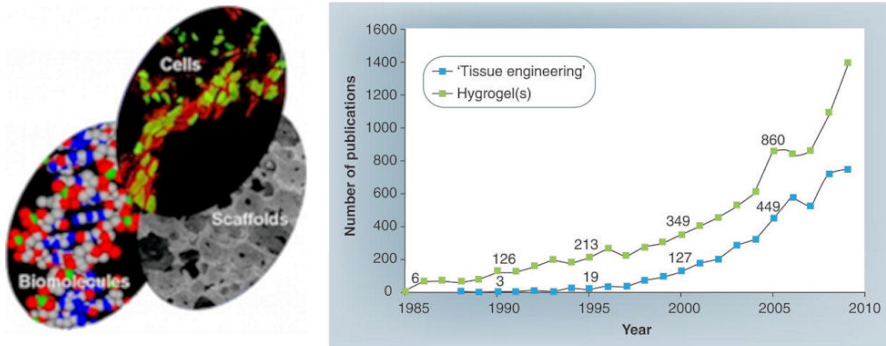


Figure 1.2: Left: classical components of a tissue engineering approach: cells, scaffolds and biomolecules. Right: The total number of publications with 'tissue engineering' and hydrogel' or hydrogels' in the title. Reproduced from [4].

the hydrogel in host tissue [5,6]. Hydrogels are preferably designed to form *in situ* as injectable systems, hence, enabling *in vivo* assembly. Injectable hydrogels present major clinical relevance since they can be applied in a minimally invasive procedure. Ultimately this may lead to the replacement of open joint surgery by an injection or an arthroscopic procedure, as illustrated in figure 1.3. Other main advantages are the excellent alignment with irregularly shaped defects and straightforward cell incorporation due to the initial fluidity of the precursor solution. By inducing gelation directly at the defect site, the precursor solution can diffuse into the host tissue, thereby enhancing adhesion potentially eliminating the need of using sutures or glues [7].

1.1 Gelation time and crosslinking density

The gelation time is an essential parameter to control when developing injectable hydrogels systems. Uncontrolled post-injection release can occur due to the time lag between the injection of the aqueous precursors and the formation of a 3-D network. This potential drawback can hamper the suitability for cartilage engineering purposes. A balance must also be achieved between gelation time and polymer viscosity which is compatible with fast gelation but avoids the clogging of the application device often a syringe [8]. Additionally, when cells are to be incorporated within the hydrogel, the gelation should occur relatively fast to avoid deposition of cells due to gravity, and, thus, non-uniform cell dispersion. Preferably, the gelation time should be approximately 1 to 5 minutes. Several gelation mechanisms can be used to form hydrogels. Each method has a direct effect on mechanical stability of the gel, its degradation properties, the crosslinking time and even cytocompatibility. Naturally

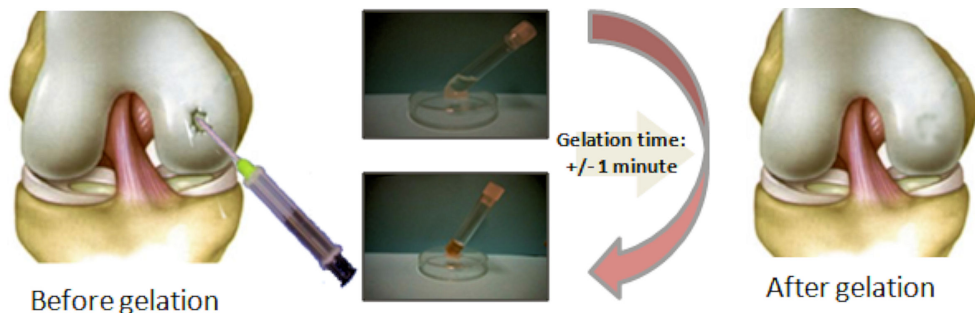


Figure 1.3: Schematic representation of an injectable hydrogel for cartilage repair.

forming hydrogels are mainly crosslinked by ionic or physical bonds and have relatively poor mechanical properties. In addition, the hydrogel can disintegrate due to a sudden change in environmental conditions, such as a change in ionic strength. Hydrogels can also be formed by covalent crosslinking, which has the major advantage of obtaining mechanically stable hydrogel properties that are resistant to changes in the environment. Covalently crosslinkable hydrogels are generally formed via radical chain polymerization or by chemical crosslinking. Yet, with these methods additional components are introduced into the system, which may possess possibly cytotoxicity. This hurdle can be overcome by using enzymatically crosslinkable hydrogels, particularly when enzymes are used that play an important role in mammalian physiology. Enzymatic crosslinking is an increasingly attractive method to induce *in situ* hydrogel assembly due to the mildness of the process. Naturally occurring enzymes such as transglutaminases and peroxidases are commonly used as the catalysts [9,10,11,12].

The network density of the crosslinked polymer affects the hydrogel properties, shaping not only its mechanical features, the diffusion coefficient of nutrients and waste products, the degradation kinetics and swelling, but also its biological properties by influencing cell behavior and, consequently, matrix deposition. Chondrocytes incorporated in hydrogels with higher crosslinking density show decreased proliferation and delayed proteoglycan production, likely due to lower mass transfer of nutrients, metabolites and other factors, such as growth factors and by hampering cell movement in the hydrogel [13]. Thus, on one hand, the crosslinking density should be high enough to assure suitable mechanical properties for cartilage repair and to retain the incorporated cells in the gel, while, on the other hand, the crosslinking density should also allow the incorporated cells to proliferate and to produce *de novo* tissue.

1.2 Degradation and mechanical properties

The structure and chemistry of the hydrogels must allow cell survival and tissue formation, at the same time as its degradation should match neo-tissue formation, as

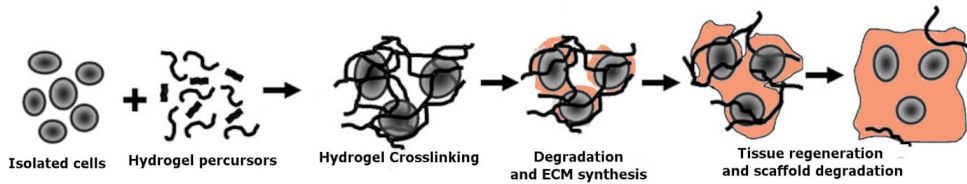


Figure 1.4: Cell incorporation by mixing with the hydrogel precursor. ECM synthesis must be synchronized with hydrogel degradation. Reproduced from [3].

illustrated in figure 1.4. Additionally, degradation products should not be detrimental to either surrounding tissues or encapsulated cells. Hydrogel degradation can be influenced by the incorporation of segments susceptible to hydrolysis, enzyme cleavage, a combination of both, or by incorporation of natural polymers which can be degraded by enzymes naturally present in our body. The used chemistry, the amount of degradable linkages, the crosslinking density, the presence of cells and the *in vivo* environment can affect the degradation of the hydrogel. Fast degradation might lead to insufficient retention of the newly synthesized proteins or even dissolution of the cell/hydrogel constructs, whereas too slow degradation can potentially limit the spatial deposition of ECM by cells to pericellular regions., impair cell movement and /or cell proliferation, which will ultimately affect the type of tissue produced [3,14]. Hydrolysis generally occurs by cleavage of ester bonds in the hydrogel when exposed to aqueous environments. Notably, *in vivo* conditions are known to accelerate the cleavage of ester bonds [15]. By controlling the crosslinking density and composition of the polymer backbone, the degradation rate can be fine tuned according to the application. Hydrogel degradation can also be cell-mediated. Cell secreted enzymes can lead to localized degradation of hydrogel segments, for example in hydrogels partially composed by hyaluronic acid, chondroitin sulphate, fibrin or collagen [16,17].

The foremost mechanical properties that determine the suitability of a hydrogel for cartilage tissue engineering are the stiffness and visco-elasticity or tensile strength. These properties are controlled by polymer concentration and crosslinking density, usually diminishing as the hydrogel degrades and no significant ECM retention is compensating this loss. The response of chondrocytes to the mechanical properties of their surroundings is an intricate orchestration of several factors such as structure, elasticity and stiffness of the hydrogel, compressive loading and finally the biosynthetic vs. catabolic behavior of the chondrocytes. The ideal mechanical properties of hydrogels for cartilage repair are not yet known. Nevertheless, when designing a hydrogel for immediate implantation into cartilage defects, one should consider that these constructs will have to withstand physiological loads and movements, otherwise they will lead to collapse of the implanted biomaterial [5].

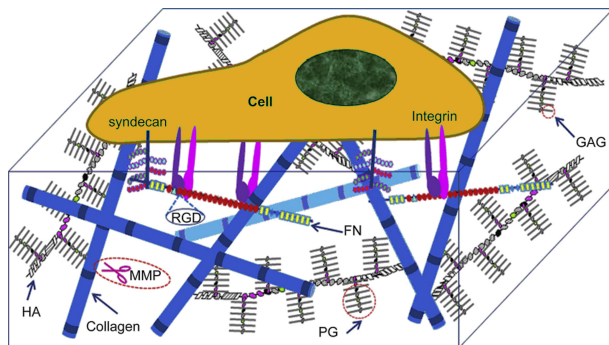


Figure 1.5: Model of cell-ECM interactions. Several strategies have been developed for the incorporation of key ECM bio-functions, such as specific cell adhesion sites, proteolytic degradation domains, and growth factor binding domains. Reproduced from [20].

1.3 Bioactivity and biomimicry

Hydrogels can be designed to interact with cells by mimicry of strategic features of the native extracellular matrix. Signaling molecules like growth factors, cytokines, or chemical compounds are commonly used to enhance cartilaginous tissue engineering [18]. Cartilaginous matrix is mainly composed of proteoglycans and collagen type II, as well as entrapped growth factors, that provide key molecular information to the chondrocytes. Indeed cells receive a plethora of biochemical cues from the surrounding ECM [19] as illustrated in figure 1.5. Cartilage is a relatively simple tissue composed of a single cell type and is avascular. The key challenges for the fabrication of functional constructs for cartilage repair are i) enhancing hyaline type cartilaginous matrix deposition, ii) providemechanical protection while keeping cells on their place when there is no ECM yet to retain them in the defect site. These prerequisites can, at least partially, be achieved by incorporation of bioactive moieties into the polymer network either as whole proteins or short oligopeptides. The tripeptide Arg-Gly-Asp (RGD) has been widely explored for this purpose to facilitate cell adhesion. Furthermore, proteolytic degradation of ECM is equally important for cell migration, tissue repair and remodelling. The majority of ECM proteins have specific cleavage sites for enzymes, such as metalloproteinases, which can also be incorporated into the polymeric structure of hydrogels to enhance mimicry. Other strategies rely on the incorporation of ECM components such as collagen, hyaluronic acid, chondroitin sulphate and other proteoglycans like heparin, which can present bioactive domains not only for cell and growth binding, but also for proteolytic degradation. Designing hydrogels that enable controlled drug release may potentially lead to enhanced cartilage repair. Hurdles such as the need of repeated administration, rapid diffusion and clearance from the defect site can be easily avoided by sustained release systems. Hydrogels are commonly used as delivery systems due to effective control over the crosslinking density (which affects the diffusion rates), charge variations (affect-

ing drug-hydrogel interactions), mildness of the hydrogel formation process rendering them highly suited for the incorporation of proteins and finally, their degradation rate can be fine tuned. The most commonly growth factors incorporated in hydrogels designed for cartilage repair, to stimulate chondrocytes proliferation, differentiation and/or cartilaginous ECM deposition, are: Insulin-like Growth Factor (IGF)-1 [21], Transforming Growth Factor- β (TGF- β)-1, 2 and 3 [22], Bone Morphogenic Protein (BMP)-2, -4, -6 and -7 [23,24], as well as basic Fibroblast Growth Factor (bFGF) [25] and Platelet-Derived Growth Factor A and B (PDGF-A or PDGF-B) [26]. The optimal regulatory effect of the signaling molecules depends on their specific intrinsic properties, such as stability, dosage, timing, cell source and culturing conditions. Recently, the trend is to combine growth factors, often with complementary effects, to maximize their impact [18,27].

1

1.4 Cell incorporation and seeding density

Chondrocytes are the cells responsible for the maintenance of the articular cartilage matrix, not only by secreting proteoglycans and collagens, which provide this tissue its structure and strength, but also by replacing degraded macromolecules. Interestingly, chondrocytes are able to respond to focal cartilage injury or degeneration by increasing matrix synthesis locally. This responses is highly suggestive for the existence of self-regenerative mechanisms within articular cartilage in response to matrix degradation or damage [28]. This self-regenerative mechanism is masked by a stronger catabolic response resulting in a net loss of cartilage. Consequently, chondrocytes are the logical choice for incorporating in a hydrogel. Yet this choice has two major drawbacks: the limited number of chondrocytes available, owing to rareness of donor tissue, and instability of these cells when cultured in monolayer, ultimately leading to de-differentiation or loss of phenotype. Multipotent MSCs are considered an attractive alternative for cartilage repair strategies due to their easy availability, and their potential for expansion while retaining differentiation capacity [29,30]. Moreover, these cells seem able to reduce host defense mechanisms and even escape immune recognition [31]. In spite of the high potential of MSCs, the drawbacks related this cell source consist of possible loss of stability in prolonged *in vivo* transplantation. Human embryonic stem cells (ESCs) can also be considered an option for cartilage tissue regeneration since they can proliferate significantly while they are still able to differentiate into the chondrogenic lineage. Yet heterogeneous populations of ESCs can lead to inferior function of the tissue engineered constructs and they have the inherent risk of form teratocarcinomas [32].

Cellular interactions during tissue homeostasis, regeneration or repair are of paramount importance. Co-culture systems based on variable ratios of chondrocytes with synovial fibroblasts, osteoblasts or MSCs have proven to be a powerful tool to guide and support cartilaginous tissue formation mediated by cellular interactions or soluble factors [33,34]. Another approach is microscale tissue engineering. Functionality arises not only from the tissue components, cells and extracellular molecules, but also from the 3-D histo-architecture, their location, and the organization of all

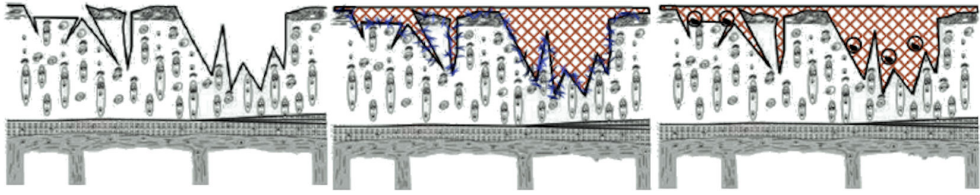


Figure 1.6: Illustrative representation of a hydrogel designed to crosslink with the components of the host tissue. The figure in the right represents the typical irregular surface of OA affected cartilage. The middle figure represents the affected cartilage surface covered with an hydrogel. The hydrogel precursor should be initially fluid to allow the coverage of the irregular surface and after gelation the hydrogel must be retained at the defect site. The figure in the left illustrates the participation of the cells incorporated within the gel or invading the gel in the regenerative mechanism. These cells should be able to deposit hyaline cartilaginous ECM for fully functional repair.

these components relative to each other [35]. By replicating these stimulating micro-environments for example by incorporating gradients of soluble cues, cell-cell and cell-ECM contact, functionality of tissue engineered constructs can be enhanced [36,37]. Seeding cells in aggregates rather than single cells can be an effective tool for fabricating biomimetic cellular micro-environments and may stimulate cartilage formation.

The quality of cartilage engineered hydrogel constructs can also be affected by the cell seeding density. Generally, the density of chondrocytes seeded within hydrogels range between 5 to 60 million cells/mL. Higher cell densities result in increased ECM deposition and, consequently, augmented mechanical properties [5]. Yet, when mechanical loading is applied in constructs with cell densities varying from 20 to 60 million cells/mL, no significant changes in mechanical properties can be detected, which might also be related to nutrient availability issues [38,39].

1.5 Biological integration/adhesive properties

One of the main challenges in tissue engineering is to obtain a sufficiently strong bond between materials with different mechanical properties, for instance hydrogels and native cartilage. The integration of neo-cartilage in an existing matrix is still a rather unresolved problem. Discontinuities between the biomaterial, and even cartilage explants, and surrounding host cartilage tissue can ultimately lead to implant failure. Several approaches have been used to circumvent this major issue, such as incorporation of fiber meshes and sutures but this only marginally improved tissue-construct integration. Better integration is observed, when cells were incorporated into these constructs [40,41]. Other approaches focus on the design of materials that crosslink with the components of the host native tissue [42,43]. Two approaches can be used to effectively allow tight integration between hydrogels and cartilage tissue: biological interactions mediated by cell remodeling and ECM deposition and/or chemical

crosslinking, as depicted in figure 1.6.

1.6 Off-the-shelf approaches and clinical relevance

The incorporation of bioactive molecules, such as growth factors (e.g. TGF- β and BMPs) and chemo-attractants (e.g. SDF1-a), have proven to be highly effective *in vitro* for tissue repair strategies [44,45]. However, inherent drawbacks are associated with these strategies: the limited stability of the components, and, consequently, short life-time, and the high costs of these molecules. To overcome the short life-time limitation, it is possible to separate the hydrogel components by using a multi-compartment application device. The bioactive supplements could be incorporated just prior to administration and their selection and dosage can be tailored for each clinical situation. Another alternative is exploring the instructive and inductive properties of the biomaterials instead of the addition of external supplementary compounds. This approach has been widely used for osteogenic applications [46,47], yet not explored to full extent for chondrogenic purposes. *In vitro* cultivation before implantation may lead to higher mechanical properties of the construct. However, this process demands longer pre-surgical procedures (biopsy collection, cell isolation and expansion which are all time costly. For clinical applications, off-the-shelf cell-free products have clear advantages. Particularly when these products are designed in such a way that they attract cells from the surrounding environment, allow cell infiltration and subsequently trigger chondrogenic differentiation of the invading cells. Moreover, cell-free systems demand less legislation for FDA approval and consequently, translation into clinical settings is faster.

Finally, multi-step aggressive procedures consisting of immobilization of the hydrogel by stitching a tissue or a membrane flap, or even exposure of tissue to UV light to allow glue solidification, are time consuming, not practical and might damage the surrounding tissue, ultimately jeopardizing the integration of the hydrogel with the host tissue. Ideally, for irregular cartilage defects, the hydrogels should be compatible with minimally invasive procedures, such as during arthroscopic procedures, by covering the damaged surface, promptly solidify and be retained within the defect site, without requiring additional surgical procedures.

1.7 Aim and outline of this thesis

A plethora of hydrogels has been recently developed for cartilage tissue engineering applications, yet several challenges remain to be addressed. The available options fail at providing, in one system, adequate mechanical properties and proper integration at the defect site, cyto/biocompatibility and bio-activity, compatible with a non-invasive injectable system.

The general aim of this thesis is to develop *in situ* forming hydrogels tailored for the treatment of local cartilage defects and degenerative cartilage diseases, such as OA, acting as healing plasters. This concept is based on a recently developed

technology platform of enzymatically crosslinkable hydrogels of natural polymers, namely dextran.

To obtain dextran molecules that can crosslink and form a hydrogel by an enzymatic peroxidase reaction, first hydroxyphenyl groups were introduced in dextran by linking tyramine residues via a urethane bond to the polymer backbone (denoted as Dex-TA). Once hydroxyphenyl groups were introduced, *in situ* gelation can be induced by an enzymatic reaction initiated by low, non-toxic concentrations of H_2O_2 and the enzyme horseradish peroxidase, which introduces covalent bonding between the hydroxyphenyl groups. These polysaccharide-based plasters are intended to induce cartilage regeneration by providing mechanical support and by delivering either cells or bioactive compounds in the diseased joint.

This thesis describes the characterization of these hydrogels and the first steps to develop these hydrogels into a plaster that can be used for treatment of cartilage defects.

Chapters 2 and 3 introduce a general overview on the tissue engineering field: **Chapter 2** offers an overall description on emerging strategies to improve cartilage repair by incorporating fundamental knowledge of developmental and cell biology in the design of optimized strategies for cell delivery at the defect site and to locally stimulate cartilage repair responses. In **Chapter 3**, enzymatic reactions currently explored for the development of hydrogels are reviewed, with focus on hydrogels that re developed for regenerative strategies. The purpose was to provide examples of combinations of enzymes and materials that offer innovative alternatives in tissue engineering.

In **Chapter 4**, the potential application of the injectable Dex-TA hydrogels for cartilage tissue engineering was evaluated. Dex-TA hydrogels with different molecular weights and conjugated with different amounts of tyramine moieties were prepared. Physical properties such as gelation time, storage moduli, glucose diffusion and morphology of the hydrogels were evaluated. The viability and metabolic activity of *in situ* incorporated chondrocytes in these Dex-TA hydrogels were determined using live-dead and MTT assays. The morphology of the chondrocytes and the formation of a cartilaginous specific matrix (glycosaminoglycans and collagen type II) in the cell/gel constructs in time were also examined.

Chapter 5 reveals a hybrid of hyaluronic acid (HA) and Dex-TA conjugates as a biomimetic hydrogel. We hypothesized that the incorporation of HA would improve the performance of Dex-TA gels in cartilage tissue engineering. These biomimetic hydrogels were designed to provide a supportive environment for chondrocyte proliferation and differentiation, as well as matrix deposition. We describe the synthesis and characterization of polysaccharide hybrids from hyaluronic acid and dextran-tyramine conjugates. The hydrogels were investigated in terms of their gelation time, storage moduli and enzymatic degradation properties. Bovine articular chondrocytes were encapsulated inside the hydrogels *in vitro* to determine cell survival and to assess matrix production.

Chapter 6 deals with biofunctional injectable hydrogels based on dextran and heparin. We hypothesized that the presence of heparin in the hydrogels may promote chondrocyte proliferation and differentiation as well as enhance cartilage regeneration.

The preparation of injectable hydrogels is described which consists of a combination of a heparin-tyramine conjugate (Hep-TA) and a Dex-TA conjugate, with varying weight ratios. The properties of the hydrogels such as gelation time, swelling and mechanical properties were investigated. Furthermore, bovine chondrocytes were incorporated in these hydrogels to evaluate their cytocompatibility, chondrocyte proliferation and matrix production.

In **Chapter 7**, we explored the potential of covalent bond formation between the hydroxyphenyl groups present in both Dex-TA and cartilage matrix components, by evaluating whether this hydrogel promotes self-attachment during the enzymatic crosslinking reaction. Additionally, we optimized the hydrogel features to enable cell homing, by incorporation of heparin components.

Chapter 8 shows that clustering chondrocytes in micro-aggregates induces a strong anabolic response stimulating neo-cartilage formation *in vitro* and *in vivo*. Our experimental data suggest that chondrocyte clusters in OA are likely part of a regenerative response of the damaged cartilage. Furthermore, seeding constructs for cartilage repair with high throughput generated clusters of chondrocytes rather than with single cells, incorporated into Dex-TA hydrogels, may be an efficient strategy, complementary to autologous chondrocyte implantation (ACI) procedures, to boost neo-cartilage formation.

In **Chapter 9**, we hypothesize that the addition of platelet lysate to Dex-TA hydrogel will improve its biological properties, accelerating remodeling and enhancing cartilaginous matrix deposition. The effects of the incorporation of platelet lysate in Dex-TA hydrogels are investigated regarding mechanical properties, cell chemotaxis, adhesion and proliferation. We evaluated the effect of the presence of this autologous growth-factor-rich constituent during chondrogenic, osteogenic and adipogenic differentiation, as well as its effect on blood vessel formation. The ultimate goal was to determine whether this system can be used as a cell free approach, based on the ability to attract MSCs or chondrocytes from the surrounding environment, and if MSCs could be directed towards the chondrogenic lineage, solely by addition of own-patient-derived source of stimuli.

Chapter 10 provides a collective overview of the obtained results and reflects about future perspectives in the development of injectable enzymatically crosslinked hydrogels for cartilage repair.

References

1. Bedi A, Feeley BT, Williams RJ, 3rd (2010) Management of articular cartilage defects of the knee. *J Bone Joint Surg Am* 92: 994-1009.
2. Farr J, Cole B, Dhawan A, Kercher J, Sherman S (2011) Clinical Cartilage Restoration: Evolution and Overview. *Clin Orthop Relat Res*.
3. Nicodemus GD, Bryant SJ (2008) Cell encapsulation in biodegradable hydrogels for tissue engineering applications. *Tissue Eng Part B Rev* 14: 149-165.
4. Geckil H, Xu F, Zhang X, Moon S, Demirci U (2010) Engineering hydrogels as extracellular matrix mimics. *Nanomedicine (Lond)* 5: 469-484.
5. Spiller KL, Mather SA, Lowman AM (2011) Hydrogels for the Repair of Articular Cartilage Defects. *Tissue Eng Part B Rev*.
6. Tortelli F, Cancedda R (2009) Three-dimensional cultures of osteogenic and chondrogenic cells: a tissue engineering approach to mimic bone and cartilage *in vitro*. *Eur Cell Mater* 17: 1-14.
7. Peretti GM, Campo-Ruiz V, Gonzalez S, Randolph MA, Wei Xu J, et al. (2006) Tissue engineered cartilage integration to live and devitalized cartilage: a study by reflectance mode confocal microscopy and standard histology. *Connect Tissue Res* 47: 190-199.
8. Lee F, Chung JE, Kurisawa M (2009) An injectable hyaluronic acid-tyramine hydrogel system for protein delivery. *Journal of Controlled Release* 134: 186-193.
9. Aeschlimann D, Mosher D, Paulsson M (1996) Tissue transglutaminase and factor XIII in cartilage and bone remodeling. *Semin Thromb Hemost* 22: 437-443.
10. Greenberg CS, Birckbichler PJ, Rice RH (1991) Transglutaminases: multifunctional cross-linking enzymes that stabilize tissues. *FASEB J* 5: 3071-3077.
11. Jin R, Moreira Teixeira LS, Dijkstra PJ, Karperien M, van Blitterswijk CA, et al. (2009) Injectable chitosan-based hydrogels for cartilage tissue engineering. *Biomaterials* 30: 2544-2551.
12. Kim KS, Park SJ, Yang JA, Jeon JH, Bhang SH, et al. (2011) Injectable hyaluronic acid-tyramine hydrogels for the treatment of rheumatoid arthritis. *Acta Biomater* 7: 666-674.
13. Bryant SJ, Anseth KS, Lee DA, Bader DL (2004) Crosslinking density influences the morphology of chondrocytes photoencapsulated in PEG hydrogels during the application of compressive strain. *J Orthop Res* 22: 1143-1149.
14. Guilak F, Alexopoulos LG, Upton ML, Youn I, Choi JB, et al. (2006) The pericellular matrix as a transducer of biomechanical and biochemical signals in articular cartilage. *Ann N Y Acad Sci* 1068: 498-512.
15. Sakurai Y, Ma SF, Watanabe H, Yamaotsu N, Hirono S, et al. (2004) Esterase-like activity of serum albumin: Characterization of its structural chemistry using p-nitrophenyl esters as substrates. *Pharmaceutical Research* 21: 285-292.
16. Gao CY, Hu XH, Li D, Zhou F (2011) Biological hydrogel synthesized from hyaluronic acid, gelatin and chondroitin sulfate by click chemistry. *Acta Biomaterialia* 7: 1618-1626.
17. Nguyen LH, Kudva AK, Guckert NL, Linse KD, Roy K (2011) Unique biomaterial compositions direct bone marrow stem cells into specific chondrocytic phenotypes

corresponding to the various zones of articular cartilage. *Biomaterials* 32: 1327-1338.

18. Kuo CK, Li WJ, Mauck RL, Tuan RS (2006) Cartilage tissue engineering: its potential and uses. *Curr Opin Rheumatol* 18: 64-73.

19. Roberts JJ, Nicodemus GD, Giunta S, Bryant SJ (2011) Incorporation of biomimetic matrix molecules in PEG hydrogels enhances matrix deposition and reduces load-induced loss of chondrocyte-secreted matrix. *Journal of Biomedical Materials Research Part A* 97A: 281-291.

20. Zhu J (2010) Bioactive modification of poly(ethylene glycol) hydrogels for tissue engineering. *Biomaterials* 31: 4639-4656.

21. Fortier LA, Mohammed HO, Lust G, Nixon AJ (2002) Insulin-like growth factor-I enhances cell-based repair of articular cartilage. *J Bone Joint Surg Br* 84: 276-288.

22. Grimaud E, Heymann D, Redini F (2002) Recent advances in TGF- β effects on chondrocyte metabolism. Potential therapeutic roles of TGF- β in cartilage disorders. *Cytokine Growth Factor Rev* 13: 241-257.

23. Kuo AC, Rodrigo JJ, Reddi AH, Curtiss S, Grotkopp E, et al. (2006) Microfracture and bone morphogenetic protein 7 (BMP-7) synergistically stimulate articular cartilage repair. *Osteoarthritis Cartilage* 14: 1126-1135.

24. Frenkel SR, Saadeh PB, Mehrara BJ, Chin GS, Steinbrech DS, et al. (2000) Transforming growth factor β superfamily members: role in cartilage modeling. *Plast Reconstr Surg* 105: 980-990.

25. Ellman MB, An HS, Muddasani P, Im HJ (2008) Biological impact of the fibroblast growth factor family on articular cartilage and intervertebral disc homeostasis. *Gene* 420: 82-89.

26. Malesud CJ (2010) Anticytokine therapy for osteoarthritis: evidence to date. *Drugs Aging* 27: 95-115.

27. Miller RE, Grodzinsky AJ, Vanderploeg EJ, Lee C, Ferris DJ, et al. (2010) Effect of self-assembling peptide, chondrogenic factors, and bone marrow-derived stromal cells on osteochondral repair. *Osteoarthritis Cartilage* 18: 1608-1619.

28. Martin JA, Buckwalter JA (2000) The role of chondrocyte-matrix interactions in maintaining and repairing articular cartilage. *Biorheology* 37: 129-140.

29. Vinatier C, Bouffi C, Merceron C, Gordeladze J, Brondello JM, et al. (2009) Cartilage tissue engineering: towards a biomaterial-assisted mesenchymal stem cell therapy. *Curr Stem Cell Res Ther* 4: 318-329.

30. Vinatier C, Mrugala D, Jorgensen C, Guicheux J, Noel D (2009) Cartilage engineering: a crucial combination of cells, biomaterials and biofactors. *Trends Biotechnol* 27: 307-314.

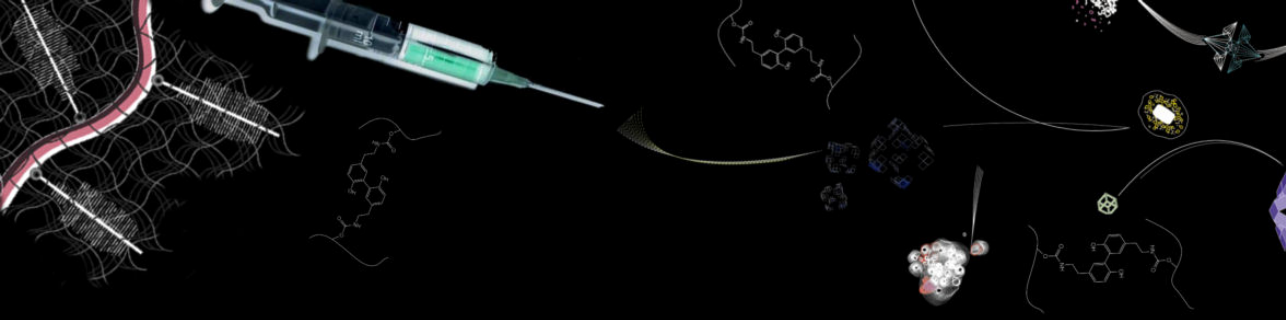
31. Noel D, Djouad F, Bouffi C, Mrugala D, Jorgensen C (2007) Multipotent mesenchymal stromal cells and immune tolerance. *Leuk Lymphoma* 48: 1283-1289.

32. Hwang NS, Varghese S, Elisseeff J (2008) Derivation of chondrogenically-committed cells from human embryonic cells for cartilage tissue regeneration. *PLoS One* 3: e2498.

33. Hendriks J, Riesle J, van Blitterswijk CA (2007) Co-culture in cartilage tissue engineering. *J Tissue Eng Regen Med* 1: 170-178.

34. Karperien M, Wu L, Leijten JCH, Georgi N, Post JN, et al. (2011) Trophic Effects of Mesenchymal Stem Cells Increase Chondrocyte Proliferation and Matrix Formation. *Tissue Engineering Part A* 17: 1425-1436.

35. Perez-Castillejos R (2010) Replication of the 3D architecture of tissues. *Materials Today* 13: 32-41.
36. Langer R, Fukuda J, Khademhosseini A, Yeo Y, Yang XY, et al. (2006) Micromolding of photocrosslinkable chitosan hydrogel for spheroid microarray and co-cultures. *Biomaterials* 27: 5259-5267.
37. Khademhosseini A, Langer R, Borenstein J, Vacanti JP (2006) Microscale technologies for tissue engineering and biology. *Proceedings of the National Academy of Sciences of the United States of America* 103: 2480-2487.
38. Mauck RL, Seyhan SL, Ateshian GA, Hung CT (2002) Influence of seeding density and dynamic deformational loading on the developing structure/function relationships of chondrocyte-seeded agarose hydrogels. *Annals of Biomedical Engineering* 30: 1046-1056.
39. Mauck RL, Wang CCB, Oswald ES, Ateshian GA, Hung CT (2003) The role of cell seeding density and nutrient supply for articular cartilage tissue engineering with deformational loading. *Osteoarthritis and Cartilage* 11: 879-890.
40. Ahsan T, Sah RL (1999) Biomechanics of integrative cartilage repair. *Osteoarthritis Cartilage* 7: 29-40.
41. Wang DA, Williams CG, Yang F, Elisseeff JH (2004) Enhancing the tissue-biomaterial interface: Tissue-initiated integration of biomaterials. *Advanced Functional Materials* 14: 1152-1159.
42. Strehin I, Nahas Z, Arora K, Nguyen T, Elisseeff J (2010) A versatile pH sensitive chondroitin sulfate-PEG tissue adhesive and hydrogel. *Biomaterials* 31: 2788-2797.
43. Wang DA, Varghese S, Sharma B, Strehin I, Fermanian S, et al. (2007) Multifunctional chondroitin sulphate for cartilage tissue-biomaterial integration. *Nat Mater* 6: 385-392.
44. Jabbari E, He XZ, Ma JY (2010) Migration of marrow stromal cells in response to sustained release of stromal-derived factor-1 alpha from poly(lactide ethylene oxide fumarate) hydrogels. *International Journal of Pharmaceutics* 390: 107-116.
45. Ratanavaraporn J, Furuya H, Kohara H, Tabata Y (2011) Synergistic effects of the dual release of stromal cell-derived factor-1 and bone morphogenetic protein-2 from hydrogels on bone regeneration. *Biomaterials* 32: 2797-2811.
46. Barradas AM, Yuan H, van Blitterswijk CA, Habibovic P (2011) Osteoinductive biomaterials: current knowledge of properties, experimental models and biological mechanisms. *Eur Cell Mater* 21: 407-429.
47. Yuan H, Fernandes H, Habibovic P, de Boer J, Barradas AM, et al. (2011) 'Smart' biomaterials and osteoinductivity. *Nat Rev Rheumatol* 7: c1; author reply c2.



Chapter 2

Cartilage tissue engineering

Liliana Moreira Teixeira*, Nicole Georgi*, Jeroen Leijten*, Ling Wu, Marcel Karperien

* Shared first co-authorship

Abstract

Cartilage tissue engineering is the art aimed at repairing defects in the articular cartilage which covers the bony ends in the joints. Since its introduction in the early 90ties of the past century, cartilage tissue engineering using autologous chondrocyte implantation (ACI) has been used in thousands of patients to repair articular cartilage defects. This review focuses on emerging strategies to improve cartilage repair by incorporating fundamental knowledge of developmental and cell biology in the design of optimized strategies for cell delivery at the defect site and to locally stimulate cartilage repair responses.

2.1 Introduction

Tissue engineering is the art of utilizing (biological) material to generate a new tissue that will replace worn out or lost native tissue that mimics its original function. Mature joint cartilage is unable to repair itself sufficiently when damaged. This results in degeneration of the cartilage and inevitably to joint failure. The need to intervene in this progressive degeneration and to restore or replace the affected cartilage effectively has created the field of cartilage tissue engineering. The main aim of cartilage tissue engineering is to repair joint or articular cartilage. Like epiphyseal growth plate cartilage, articular cartilage is a hyaline cartilage of which the extracellular matrix is rich in glycosaminoglycans and collagen type 2 as the most abundant protein. Unlike

for articular cartilage, there is no clear clinical need for epiphyseal cartilage tissue engineering. Thus if one speaks about cartilage tissue engineering, we are specifically talking about articular cartilage.

This review first discusses the development of cartilage focusing on the development of long bones, the growth plate and in particular articular cartilage. Many of the molecular mechanisms identified in the developing long bones can be applied in tissue engineering strategies. In addition to the biological knowledge, it is important to understand the history of clinical applications of articular cartilage repair and how this led to presently used tissue engineering strategies. Another essential element for the creation of an optimal and effective therapy is, in case cells are used, the cell source. For this the focus will be on historically used cell sources, the current trend and options for future therapy. The use of currently available commercial biomaterials and their use in cartilage tissue engineering, as well as emerging smart materials that are adapted to certain selected requirements are highlighted. Finally this review gives a perspective on the future of cartilage tissue engineering.

2

2.2 Development of cartilage

2.2.1 Joint formation

The main purpose of tissue engineering is to generate new tissue that can mimic the original functions to replace worn out or lost native tissues. Fundamental knowledge on the tissue of interest, as well as its natural development, is therefore of paramount importance. Chondrogenesis is heralded from three different origins: the cranial neural crest that forms craniofacial cartilage, the somites leading to the axial skeleton and the lateral plate mesoderm resulting in the formation of limbs. From here on we will focus on the latter, since cartilage tissue engineering mostly focuses on the joints of the limbs [1].

Secretion of fibroblast growth factor (FGF) 7 from the lateral plate mesoderm initiates the formation of the limb organizing apical ectodermal ridge (AER). Subsequently a signalling loop between FGF 10 in the limb mesoderm and FGF 8 in the AER directs the proximal distal outgrowth of the limb buds. Cartilage formation starts with the mesenchymal condensations in these developing limb buds and is formed from a seemingly heterogeneous cell population. The up-regulation of TGF- β , a member of the BMP superfamily, leads to enhanced expression of numerous molecules including N-cadherin, N-CAM, fibronectin and Tenascin-C, which are all implicated in the condensation of the mesenchymal cells [2].

Initiation of the expression of the cartilage master regulator SOX-9 instigates chondrogenesis and is associated with the expression of collagen type IIA and at a later stage its splice variant collagen type IIB. Under the influence of a growth factor cocktail, including amongst others insulin growth factor-1, FGF2 and BMP's 2/4/7/14, the mesenchymal condensation develops into a cartilage anlage.

The determination of the location of the joint is dependent on a site called the interzone. Although the mechanism behind this phenomenon is largely unknown, the involvement of several molecules such as Wnt-14, GDF-5 and Chordin has been im-

plicated. The cells in the interzone start producing lubricin, which is suggested to play a role in the cavitation and separation of the original cartilage anlage resulting in the formation of the joint itself [3]. When fully formed, the articulated ends of the joints are still lined with lubricin producing cells that will allow almost frictionless movement. In the mid-section of the remaining cartilage anlage the primary centre starts to mineralize and is eventually replaced by bone in a process called endochondral ossification. Postnatally, a second centre of ossification appears in the primary growth plate that effectively separates the articular cartilage covering the distal ends of the long bone from the epiphyseal growth plate cartilage entrapped between the epiphysis and metaphysis. Unlike epiphyseal growth plate cartilage which disappears at the end of puberty by growth plate fusion, healthy articular cartilage is resistant to endochondral ossification and does not disappear after puberty.

2.2.2 Growth plate cartilage

Being primarily responsible for longitudinal growth, the activity of the epiphyseal growth plate is tightly orchestrated by multiple autocrine, paracrine and endocrine factors. After the initial mesenchymal condensation and chondrogenic differentiation, the chondrocytes in the centre of the cartilage anlage start to undergo hypertrophic differentiation. This terminal differentiation allows for the formation of a mineralized matrix, in growth of blood vessels and eventually chondrocyte death, most likely via apoptosis. On the remaining cartilage anlage, osteoblasts start producing bone, forming the primary spongiosa. At the opposing end of the hypertrophic chondrocytes, chondrocyte proliferation continues in vertical columns further lengthening the long bones. These proliferating chondrocytes are recruited from the resting zone which covers the distal ends of the long bones. After the formation of the secondary ossification center the resting zone is located directly adjacent to the epiphysis [4] and contains the growth plate stem cells. The continuous cycle of stem cell recruitment, proliferation, hypertrophic differentiation and chondrocyte death is tightly regulated by a plethora of signalling molecules. The feedback loop between Indian Hedgehog and Parathyroid Hormone-related Protein is demonstrated to be one of the key regulators of endochondral ossification. Additionally, many other factors have been shown to play (major) roles in endochondral ossification including paracrine factors like Fibroblast Growth Factors (FGFs), Bone Morphogenetic Proteins (BMPs), WNTs, and endocrine regulators such as Thyroid Hormone, Growth Hormone, Insulin-like Growth Factor 1, testosterone and estrogens [5]. Many of these factors are currently explored for application in tissue engineering strategies for cartilage repair.

2.2.3 Articular cartilage

As already indicated, the main focus of cartilage tissue engineering is on restoration of the articulated surface of the joint, the articular cartilage. In its healthy mature form the tissue has an extremely high matrix/cell ratio: only 2-3 percent of its mass consists of chondrocytes, the only residing cells in articular cartilage. For the remaining it consists out of 65-80 percent of water, 12-21 percent of collagens being predominantly

collagen type II, 6-10 percent of proteoglycans and approximately 2-3.5 percent other proteins. The arch-like orientation of collagen type II fibrils, being almost horizontal in the superficial zone and almost fully vertical in the deep zone, gives the articular cartilage its anisotropic nature and allows it to transduce mechanical forces throughout the entire tissue. Additionally, the different zones do not contain the same (ratio of) molecules, having different (levels of) glycosaminoglycans and collagens as well as other more characteristic features such as the calcification of the cartilage near the subchondral bone and the production of lubricin in the superficial zone [6]. An important characteristic of healthy articular cartilage is that they are resistant to endochondral ossification. In joint degenerative diseases such as osteoarthritis, this resistance disappears and it is described that the degeneration is, at least in part, caused by endochondral ossification [7]. Articular and epiphyseal chondrocytes have many features in common and it has been long believed that they have a common progenitor. In the past years, however, preliminary proof has been provided that articular and epiphyseal growth plate chondrocytes arise from distinct cell populations. At present, the mechanisms by which articular chondrocytes are formed and by which they are able to resist hypertrophic differentiation and subsequent endochondral ossification remains unknown.

2.3 History of clinical applications in cartilage repair

The clinical and biological need to develop new cartilage repair strategies arises from the fact that cartilage has a low capacity of self repair. When damaged by either trauma or degenerative diseases it will progressively degrade and thereby destabilizing the joint. The majority of cartilage engineering strategies focus on the repair of cartilage lesions induced by trauma, since progressively diseased cartilage, such as seen in osteoarthritis needs different repair approach.

If left untreated, acute trauma will inevitably result in joint degeneration necessitating unicompartamental or total joint replacement as the only possible solution to treat the degenerated joint. To avoid total joint replacement the surgeon has a number of treatment options all with inherent drawbacks. The most popular clinical cartilage repair approaches of the last 20 years are osteochondral transplantation (OT), marrow stimulation techniques e.g. microfracture (MF) and autologous chondrocyte implantation (ACI).

OT can be divided into autologous mosaicplasty and allograft osteochondral transplantation. In the more recently developed mosaicplasty, [8] cylindrical osteochondral grafts are harvested from a non-load bearing site of the donor and will then be press fitted in pre-drilled osteochondral holes of the defect area. During the healing process, space between the grafts will be filled with fibrocartilaginous tissue. This strategy carries the risk of bone collapse at the donor and recipient site but shows acceptable results in long term follow up. Since mosaicplasty can only be applied to smaller lesions, allograft osteochondral transplantation with matching fresh or frozen cartilage pieces from organ donors is an alternative option.

During MF the subchondral bone of the affected cartilage is perforated leading to

blood clot formation at the defect site and, after the invasion of progenitor cells, to cartilage matrix formation. This cost saving and fast technique, based on the self-healing capacity of invading bone marrow cells, was first introduced by Steadman et al [9] in the early 90s. The procedure of MF leads to satisfactory outcome, but has been reported to induce fibrous cartilage formation with poor mechanical properties in some cases, questioning the long term performance of the de novo formed tissue. Next to MF, ACI gained popularity after its introduction by Brittberg et al in 1994. ACI is the first cell based therapeutic cartilage tissue engineering strategy [10]. This two step surgical procedure requires donor cartilage harvest from a non-load bearing site for chondrocyte isolation, followed by upto 6 weeks of cell expansion ex vivo and finally re-implantation of the expanded cells at the defect site. During re-implantation, the cartilage defect is first covered with a periosteal flap sealed with fibrin glue before injecting the cultured chondrocytes underneath the periosteal flap (Figure 1). This time consuming and costly technique has been shown to promote the formation of hyaline like cartilage with functional improvement in most patients, whereas other studies provide evidence for the abundance of substantial amounts of fibrous cartilage [11]. In the last decade, various studies compared microfracture to ACI with conflicting results. The findings indicate that ACI and MF lead to similar outcomes in the repair of small lesions, but the repair of large defects might have a superior outcome after ACI. In 2008, Saris et al [12] introduced characterised chondrocyte implantation (CCI) to overcome existing problems with the quality of the engineered cartilage obtained by ACI. The strategy of this CCI relies on the pre-assessment of chondrocyte populations with a greater potential to form hyaline cartilage. Compared with MF, this technique was shown to result in noticeably better clinical outcome after 36 months [13].

Although all these described cartilage repair strategies support enhanced joint function and pain relief for the patient, they do not succeed in restoring the natural cartilage structure with its associated biomechanical properties. Recent cartilage tissue engineering approaches include established methods in combination with the delivery of cells and/or bioactive molecules via a biomaterial scaffold. Bartlett et al described two variations of the traditional ACI. In the first variation, periosteal flap is replaced with a porcine-derived type I/type III collagen (ACI-C) matrix. In the second variation, before implantation chondrocytes were first seeded in a collagen bilayer (matrix-induced ACI-MACI). Both methods resulted in an improvement of ACI based on the Cincinnati knee score and International Cartilage Repair Society score, which provide both a measure for cartilage and joint quality.

2.4 Cell sources for cartilage engineering

Presently, cartilage tissue engineering is primarily based on the use of two cell types: chondrocytes or mesenchymal stromal cells (MSCs). As the most intuitive cell source for cartilage regeneration, autologous chondrocytes, have been successfully used in many studies of cartilage repair with or without the use of a scaffold [10]. However, using chondrocytes in cartilage repair applications obviously has some disadvantages.

One problem could be injury of healthy cartilage from which chondrocytes are harvested. Although donor cartilage is taken from low weight bearing sites of joint, this procedure often results in morbidity at donor sites. Another problem of using autologous chondrocytes in cartilage engineering is that they can only be harvested from small biopsies of articular cartilage. To obtain sufficient chondrocytes for cartilage repair, *in vitro* expansion is necessary. Culture expansion of chondrocytes results in a gradual loss of the chondrocyte phenotype with increasing passage number, a process known as chondrocyte dedifferentiation.

2 After several passages of expansion in two-dimensional culture environment, chondrocytes lose their initial characteristics and become fibroblast-like cells [14]. Expanding chondrocytes on microcarriers instead of tissue culture plastic can omit subculture steps in flask, thus can prevent dedifferentiation of chondrocytes. It is also believed that dedifferentiated chondrocytes may regain the ability to produce cartilage matrix when cultured in a 3D environment (e.g., suspension in hydrogel), or in chondrogenic differentiation medium containing transforming growth factor- β (TGF- β). This growth factor plays an important role in cartilage formation during organogenesis in the embryo. However, the cartilage phenotypes obtained by these treatments are significantly inferior when compared to native cartilage [15]. Yet the complex molecular events occurring in the induction and maintenance of the chondrogenic phenotype should still be enlightened for further identification of the bioactive levels and kinetics of the key factors involved in cartilage repair. Moreover, integration of repair cartilage with the native tissue and reestablishment of the zonal organization of articular cartilage are still challenging and only partly resolved. To improve the quantity of regenerated cartilage, mesenchymal stromal cells (MSC) are considered to be a promising alternative cell source. MSCs are adult stem cells isolated from somatic tissue. They have been found to be multipotent, showing the ability to differentiate into chondrocyte, osteoblast, adipocytes and endothelial cells. MSCs isolated from different origins like bone marrow, fat tissue, synovium and muscles all show potency of chondrogenic differentiation and may have possible applications in cartilage tissue engineering [16]. Most clinical studies use autologous MSCs, though allograft MSCs may be used in some cases. Traditionally, *ex vivo* chondrogenic differentiation of MSCs is induced by culturing high-density cell pellets in serum-free medium containing transforming factor- β (TGF- β). High-density pellets mimics the first step of cartilage formation in the embryo, namely the condensation of mesenchymal cells. For MSCs isolated from fat tissue, bone morphogenetic protein-6 (BMP-6) is often added to the differentiation medium. In recent years, it has been reported that culturing MSCs in gel-like biomaterials made of collagen or fibrin increases chondrogenic differentiation of MSCs when compared with pellet culture [17]. When using MSCs for cartilage engineering, the greatest challenge is not the differentiation of the cells into chondrocytes per se but to prevent the chondrogenically differentiated MSCs from undergoing endochondral ossification. Substantial evidence indicates that the chondrogenically differentiated MSCs acquire an epiphyseal growth plate phenotype rather than an articular phenotype [18]. To direct differentiation of MSCs in the articular cartilage lineage instead of a growth plate lineage is an active area of research.

To reduce the number of chondrocytes needed for cartilage engineering, MSCs

started to be co-cultured with chondrocytes. Interestingly, it was reported that co-cultures of bone marrow MSCs with articular chondrocytes produced more matrix compared to chondrocytes alone [19]. This phenomenon of increased cartilage formation was not only observed in differentiation medium containing TGF- β , but also in medium without any growth factors. Enhancement of cartilage matrix formation was also found in co-culture of articular chondrocytes with other sources of MSCs [20]. This effect has been attributed to the chondrogenic differentiation of MSCs stimulated by the chondrocytes. In recent years, it has been suggested that lineage commitment of MSCs, however, cannot fully explain their benefits on tissue remodelling and repair. Many studies have suggested a role for MSCs in secreting trophic mediators that stimulate local tissue repair mechanisms. These factors promote tissue specific cells to restore the damaged or lost tissue. A combination of MSCs and autologous chondrocytes may be a promising strategy for cartilage engineering in which the trophic effects of MSCs support and facilitate the chondrocytes to repair cartilage defects. The strategy also reveals possibility of omitting *in vitro* expansion of chondrocytes in traditional ACI procedures. The mixture of chondrocyte and MSCs may lead to a single step surgery for cartilage treatment, in which chondrocytes are isolated, mixed with bone marrow cells from the same patient, loaded on a scaffold and directly re-implanted into the patient.

Many aspects of ACI still need further optimization. For example, the integration of the neo tissue is still far from optimal. It can be hindered by cell loss, either by apoptosis or necrosis caused by, for example inflammatory cytokines or mechanical stress, or due to leakage of the cells. The relatively limited ECM production by the implanted cells, and the dissimilarities in structure and/or composition compared to native cartilage can also lead to integration failure. Thus, strategies that circumvent these complex molecular events, such as the delivery of anti-apoptotic or anti-differentiating factors, combined with a structural orchestration of cells and soluble factors is thought to play an essential role in future therapies.

2.5 Biomaterials for cartilage repair

The commonly used strategy of tissue engineering is, in general terms, to seed cells in a scaffold that can be implanted into the damaged site, as illustrated in figure 2.1. Initially, the main purpose of the scaffold is to provide structural support and allow attachment, proliferation and differentiation of cells in a 3D environment. The mechanical support provided by the scaffold would lead to a decrease in the rehabilitation time for the patient. Nowadays, tissue engineered scaffolds may be developed to trigger, interact and instruct cells by mimicry of key molecular features of the native extracellular matrix (ECM), conferred by both macromolecules (proteoglycans, collagens, fibronectin and laminins) and sequestered growth factors [21].

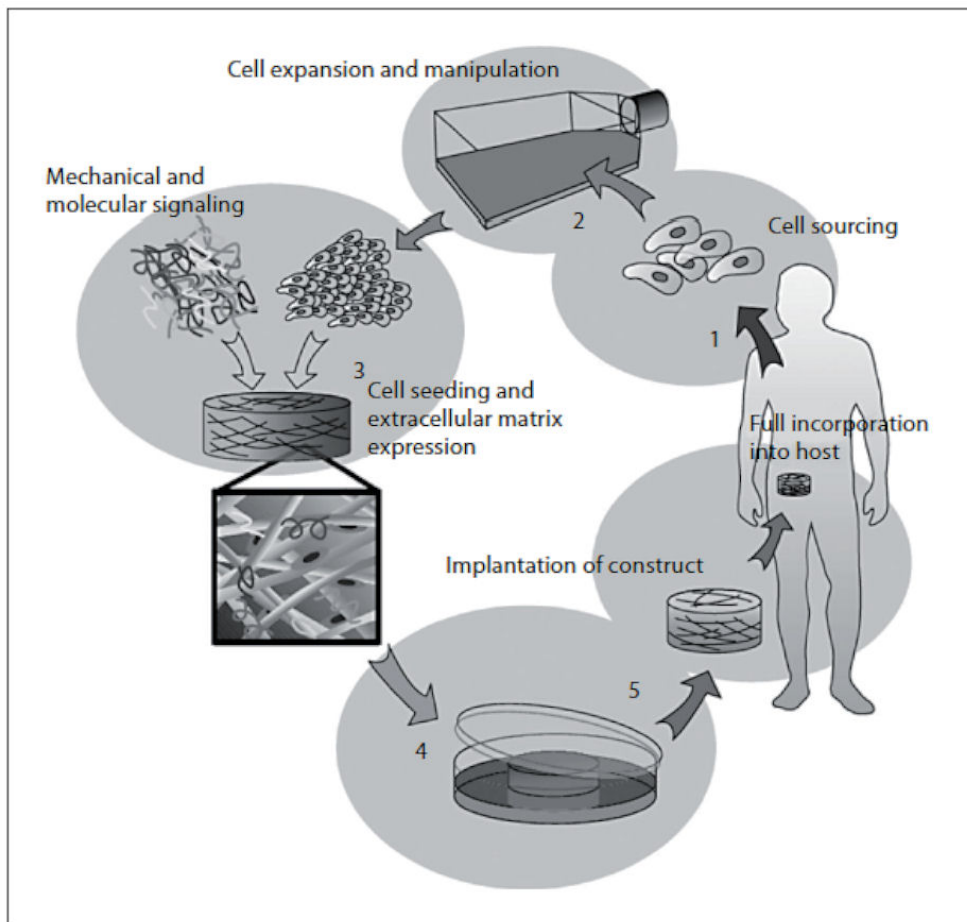


Figure 2.1: The tissue engineering approach. Adapted from: C.A. v Blitterswijk, Tissue Engineering. Academic Press Series in Biomedical Engineering [Elsevier / Academic press, Amsterdam; London, 2008] pp. xvi, 740 p.

2.5.1 Chondro-conducting scaffolds: natural and synthetic biomaterials

A myriad of biomaterials has been used as scaffolds for 3D culture of chondrocytes *in vitro* and *in vivo*, as well as for medical applications. Scaffolds can vary depending on material chemistry, 3D geometry, structure, mechanical properties and speed of degradation. The structure, mainly described in terms of pore distribution, orientation and connectivity, should maximize exchange of nutrients, metabolites and regulatory factors, as well as limit oxygen gradients and influence cell-cell interactions. The chemistry can play an instructional role and, overall, the scaffold should be biocompatible and biodegrade at a similar rate as ECM deposition, to ensure continuity and stability of the neo-tissue [22]. Additionally, the scaffolds' mechanical integrity and integration should not only be sufficient to support or match the native tissue, but also mediate mechanical stimulus to the cells during loading [23].

Scaffold materials for cartilage repair can be distinguished according to their source: natural or synthetic, as shown in table 2.1. Natural biomaterials can also be divided in of two types: protein- and polysaccharide-based. Many of these natural materials can be degraded by human enzymes, with non-toxic degradation products. Yet these materials have some drawbacks, mainly related to batch variation, processing and potential pathogen transfer. The main natural materials used for cartilage tissue engineering are collagen, hyaluronic acid, chitosan, agarose, alginate and fibrin glue [24]. These materials can be used either as temporary scaffolds and/or vehicles for cell and drug delivery or can be directly implanted or injected into the defect site.

Synthetic polymers are widely used in tissue engineering due to their flexibility in design and absence of the possibility of disease transmission; yet the disadvantages are related to their relatively poor biocompatibility for example of degradation products, which can lead to severe inflammatory responses. Synthetic materials, such as polylactide, polyglycolide and polyurethane, have been explored as suitable candidates for cartilage repair [24]. Figure 2.2 shows some protein-based membranes and gels which are currently explored in ACI procedures.

Scaffolds developed for cartilage tissue engineering can be either solid, like foams meshes or sponges, or gel-like, also termed as hydrogels. Hydrogels have been largely explored for cartilage repair strategies, because they consist of 3D hydrophilic networks and their high water content mimics native cartilage, unlike solid-type materials. Additionally, due to high diffusion rates, hydrogels allow efficient transport of nutrients and waste products. Hydrogels can be composed of natural and/or synthetic polymers that form a gellified network by physical, ionic or covalent crosslinking. Some hydrogels can be thermo-reversible (liquid at approximately 25 degrees Celsius or below, only solidifying at body temperature, around 37 degrees Celsius), be chemically crosslinked (for example by enzymes), or by photo-polymerization (using visible or ultraviolet light). *in situ* forming hydrogels allow for replacement of open surgeries by a minimal invasive procedure that offers great advantages in integration with native tissue and limits the trauma caused by surgery.

| Material source | Examples | Advantages/disadvantages |
|-----------------|---|---|
| Natural | Collagen based | Advantage: providers of molecular cues to the cells, stimulating them to produce more collagen. Disadvantage: poor mechanical properties and can undergo contraction due to interactions with cells when not combined with other materials. |
| | Hyaluronic acid | Advantage: bioactive properties, with the ability of interacting with chondrocytes (via CD44). Disadvantage: poor mechanical properties of the unmodified hyaluronic acid; the combination or engraftment with other materials, such as polyethylene glycol or dextran, allowed optimization of the biomechanical properties of the hyaluronic acid-based scaffolds. |
| | Fibrin glue | Advantage: extensively used for wound healing and, additionally for its use as fixative for scaffolds to native tissue. It can also be used as a matrix. Disadvantage: enhancement of cartilage repair is limited. |
| | Chitosan, agarose and alginate | Advantage: used as either hydrogels, sponges or pads. Disadvantage: still not available for clinical applications. |
| Synthetic | Poly lactide, polyglycolide, polyethylene glycol and polyurethane | Advantage: no batch variation. Disadvantage: possible inflammatory response against degradation products. |

Table 2.1: Scaffold materials for cartilage repair.

2.5.2 Emerging "smart" biomaterials

Novel scaffolds based on modification of natural polymers, such as dextran, silk, heparin and cellulose, or of synthetic polymers, such as polycaprolactone or co-polymers of polyether-esters have been studied to support cartilage regeneration. Several of these studies have focused on the optimization of these materials and have shown that the combination of different materials may improve properties [24]. Hybrid materials can be designed to mimic ECM structure, for example by adding hyaluronic acid or chondroitin-6-sulfate, and, therefore, providing direct interaction with the chondrocytes by the enabling necessary signals to trigger tissue repair. The communication between the cells and ECM can also be mediated by integrins, surface-specific receptors that react with proteins, such as collagens, fibronectin and laminin, which affect cell survival, proliferation and differentiation. To facilitate these type of interactions, short synthetic peptides such as the Arg-Gly-Asp (RGD) sequence, can be incorpo-

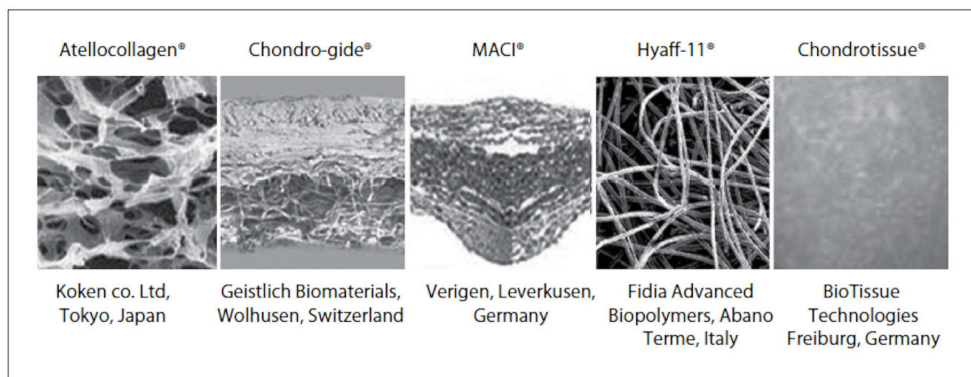


Figure 2.2: Protein-based membranes and gels already available for autologous chondrocyte implantation.

rated into scaffolds to increase the interaction between biomaterials and cells. These recognition sequences have proven to be of great value in the case of synthetic materials that lack cell-attachment signals. Yet the involvement of the RGD sequence in inducing or supporting chondrogenic differentiation of MSCs is still controversial. In addition to these peptides, the controlled local delivery of growth and differentiation factors, including Insulin-like Growth Factor-1 (IGF-1), Transforming Growth Factor β (TGF- β 1 and TGF- β 3) or Bone Morphogenic Proteins (BMP-2 and BMP-6), have been successfully combined with scaffolds. These growth factors have been selected based on their proven role during cartilogenesis in the developing embryo. Hybrid scaffolds can either be designed to locally release the bioactive factors or produced in such a way that they mimic properties of the ECM. The release of growth factors by synthetic polymers is still highly dependent on the diffusion and degradation rates of the polymers.

Recently, surface-eroding scaffolds and materials of which the release occurs by cellular demand have been developed to allow a better and more effective control of the release profiles. By incorporation in the scaffold of peptide sequences which can be recognized by e.g. matrix metalloproteinases (MMPs), release of growth factors can be locally controlled [25]. This responsive feature of the scaffold can be of great interest as the release of the growth factor in these cases can be tailored to depend on the disease-activity. For example, MMP-13 is a factor that is significantly elevated in osteoarthritis and can be used as a trigger to release scaffold bound drugs [24]. Other strategies to improve scaffold design include the development of biphasic scaffolds. Such scaffolds can also be used *in vitro* for tissue formation prior to implantation, where the design prevents cell migration between regions of the scaffold [23]. Like the growth plate, articular cartilage has a zonal organization. Strategies have been developed that use predefined geometries (for example by using rapid prototyping technologies), or have incorporated physical and chemical gradients in the scaffold to recreate the zonal organization in tissue engineered constructs [26]. Using these

strategies, the mimicry of the native cartilage-tissue anisotropy can be achieved. Gene therapy approaches can also be taken into account in scaffold design. In recent years promising results for cartilage repair strategies have been obtained by transfecting chondro-generative growth factor genes and/or chondro-protective cartilage catabolic inhibitor genes [23].

Starting from structural variations from nano to macroscale, the new generation of scaffolds often with a bioinspired design, aim at creating the optimal microenvironment for the formation of a *de novo* extracellular cartilaginous matrix by either chondrocytes, MSCs or a combination of both cell types.

2

2.6 Future of cartilage tissue engineering

Although a wide range of possible cartilage repair strategies have been described, none of them successfully restores the function and organisation of cartilage in long term studies. At the moment, numerous possible novel repair strategies arise. In general, the optimal approach will be determined by three major components: cells, biomaterials and bioactive compounds.

Cellular and molecular studies including improved cell culture, co-culture, cell tracking, gene therapy, gene arrays and proteomics will provide further cues for possible strategies in joint surface regeneration. The complex molecular events occurring in the induction and maintenance of the chondrogenic phenotype during embryogenesis may lead to the identification of novel mechanisms involved in cartilage formation. It seems promising to translate the findings from developmental biology into strategies for cartilage tissue formation. Beside optimised allogenic and autologous cartilage or cell transplants, progenitor cells, like autologous bone marrow derived stromal cells (MSCs), are likely to play an important role in future strategies for cartilage tissue repair being an alternative or supplementary cell source. Until now, however, the fate of these cells, the choice of cell fraction and optimal culture parameters are not determined and additional research is needed to clarify their applicability to articular cartilage engineering.

As indicated above, growth factors may play an important role in further optimization of cartilage tissue engineering. Presently, application of growth factors in cartilage tissue engineering is controversial and more robust studies are needed to demonstrate their applicability. The choice of the optimal combination of growth factor and method of delivery will very likely depend on the used cell type. For example different growth factors may be needed when MSCs or expanded primary chondrocytes are used for cartilage repair. Improvements in growth factor delivery should reflect an extended release profile, with protection of the proteins against fast degradation and must aim at targeting specific cell types. Multistep release, as a poly-therapy approach instead of single delivery systems, could be an additional improvement for cartilage repair strategies.

The third pillar of cartilage tissue engineering is formed by biomaterials. At the moment evermore biomaterials are being developed that show better bioaffinity and manage to mimic the native environment of cartilage. An example of these new gen-

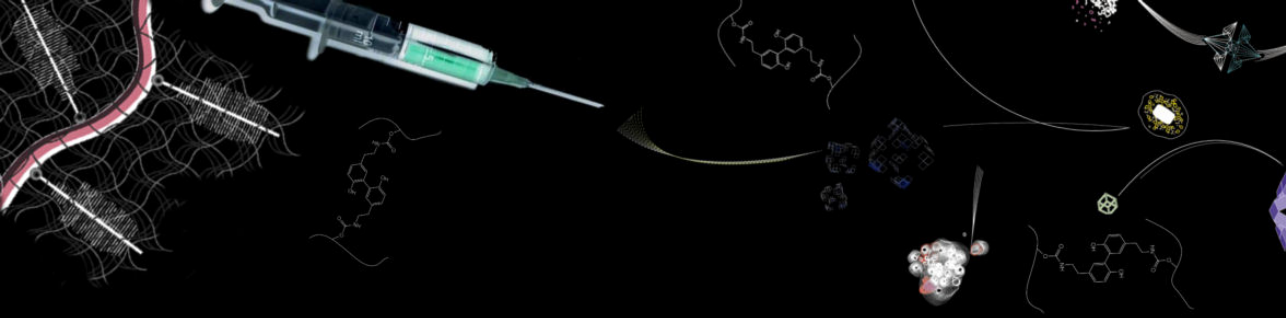
erations of biomaterials are *in situ* gelating hydrogels, which mimic the natural ECM and can perfectly fill up irregular defect sites. Importantly, *in situ* gelating hydrogels can be used in minimal invasive strategies, which will significantly reduce the burden for the individual patient. Smart” hydrogels sensitive to external stimuli such as temperature, pH or certain biomolecules, that can trigger swelling or degradation, have been developed. Recently, dynamic hydrogels have been investigated, offering the ability to precisely control temporal and spatial behaviour of the cells, by creating a tissue-like hierarchical organization. This strategy can be combined with tailored delivery of bioactive signals that stimulate tissue repair.

Translating fundamental knowledge in chondrogenesis and articular cartilage homeostasis into the design of novel smart materials is an active field of research, which undoubtedly will result in the development of improved strategies for cartilage repair in the near future.

References

1. Olsen BR, Reginato AM, Wang W. Bone development. *Annu Rev Cell Dev Biol* 2000;16:191-220.
2. Chimal-Monroy J, Diaz de Leon L. Expression of N-cadherin, N-CAM, fibronectin and tenascin is stimulated by TGF- β 1, β 2, β 3 and β 5 during the formation of pre-cartilage condensations. *Int J Dev Biol* 1999;43:59-67.
3. Pacifici M, Koyama E, Iwamoto M. Mechanisms of synovial joint and articular cartilage formation: recent advances, but many lingering mysteries. *Birth Defects Res C Embryo Today* 2005;75:237-48.
4. Zuscik MJ, Hilton MJ, Zhang X, Chen D, O'Keefe RJ. Regulation of chondrogenesis and chondrocyte differentiation by stress. *J Clin Invest* 2008;118:429-38.
5. Grumbach MM. Estrogen, bone, growth and sex: a sea change in conventional wisdom. *J Pediatr Endocrinol Metab* 2000;13 Suppl 6:1439-55.
6. Poole AR, Kojima T, Yasuda T, Mwale F, Kobayashi M, Lavery S. Composition and structure of articular cartilage: a template for tissue repair. *Clin Orthop Relat Res* 2001:S26-33.
7. Kawaguchi H. Regulation of osteoarthritis development by Wnt- β -catenin signaling through the endochondral ossification process. *J Bone Miner Res* 2009;24:8-11.
8. Hangody L, Kish G, Karpati Z, Szerb I, Udvarhelyi I. Arthroscopic autogenous osteochondral mosaicplasty for the treatment of femoral condylar articular defects. A preliminary report. *Knee Surg Sports Traumatol Arthrosc* 1997;5:262-7.
9. Steadman JR, Rodkey WG, Briggs KK, Rodrigo JJ. [The microfracture technique in the management of complete cartilage defects in the knee joint]. *Orthopade* 1999;28:26-32.
10. Brittberg M, Lindahl A, Nilsson A, Ohlsson C, Isaksson O, Peterson L. Treatment of deep cartilage defects in the knee with autologous chondrocyte transplantation. *N Engl J Med* 1994;331:889-95.
11. McNickle AG, L'Heureux DR, Yanke AB, Cole BJ. Outcomes of autologous chondrocyte implantation in a diverse patient population. *Am J Sports Med* 2009;37:1344-50.
12. Saris DB, Vanlauwe J, Victor J, et al. Characterized chondrocyte implantation results in better structural repair when treating symptomatic cartilage defects of the knee in a randomized controlled trial versus microfracture. *Am J Sports Med* 2008;36:235-46.
13. Saris DB, Vanlauwe J, Victor J, et al. Treatment of symptomatic cartilage defects of the knee: characterized chondrocyte implantation results in better clinical outcome at 36 months in a randomized trial compared to microfracture. *Am J Sports Med* 2009;37 Suppl 1:10S-9S.
14. Schnabel M, Marlovits S, Eckhoff G, et al. Dedifferentiation-associated changes in morphology and gene expression in primary human articular chondrocytes in cell culture. *Osteoarthritis Cartilage* 2002;10:62-70.
15. Mukaida T, Urabe K, Naruse K, et al. Influence of three-dimensional culture in a type II collagen sponge on primary cultured and dedifferentiated chondrocytes. *J Orthop Sci* 2005;10:521-8.

16. Sakaguchi Y, Sekiya I, Yagishita K, Muneta T. Comparison of human stem cells derived from various mesenchymal tissues: superiority of synovium as a cell source. *Arthritis Rheum* 2005;52:2521-9.
17. Mueller MB, Tuan RS. Functional characterization of hypertrophy in chondrogenesis of human mesenchymal stem cells. *Arthritis Rheum* 2008;58:1377-88.
18. Tsuchiya K, Chen GP, Ushida T, Matsuno T, Tateishi T. The effect of coculture of chondrocytes with mesenchymal stem cells on their cartilaginous phenotype *in vitro*. *Mat Sci Eng C-Bio S* 2004;24:391-6.
19. Hildner F, Concaro S, Peterbauer A, et al. Human Adipose-Derived Stem Cells Contribute to Chondrogenesis in Coculture with Human Articular Chondrocytes. *Tissue Eng Pt A* 2009;15:3961-9.
20. Gneccchi M, He H, Liang OD, et al. Paracrine action accounts for marked protection of ischemic heart by Akt-modified mesenchymal stem cells. *Nat Med* 2005;11:367-8.
21. Place ES, Evans ND, Stevens MM. Complexity in biomaterials for tissue engineering. *Nat Mater* 2009;8:457-70.
22. Vunjak-Novakovic G. The fundamentals of tissue engineering: scaffolds and bioreactors. *Novartis Found Symp* 2003;249:34-46; discussion -51, 170-4, 239-41.
23. Woodfield TB, Bezemer JM, Pieper JS, van Blitterswijk CA, Riesle J. Scaffolds for tissue engineering of cartilage. *Crit Rev Eukaryot Gene Expr* 2002;12:209-36.
24. Stoop R. Smart biomaterials for tissue engineering of cartilage. *Injury* 2008;39 Suppl 1:S77-87.
25. Raeber GP, Lutolf MP, Hubbell JA. Mechanisms of 3-D migration and matrix remodeling of fibroblasts within artificial ECMs. *Acta Biomater* 2007;3:615-29.
26. Klein TJ, Malda J, Sah RL, Hutmacher DW. Tissue engineering of articular cartilage with biomimetic zones. *Tissue Eng Part B Rev* 2009;15:143-57.



Chapter 3

3

Enzyme-catalyzed crosslinkable hydrogels: emerging strategies for tissue engineering

Liliana Moreira Teixeira, Jan Feijen, Clemens van Blitterswijk, Piet Dijkstra, Marcel Karperien

Abstract

State of the art bioactive hydrogels can easily and efficiently be formed by enzyme-catalyzed mild-crosslinking reactions *in situ*. Yet this cell-friendly and substrate-specific method remains under explored. Hydrogels prepared by using enzyme systems like tyrosinases, transferases and lysyl oxidases show interesting characteristics as dynamic cell scaffolds and as systems for controlled release. Increased attention is currently paid to hydrogels obtained via crosslinking of precursors by transferases or peroxidases, as catalysts. Enzyme-mediated crosslinking has proven its efficiency and attention has now shifted to the development of enzymatically crosslinked hydrogels with higher degrees of complexity, mimicking extracellular matrices. Moreover, bottom-up approaches combining biocatalysts and self-assembly are being explored for the development of complex nano-scale architectures. In this review, the use of enzymatic crosslinking for the preparation of hydrogels as an innovative alternative to other crosslinking methods, such as the commonly used UV-mediated photo-crosslinking or physical crosslinking, will be discussed. Photo-initiator-based crosslinking may compromise the biocompatibility of the gels formed, whereas physical crosslinking may lead to gels which do not have sufficient mechanical strength and

stability. These limitations can be overcome by the use of enzymes to form covalently crosslinked hydrogels. Herewith, we report the mechanisms involved and innovative applications, focusing on emerging strategies for tissue engineering and regenerative medicine.

3.1 Introduction

Hydrogels are hydrophilic polymeric networks able to absorb and retain high quantities of water while retaining its shape [1,2]. Their three-dimensional (3D) structure is excellent to mimic cell and tissue culture environments and, consequently, they are frequently used to encapsulate cells in a 3D-microenvironment. Additionally, hydrogels have proven to be very efficient for the delivery of biologically active molecules, such as growth factors, as well as providing organization of cells and tissues, due to the possibility to create multilayered systems [3,4,5,6].

In the last few years, mild crosslinking methods have been successfully developed to form artificial matrixes. Major advances have been achieved in both physically or chemically crosslinked gels [7]. In physically crosslinked gels, interactions between polymers chains in amphiphilic block and graft copolymers [8], are established by ionic and/or hydrophobic interactions [9], or crystallization [10]. On one hand, this type of crosslinking has the advantages of reversibility and absence of chemical reactions potentially harmful to the integrity of incorporated bioactive agents or cells. On the other hand, their stability *in vivo* might be severely affected by interactions with bodily functions, both physiological and mechanical. Examples of these functions include weight bearing actions, for example in the bone and joints, for which these gels might provide insufficient mechanical strength. Another example is the sudden change in ion concentration or changes in pH, occurring in a normal inflammatory response, which can ultimately lead to gel collapse. In chemically crosslinked gels, covalent bonds are formed between polymer chains. In contrast, chemical crosslinking allows the formation of gels with controllable mechanical strength and superior physiological stability. The crosslinks in these type of gels can be generated via e.g. radical polymerization, chemical reaction of complementary groups, by using high energy radiation or by mimicking of biological crosslinking methods using enzymes [11].

Recently, increasing interest has been devoted to enzymatically crosslinked hydrogels, mainly due to the mildness of this type of reaction. The majority of the enzymes involved in the crosslinking are common to the enzymes catalyzing reactions naturally occurring in our body [12,13,14,15,16,17,18,19,20]. Enzymatic reactions are catalyzed by most enzymes at neutral pH, in an aqueous milieu and at moderate temperatures implying that they also can be used to develop *in situ* forming hydrogels. Additionally, unwanted side reactions or toxicity, that can occur with photo-initiators or organic solvents mediated reactions, are avoided due to one of the best characteristics of this type of reaction: the substrate specificity of the enzyme. Another major advantage relates to the mildness of the enzymatic reactions at normal physiological conditions, which highlights the advantages of this method for the crosslinking of

natural polymers that cannot withstand harsh chemical conditions. Possible loss of bioactivity is, therefore, avoided. The polymerization reaction can be directly controlled by modulation of the enzyme activity [21]. Smart enzyme-responsive systems can be designed not only to recreate native extracellular matrixes (ECM) [22], but also to form and degrade biomaterials. These events capture, in essence, the intricacy of one of the most important biological functionalities of ECM, which is remodeling. In addition to degradability, tailoring the gelation rate is fundamental for applications such as drug delivery and tissue regeneration strategies. A controlled gelation rate is essential to prevent diffusion of the precursors, to ensure localized drug delivery, to obtain a suitable cell distribution, and, finally to properly integrate the gel with the surrounding tissues (mainly for irregular-shape filling applications).

Minimally invasive procedures are highly advantageous in tissue engineering therapies, presenting an attractive alternative for the replacement of cartilage. *In situ* crosslinkable gels are based on aqueous mixtures of gel precursors with bioactive agents that can be administrated via a syringe [23,24]. Injectable matrices abolish the need of complicated surgical interventions and reduce both the discomfort and complications for the patient [25]. For this purpose, artificial matrices should be biocompatible, non-inflammatory, easy to inject, stable after gelation, and, lastly, their resorption rate should match the rate of formation of new tissue [26]. Moreover, injectable enzymatically crosslinked hydrogels offer a plausible solution for the generation of functional tissue substitutes due to the similarities in the mechanical and swelling properties of these gels and native tissue, thereby maintaining the cell phenotype. This feature is highly relevant for tissues such as cartilage, where cells tend to de-differentiate when placed in a 2D environment [27,28]. Importantly, integration within wounds and tissue defects, even oddly shaped, is permitted by *in situ* forming hydrogels. These hydrogels can be applied during endoscopic or arthroscopic procedures, due to the initial fluidity of the gel precursors prior to gelation.

In this contribution, enzymatically crosslinked gels will be reviewed, focusing on their application in regenerative strategies. The purpose of this review is to provide examples of combinations of enzymes and materials that offer innovative avenues for further exploration in tissue engineering applications.

3.2 Enzymatically crosslinked hydrogels

3.2.1 Transglutaminase

Transglutaminases are a wide family of thiol enzymes that catalyze post-translational protein modification mainly by inducing isopeptide bond formation, but also through the covalent conjugation of polyamines, lipid esterification, or the deamination of glutamine residues. Transglutaminases are a mild alternative to chemical crosslinking, catalyzing the formation of covalent bonds between a free amine group from a protein or peptide-bound lysine and the -carboxamide group of a protein or peptide-bound glutamine (table 3.1). Once formed, these bonds are highly resistant to proteolytic degradation. Consequently, stable polymeric networks are assembled, without addition of co-factors. The biochemical role of transglutaminases was discovered in

| Mechanism of the reaction: | |
|--|---|
| | |
| Advantages | Drawbacks |
| <ul style="list-style-type: none"> Involved in wound healing and blood clot formation Acts as "biological glue", participation in cell-matrix interactions and general maintenance of tissue integrity [34] No co-factors are needed; only requires the binding of Ca^{2+} in supra-physiological concentrations [35] Relatively fast gel formation (from 5 to 20 minutes) [36] The gels formed are generally highly cytocompatible and with suitable transport properties [20] | <ul style="list-style-type: none"> Short-lived proteins (half-life of type 2 tissue transglutaminase is about 11 hours) [37] Large enzymes, difficult to produce recombinantly [38] Involvement in chronic inflammatory diseases of the joint, activating pro-inflammatory cytokines that might lead to mineralization and disease progression [39,40] Poor mechanical properties (storage modulus up to 1kPa) [36] |

Table 3.1: Mechanism of the enzymatic reaction mediated by transglutaminases, advantages and drawbacks

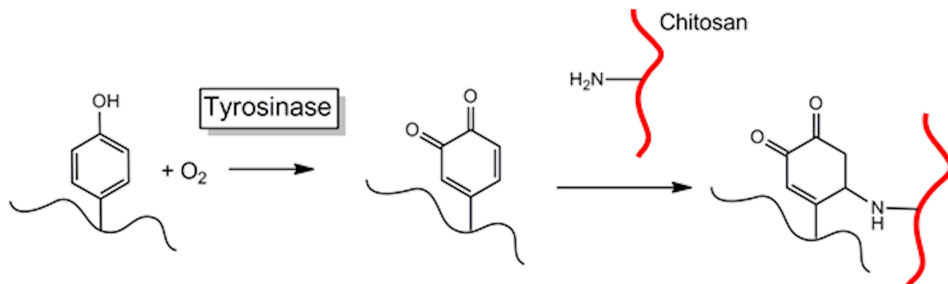
1968, when the function of isozyme factor XIII in blood coagulation was revealed as a fibrin-stabilizing factor [29]. These enzymes are found in a variety of tissues, such as skin and the brain [30,31,32]. Transglutaminases are responsible for the formation of fibrin clots and cornified epidermis. Consequently, the absence of these enzymes severely hampers wound healing [33]. Using this system, Davis *et al.* have reported a modular hydrogel with tunable characteristics that is formed within 2 minutes. Additionally, bioactive peptides could be engrafted, allowing customizable cell-signaling requirements [12]. Fibrin matrices are formed by factor XIII, which is the circulatory form of transglutaminases. These matrices have been studied both *in vitro* and *in vivo* for several applications, including angiogenesis, nerve repair and cartilage tissue engineering [41,42,43,44]. Ehrbar *et al.* used activated transglutaminase factor XI-IIa to simultaneously couple site-specific cell-adhesion ligands and crosslink modified multi-arm poly(ethylene glycol) (PEG) precursors. Interestingly, in their system, the material building blocks are responsive to two enzymatic systems, one responsible for matrix formation and the other one for degradation [36]. The enzyme-mediated site-specific coupling of ligands allowed extensive cell spreading, proliferation and migration, as well as proteolytic matrix degradation by cell-derived matrix metal-

loproteinases (MMPs). Elegant strategies also reporting the use of factor XIIIa to cross-link star-shaped PEG, functionalized by either a glutamine acceptor or donor, to tether growth factors to surfaces were provided [45]. In this study, consecutive enzymatic reactions allowed for site-specific immobilization of large quantities of biologically active substances. This system highlights the advantages of the use of enzymatic crosslinking, as their mild conditions and high specificity do not jeopardize proteins bioactivity, providing the cells simultaneously with adhesive sites and morphogens. Tissue transglutaminase shows a high degree of sequence similarity with other transglutaminases, such as factor XIII, however, requiring no proteolysis for activation. Moreover, tissue transglutaminases present stronger adhesiveness than fibrin-based glues and less susceptibility to physical parameters like humidity [46]. The combination between PEG and tissue transglutaminases has been described by Sperinde and Griffith. In their model, the gelation time was dependent on polymer functionalities, initial stoichiometric ratios and substrate kinetics [47,48]. Hu and Messersmith, reported the high adhesive strength of the *in situ* forming peptide conjugated polymer hydrogels crosslinked by transglutaminase [49]. Transglutaminase has also been used to prepare gelatin-based hydrogels. These gels can be used for incorporation of cells showing excellent cytocompatibility and promising features for TE applications. In addition, they show excellent transport properties, which facilitate sustained drug delivery [20,50]. Genetically engineered elastin-like polypeptide hydrogels and peptide-PEG conjugates crosslinked by transglutaminases have shown promising features as injectable hydrogels for cartilage repair [51,52]. In the study published by Jones *et al.*, reactive ECM components have been identified, that allowed the coupling of peptide and peptide-polymer conjugates via tissue transglutaminase [52]. The possibility to broaden the application of this strategy to a variety of tissue surfaces highlights the versatility of this method. Using this method, surfaces can be modified with molecules such as growth factors, therapeutic drugs or functional moieties. Transglutaminases are enzymes that rely on the presence of Ca_{2+} . Interestingly, Ca_{2+} independent transglutaminase-catalyzed gel formation has also been described with the ability to entrap and release cells. These gels appear especially useful for micro-fluidic biosensor systems [53].

3.2.2 Tyrosinase

Similarly to transglutaminases, tyrosinases, also known as phenoloxidase and monophenol monooxygenase, catalyze macromolecular network formation in the absence of co-factors. Tyrosinase is a copper-containing enzyme that catalyses the oxidation of phenols, such as in tyrosine residues and dopamine, into activated quinones [54], in the presence of O_2 . Activated quinones can react with a hydroxyl group or amino group mainly via a Michael type addition reaction [55]. Tyrosinases are present in plants and animals. These enzymes are involved in melanin production, browning of food and also cuticle hardening in insects [56]. In most plants and animals, tyrosinases have rather broad substrate specificity. In contrast, substrate specificity is restricted to the L-form of tyrosine or DOPA in mammalian tyrosinases. Chen *et al.* compared gels of gelatin and chitosan (table 3.2) formed upon crosslinking using

 Mechanism of the reaction:



| Advantages | Drawbacks |
|--|--|
| <ul style="list-style-type: none"> • High adhesiveness [57] • No co-factors are needed | <ul style="list-style-type: none"> • Instability of the gel networks [56] • Not yet tested in hydrogel formation for biomedical applications |

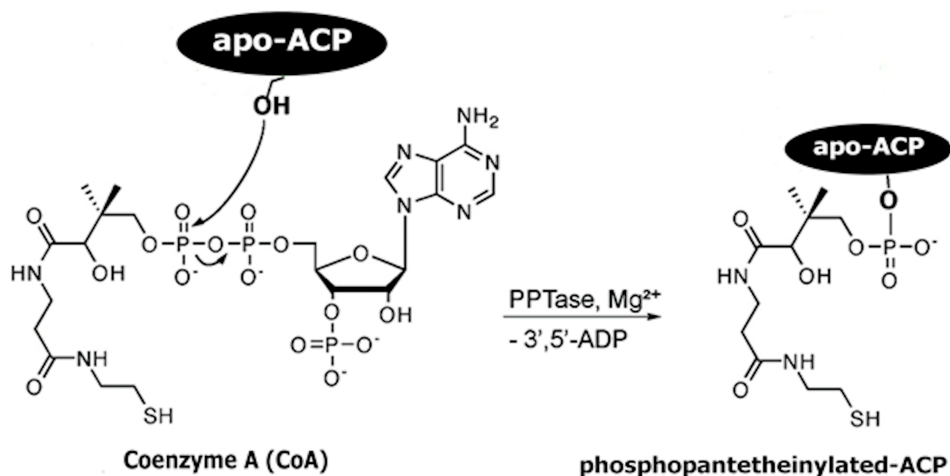
Table 3.2: Mechanism of the enzymatic reaction mediated by tyrosinases, advantages and drawbacks

tyrosinase or transglutaminase and concluded that tyrosinase induced faster gelation. However, the hydrogels catalyzed by tyrosinase only formed in the presence of chitosan and were mechanically weaker or unstable [56,58]. This and similar studies, suggested that the gels formed by tyrosinase were mainly suitable as glue [59], and wound dressings or could be used for protein immobilization [60], due to their fast degradation. Kang *et al.* reported the efficacy of tyrosinase crosslinking of silk fibroin and chitosan conjugates [57]. Other applications of tyrosinase involve the crosslinking of tyrosine residues in silk, fibroin and sericin, yielding protein-polysaccharide conjugates [61,62]. These hydrogels showed potential for biomedical applications, due to their unique mechanical properties, adhesiveness and non-toxicity. However, no specific descriptions as TE approaches were reported.

3.2.3 Phosphopantetheinyl transferase

Phosphopantetheinyl transferase is a small enzyme that can be obtained with high expression yields, thus, offering an alternative to transglutaminases, which are larger and have limited recombinant production. Transferases, which are expressed mainly in the cytosolic compartment in a wide range of tissues, both in yeast and animal cells, comprise large multifunctional polypeptides that contain all of the catalytic components required for the synthesis of long-chain fatty acids [63]. The general mechanism of transferase catalysis to form synthetic hydrogels occurs by transfer of

Mechanism of the reaction [38]:



| Advantages | Drawbacks |
|--|---|
| <ul style="list-style-type: none"> • Small size enzyme with very high specificity • Efficient recombinant production with high expression yields and easy purification | <ul style="list-style-type: none"> • Slow crosslinking • Soft gels • Requirement of coenzyme A |

Table 3.3: Mechanism of the enzymatic reaction mediated by phosphopantetheinyl transferase, advantages and drawbacks

a phosphopantethein prosthetic group of coenzyme A-functionalized PEG macromers to a serine residue of engineered carrier proteins. The use of phosphopantetheinyl transferase-catalyzed formation of polymer hydrogels (table 3.3) was recently reported by Mosiewicz *et al.* [38]. Hybrid hydrogels were formed by mixing the precursors of 8-arm-PEG-coenzymeA, at 37 degrees Celsius, neutral pH and in the presence of Mg^{2+} . The gelation was rather slow and occurred in approximately 15 minutes. The hydrogel reached an elastic modulus value of 2.3 kPa. Furthermore, in this study they also explored the potential to incorporate bioactive peptides, more specifically the integrin receptor binding motifs, such as RGDs (Arg-Gly-Asp), which enable cell attachment and spreading [64]. With this method, selective covalent formation and modification of these transferase-catalyzed hydrogels with bioactive peptide ligands occurred simultaneously. This type of reaction is, on one hand highly attractive for

cell biology and tissue engineering applications, but, on the other hand, still under explored due to its novelty.

3.2.4 Lysyl oxidase and plasma amine oxidase

Lysyl oxidase is a key component in the formation and repair of the native extracellular matrix. This ubiquitous enzyme oxidizes primary amines of lysines to aldehydes (table 3.4). The formed reactive aldehydes react further to cross-link the extracellular matrix [65]. Lysyl oxidase is responsible for the covalent crosslinkages which stabilize collagen and elastin fibrous proteins. Consequently, lysyl oxidase is involved in the morphogenesis and regeneration potential of many connective tissues including skeleton, respiratory tract and cardiovascular tissue [66]. Plasma amine oxidase also functions by oxidation of primary amines and has the major advantage that it is commercially available [65]. Interestingly, both these enzymes can be used as matrix crosslinkers, not only to improve tissue or biomaterial strength over time, but also to enhance matrix formation [67,68]. Bakota *et al.* used lysyl oxidase to fabricate nanofibers of multidomain peptides, by oxidative crosslinking of lysine residues. Interestingly, unlike other hydrogel systems that degrade overtime, the hydrogels formed by this enzyme family become more robust due to the continuous activity of lysyl oxidase. This interesting feature leads to continuous increase in the mechanical stability of hydrogels composed of biopolymers rich in lysine. Lysyl oxidase is abundantly present in serum. Thus, in serum containing conditions, crosslinking of lysine containing polymers spontaneously occurs without addition of an exogenous enzyme source [65]. Lysyl oxidase shows great value in tissue engineering using lysine-rich peptide-based hydrogels [69,70]. It might be explored to enhance extracellular matrix production by cells incorporated in the hydrogel. Moreover, it may also improve the intrinsic mechanical properties of tissue engineered constructs over time and allow hydrogel fixation with native tissue by covalent bond formation between the lysine rich polymers of the hydrogel and primary amines in native tissue proteins.

3.2.5 Phosphatase, thermolysin, β -lactamase and phosphatase/kinase

Enzyme catalysis mediated by phosphatases, thermolysin, β -lactamase or phosphatase/kinase can change the amphiphilicity of small peptide derivatives, for example, by phosphorylation mediated by a kinase or dephosphorylation mediated by a phosphatase. This change can, subsequently, trigger the self-assembly and non-covalent interactions of the amphiphilic peptides in nanofibers, ultimately resulting in hydrogel formation, as represented in table 3.5 [71,72]. These small peptide derivatives are usually organic or bioactive molecules, which tolerate the addition of bioactive components. Phosphatases catalyze the removal of phosphate groups from a substrate, which becomes more hydrophobic. In an aqueous milieu, these hydrophobic substrates may self-assemble into a 3D nanofiber network by non-covalent interactions (for example, hydrogen bonding and charge interactions) that allow gel formation [75]. In this respect, alkaline phosphatases are particularly interesting classes of enzymes to

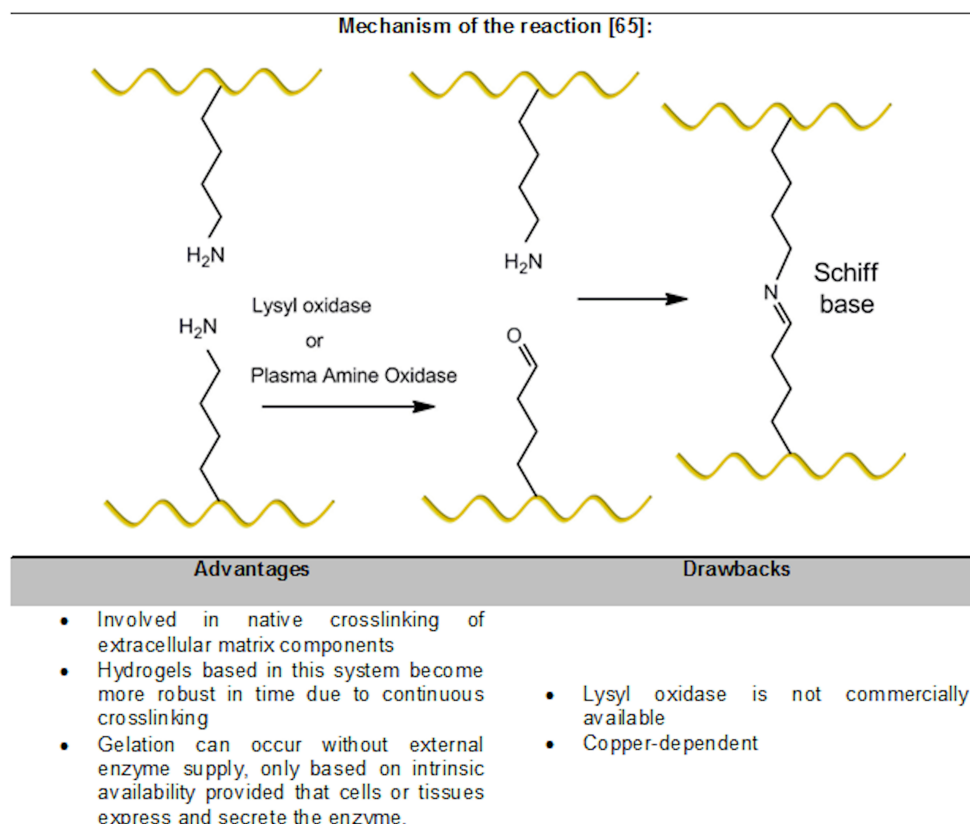
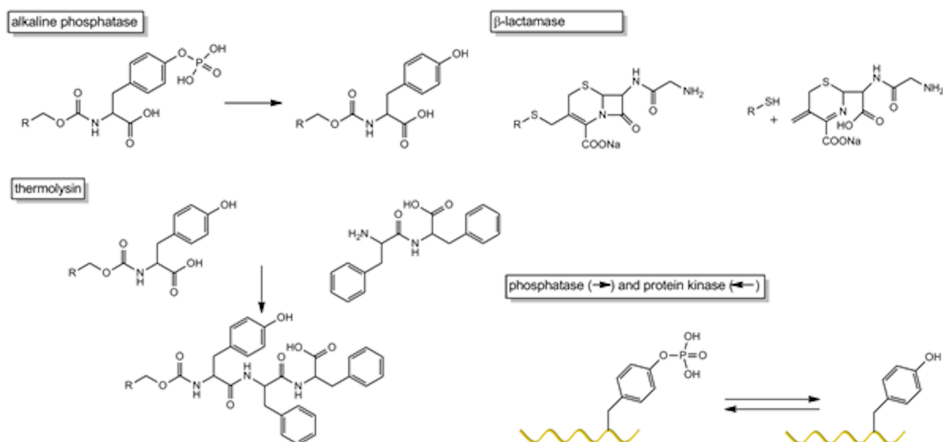


Table 3.4: Mechanism of the enzymatic reaction mediated by lysyl oxidase and plasma amine oxidase, advantages and drawbacks

Mechanism of the reaction [72]:



Advantages

- Catalysts for molecular self-assembly
- Kinase/phosphatase switches enable reversibility of the reactions [73], highly interesting as dynamic cell scaffolds and for controlled drug release
- Control over spatial organization of hydrogels

Drawbacks

- Spatial-temporal control of self-assembly and nucleation is a major challenge [74]
- Poor mechanical properties

Table 3.5: Mechanism of the enzymatic reaction mediated by phosphatases, thermolysin, β-lactamase and phosphatase/kinase, advantages and drawbacks

form hydrogels due to their involvement in mineralization of skeletal tissues. Schnepf *et al.* exploited this property of alkaline phosphatase by fabricating materials with a range of mineral loadings. Interestingly, these materials maintained their viscoelasticity rendering them suitable as biomaterials for application in tissue engineering, wound healing, and drug release purposes [76]. Instead of breaking the covalent bonds between the peptide and the phosphate group, as it occurs with phosphatases, thermolysin exploits another way of changing the amphiphilicity of a peptide. Thermolysin catalyzes the formation of bonds between peptides by reverse hydrolysis. This enzyme can be used to couple two distinct peptide derivatives, reducing the solubility of one of the peptides. This new block peptide can then self-assemble into a hydrogel by hydrophobic interactions. Thermolysin favors hydrophobic, aromatic residues on the amine side of the peptide bond. This system has been reported by

Toledano *et al.* with possible applications in the production of nanofibrous hydrogel scaffolds for cell culture [77]. β -Lactamases and esterases are two other enzymes that can be used as catalysts for molecular self-assembly. If the self-assembly occurs in an aqueous medium, the gels are referred to as a supramolecular hydrogels, and the small molecules are referred to as supramolecular hydrogelators. Both enzymes couple with the formation of hydrogelators. β -Lactamases are produced by some bacteria and are responsible for their resistance to β -lactam antibiotics, such as penicillin. The lactamase breaks a four-atom ring present in the molecular structure of antibiotics, known as β -lactam. As this ring opens, the molecule's antibacterial properties are deactivated. Upon the action of a lactamase, the lactam ring of the hydrogel precursor molecules opens and the hydrogelator is released. This release results in their self-assembly, subsequent nanofiber assembly and hydrogel formation. The presence of lactamases in bacterial lysate are able to convert the precursor to an hydrogelator, which triggers supramolecular hydrogel formation. The intracellular self-assembly of a hydrogels mediated by β -lactamases or esterases can potentially be used as in bacterial assays or to trigger specific cell death, as the formation of these supramolecular hydrogels can occur inside the cells [78,79].

Most enzymatic reactions are irreversible, thus, leading to irreversible modification of the peptide backbone of the crosslinked hydrogel. To allow reversibility of the enzymatic reactions, Yang *et al.* proposed a kinase/phosphatase switch to control supramolecular hydrogels. This enzyme switch regulates the phase transition of the peptide backbone of the hydrogel. This occurs by either adding or removing a hydrophilic phosphate group from the peptide backbone, thereby, controlling both dissociation and formation of the self-assembled nanostructures. Exploiting this enzymatic switch allows precise control of biomaterial organization at the molecular level over time. This may have a wide range of applications in tissue engineering [73]. In contrast to the random formation of polymer chains obtained by other ways of enzymatic crosslinking of polymeric hydrogels, the self-assembly of supramolecular hydrogels allows an ordered molecular arrangement within the nanofibers (hierarchical nanostructures) that ultimately leads to hydrogel formation. These are unique features of enzymatically formed supramolecular hydrogels [74,80].

3.2.6 Peroxidases

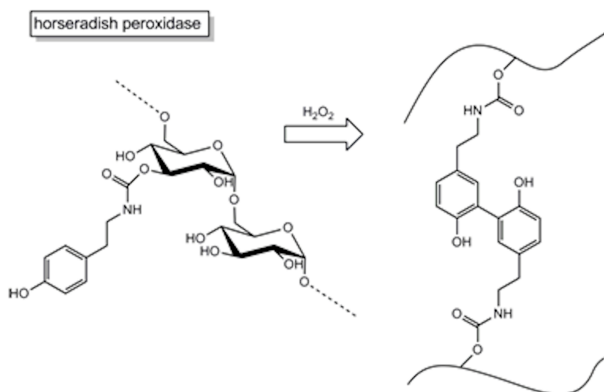
Peroxidases are a wide family of enzymes that typically catalyze the following reaction: $\text{ROOR}' + \text{electron donor (2 e}^-) + 2\text{H}^+ \rightarrow \text{ROH} + \text{R}'\text{OH}$. The majority of the peroxidases use hydrogen peroxide as substrate. This family consists up to 42 isozymes, which becomes a challenge when defining the *in vivo* function [81]. The most commonly used peroxidases in hydrogel formation are horseradish peroxidase and soy bean peroxidase. Both are plant enzymes and are explored as useful tools for biosciences and biotechnology, even though soy bean peroxidase has only become known in the last 20 years. Horseradish peroxidase is a single-chain β -type hemoprotein responsible for the catalysis of the conjugation of phenol and aniline derivatives in the presence of hydrogen peroxide [82]. In this reaction the horseradish peroxidase promptly combines with hydrogen peroxide and the formed complex can oxidize

hydroxyphenyl groups. Such groups are present for instance in tyramine, tyrosine and 4-hydrophenyl acetic acid [83]. Soybean peroxidase is a suitable alternative to horseradish peroxidase, due to comparable stability and mechanism of action. The family of human peroxidases includes myeloperoxidase, lactoperoxidase, eosinophil peroxidase, thyroid peroxidase and prostaglandin H synthases. Mammalian enzymes contribute mainly in host defense against infection, hormone synthesis and pathogenesis. Plant peroxidases differ from human peroxidases in size and how the heme-group is bound. Plant peroxidases consist of approximately 300 aminoacids and the heme-domain is not covalently bound, whereas mammalian peroxidases are larger, ranging from 576 to 738 aminoacids, with heme covalently bound [84,85]. Although human peroxidases have been widely investigated, to our knowledge, only plant peroxidases have been explored for enzymatic crosslinking to form hydrogels. Sofia *et al.* reported the use of peroxidases to catalyze the crosslinking of functionalized polyaspartic acid-based hydrogels. This study is one of the first comparing the activity of several peroxidases and their efficiency to form hydrogel networks [21]. The use of this enzyme was further explored due to its high biocompatibility and potential to crosslink *in situ*. Recently, novel biomaterials have been developed taking advantage of this system for the crosslinking of tyramine conjugated polymers. Darr *et al.* have characterized tyramine-based hyaluronan hydrogels that have shown *in vivo* biocompatibility and resistance to degradation after subcutaneous injection, while preserving most of the negative charge from the carboxyl groups in hyaluronic acid, essential for the contribution of the physio-mechanical properties of tissue [87]. Other studies have reported the use of hyaluronic acid-tyramine conjugates crosslinked by horseradish peroxidase, highlighting excellent biocompatibility and biodegradability and it has been postulated that these materials possess, promising features for controlled drug delivery and for application as injectable *in situ* forming gels [88,89]. The success of crosslinking system using peroxidases was extended to the use of other polysaccharide-derived polymers such as chitosan [90,91], alginate [18], carboxymethylcellulose [16] and dextran [86]. Horseradish crosslinkable dextran-tyramine hydrogels (table 3.6) also in combination with hyaluronic acid and heparin have recently shown high potential as artificial extracellular matrixes for cartilage tissue engineering [13,14,15]. These polysaccharide hybrids were designed to mimic the molecular structure of the extracellular matrix of native cartilage. Similarly, injectable hyaluronic acid-tyramine has been described by Kim *et al.* as an effective drug carrier for the treatment of rheumatoid arthritis [92]. Other recent polymer combinations using horseradish peroxidase to induce gelation include tetronic-tyramine conjugates and supramolecular hydrogels based on tyramine-terminated PEG [83,93]. The major advantage of this enzyme in comparison to the above mentioned enzymes, such as transglutaminase, is the fast gelation that can occur within seconds.

3.2.7 Horseradish peroxidase mimetic enzymes

Even though natural enzymes are remarkably specific, in general, these biomolecules are expensive, unstable and prone to deactivation when in solution. Thus, artificial enzymes with similar selectivity and catalytic activity have been developed, with su-

Mechanism of the reaction [14]:



| Advantages | Drawbacks |
|--|--|
| <ul style="list-style-type: none"> • Peroxidases are involved in several processes in our body and are used in a wide range of biotechnological tools [81] • Both horseradish and soybean peroxidases are highly stable • Induce fast gelation, ranging from seconds to a few minutes [86] • No co-factors are necessary [21] • The gels formed are overall highly cytocompatible and are suitable for drug delivery [13,14,15] • High mechanical strength | <ul style="list-style-type: none"> • Despite the several <i>in vitro</i> applications of horseradish peroxidase, the <i>in vivo</i> role is not fully elucidated • No human peroxidase has been reported to induce <i>in situ</i> hydrogel formation |

Table 3.6: Mechanism of the enzymatic reaction mediated by peroxidases, advantages and drawbacks

| Advantages | Drawbacks |
|--|--|
| <ul style="list-style-type: none"> • Artificial enzymes with similar selectivity to the native form • Superior stability | <ul style="list-style-type: none"> • Not yet explored for biomedical applications |

Table 3.7: Advantages and drawbacks the enzymatic reaction mediated by horseradish peroxidase mimetic enzymes

3

perior stability compared to the natural enzymes [94,95,96,97]. Chen *et al.* have described a catalytic system, which is a water dispersible imprinted hydrogel based on a tetrapolymer of 4-vinylpyridine, hemin, acrylamide, and N-isopropylacrylamide. Hemin, also named chloro[3,7,12,17-tetramethyl-8,13-divinylporphyrin-2,18-dipropionate(2-)]-iron(III) or Fe(III)protoporphyrin(IX) chloride, are co-functional monomers that act as the catalytic centers. This tetrapolymer was crosslinked by ethylene glycol dimethacrylate with homovanillic acid as template molecule, designed as an enzyme mimic of horseradish peroxidase [94]. Wang *et al.* have previously reported a supramolecular hydrogel with encapsulated hemin as an artificial enzyme to mimic peroxidases, reaching approximately 90 percent of the activity of horseradish peroxidase. This artificial enzyme allowed catalysis with operational stability and reusability [96,97]. Additionally, poly(NIPAAm/MBA/hemin) has been reported by Li *et al.* as a new substitute for peroxidase [95]. In addition to hemin, two other biocatalysts, microperoxidase-11 and cytochrome c, display peroxidase activity when activated by an electron receptor. These novel alternatives based on hemin, microperoxidases, or cytochrome c to mimic natural peroxidases have shown great promise for industrial purposes [98], although not yet explored for biomedical applications.

3.3 Conclusions and future perspectives

As outlined, enzyme-mediated systems are a relatively recent concept, pointing a new direction in hydrogel design. Despite the major advances and advantages of using biocatalysts, there are still challenges to be overcome. These relate mainly to the slender amount of studies *in vivo*, instability of some of the enzyme types, such as transglutaminases and tyrosinases, and limited mechanical properties of the gels formed. The reduced *in vivo* applications are essentially due to the novelty of these systems. Additionally, the stability and availability of enzymes can be enhanced by the development of more recombinant enzyme types. Lastly, the poor or limited mechanical properties of some hydrogels can, in principle, be improved by combining enzyme types, after adjusting the material design. Predominantly, transglutaminases and horseradish peroxidases can be highlighted as the best studied enzyme systems involved in hy-

| Gel type/composition | Enzyme type | Potential applications | Reference |
|--|--|---|----------------|
| Modular protein hydrogel of lysine and glutamine | - Animal derived tissue transglutaminase - Recombinant human transglutaminase | Non-specific TE applications | [12] |
| Fibrin gel | Factor XIIIa (transglutaminase isoenzyme) | Angiogenesis Neurite extension Bone and cartilage tissue repair | [41,42,43,44] |
| 8-arm PEG-peptide conjugates | Factor XIIIa (transglutaminase isoenzyme) | Drug delivery systems Smart implants for <i>in situ</i> TE | [36,45] |
| Multi-arm comb PEG | Tissue transglutaminase | Gelation model | [47] |
| Elastin-like polypeptide gels | Tissue transglutaminase | Cartilage tissue repair | [51] |
| PEG-peptide conjugates | Tissue transglutaminase | Surgical tissue adhesives Cartilage tissue repair | [49,52] |
| Gelatin | Microbial transglutaminase | Scaffolds for TE Sustained drug release devices | [20,50,99,100] |
| Gelatin | Calcium-independent microbial transglutaminase | Microfluidic biosensor systems | [53] |
| Casein | Microbial transglutaminase | Sustained drug release | [101] |
| Gelatin-chitosan conjugates | Tyrosinase | Tissue glue Wound dressings | [56,59] |
| Silk fibroin/chitosan conjugates | Tyrosinase | Scaffolds for TE | [57] |
| Gelatin-chitosan conjugates | - Tyrosinase - Microbial transglutaminase | Film biofabrication Scaffolds for TE | [54,58] |
| Coil-chitosan bioconjugate | Tyrosinase | Protein immobilization | [60] |
| Coenzyme A-functionalized PEG | Phosphopantetheinyl transferase (surfactin synthetase) | Cell biology and TE | [38] |
| Nanofibrous lysine-rich peptide hydrogel | Lysyl oxidase Plasma amine oxidase | No application described | [65] |
| Supramolecular tyrosine-based hydrogel | Alkaline phosphatase | Assay platform for enzyme inhibitors | [75] |
| Supramolecular tyrosine-phosphate-based hydrogel | Alkaline phosphatase | Scaffolds to assist biomineralization | [76] |
| Fmoc-(Phe) ₃ hydrogel | Thermolysin | Nanofibrous scaffolds for cell culture | [77] |

Table 3.8: Enzyme-catalyzed crosslinkable hydrogels and potential applications

| | | | |
|---|------------------------|---|---------------|
| Pentapeptidic hydrogelator (Nap-FFGEY) | Kinase/phosphatase | Non-specific TE applications | [73] |
| Functionalized polyaspartic acid | Peroxidases | Drug delivery, wound healing and TE | [21] |
| Chitosan derivative | Horseradish peroxidase | Drug delivery and TE | [90] |
| Chitosan-glycolic acid conjugates modified with phloretic acid | Horseradish peroxidase | Cartilage tissue repair | [91] |
| Hyaluronic acid-tyramine | Horseradish peroxidase | Protein delivery Non-specific TE applications Cartilage tissue repair | [87,88,89,92] |
| Alginate-phenol tyramine conjugates | Horseradish peroxidase | Multicellular spheroids for TE | [18] |
| Carboxymethylcellulose | Horseradish peroxidase | Biomedical applications | [16] |
| Dextran-tyramine conjugates | Horseradish peroxidase | Protein delivery and TE Cartilage tissue repair | [14,86] |
| Dextran-hyaluronic acid conjugates | Horseradish peroxidase | Cartilage tissue repair | [15] |
| Dextran-heparin | Horseradish peroxidase | Cartilage tissue repair | [13] |
| Tetronic-tyramine conjugates (propylene oxide and ethylene oxide) | Horseradish peroxidase | Drug delivery and TE | [93] |
| Tyramine-terminated PEG | Horseradish peroxidase | Drug delivery and TE | [83] |

Table 3.9: (Continuation of table 3.8) Enzyme-catalyzed crosslinkable hydrogels and potential applications

drogel crosslinking for tissue engineering approaches. Transglutaminases are highly interesting since they offer intimate integration between the *in situ* formed gel and the native host tissue. The gels formed act as biological glues, due to the ubiquitous bodily distribution and equal supply of natural substrates [48]. Additionally, these enzymes have proven to successfully catalyze the crosslinking reaction of very different types of materials, such as PEG, elastin and gelatin. Horseradish peroxidases are equally attractive due to their high stability, easy purification and availability mainly directly from the horseradish but also of recombinant forms [102]. Engineered peroxidases with even higher stability and catalytic efficiency are currently being developed, which is indicative that, in the near future, further applications using this enzyme type will be developed and continue to prosper in the tissue engineering field.

Overall, enzyme catalysis allows exceptional control over hydrogel formation, providing a step forward regarding higher complexity, biocompatibility and non-invasiveness, vitally desired for the next generation of biomaterials for tissue engineering and regenerative medicine.

References

1. Elisseeff J (2008) Hydrogels: structure starts to gel. *Nat Mater* 7: 271-273.
2. Nguyen MK, Lee DS (2010) Injectable biodegradable hydrogels. *Macromol Biosci* 10: 563-579.
3. Davis HE, Leach JK (2011) Designing bioactive delivery systems for tissue regeneration. *Ann Biomed Eng* 39: 1-13.
4. Elisseeff J, Puleo C, Yang F, Sharma B (2005) Advances in skeletal tissue engineering with hydrogels. *Orthod Craniofac Res* 8: 150-161.
5. Zhang H, Wang G, Yang H (2011) Drug delivery systems for differential release in combination therapy. *Expert Opin Drug Deliv* 8: 171-190.
6. Lutolf MP (2009) Biomaterials: Spotlight on hydrogels. *Nat Mater* 8: 451-453.
7. Hennink WE, van Nostrum CF (2002) Novel crosslinking methods to design hydrogels. *Adv Drug Deliv Rev* 54: 13-36.
8. Kopecek J, Yang J (2009) Peptide-directed self-assembly of hydrogels. *Acta Biomater* 5: 805-816.
9. Zhao X, Huebsch N, Mooney DJ, Suo Z (2010) Stress-relaxation behavior in gels with ionic and covalent crosslinks. *J Appl Phys* 107: 63509.
10. Gupta S, Pramanik AK, Kailath A, Mishra T, Guha A, *et al.* (2009) Composition dependent structural modulations in transparent poly(vinyl alcohol) hydrogels. *Colloids Surf B Biointerfaces* 74: 186-190.
11. Langer RS, Peppas NA (1981) Present and future applications of biomaterials in controlled drug delivery systems. *Biomaterials* 2: 201-214.
12. Davis NE, Ding S, Forster RE, Pinkas DM, Barron AE (2010) Modular enzymatically crosslinked protein polymer hydrogels for *in situ* gelation. *Biomaterials* 31: 7288-7297.
13. Jin R, Moreira Teixeira LS, Dijkstra PJ, van Blitterswijk CA, Karperien M, *et al.* (2011) Chondrogenesis in injectable enzymatically crosslinked heparin/dextran hydrogels. *J Control Release*.
14. Jin R, Moreira Teixeira LS, Dijkstra PJ, Zhong Z, van Blitterswijk CA, *et al.* (2010) Enzymatically crosslinked dextran-tyramine hydrogels as injectable scaffolds for cartilage tissue engineering. *Tissue Eng Part A* 16: 2429-2440.
15. Jin R, Teixeira LS, Dijkstra PJ, van Blitterswijk CA, Karperien M, *et al.* (2010) Enzymatically-crosslinked injectable hydrogels based on biomimetic dextran-hyaluronic acid conjugates for cartilage tissue engineering. *Biomaterials* 31: 3103-3113.
16. Ogushi Y, Sakai S, Kawakami K (2007) Synthesis of enzymatically-gellable carboxymethylcellulose for biomedical applications. *J Biosci Bioeng* 104: 30-33.
17. Sakai S, Hirose K, Taguchi K, Ogushi Y, Kawakami K (2009) An injectable, *in situ* enzymatically gellable, gelatin derivative for drug delivery and tissue engineering. *Biomaterials* 30: 3371-3377.
18. Sakai S, Ito S, Ogushi Y, Hashimoto I, Hosoda N, *et al.* (2009) Enzymatically fabricated and degradable microcapsules for production of multicellular spheroids with well-defined diameters of less than 150 microm. *Biomaterials* 30: 5937-5942.
19. Sakai S, Ogushi Y, Kawakami K (2009) Enzymatically crosslinked carboxymethyl-

cellulose-tyramine conjugate hydrogel: cellular adhesiveness and feasibility for cell sheet technology. *Acta Biomater* 5: 554-559.

20. Yung CW, Bentley WE, Barbari TA (2010) Diffusion of interleukin-2 from cells overlaid with cytocompatible enzyme-crosslinked gelatin hydrogels. *J Biomed Mater Res A* 95: 25-32.

21. Sofia SJ, Singh A, Kaplan DL (2002) Peroxidase-catalyzed crosslinking of functionalized polyaspartic acid polymers. *Journal of Macromolecular Science-Pure and Applied Chemistry A39*: 1151-1181.

22. Hubbell JA (2003) Materials as morphogenetic guides in tissue engineering. *Curr Opin Biotechnol* 14: 551-558.

23. Getgood A, Brooks R, Fortier L, Rushton N (2009) Articular cartilage tissue engineering: today's research, tomorrow's practice? *J Bone Joint Surg Br* 91: 565-576.

24. Elisseeff J (2004) Injectable cartilage tissue engineering. *Expert Opinion on Biological Therapy* 4: 1849-1859.

25. Kretlow JD, Klouda L, Mikos AG (2007) Injectable matrices and scaffolds for drug delivery in tissue engineering. *Adv Drug Deliv Rev* 59: 263-273.

26. Gutowska A, Jeong B, Jasionowski M (2001) Injectable gels for tissue engineering. *Anat Rec* 263: 342-349.

27. Lin Z, Willers C, Xu J, Zheng MH (2006) The chondrocyte: biology and clinical application. *Tissue Eng* 12: 1971-1984.

28. Spiller KL, Maher SA, Lowman AM (2011) Hydrogels for the Repair of Articular Cartilage Defects. *Tissue Eng Part B Rev*.

29. Pisano JJ, Finlayson JS, Peyton MP (1968) [Cross-link in fibrin polymerized by factor 13: epsilon-(gamma-glutamyl)lysine]. *Science* 160: 892-893.

30. Kim SY, Grant P, Lee JH, Pant HC, Steinert PM (1999) Differential expression of multiple transglutaminases in human brain. Increased expression and cross-linking by transglutaminases 1 and 2 in Alzheimer's disease. *J Biol Chem* 274: 30715-30721.

31. Priglinger SG, Alge CS, Kook D, Thiel M, Schumann R, *et al.* (2006) Potential role of tissue transglutaminase in glaucoma filtering surgery. *Invest Ophthalmol Vis Sci* 47: 3835-3845.

32. Priglinger SG, Alge CS, Kreutzer TC, Neubauer AS, Haritoglou C, *et al.* (2006) Keratinocyte transglutaminase in proliferative vitreoretinopathy. *Invest Ophthalmol Vis Sci* 47: 4990-4997.

33. Griffin M, Casadio R, Bergamini CM (2002) Transglutaminases: nature's biological glues. *Biochem J* 368: 377-396.

34. Greenberg CS, Birckbichler PJ, Rice RH (1991) Transglutaminases: multifunctional cross-linking enzymes that stabilize tissues. *FASEB J* 5: 3071-3077.

35. Burgoyne RD, Weiss JL (2001) The neuronal calcium sensor family of Ca²⁺-binding proteins. *Biochem J* 353: 1-12.

36. Ehrbar M, Rizzi SC, Schoenmakers RG, Miguel BS, Hubbell JA, *et al.* (2007) Biomolecular hydrogels formed and degraded via site-specific enzymatic reactions. *Biomacromolecules* 8: 3000-3007.

37. Verderio E, Nicholas B, Gross S, Griffin M (1998) Regulated expression of tissue transglutaminase in Swiss 3T3 fibroblasts: effects on the processing of fibronectin, cell attachment, and cell death. *Exp Cell Res* 239: 119-138.

38. Mosiewicz KA, Johnsson K, Lutolf MP (2010) Phosphopantetheinyl transferase-catalyzed formation of bioactive hydrogels for tissue engineering. *J Am Chem Soc* 132: 5972-5974.
39. Plenz A, Fritz P, Konig G, Laschner W, Saal JG (1996) Immunohistochemical detection of factor XIIIa and factor XIIs in synovial membranes of patients with rheumatoid arthritis or osteoarthritis. *Rheumatol Int* 16: 29-36.
40. Aeschlimann D, Mosher D, Paulsson M (1996) Tissue transglutaminase and factor XIII in cartilage and bone remodeling. *Semin Thromb Hemost* 22: 437-443.
41. Eyrich D, Brandl F, Appel B, Wiese H, Maier G, *et al.* (2007) Long-term stable fibrin gels for cartilage engineering. *Biomaterials* 28: 55-65.
42. Hall H, Baechi T, Hubbell JA (2001) Molecular properties of fibrin-based matrices for promotion of angiogenesis *in vitro*. *Microvasc Res* 62: 315-326.
43. Peretti GM, Xu JW, Bonassar LJ, Kirchhoff CH, Yaremchuk MJ, *et al.* (2006) Review of injectable cartilage engineering using fibrin gel in mice and swine models. *Tissue Eng* 12: 1151-1168.
44. Schense JC, Bloch J, Aebischer P, Hubbell JA (2000) Enzymatic incorporation of bioactive peptides into fibrin matrices enhances neurite extension. *Nat Biotechnol* 18: 415-419.
45. Sala A, Ehrbar M, Trentin D, Schoenmakers RG, Voros J, *et al.* (2010) Enzyme mediated site-specific surface modification. *Langmuir* 26: 11127-11134.
46. Jurgensen K, Aeschlimann D, Cavin V, Genge M, Hunziker EB (1997) A new biological glue for cartilage-cartilage interfaces: Tissue transglutaminase. *Journal of Bone and Joint Surgery-American Volume* 79A: 185-193.
47. Sperinde JJ, Griffith LG (2000) Control and prediction of gelation kinetics in enzymatically cross-linked poly(ethylene glycol) hydrogels. *Macromolecules* 33: 5476-5480.
48. Sperinde JJ, Griffith LG (1997) Synthesis and characterization of enzymatically-cross-linked poly(ethylene glycol) hydrogels. *Macromolecules* 30: 5255-5264.
49. Hu BH, Messersmith PB (2005) Enzymatically cross-linked hydrogels and their adhesive strength to biosurfaces. *Orthod Craniofac Res* 8: 145-149.
50. Yung CW, Wu LQ, Tullman JA, Payne GF, Bentley WE, *et al.* (2007) Transglutaminase crosslinked gelatin as a tissue engineering scaffold. *J Biomed Mater Res A* 83: 1039-1046.
51. McHale MK, Setton LA, Chilkoti A (2005) Synthesis and *In vitro* evaluation of enzymatically cross-linked elastin-like polypeptide gels for cartilaginous tissue repair. *Tissue Eng* 11: 1768-1779.
52. Jones ME, Messersmith PB (2007) Facile coupling of synthetic peptides and peptide-polymer conjugates to cartilage via transglutaminase enzyme. *Biomaterials* 28: 5215-5224.
53. Chen T, Small DA, McDermott MK, Bentley WE, Payne GF (2003) Enzymatic methods for *in situ* cell entrapment and cell release. *Biomacromolecules* 4: 1558-1563.
54. Wu LQ, Bentley WE, Payne GF (2011) Biofabrication with biopolymers and enzymes: potential for constructing scaffolds from soft matter. *Int J Artif Organs* 34: 215-224.
55. Yamamoto H, Kuno S, Nagai A, Nishida A, Yamauchi S, *et al.* (1990) Insol-

ubilizing and adhesive studies of water-soluble synthetic model proteins. *Int J Biol Macromol* 12: 305-310.

56. Chen T, Embree HD, Brown EM, Taylor MM, Payne GF (2003) Enzyme-catalyzed gel formation of gelatin and chitosan: potential for *in situ* applications. *Biomaterials* 24: 2831-2841.

57. Kang GD, Lee KH, Ki CS, Nahm JH, Park YH (2004) Silk fibroin/chitosan conjugate crosslinked by tyrosinase. *Macromolecular Research* 12: 534-539.

58. Chen T, Embree HD, Wu LQ, Payne GF (2002) *in vitro* protein-polysaccharide conjugation: tyrosinase-catalyzed conjugation of gelatin and chitosan. *Biopolymers* 64: 292-302.

59. Yamada K, Chen T, Kumar G, Vesnovsky O, Topoleski LD, *et al.* (2000) Chitosan based water-resistant adhesive. Analogy to mussel glue. *Biomacromolecules* 1: 252-258.

60. Demolliens A, Boucher C, Durocher Y, Jolicoeur M, Buschmann MD, *et al.* (2008) Tyrosinase-catalyzed synthesis of a universal coil-chitosan bioconjugate for protein immobilization. *Bioconjug Chem* 19: 1849-1854.

61. Anghileri A, Lantto R, Kruus K, Arosio C, Freddi G (2007) Tyrosinase-catalyzed grafting of sericin peptides onto chitosan and production of protein-polysaccharide bioconjugates. *J Biotechnol* 127: 508-519.

62. Freddi G, Anghileri A, Sampaio S, Buchert J, Monti P, *et al.* (2006) Tyrosinase-catalyzed modification of Bombyx mori silk fibroin: grafting of chitosan under heterogeneous reaction conditions. *J Biotechnol* 125: 281-294.

63. Joshi AK, Zhang L, Rangan VS, Smith S (2003) Cloning, expression, and characterization of a human 4'-phosphopantetheinyl transferase with broad substrate specificity. *J Biol Chem* 278: 33142-33149.

64. D'Souza SE, Ginsberg MH, Plow EF (1991) Arginyl-glycyl-aspartic acid (RGD): a cell adhesion motif. *Trends Biochem Sci* 16: 246-250.

65. Bakota EL, Aulisa L, Galler KM, Hartgerink JD (2011) Enzymatic cross-linking of a nanofibrous peptide hydrogel. *Biomacromolecules* 12: 82-87.

66. Kagan HM, Li W (2003) Lysyl oxidase: properties, specificity, and biological roles inside and outside of the cell. *J Cell Biochem* 88: 660-672.

67. Kothapalli CR, Ramamurthi A (2009) Lysyl oxidase enhances elastin synthesis and matrix formation by vascular smooth muscle cells. *J Tissue Eng Regen Med* 3: 655-661.

68. Lau YK, Gobin AM, West JL (2006) Overexpression of lysyl oxidase to increase matrix crosslinking and improve tissue strength in dermal wound healing. *Ann Biomed Eng* 34: 1239-1246.

69. Hwang JJ, Stupp SI (2000) Poly(amino acid) bioadhesives for tissue repair. *J Biomater Sci Polym Ed* 11: 1023-1038.

70. Grieshaber SE, Nie T, Yan C, Zhong S, Teller SS, *et al.* (2011) Assembly Properties of an Alanine-Rich, Lysine-Containing Peptide and the Formation of Peptide/Polymer Hybrid Hydrogels. *Macromol Chem Phys* 212: 229-239.

71. Gao Y, Kuang Y, Guo ZF, Guo Z, Krauss IJ, *et al.* (2009) Enzyme-instructed molecular self-assembly confers nanofibers and a supramolecular hydrogel of taxol derivative. *J Am Chem Soc* 131: 13576-13577.

72. Yang Z, Liang G, Xu B (2008) Enzymatic hydrogelation of small molecules. *Acc Chem Res* 41: 315-326.
73. Yang Z, Liang G, Wang L, Xu B (2006) Using a kinase/phosphatase switch to regulate a supramolecular hydrogel and forming the supramolecular hydrogel *in vivo*. *J Am Chem Soc* 128: 3038-3043.
74. Williams RJ, Mart RJ, Ulijn RV (2010) Exploiting Biocatalysis in Peptide Self-Assembly. *Biopolymers* 94: 107-117.
75. Yang ZM, Gu HW, Fu DG, Gao P, Lam JK, *et al.* (2004) Enzymatic formation of supramolecular hydrogels. *Advanced Materials* 16: 1440-+.
76. Schnepf ZAC, Gonzalez-McQuire R, Mann S (2006) Hybrid biocomposites based on calcium phosphate mineralization of self-assembled supramolecular hydrogels. *Advanced Materials* 18: 1869-+.
77. Toledano S, Williams RJ, Jayawarna V, Ulijn RV (2006) Enzyme-triggered self-assembly of peptide hydrogels via reversed hydrolysis. *J Am Chem Soc* 128: 1070-1071.
78. Yang Z, Ho PL, Liang G, Chow KH, Wang Q, *et al.* (2007) Using β -lactamase to trigger supramolecular hydrogelation. *J Am Chem Soc* 129: 266-267.
79. Yang Z, Liang G, Guo Z, Xu B (2007) Intracellular hydrogelation of small molecules inhibits bacterial growth. *Angew Chem Int Ed Engl* 46: 8216-8219.
80. Williams RJ, Smith AM, Collins R, Hodson N, Das AK, *et al.* (2009) Enzyme-assisted self-assembly under thermodynamic control. *Nat Nanotechnol* 4: 19-24.
81. Ryan BJ, Carolan N, O'Fagain C (2006) Horseradish and soybean peroxidases: comparable tools for alternative niches? *Trends Biotechnol* 24: 355-363.
82. Kobayashi S, Uyama H, Kimura S (2001) Enzymatic polymerization. *Chem Rev* 101: 3793-3818.
83. Tran NQ, Joung YK, Lih E, Park KM, Park KD (2010) Supramolecular hydrogels exhibiting fast *in situ* gel forming and adjustable degradation properties. *Biomacromolecules* 11: 617-625.
84. Obinger C (2006) Chemistry and biology of human peroxidases. *Arch Biochem Biophys* 445: 197-198.
85. O'Brien PJ (2000) Peroxidases. *Chem Biol Interact* 129: 113-139.
86. Jin R, Hiemstra C, Zhong Z, Feijen J (2007) Enzyme-mediated fast *in situ* formation of hydrogels from dextran-tyramine conjugates. *Biomaterials* 28: 2791-2800.
87. Darr A, Calabro A (2009) Synthesis and characterization of tyramine-based hyaluronan hydrogels. *J Mater Sci Mater Med* 20: 33-44.
88. Kurisawa M, Chung JE, Yang YY, Gao SJ, Uyama H (2005) Injectable biodegradable hydrogels composed of hyaluronic acid-tyramine conjugates for drug delivery and tissue engineering. *Chem Commun (Camb)*: 4312-4314.
89. Lee F, Chung JE, Kurisawa M (2009) An injectable hyaluronic acid-tyramine hydrogel system for protein delivery. *Journal of Controlled Release* 134: 186-193.
90. Sakai S, Yamada Y, Zenke T, Kawakami K (2009) Novel chitosan derivative soluble at neutral pH and *in situ* gellable via peroxidase-catalyzed enzymatic reaction. *Journal of Materials Chemistry* 19: 230-235.
91. Jin R, Moreira Teixeira LS, Dijkstra PJ, Karperien M, van Blitterswijk CA, *et al.* (2009) Injectable chitosan-based hydrogels for cartilage tissue engineering. *Bio-*

materials 30: 2544-2551.

92. Kim KS, Park SJ, Yang JA, Jeon JH, Bhang SH, *et al.* (2011) Injectable hyaluronic acid-tyramine hydrogels for the treatment of rheumatoid arthritis. *Acta Biomater* 7: 666-674.

93. Park KM, Shin YM, Joung YK, Shin H, Park KD (2010) *in situ* forming hydrogels based on tyramine conjugated 4-Arm-PPO-PEO via enzymatic oxidative reaction. *Biomacromolecules* 11: 706-712.

94. Chen ZY, Xu L, Liang Y, Zhao MP (2010) pH-Sensitive Water-Soluble Nanospheric Imprinted Hydrogels Prepared as Horseradish Peroxidase Mimetic Enzymes. *Advanced Materials* 22: 1488-+.

95. Li YZ, He N, Wang XQ, Chang WB, Ci YX (1998) Mimicry of peroxidase by immobilization of hemin on N-isopropylacrylamide-based hydrogel. *Analyst* 123: 359-364.

96. Wang Q, Yang Z, Ma M, Chang CK, Xu B (2008) High catalytic activities of artificial peroxidases based on supramolecular hydrogels that contain heme models. *Chemistry* 14: 5073-5078.

97. Wang Q, Yang Z, Zhang X, Xiao X, Chang CK, *et al.* (2007) A supramolecular-hydrogel-encapsulated hemin as an artificial enzyme to mimic peroxidase. *Angew Chem Int Ed Engl* 46: 4285-4289.

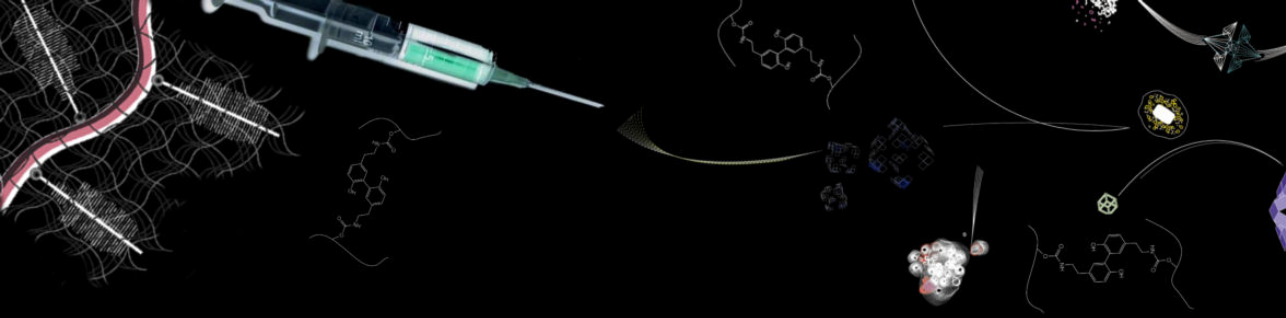
98. Laszlo JA, Compton DL (2002) Comparison of peroxidase activities of hemin, cytochrome c and microperoxidase-11 in molecular solvents and imidazolium-based ionic liquids. *Journal of Molecular Catalysis B-Enzymatic* 18: 109-120.

99. Broderick EP, O'Halloran DM, Rochev YA, Griffin M, Collighan RJ, *et al.* (2005) Enzymatic stabilization of gelatin-based scaffolds. *J Biomed Mater Res B Appl Biomater* 72: 37-42.

100. Crescenzi V, Francescangeli A, Taglienti A (2002) New gelatin-based hydrogels via enzymatic networking. *Biomacromolecules* 3: 1384-1391.

101. Song F, Zhang LM, Shi JF, Li NN (2010) Novel casein hydrogels: formation, structure and controlled drug release. *Colloids Surf B Biointerfaces* 79: 142-148.

102. Veitch NC (2004) Horseradish peroxidase: a modern view of a classic enzyme. *Phytochemistry* 65: 249-259.



Chapter 4

Enzymatically Crosslinked Dextran-tyramine Hydrogels as Injectable Scaffolds for Cartilage Tissue Engineering

4

Liliana Moreira Teixeira*, Rong Jin*, Piet Dijkstra, Zhiyuan Zhong, Marcel Karperien, Clemens van Blitterswijk, Jan Feijen

* Shared first co-authorship

Abstract

Enzymatic crosslinking of dextran-tyramine (Dex-TA) conjugates in the presence of horseradish peroxidase and hydrogen peroxide was successively applied in the preparation of hydrogels. Depending on the molecular weight of the dextran (M_n , GPC of 14000 or 31000 g/mol) and the degree of substitution (DS of 5, 10 or 15) with tyramine (TA) groups, the gelation times ranged from 20 s to 1 min. Hydrogels prepared from Dex31k-TA with a DS of 10 had storage moduli up to 60 kPa. Similar values were found when chondrocytes were incorporated into the hydrogels. Chondrocyte-seeded Dex-TA hydrogels were prepared at a molar ratio of H_2O_2 /TA of 0.2 and cultured in a chondrocyte medium. A live-dead assay and a MTT assay revealed that almost all chondrocytes retained their viability after 2 weeks. SEM analysis showed that the encapsulated chondrocytes were capable of maintaining their round shape. Histology and immunofluorescent staining demonstrated the production of glycosaminoglycans (GAGs) and collagen type II after culturing for 14 and 21 days. Biochemical analysis

showed that GAG accumulation increased with time inside Dex-TA hydrogels. Besides, GAG/DNA for Dex-TA hydrogels was higher than that for agarose at day 28. These results indicate that Dex-TA hydrogels are promising 3D scaffolds for cartilage tissue engineering applications.

4.1 Introduction

Injured cartilage tissue is known to have a limited capacity of self-healing due to its avascular nature. Tissue engineering holds great promise for the regeneration of damaged cartilage. In this approach mature or progenitor cells are incorporated in a tissue-engineered scaffold that can be placed at the cartilage defect site. An ideal scaffold for cartilage regeneration is expected to have a controlled degradability, provides an adequate mechanical strength, promotes cell survival and differentiation, and allows nutrient diffusion, adhesion and integration with the surrounding native cartilage [1].

Hydrogels are biocompatible hydrated, elastic three-dimensional networks that mimic the micro-environment for cells in soft tissues. Over the past decades, a number of hydrogels as scaffolds for cartilage tissue engineering have been developed [1-4]. Among these materials, injectable hydrogels, which can be placed locally as a viscous solution and gel *in situ*, have received much attention [5, 6]. They can be applied using a minimally invasive procedure and can readily fill in cartilage defects of various sizes and shapes. Moreover, cultured cells can be homogeneously distributed in the hydrogels by suspending cells in the precursor solutions prior to injection and gelation.

In the development of injectable hydrogels for cartilage regeneration, several approaches have been employed using natural or synthetic polymers such as chitosan [7, 8], hyaluronic acid [9-11] and poly(ethylene glycol)-based copolymers [12-14]. Radical polymerization using redox- or photo-initiators is one of the most commonly used methods to prepare chemically crosslinked injectable hydrogels [10, 15-17]. Burdick et al. reported on photopolymerized hyaluronic acid-based hydrogels. The mechanical properties of the hydrogels could be adjusted by varying the hyaluronic acid concentration and molecular weight. An increase in the network cross-linking density resulted in higher compressive moduli. However, this compromised the cell viability due to a limited exchange of nutrients and waste products to the surrounding culture media [15]. Hong et al. prepared methacrylated chitosan hydrogels using a redox initiator at low concentrations. A significant decrease in the DNA content of encapsulated chondrocytes after *in vitro* culturing for 6 days was observed because of cell loss or cell death [17].

Alternatively, injectable hydrogels can be prepared under mild conditions via Michael-type addition reactions [18-20]. Hubbell et al. reported on biodegradable PEG-peptide injectable hydrogels via Michael-type addition for cartilage repair [20]. The reaction between thiols and vinyl sulfone groups had no adverse effect on the chondrocytes in the gels, and culturing periods over one month showed that <90% cells were still viable. However, gelation times to form stable gels from these materials appeared rather long (ca. 20 min) [21]. Recently, a new approach which makes

use of enzymatic crosslinking was introduced to prepare injectable hydrogels [22-28]. We previously reported on the enzyme-mediated in-situ formation of hydrogels from dextran-tyramine conjugates (Dex-TA) [25]. In this approach, horseradish peroxidase (HRP) in combination with hydrogen peroxide (H_2O_2) was used to induce crosslinking of the tyramine (TA) units conjugated to the dextran. By varying the ratios of HRP/TA, H_2O_2 /TA and the degree of substitution (DS) of tyramine groups to the dextran, the gelation times, mechanical properties (e.g. storage and loss moduli) and degradation properties of the hydrogels can be tuned.

In this study, the potential application of the injectable Dex-TA hydrogels for cartilage tissue engineering was evaluated. Therefore, Dex-TA hydrogels with different molecular weights (Mn) and conjugated with different numbers of tyramine groups were prepared. Physical properties like gelation times, storage moduli, glucose diffusion and morphology of the hydrogels were studied. The viability and metabolic activity of in-situ incorporated chondrocytes in these Dex-TA hydrogels were determined using live-dead and MTT assays. The morphology of the chondrocytes and the formation of a cartilaginous specific matrix (glycosaminoglycan and collagen type II) in the cell/gel constructs in time were also examined.

4.2 Materials and methods

4.2.1 Materials

Dextrans (Mn, GPC=1.4104 g/mol, Mw/Mn=1.45, denoted as Dex14k, and Mn, GPC=3.1104 g/mol, Mw/Mn=1.38, denoted as Dex31k) were purchased from Fluka. Dextran-tyramine conjugates (denoted as Dex-TA) were prepared as reported previously [25]. Hydrogen peroxide (H_2O_2), dextranase (10-25 units/mg solid) and deuterium oxide (D_2O) were obtained from Aldrich-Sigma. Horseradish peroxidase (HRP, type VI, ~300 purpurogallin unit/mg solid) was purchased from Aldrich and used without further purification. Phosphate buffered saline (PBS, pH 7.4, without calcium or magnesium) was purchased from Invitrogen. Bovine chondrocytes were isolated as previously reported and cultured in a chondrocyte expansion medium composed of DMEM high glucose (Invitrogen), 10 mM HEPES (Invitrogen), 10 % of fetal bovine serum (FBS, Cambrex), 100 U/mL penicillin (Invitrogen), 100 μ g/mL streptomycin (Invitrogen), 0.2 mM ascorbic acid (ASAP, Sigma), 0.1 mM non-essential amino acids (NEAA, Sigma) and 0.4 mM proline (Sigma) [26].

4.2.2 Hydrogel formation and characterization

Hydrogel samples (~0.5 mL) were prepared in vials by the addition of a mixture of H_2O_2 and HRP in PBS to stock solutions of Dex-TA. In a typical example, to a PBS solution of Dex14k-TA DS15 (400 μ L, 12.5 wt %), a freshly prepared solution of H_2O_2 (61.5 μ L of 0.4 wt % stock solution) and HRP (40.5 μ L of 0.25 mg/mL stock solution) in PBS were added. The contents were gently mixed. The final concentration of Dex-TA was 10 wt %. The amount of HRP used was fixed at 0.25 mg per mmol of tyramine moieties. Molar ratios of H_2O_2 /TA ranging from 0.1 to 0.5 were applied in

the preparation of the hydrogels. The time to form a gel (denoted as gelation time) was determined using the vial tilting method. No flow within 1 min upon inverting the vial was regarded as the gel state. Semi-spherical hydrogel samples of 4 mm in diameter and 2 mm in height were prepared for microstructural characterization. Freeze-dried hydrogels were prepared by first freezing the gels at -20 degrees Celsius for 4 hours and then in liquid nitrogen, followed by freeze-drying. The constructs were analyzed with a Philips XL 30 ESEM-FEG scanning electron microscopy (SEM) operating at a voltage of 10kV. Samples were gold sputtered (Carrington) before SEM analysis.

4.2.3 Nutrient transport

The diffusion of glucose in Dex-TA hydrogels was measured. The diffusion setup is similar as described in literature and is made of two Perspex chambers of 70 mL each, divided by a Perspex plate, and held together with screws [29]. One chamber (A) contained the glucose solution (initial concentration: 10 g/L in H₂O), whereas the other (B) contained distilled water. The Dex-TA hydrogel (average thickness ~0.5 mm, which was measured by a micrometer (Mitutoyo Corp.)) was placed in a circular opening in the Perspex plate (diameter 17 mm) and subsequently immersed in PBS at 37 degrees Celsius to allow swelling. The PBS was changed every day to remove uncrosslinked/unreacted residues. After 3 days, the Perspex plate with the gel was removed from the PBS solution, and the gel was supported by a round mesh (Flow-Mesh gel and membrane support, Sigma), and placed between the A and B chambers. Both chambers were double-walled and kept at 37 degrees Celsius with circulating water. The glucose concentrations in chambers A and B were determined using an enzymatic assay (PGO Enzymes, Sigma) and analyzed at $\lambda = 450$ nm using a UV spectrophotometer (Varian Cary 300 scan) [30]. The glucose diffusion was determined by measuring the glucose concentration after 72 h. The percentage of glucose diffused after 72 h was expressed as the glucose concentration in chamber B divided by the equilibrium concentration of 5g/L times 100 %.

4.2.4 Rheological analysis

Rheological experiments were carried out with a MCR 301 rheometer (Anton Paar) using a parallel plate (25 mm diameter, 0 degrees) configuration and at 37 degrees Celsius in the oscillatory mode. In a typical experiment, 123 μ L of a H₂O₂ stock solution (0.4 wt %, in PBS) and 81 μ L of a HRP stock solution (0.25 mg/mL, in PBS) were mixed. The HRP/H₂O₂ solution was then immediately mixed with 800 μ L of a solution of Dex14k-TA DS 15 (12.5 wt % in PBS) using a double syringe (2.5 mL, 1:4 volume ratio) equipped with a mixing chamber (Mixpac). After the sample was applied to the rheometer, the upper plate was immediately lowered to a measuring gap size of 0.5 mm, and the measurement was started. To prevent evaporation of water, a layer of oil was introduced around the polymer sample. Similar experiments were performed with chondrocytes (cell density 5×10^6 /mL) in the polymer solution using the same procedure as described above. The evolution of the storage (G') and

loss (G'') moduli were recorded as a function of time. A frequency of 0.5 Hz and a strain of 0.1 % were applied in order to maintain the linear viscoelastic regime.

4.2.5 *In situ* chondrocyte incorporation

Hydrogels containing bovine chondrocytes were prepared under sterile conditions by mixing a Dex-TA/cell suspension with a freshly prepared mixture of HRP and H_2O_2 . Solutions of Dex-TA were made using medium and HRP and H_2O_2 stock solutions were made using PBS. All solutions were sterilized by filtration through filters with a pore size of 0.22 μm . Chondrocytes were incorporated in hydrogels prepared analogously as without cells. As an example: Chondrocyte/polymer suspensions were prepared by mixing 200 μL of a Dex14k-TA DS 15 solution (25 wt %) with 200 μL of medium containing chondrocytes. To 100 μL of the resulting cell/polymer suspension, 25 μL of a HRP/ H_2O_2 mixture was added and the suspension was gently mixed. The HRP/ H_2O_2 mixture was prepared by adding 61.5 μL of the HRP stock solution to 40.5 μL of the H_2O_2 stock solution. Before gelation, the precursor was quickly transferred to a culture plate. The final polymer concentration was 10 wt % and the cell seeding density in the gels was $510^6/mL$. For cytotoxicity and morphology studies, the cell/gel constructs were cultured in a chondrocyte expansion medium. For matrix production studies, the constructs were cultured in a chondrocyte differentiation medium composed of DMEM high glucose with 0.1 μM dexamethasone (Sigma), 100 $\mu g/mL$ sodium pyruvate (Sigma), 0.2 mM ascorbic acid, 50 mg/mL insulin-transferrin-selenite (ITS+Premix, BD biosciences), 100 U/ml penicillin, 100 $\mu g/mL$ streptomycin and 10 ng/mL transforming growth factor $\beta 3$ (TGF- $\beta 3$, RD system). In all experiments, samples were incubated at 37 degrees Celsius and 5 % of CO_2 , and the medium was replaced every 2 or 3 days.

4.2.6 Cytotoxicity assay

A viability study on Dex-TA hydrogels encapsulated chondrocytes (Passage 3-4) was performed with a live-dead assay and an MTT (3-(4,5-dimethyl-2-thiazolyl)-2,5-diphenyl-2H-tetrazolium bromide) assay. For the Live/Dead assay, at days 7 and 14, the hydrogel constructs were rinsed with PBS and stained with calcein AM/ethidium homodimer using the Live/Dead assay Kit (Invitrogen), according to the manufactures instructions [31]. Agarose hydrogels (0.5 wt %) with a similar chondrocyte density were used as a control. Hydrogel/cell constructs were visualized using fluorescence microscopy (Zeiss). As a result living cells fluoresce green and the nuclei of dead cells red. An MTT staining was performed using 1 % (total medium volume) of a MTT solution (5 mg/mL, Gibco) and an incubation time of 2 h. Hydrogel/cell constructs were then visualized using a light microscope.

To quantitatively measure the metabolic activity of chondrocytes encapsulated in the hydrogels, samples were first washed with PBS and 10 % (total medium volume, without phenol red) MTT solutions were added to the hydrogels. The constructs were incubated at 37 degrees Celsius. After 4 h, MTT solutions were removed and 500 μL of dextranase solution (100 U/mL in PBS) was added to each gel to disrupt

the gels. After centrifugation and removal of the solutions, the formazan formed by cells presenting mitochondrial metabolic activity was thoroughly extracted from the gel pieces by addition of DMSO under vortexing. The extracts were centrifuged and the supernatants were transferred to a 96-well plate. The absorbance at 540 nm was recorded using a microplate reader (Bio-TEK Instruments). Values were corrected for background staining of hydrogels without chondrocytes. The experiments were performed in triplicate. The percentage of metabolic activity (percentage of chondrocytes was calculated relative to values determined for cells cultured in agarose gels (control) at day 1 (considered as a starting value for metabolic activity).

4.2.7 Chondrocyte morphology

The morphology of the chondrocytes in the hydrogels was studied using a Philips XL 30 ESEM-FEG scanning electron microscope (SEM) or a LEO Gemini 1550 FEG-SEM. After 14 days' *in vitro* culturing in expansion medium, the hydrogel/cell constructs were fixed with formalin by sequential dehydration and critical point drying. These samples were gold sputtered (Carrington) and analyzed with SEM.

4.2.8 Histology and immunofluorescent staining

After 14 and 21 days, the hydrogel/cell constructs were washed with PBS and fixed in a 10 % buffered formalin solution for 1 hour. After dehydration with a standard series of ethanol followed by butanol incubation overnight, samples were embedded in paraffin and sectioned using a microtome to yield sections of 5 μm in thickness. Sections were stained with Alcian Blue (Sigma-Aldrich, used as 1 % w/v solution) for 30 min, and destained for 5 min in 1 % acetic acid. Afterwards, the sections were washed with water and dehydrated. The staining for glycosaminoglycans (GAGs) was examined under a light microscope (Nikon Eclipse E400). For immunofluorescence analysis of collagen type II, sections were rehydrated with xylene and a standard series of ethanol. Afterwards, the samples were treated with 10 mM citric acid buffer (pH 6.0) for 10 min, and then washed with PBS/BSA 1 %. Col2A1 monoclonal antibody (Purified mouse immunoglobulin IgG1, clone 3HH1-F9, Abnova) was diluted at 1:100 in PBS/BSA 1 % and let to react overnight at room temperature. After washing twice for 5 min in PBS/BSA 1 %, the sections were incubated with Alexa Fluor 488-Goat anti-Mouse IgG1 (γ 1) (Invitrogen, Molecular Probes, 1:1000) for 1 h. After extensive washing, the sections were mounted with VECTASHIELD Mounting Medium containing 4',6'-diamidino-2-phenylindole dihydrochloride (DAPI, Vector Laboratories, Burlingame, CA) to stain the nuclei. The sections not incubated with primary antibodies were used as a negative control and a pellet of human chondrocytes cultured for 21 days in chondrocyte differentiation medium was used as a positive control.

4.2.9 Biochemical analysis

To quantitatively analyze the GAG production inside the hydrogels, a DMMB assay was performed. The constructs were taken from the chondrocyte differentiation

medium after 14, 21 and 28 days. Samples were washed with PBS and frozen at 80 degrees Celsius. After thawing, the constructs were digested in proteinase-K (Sigma) at 56 degrees Celsius (<16 h). Quantification of total DNA was done by a Cyquant dye kit (Molecular Probes) using a fluorescent plate reader (Perkin-Elmer). The amount of GAG was determined spectrophotometrically after reaction with a dimethylmethylene blue dye (DMMB, Sigma-Aldrich). The intensity of the color was quantified immediately in a microplate reader (Bio-TEK Instruments) by measuring the absorbance at 540 nm. The amount of GAG was calculated based on a calibration curve using chondroitin sulphate A or B (Sigma-Aldrich). All values were corrected for the background staining of gels without cells and normalized to the DNA amount (expressed as the GAG/DNA ($\mu\text{g}/\mu\text{g}$) ratio). Data (n=3, measured in triplicates) are expressed as mean \pm standard deviation (SD). Statistical significance was determined by one-way ANOVA with Turkeys post-hoc analysis.

4.3 Results and discussion

4.3.1 Hydrogel formation and gelation time

In foregoing research, it was shown that the enzymatic crosslinking of dextran-tyramine (Dex-TA) conjugates using horseradish peroxidase (HRP) and hydrogen peroxide (H_2O_2) is a highly efficient method to prepare *in situ* forming hydrogels [25]. The gelation time depends on relative ratios of HRP and H_2O_2 to tyramine (TA) groups present. In this study, Dex-TA conjugates with different molecular weights of dextran (Mn of 14k and 31k) and degrees of substitution (DS) of tyramine groups, i.e. Dex14k-TA with a DS of 5, 10 or 15 tyramine groups and Dex31k-TA with a DS of 5 or 10 tyramine groups, were synthesized (Figure 4.1) [25]. The hydrogels were prepared by mixing PBS solutions of Dex-TA conjugates and freshly-made PBS solutions of HRP and H_2O_2 . To apply these hydrogels as an injectable matrix material for cartilage tissue engineering, the crosslinking reaction was optimized with respect to suitable gelation times and use of hydrogen peroxide. It was expected that the use of high concentrations of H_2O_2 would have a detrimental effect on chondrocytes during the crosslinking reaction [32, 33]. To this end, the gelation times of Dex-TA at low molar ratios of H_2O_2 /TA ranging from 0.05 to 0.5 were investigated. Concentrations of Dex-TA conjugates of 10 wt % and 0.25 mg of HRP per mmol tyramine moieties were applied in the hydrogel preparation. The gelation times of the Dex-TA hydrogels were determined by the vial tilting method. As shown in Figure 4.2, the gelation times of the hydrogels prepared from Dex14k-TA and Dex31k-TA conjugates (DS=10) increased with increasing molar ratios of H_2O_2 /TA from 0.1 to 0.5. No gelation occurred when H_2O_2 /TA ratios at and below 0.05 were used (data not shown). Moreover, at the same H_2O_2 /TA ratio, a shorter gelation time was observed for the hydrogels comprising a higher molecular weight Dex-TA. Additionally, the DS values of the Dex14k-TA and Dex31k-TA conjugates have an influence on the gelation time of the hydrogels (Table 4.1). By increasing the number of tyramine groups conjugated to the dextran from 5 to 15 per 100 anhydroglucose rings of dextran, the gelation times of the hydrogels of the Dex14k-TA conjugates decreased from about 60 to 20

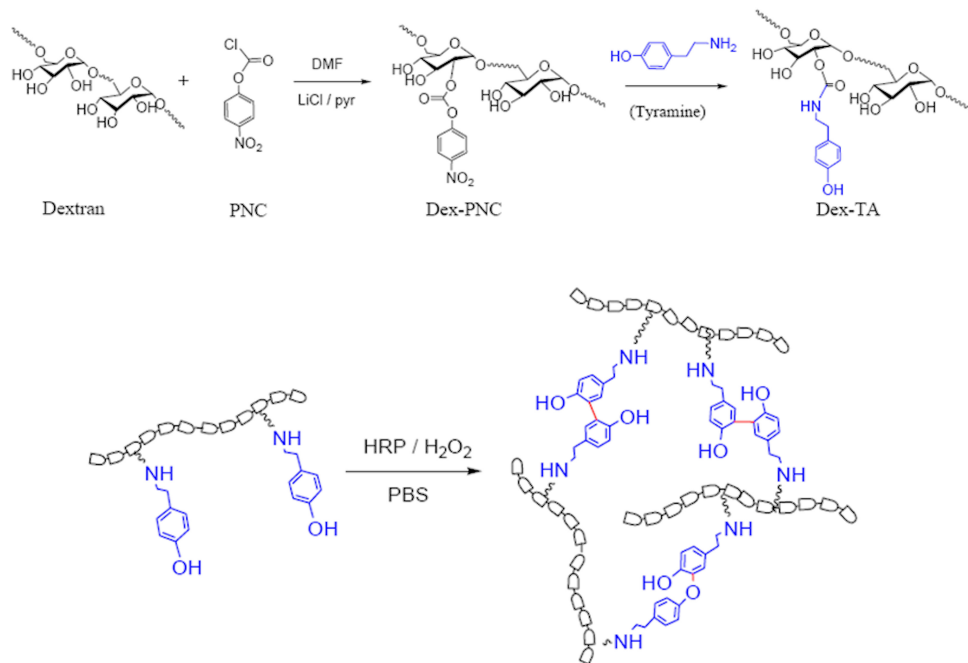


Figure 4.1: Synthesis of dextran-tyramine conjugates (Dex-TA) and hydrogel formation via enzymatic crosslinking.

seconds. Taken together, the hydrogels prepared from Dex14k-TA with a DS of 10 or 15, and Dex31k-TA with a DS of 10 showed short gelation times and were regarded suitable as injectable cell carriers for the retention of cells inside the gels. Since fast gelation (less than 60 sec) was generally observed at a H₂O₂/TA molar ratio of 0.2 ([H₂O₂] = 12 and 16 mM for Dex-TA DS 10 and DS 15, respectively), this ratio was used in the preparation of cell/gel constructs and evaluation of their properties.

4.3.2 Hydrogel characterization

The mechanical properties of the Dex-TA hydrogels were studied by oscillatory rheology experiments at 37degrees Celsius [34] . The storage moduli of Dex-TA hydrogels are listed in Table 4.1. The storage moduli of the Dex-TA hydrogels largely increased with increasing DS of tyramine groups from 5 to 15. For example, the storage moduli of the Dex14k-TA hydrogels increased from about 1.4 kPa to 40 kPa by increasing the DS from 5 to 15. An even higher storage modulus of about 60 kPa was obtained in the hydrogels prepared from Dex31k-TA with a DS of 10. Interestingly, the Dex-TA hydrogels containing chondrocytes (5 million cells/mL gel) had storage and loss moduli that were close to the gels without cells (data not shown), indicating that the presence of chondrocytes in the hydrogels did not influence their mechanical properties.

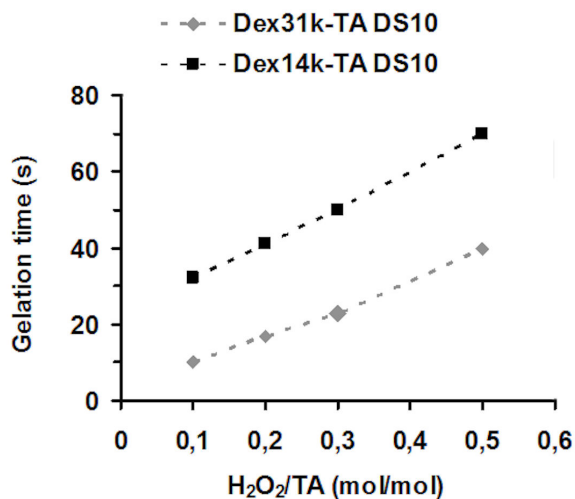


Figure 4.2: Gelation times of Dex-TA conjugates (10 wt %) as a function of the H₂O₂/TA molar ratio. Reaction conditions: 0.25 mg HRP per mmol phenol groups; 37 degrees Celsius, PBS.

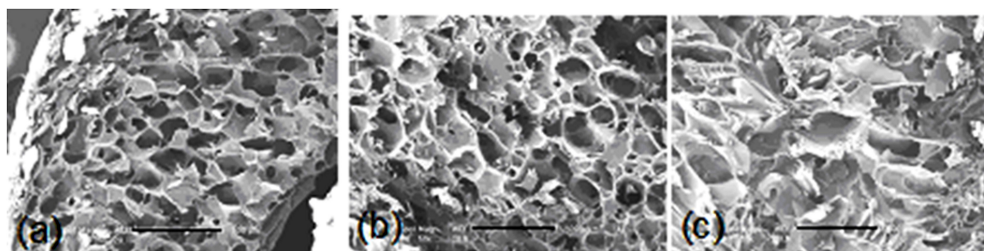


Figure 4.3: SEM images of freeze dried hydrogel samples: (a) Dex31k-TA DS 10, (b) Dex14k-TA DS 10 and (c) Dex14k-TA DS 5. Reaction conditions: 0.25 mg HRP per mmol phenol groups; molar ratio of H₂O₂/TA = 0.2. (Scale bar 500 μ m)

The morphology of freeze-dried hydrogels prepared from the Dex-TA conjugates was determined using scanning electron microscopy (SEM) (Figure 4.3). In all cases, the Dex-TA hydrogels appeared to be highly porous and had a well-interconnected pore structure. It appeared that the pore size of these hydrogels is mainly influenced by the DS rather than by the Mn of the polymers. Freeze-dried samples of hydrogels prepared from Dex14k-TA with a DS of 5 had a larger average pore size ($351 \pm 71 \mu\text{m}$) than those of Dex14k-TA with a DS of 10 ($206 \pm 93 \mu\text{m}$) (Figure 4.2 b vs. c) and the hydrogel prepared from Dex31k-TA with a DS of 10 had an average pore size similar to the Dex14k-TA with the same DS of 10 (Figure 4.3 a vs. b).

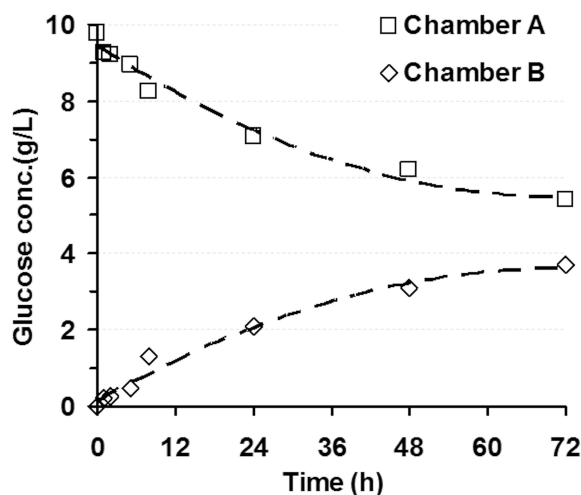


Figure 4.4: Typical graph of glucose (in water) diffusion from chamber A towards the chamber B using a Dex14k-TA DS 15 hydrogel as function of time at 37 degrees Celsius.

To allow cell growth over prolonged periods of time, sufficient nutrient diffusion in the hydrogels is highly desired. The permeability of the Dex-TA hydrogels was evaluated by determining the glucose diffusion through the hydrogels. The setup consisted of two chambers separated by a plate with a circular opening in which a hydrogel film was placed. Glucose is a representative nutrient in the cell culture medium. Figure 4.3 shows typical results of the glucose diffusion in time through a Dex14k-TA DS 15 hydrogel. As can be expected, the concentration of the glucose in chamber A decreased over time, while there was a corresponding increase in the concentration of glucose in chamber B. After 72h, the glucose concentrations in both chambers almost reached a plateau. The diffusion coefficient of glucose through a Dex14k-TA DS 15 hydrogel was determined in time from the glucose concentrations in both chambers [35]. The diffusion coefficient was calculated to be $3.2 \cdot 10^{-6} \text{ cm}^2/\text{s}$, which was close to that of glucose diffusion in cartilage tissue ($\sim 2 \cdot 10^{-6} \text{ cm}^2/\text{s}$) [36]. In Table 4.1, the percentage of glucose diffused after 72 h using various Dex-TA hydrogels is presented. Similar values of 79 % were determined for hydrogels prepared from Dex14k-TA and Dex31k-TA with a DS value of 10. A slightly lower percentage of 74 % was determined for the Dex14k-TA hydrogels with a higher DS of 15. The slower diffusion can be attributed to a more compact network of the hydrogel prepared from Dex14k-TA DS 15 than that of Dex14k-TA DS 10. In all cases, the glucose diffusion reached over 70 % of the equilibrium glucose concentration within 72 h, indicating that cells may efficiently interact with nutrients in these hydrogels.

| | DS ^b | Gelation time (s) | Storage modulus G' (kPa) | Percentage of glucose diffused after 72 h ^c |
|-----------|-----------------|-------------------|--------------------------|--|
| Dex14k-TA | 5 | 60 | 1.4 | n.d. |
| | 10 | 41 | 15.1 | 79% |
| | 15 | 20 | 40.2 | 74% |
| Dex31k-TA | 5 | 42 | 8.2 | 83% |
| | 10 | 17 | 60.4 | 79% |

Table 4.1: Gelation times, storage moduli and glucose diffusion for Dex-TA hydrogels (a). a: Reaction conditions: 10 % wt polymer concentration; molar ratio of H₂O₂/TA is 0.2; 0.25 mg HRP per mmol phenol groups; 37 degrees Celsius, PBS. b: DS (Degree of substitution, defined as the number of tyramine units per 100 anhydroglucose rings in dextran) was determined using ¹H NMR. c: The percentage of glucose diffused after 72 h was expressed as the ratio of the glucose concentration in chamber B and the equilibrium conc. of 5 g/L, multiplied by 100 %.

4.3.3 Cell viability of chondrocytes in Dex-TA hydrogels

Chondrocytes were cultured in the hydrogels of Dex14k-TA and Dex31k-TA with different DS for 14 days. Cell survival of the chondrocytes in the hydrogels was evaluated using a live-dead assay, in which living cells stained green and dead cells red. As is shown in Figure 4, over 95 % cells in these hydrogels were alive, similar to those embedded in an agarose gel which was used as a control. Moreover, a homogeneous distribution of metabolically active chondrocytes that stained purple with a MTT solution was observed in all Dex-TA hydrogels after 1, 7 and 14 days (Figure 4.5). Cell viability experiments, evaluated by the MTT assay, showed that the metabolic activities (percentage) of chondrocytes in the hydrogels of Dex31k-TA DS 10, Dex14k-TA DS 10 and Dex14k-TA DS 15 were comparable to the agarose control over the culturing periods, indicating good biocompatibility and low cytotoxicity (Figure 4.6a). Notably, the metabolic activity values of chondrocytes in the Dex14k-TA DS 10 hydrogel after 14 days in culture is statistically higher than the value at day 1 ($p < 0.05$). These results suggested that chondrocyte proliferation might occur in the Dex14k-TA DS 10 hydrogels. Support for this hypothesis was found by the live-dead assay. Nests of doublets that are indicative of chondrocyte division were observed in the Dex14k-TA DS 10 hydrogel after 14 days in culture (Figure 6b).

4.3.4 Chondrocyte morphology and matrix production

In native cartilage, chondrocytes are surrounded by an extracellular matrix that consists of negatively charged glycosaminoglycan (GAG), like hyaluronic acid and chondroitin sulfate, as well as collagen type II fibrils. The ability of these Dex-TA hydrogels

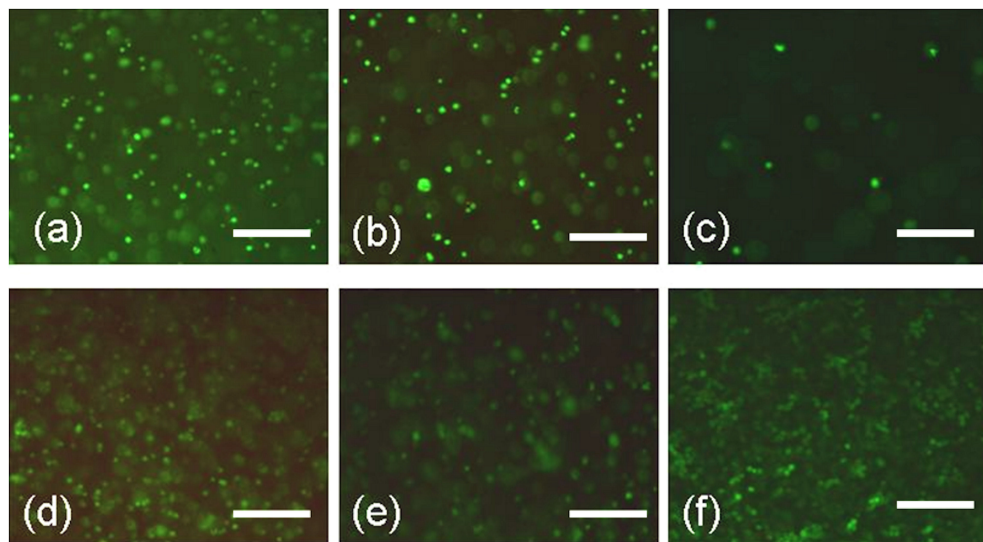


Figure 4.5: Live-dead assay of chondrocytes in Dex-TA hydrogels at day 14: (a) Dex14k-TA DS 15, (b) Dex14k-TA DS 10, (c) Dex14k-TA DS 5, (d) Dex31k-TA DS 10 and (e) Dex31k-TA DS 5. Agarose gels (0.5 wt %) were used as a control (f). Reaction conditions: 0.25 mg HRP per mmol phenol groups; molar ratio of $\text{H}_2\text{O}_2/\text{TA} = 0.2$. Cells were stained with calcein-AM/ethidium Homodimer (living cells stained green and dead cells red). The chondrocyte seeding density was 5 million cells/mL. Scale bar: 200 μm .

to function as a scaffold for cartilage tissue formation was investigated by examining the cell morphology and the ability to produce a cartilaginous specific matrix. It is known that chondrocytes in culture may rapidly lose chondrocytic characteristics and obtain a fibroblast-like phenotype, a process termed dedifferentiation [37]. A round cell shape is correlated with the maintenance of the chondrocyte phenotype. The morphology of the chondrocytes incorporated in the Dex-TA and agarose hydrogels was evaluated by SEM after culturing for 14 days in chondrocyte expansion medium. In Figure 4.7 it is shown that the chondrocytes incorporated in Dex31k-TA DS 10 and Dex14-TA DS 10 and 15 hydrogels exhibited a distinctly round cell shape. Notably, as a typical example, the chondrocytes inside Dex14k-TA DS 15 hydrogels after culturing for 21 days, were located adjacent to a fibrous pericellular matrix (Figure 4.8a) [38]. SEM examinations revealed that this fibrous matrix consisted of collagen fibrils, which was confirmed by the observation of the typical D-period in the fibrils (Figure 4.9b-c).

GAG production by chondrocytes in the Dex-TA hydrogels was examined by histology using Alcian Blue staining. Histology showed that the chondrocytes incorporated in these Dex-TA hydrogels produced abundant ECMs rich in GAGs after 14 and 21 days, as confirmed by the dense GAG staining in these gels (Figure 4.10).

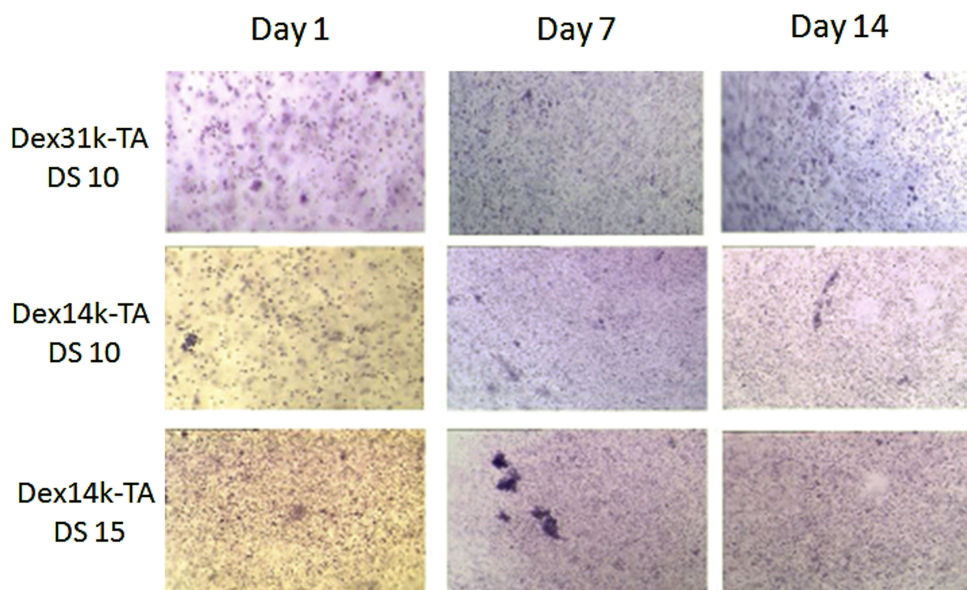


Figure 4.6: MTT staining of chondrocytes in Dex31k-TA DS 10, Dex14k-TA DS 15 and DS 10 hydrogels after 1, 7 and 14 days in culture. Metabolically active cells stained purple. Reaction conditions: $\text{H}_2\text{O}_2/\text{TA}$ molar ratio is 0.2; 0.25 mg HRP per mmol phenol groups. The chondrocyte seeding density was 5 million cells/mL.

No staining was observed for the Dex-TA gels without chondrocytes or for the Dex-TA/cell constructs at day 1 (data not shown). Moreover, at day 14, the GAGs were mainly located in the pericellular matrix around spherical cells, but at day 21, the GAGs were more evenly distributed throughout the gels both in the pericellular and interterritorial matrix.

The synthesis of collagen by chondrocytes in the Dex-TA hydrogels was also examined. The type of collagen present in articular cartilage is primarily collagen type II [39]. An immunofluorescent staining demonstrated the presence of collagen type II inside Dex-TA hydrogels (Figure 4.11a). In the positive control, the nuclei of the chondrocytes fluoresced blue due to the counterstaining with DAPI and the collagen type II fluoresced green. In the negative control, only the staining of the nuclei was observed. These results indicated that chondrocytes cultured inside Dex-TA hydrogels were capable of maintaining their phenotype and producing a cartilaginous specific matrix.

The amounts of glycosaminoglycan (GAG) secreted by chondrocytes inside the hydrogels at different times in culture were determined by a DMMB assay. Agarose gel, a well-known polysaccharide hydrogel system for chondrocyte culturing, was used as a positive control [40, 41]. In Figure 4.12a the time-dependent accumulation of the

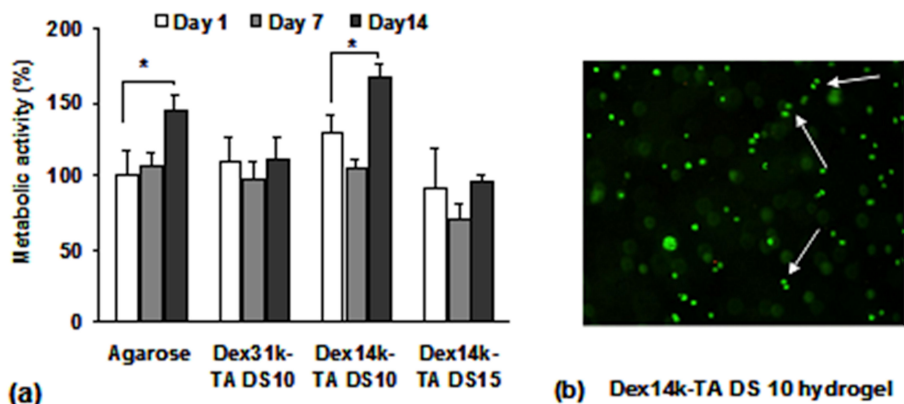


Figure 4.7: (a) Quantitative determination of the metabolic activity of chondrocytes inside Dex-TA hydrogels (Students t-test, * $p < 0.05$). (b) Live-dead assay showing chondrocytes incorporated in a Dex14k-TA DS10 hydrogel after 14 days in culture (chondrocyte division is indicated by arrows, original amplification: 100x). Reaction conditions: the H_2O_2 /TA molar ratio is 0.2; 0.25 mg HRP per mmol phenol groups. The chondrocyte seeding density was 5 million cells/mL.

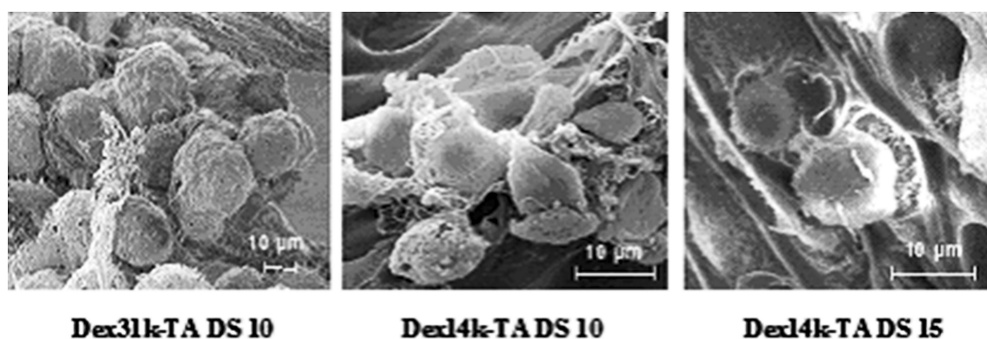


Figure 4.8: SEM images of chondrocytes in Dex-TA hydrogels after 14 days in culture.

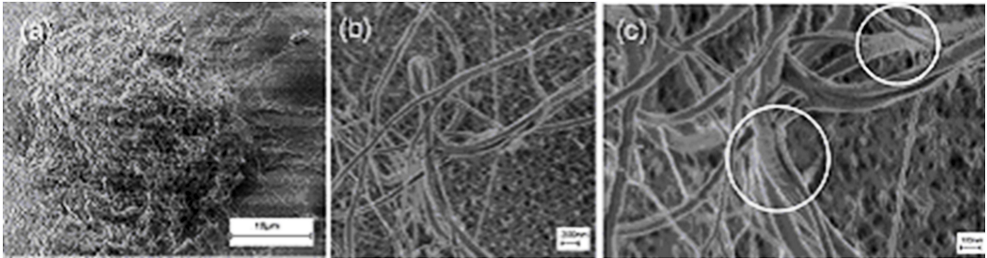


Figure 4.9: SEM images of (a) a single chondrocyte in a Dex14k-TA DS 15 hydrogel (21 days) was surrounded by a fibrous matrix on the gel surface, (b) fibrous matrix at high magnification (c) Circles point to collagen fibrils with a visible D-period at high magnification.

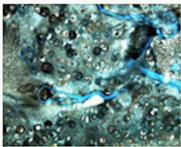
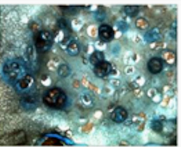
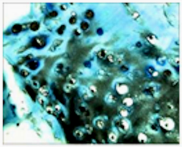
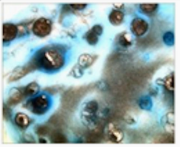
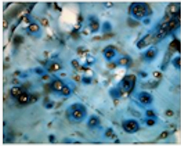
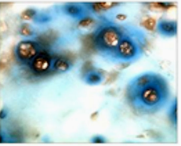
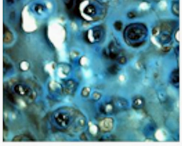

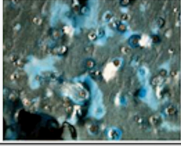
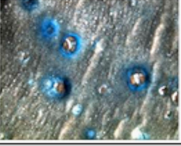
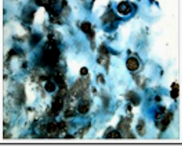
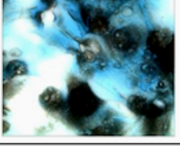
| Day | Day 14 | | Day 21 | |
|------------------------|---|---|---|--|
| Original magnification | 200× | 400× | 200× | 400× |
| Dex14k-TA DS15 |  |  |  |  |
| Dex14k-TA DS10 |  |  |  |  |
| Dex31k-TA DS10 |  |  |  |  |

Figure 4.10: Alcian blue staining of Dex-TA hydrogels with chondrocytes after culturing for 14 and 21 days in differentiation medium. GAGs were stained blue/green. The chondrocyte seeding density was 5 million cells/mL.

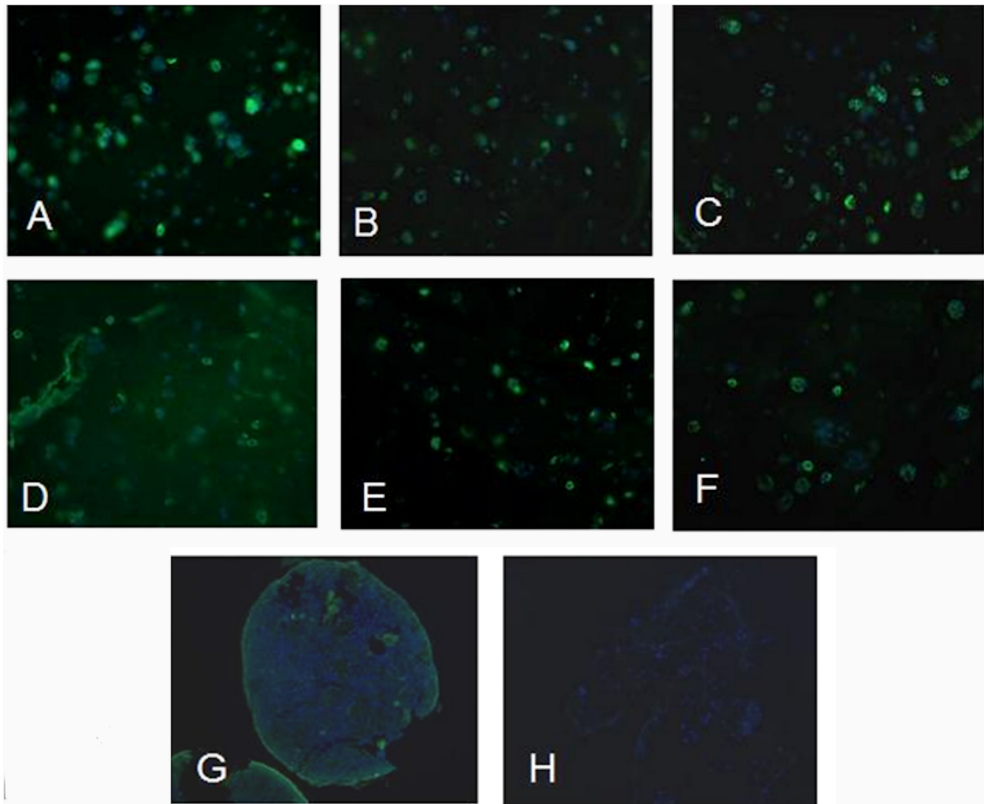


Figure 4.11: Collagen type II staining of Dex14k-TA DS 15 (A and D), Dex14k-TA DS 10 (B and E), and Dex31k-TA DS 10 (C and F) hydrogels after culturing for 14 (A-C) and 21 (D-F) days in differentiation medium; The chondrocyte seeding density was 5 million cells/mL. A pellet of human chondrocytes cultured for 21 days in chondrocyte differentiation medium was used as a positive control (G) and the section without incubation with primary antibodies was used as a negative control (H). Collagen type II fluoresced green and nuclei of the cells were stained with DAPI (blue).

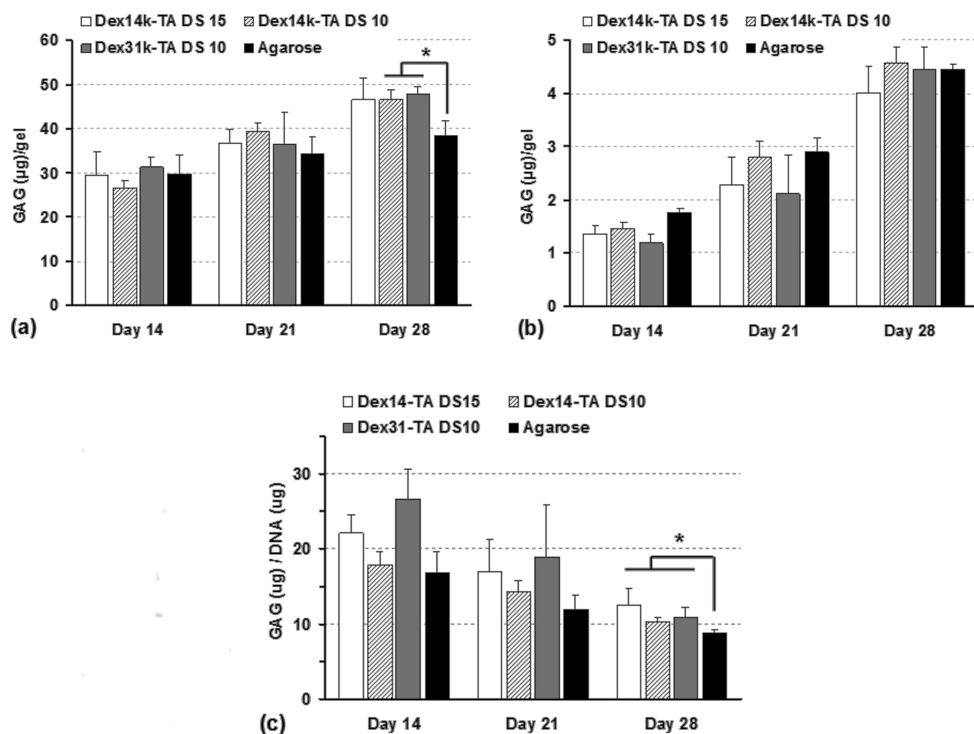


Figure 4.12: GAG accumulation in Dex-TA and agarose hydrogels containing chondrocytes after *in vitro* culturing for 14, 21 and 28 days in differentiation medium. (a) GAG and (b) DNA content per hydrogel sample; (c) GAG accumulation normalized to the DNA content per gel sample. (Cell seeding density: 5 million/mL, ANOVA: * $p < 0.05$).

GAG in the Dex-TA and agarose hydrogels is presented. All hydrogels demonstrated a significant increase in GAG production with increasing culturing times from 14 to 28 days ($p < 0.05$). These results are consistent with the histology results using Alcian blue staining, which showed a denser staining of GAGs at day 21 than that at day 14. Notably, the GAG contents in the hydrogels from Dex14k-TA DS 10 and Dex31k-TA DS 10 are significantly higher than that in the agarose gel at day 28 ($p < 0.05$). The GAG amount for these Dex-TA hydrogels at the same culturing time did not differ.

To compare the described hydrogels with other injectable hydrogel systems reported in literature, the amounts of GAG in each gel were normalized to their DNA content (GAG/DNA) at the different culturing time points (Figure 4.12c). The GAG/DNA values remained statistically constant at day 14 and day 21 ($p < 0.05$). However, the values decreased at day 28 compared to day 14 ($p < 0.05$) because of the increased DNA content per gel as a result of cell proliferation (Figure 4.12b) [42]. Moreover, the GAG/DNA ratios for Dex-TA hydrogels were higher than for agarose

gels (10.9-12.5 $\mu\text{g}/\mu\text{g}$ for Dex-TA vs. 8.7 $\mu\text{g}/\mu\text{g}$ for agarose, $p < 0.05$) at day 28. The GAG/DNA values for the Dex-TA hydrogels at day 14 (17.8-26.7 $\mu\text{g}/\mu\text{g}$) are comparable with those for other injectable hydrogel systems, such as self-assembled peptide hydrogels (~ 22 $\mu\text{g}/\mu\text{g}$ at day 15) and photopolymerized PEG hydrogels (ca. ~ 26 $\mu\text{g}/\mu\text{g}$ at day 14) [43, 44]. Taken together, these results reveal the high potential of these injectable Dex-TA hydrogels for cartilage tissue engineering.

4.4 Conclusions

The enzymatic crosslinking of dextran-tyramine (Dex-TA) conjugates in the presence of horseradish peroxidase and hydrogen peroxide is a highly efficient method to prepare in-situ forming hydrogels. Increasing the molecular weight of dextran and degree of substitution of tyramine moieties resulted in decreasing gelation times and increasing storage moduli. Chondrocytes incorporated in the hydrogels showed a high cell viability after 2 weeks and retained their round cell morphology. Besides, the cells were capable of producing a cartilaginous specific matrix rich in GAGs and collagen type II. These studies indicated that injectable hydrogels from Dex-TA conjugates have a high potential as injectable scaffolds for cartilage tissue engineering.

References

1. Drury JL, Mooney DJ. Hydrogels for Tissue Engineering: Scaffold Design Variables and Applications. *Biomaterials* 2003;24: 4337-4351.
2. Frenkel SR, Di Cesare PE. Scaffolds for Articular Cartilage Repair. *Ann. Biomed. Eng.* 2004;32: 26-34.
3. Lee S-H, Shin H. Matrices and Scaffolds for Delivery of Bioactive Molecules in Bone and Cartilage Tissue Engineering. *Adv. Drug Deliver. Rev.* 2007;59: 339-359.
4. J Elisseeff, Puleo C, Yang F, Sharma B. Advances in Skeletal Tissue Engineering with Hydrogels. *Orthod. Craniofac. Res.* 2005;8: 150-161.
5. Van Tomme SR, Storm G, Hennink WE. *in situ* Gelling Hydrogels for Pharmaceutical and Biomedical Applications. *Int. J. Pharm.* 2008;355: 1-18.
6. Kretlow JD, Klouda L, Mikos AG. Injectable Matrices and Scaffolds for Drug Delivery in Tissue Engineering. *Adv. Drug Deliver. Rev.* 2007;59: 263-273.
7. Francis Suh JK, Matthew HWT. Application of Chitosan-Based Polysaccharide Biomaterials in Cartilage Tissue Engineering: A Review. *Biomaterials* 2000;21: 2589-2598.
8. Chen J-P, Cheng T-H. Thermo-Responsive Chitosan-graft-Poly(N-Isopropylacrylamide) Injectable Hydrogel for Cultivation of Chondrocytes and Meniscus Cells. *Macromol. Biosci.* 2006;6: 1026-1039.
9. Chung C, Mesa J, Miller GJ, Randolph MA, Gill TJ, Burdick JA. Effects of Auricular Chondrocyte Expansion on Neocartilage Formation in Photocrosslinked Hyaluronic Acid Networks. *Tissue Eng.* 2006;12: 2665-2673.
10. Chung C, Mesa J, Randolph MA, Yaremchuk M, Burdick JA. Influence of Gel Properties on Neocartilage Formation by Auricular Chondrocytes Photoencapsulated in Hyaluronic Acid Networks. *J. Biomed. Mater. Res. A* 2006;77A: 518-525.
11. Chung C, Erickson IE, Mauck RL, Burdick JA. Differential Behavior of Auricular and Articular Chondrocytes in Hyaluronic Acid Hydrogels. *Tissue Eng. A* 2008;14: 1121-1131.
12. Fisher JP, Jo S, Mikos AG, Reddi AH. Thermoreversible Hydrogel Scaffolds for Articular Cartilage Engineering. *J. Biomed. Mater. Res. A* 2004;71A: 268-274.
13. Park H, Temenoff JS, Holland TA, Tabata Y, Mikos AG. Delivery of TGF- β 1 and Chondrocytes Via Injectable, Biodegradable Hydrogels for Cartilage Tissue Engineering Applications. *Biomaterials* 2005;26: 7095-7103.
14. Dadsetan M, Szatkowski JP, Yaszemski MJ, Lu L. Characterization of Photo-Cross-Linked Oligo[poly(ethylene glycol) Fumarate] Hydrogels for Cartilage Tissue Engineering. *Biomacromolecules* 2007;8: 1702-1709.
15. Burdick JA, Chung C, Jia X, Randolph MA, Langer R. Controlled Degradation and Mechanical Behavior of Photopolymerized Hyaluronic Acid Networks. *Biomacromolecules* 2005;6: 386-391.
16. Hong Y, Mao Z, Wang H, Gao C, Shen J. Covalently Crosslinked Chitosan Hydrogel Formed at Neutral Ph and Body Temperature. *J. Biomed. Mater. Res. A* 2006;79A: 913-922.
17. Hong Y, Song H, Gong Y, Mao Z, Gao C, Shen J. Covalently Crosslinked Chitosan Hydrogel: Properties of *in vitro* Degradation and Chondrocyte Encapsulation.

Acta Biomater. 2007;3: 23-31.

18. Hiemstra C, vanderAa LJ, Zhong Z, Dijkstra PJ, Feijen J. Novel *in situ* Forming, Degradable Dextran Hydrogels by Michael Addition Chemistry: Synthesis, Rheology, and Degradation. Macromol. 2007;40: 1165-1173.

19. Hiemstra C, vanderAa LJ, Zhong Z, Dijkstra PJ, Feijen J. Rapidly *in situ*-Forming Degradable Hydrogels from Dextran Thiols through Michael Addition. Biomacromolecules 2007;8: 1548-1556.

20. Park Y, Lutolf MP, Hubbell JA, Hunziker EB, Wong M. Bovine Primary Chondrocyte Culture in Synthetic Matrix Metalloproteinase-Sensitive Poly(ethylene glycol)-Based Hydrogels as a Scaffold for Cartilage Repair. Tissue Eng. 2004;10: 515-522.

21. Nicodemus GD, Bryant SJ. Cell Encapsulation in Biodegradable Hydrogels for Tissue Engineering Applications. Tissue Eng. B 2008;14: 149-165.

22. Lee F, Chung JE, Kurisawa M. An Injectable Enzymatically Crosslinked Hyaluronic Acid-Tyramine Hydrogel System with Independent Tuning of Mechanical Strength and Gelation Rate. Soft Mat. 2008;4: 880-887.

23. Sakai S, Ogushi Y, Kawakami K. Enzymatically Crosslinked Carboxymethylcellulose-Tyramine Conjugate Hydrogel: Cellular Adhesiveness and Feasibility for Cell Sheet Technology. Acta Biomater. 2009;5: 554-559.

24. Sakai S, Kawakami K. Synthesis and Characterization of Both Ionically and Enzymatically Cross-Linkable Alginate. Acta Biomater. 2007;3: 495-501.

25. Jin R, Hiemstra C, Zhong Z, Feijen J. Enzyme-Mediated Fast *in situ* Formation of Hydrogels from Dextran-Tyramine Conjugates. Biomaterials 2007;28: 2791-2800.

26. Jin R, Moreira Teixeira LS, Dijkstra PJ, Karperien M, van Blitterswijk CA, Zhong ZY, and Feijen J. Injectable Chitosan-Based Hydrogels for Cartilage Tissue Engineering. Biomaterials 2009;30: 2544-2551.

27. Sakai S, Yamada Y, Zenke T, Kawakami K. Novel Chitosan Derivative Soluble at Neutral Ph and *in-Situ* Gellable Via Peroxidase-Catalyzed Enzymatic Reaction. J. Mater. Chem. 2009;19: 230-235.

28. Sakai S, Hirose K, Taguchi K, Ogushi Y, Kawakami K. An Injectable, *in situ* Enzymatically Gellable, Gelatin Derivative for Drug Delivery and Tissue Engineering. Biomaterials 2009;30: 3371-3377.

29. Papenburg BJ, Vogelaar L, Bolhuis-Versteeg LAM, Lammertink RGH, Stamatialis D, Wessling M. One-Step Fabrication of Porous Micropatterned Scaffolds to Control Cell Behavior. Biomaterials 2007;28: 1998-2009.

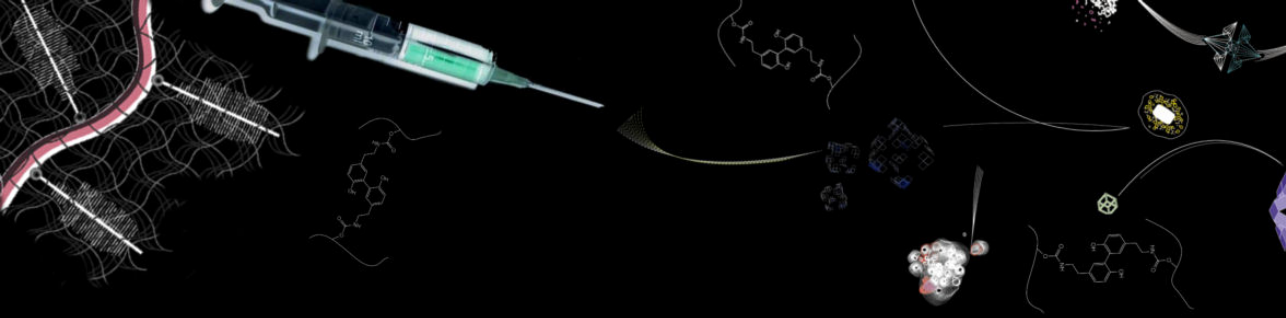
30. Alexandre E, Schmitt B, Boudjema K, Merrill EW, Lutz PJ. Hydrogel Networks of Poly(Ethylene Oxide) Star-Molecules Supported by Expanded Polytetrafluoroethylene Membranes: Characterization, Biocompatibility Evaluation and Glucose Diffusion Characteristics. Macromol. Biosci. 2004;4: 639-648.

31. Jukes JM, Moroni L, van Blitterswijk CA, de Boer J. Critical Steps toward a Tissue-Engineered Cartilage Implant Using Embryonic Stem Cells. Tissue Eng. A 2008;14: 135-147.

32. Burdon RH. Superoxide and Hydrogen Peroxide in Relation to Mammalian Cell Proliferation. Free Radic. Biol. Med. 1995;18: 775-794.

33. Asada S, Fukuda K, Oh M, Hamanishi C, Tanaka S. Effect of Hydrogen Peroxide on the Metabolism of Articular Chondrocytes. Inflamm. Res. 1999;48: 399-403.

34. van de Manakker F, Vermonden T, el Morabit N, van Nostrum CF, Hennink WE. Rheological Behavior of Self-Assembling PEG-b-Cyclodextrin/PEG-Cholesterol Hydrogels. *Langmuir* 2008;24: 12559-12567.
35. Baker RW, Lonsdale HK (1974) *Controlled Release of Biologically Active Agents*, Plenum Press, New York.
36. Maroudas A. Distribution and Diffusion of Solutes in Articular Cartilage. *Biophys. J.* 1970;10: 365-379.
37. Yoon Y-M, Kim S-J, Oh C-D, Ju J-W, Song WK, Yoo YJ, Huh T-L, and Chun J-S. Maintenance of Differentiated Phenotype of Articular Chondrocytes by Protein Kinase C and Extracellular Signal-Regulated Protein Kinase. *J. Biol. Chem.* 2002;277: 8412-8420.
38. DiMicco MA, Kisiday JD, Gong H, Grodzinsky AJ. Structure of Pericellular Matrix around Agarose-Embedded Chondrocytes. *Osteoarthr. Cartilage* 2007;15: 1207-1216.
39. Aigner T, Stove J. Collagens—Major Component of the Physiological Cartilage Matrix, Major Target of Cartilage Degeneration, Major Tool in Cartilage Repair. *Adv. Drug Deliver. Rev.* 2003;55: 1569-1593.
40. Buschmann MD, Gluzband YA, Grodzinsky AJ, Kimura JH, Hunziker EB. Chondrocytes in Agarose Culture Synthesize a Mechanically Functional Extracellular Matrix. *J. Orthop. Res.* 1992;10: 745-758.
41. Benya PD, Shaffer JD. Dedifferentiated Chondrocytes Reexpress the Differentiated Collagen Phenotype When Cultured in Agarose Gels. *Cell* 1982;30: 215-224.
42. Toh WS, Yang Z, Liu H, Heng BC, Lee EH, Cao T. Effects of Culture Conditions and Bone Morphogenetic Protein 2 on Extent of Chondrogenesis from Human Embryonic Stem Cells. *Stem Cells* 2007;25: 950-960.
43. Kisiday J, Jin M, Kurz B, Hung H, Semino C, Zhang S, and Grodzinsky AJ. Self-Assembling Peptide Hydrogel Fosters Chondrocyte Extracellular Matrix Production and Cell Division: Implications for Cartilage Tissue Repair. *Proc. Natl. Acad. Sci. USA* 2002;99: 9996-10001.
44. Bryant SJ, Anseth KS. Hydrogel Properties Influence ECM Production by Chondrocytes Photoencapsulated in Poly(ethylene glycol) Hydrogels. *J. Biomed. Mater. Res.* 2002;59: 63-72.



Chapter 5

Enzymatically-Crosslinked Injectable Hydrogels Based on Biomimetic Dextran-Hyaluronic Acid Conjugates for Cartilage Tissue Engineering

5

Rong Jin, Liliana Moreira Teixeira, Piet Dijkstra, Marcel Karperien, Clemens van Blitterswijk, Jan Feijen

Abstract

Novel polysaccharide hybrids consisting of hyaluronic acid (HA) grafted with a dextran-tyramine conjugate (Dex-TA) were synthesized and investigated as injectable biomimetic hydrogels for cartilage tissue engineering. The design of these hybrids (denoted as HA-g-Dex-TA) is based on the molecular structure of proteoglycans present in the extracellular matrix of native cartilage. Hydrogels of HA-g-Dex-TA were rapidly formed within 2 minutes via enzymatic crosslinking of the tyramine residues in the presence of horseradish peroxidase and hydrogen peroxide. The gelation time, equilibrium swelling and storage modulus could be adjusted by varying the degree of substitution of tyramine residues and polymer concentration. Bovine chondrocytes incorporated in the HA-g-Dex-TA hydrogels remained viable, as shown by the Live-dead assay. Moreover, enhanced chondrocyte proliferation and matrix production were observed in the HA-g-Dex-TA hydrogels compared to Dex-TA hydrogels. These results suggest

that HA-g-Dex-TA hydrogels have a high potential as injectable scaffolds for cartilage tissue engineering.

5.1 Introduction

Tissue engineering represents a promising approach in the treatment of damaged cartilage. This approach generally involves the use of three-dimensional (3-D) scaffolds, which can support the growth, proliferation and differentiation of incorporated chondrocytes and/or progenitor cells. Because hydrogels are 3-D elastic networks having high water content, they mimic hydrated native cartilage tissue and are considered suitable scaffolds for cartilage tissue engineering.

Injectable hydrogels are highly desirable in clinical applications since they can be applied via a minimally invasive procedure. After injection in the form of a solution, the precursor gels *in situ* and fills the irregularly shaped defect. Meanwhile, cells and/or bioactive molecules can be easily incorporated. Injectable hydrogels can be obtained via a chemical crosslinking method, for example, photopolymerization. In this approach, a solution of a vinyl-containing polymer converts into a gel by exposure to visible or ultraviolet light in the presence of photo-initiators [1-7]. Photocrosslinked hydrogels generally have a short gelation time and are chemically stable and mechanically strong. However, cytotoxic photo-initiators and UV light required for the photopolymerization reaction may induce cell death [8, 9]. In addition, the reaction may be exothermic, which may harm the incorporated cells and induce local necrosis [10]. Alternatively, injectable hydrogels can be generated via Michael type addition reactions of thiol groups to (meth)acrylate, (meth)acrylamide, or vinyl sulfone groups [11-16]. In this approach, thiol-bearing bioactive molecules such as adhesion peptides and matrix metalloproteinase substrate peptides can be relatively easily incorporated creating biomimetic hydrogels [15, 17]. However, in general the rate of gelation induced by a Michael type addition reaction was found to be too slow (~ 30 min or longer) [14, 18], which hampers clinical applications. Recently, an enzymatic crosslinking method, which induces fast gelation, has been developed [19-24]. We previously reported on dextran- and chitosan-based injectable hydrogels based on this approach [20, 23]. Crosslinking takes place via an oxidative coupling reaction of phenol moieties in the presence of horseradish peroxidase (HRP) and H_2O_2 . These hydrogels were formed rapidly within minutes. They showed good biocompatibility and support chondrocyte survival and differentiation [23, 25, 26].

Various natural and synthetic polymers, as well as combinations thereof have been used for the preparation of injectable hydrogels [27-29]. Among these materials, polysaccharides, such as hyaluronic acid, dextran, and chitosan, have received wide-spread interest particularly for applications in cartilage tissue engineering [30]. This is based on the presence of large quantities of glycosaminoglycans (GAGs), such as hyaluronic acid, heparan sulfate, and chondroitin sulfate, in the extracellular matrix (ECM) of native cartilage. It has been demonstrated that polysaccharide-based hydrogels are biocompatible and capable of maintaining the phenotype of chondrocytes incorporated. Gel/cell constructs show accumulation of a newly-formed ECM

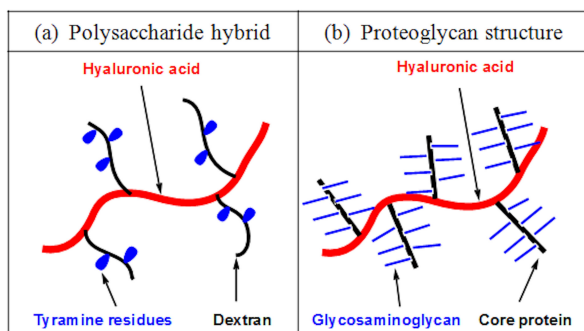


Figure 5.1: Chemical structure of (a) polysaccharide hybrids based on hyaluronic acid and dextran-tyramine conjugates and (b) structure of a proteoglycan.

matrix over time *in vitro* and/or *in vivo* [25, 31, 32]. Additionally, polysaccharides have abundant functional groups such as hydroxyl groups, amino groups and/or carboxylic acid groups, amenable to various types of chemical modifications. This offers the opportunity to introduce crosslinkable or bioactive moieties into polysaccharide precursors of hydrogels. In this way, biofunctional scaffolds can be created to modulate cell adhesion, migration, proliferation and differentiation as well as direct new tissue formation [33, 34].

In our current research, we present a first step towards a strategy to prepare biomimetic polysaccharide-based injectable hydrogels for cartilage tissue engineering. Novel polysaccharide hybrids were designed, in which tyramine-conjugated dextrans were grafted onto hyaluronic acid (HA). These polysaccharide hybrids resemble the macromolecular structure of proteoglycans (Figure 5.1) present in the ECM of native cartilage. The tyramine residues enable subsequent enzymatic crosslinking of the hybrid molecules in the presence of HRP and H_2O_2 . HA was chosen because it is an important component of the ECM in cartilage tissue. HA interacts with chondrocytes through surface receptors like CD44, enabling modulation of cell activity [35–37]. In previous research, tyramine-conjugated dextrans showed a fast gelation and good mechanical properties using HRP-mediated crosslinking [20]. In this study, a hybrid of HA and dextran-tyramine (Dex-TA) conjugates would afford a biomimetic hydrogel. We hypothesized that the incorporation of HA would improve the performance of Dex-TA gels in cartilage tissue engineering. These biomimetic hydrogels may provide a supportive environment for chondrocyte proliferation and differentiation as well as matrix deposition. In this chapter, we describe the synthesis and characterization of polysaccharide hybrids from hyaluronic acid and dextran-tyramine conjugates. The hydrogels were investigated in terms of their gelation times, storage moduli and enzymatic degradation properties. Besides, bovine articular chondrocytes were encapsulated inside the hydrogels *in vitro* to determine cell survival and to assess matrix production.

5.2 Materials and methods

5.2.1 Materials

Dextran ($M_r=6,000$, Fluka) was dried by azeotropic distillation from dry toluene. N-Boc-1,4-diaminobutane, p-nitrophenyl chloroformate (PNC), N-ethyl-N-(3-dimethylaminopropyl) carbodiimide hydrochloride (EDAC) and sodium cyanoborohydride (NaBH_3CN) were purchased from Fluka. Tyramine (TA), 4-morpholino ethanesulfonic acid (MES), trifluoroacetic acid (TFA), hydrogen peroxide (H_2O_2), pyridine (anhydrous), deuterium oxide (D_2O), phosphorus pentoxide, hyaluronidase (HAse, ~ 300 U/mg), lithium chloride (LiCl) and N-hydroxysuccinimide (NHS) were obtained from Aldrich-Sigma. Horseradish peroxidase (HRP, type VI, 300 purpurogallin unit/mg solid) was purchased from Aldrich and used without further purification. Sodium hyaluronate (15-30 kg/mol, laboratory grade) was purchased from CPN Shop. N,N-Dimethylformamide (DMF) was dried over CaH_2 , distilled under vacuum and stored over molecular sieves (4 Å). LiCl was dried at 80 degrees Celsius under vacuum over phosphorus pentoxide. All other solvents were used as received. Dextran-tyramine (denoted as Dex-TA) conjugates were prepared as reported previously [20].

5.2.2 Synthesis of amine-terminated dextran-tyramine conjugates

Amine-terminated dextran-tyramine conjugates (denoted as Dex-TA-NH₂) were synthesized by a two-step procedure. Dex-TA conjugates were first reacted with N-Boc-1,4-diaminobutane and sodium cyanoborohydride to end functionalize the dextran. The protecting t-butyloxycarbonyl group was removed by reaction with TFA. Typically, Dex-TA (5 g), dissolved in 25 mL of deionized water, was treated with N-Boc-1,4-diaminobutane (3.9 g, 21 mmol) and stirred for 2 h under nitrogen. NaBH_3CN (3.9 g, 63 mmol) was then added in portions, and the reaction mixture was stirred at room temperature. After 3 d, the solution was neutralized with 1 M HCl solution to pH 7. The Boc-amine-terminated Dex-TA (denoted as Dex-TA-NH-Boc) was purified by ultrafiltration (MWCO 1000) and isolated as a white foam after freeze-drying. Yield: 4.4 g (88 %). ^1H NMR (D_2O): δ 1.3-1.4 (Boc, $-\text{C}(\text{CH}_3)_3$), 1.4-1.7 ($-\text{NH}-\text{CH}_2-\text{C}_2\text{H}_4-\text{CH}_2-\text{NH}-$), 2.6 and 3.0 ($-\text{C}_2\text{H}_4-\text{C}_6\text{H}_4-\text{OH}$ and $-\text{NH}-\text{CH}_2-\text{C}_2\text{H}_4-\text{CH}_2-\text{NH}-\text{Boc}$), 3.2-4.1 (dextran glucosidic protons), 5.0 (dextran anomeric proton), 6.9 and 7.2 ($-\text{C}_2\text{H}_4-\text{C}_6\text{H}_4-\text{OH}$).

In the second step, Dex-TA-NH-Boc (4.4 g) was dissolved in 110 mL of deionized water and after addition of 4.4 mL of TFA, the mixture was stirred overnight under nitrogen. The solution was then neutralized with 4 M NaOH to pH 7. The obtained amine-terminated Dex-TA (denoted as Dex-TA-NH₂) was purified by ultrafiltration (MWCO 1000) and subsequently freeze-dried. Yield: 3.4 g (78 %). ^1H NMR (D_2O): δ 1.5-1.6 ($-\text{NH}-\text{CH}_2-\text{C}_2\text{H}_4-\text{CH}_2-\text{NH}_2$), 2.6 and 3.0 ($-\text{C}_2\text{H}_4-\text{C}_6\text{H}_4-\text{OH}$ and $-\text{NH}-\text{CH}_2-\text{C}_2\text{H}_4-\text{CH}_2-\text{NH}_2$), 3.2-4.1 (dextran glucosidic protons), 5.0 (dextran anomeric proton), 6.9 and 7.2 ($-\text{C}_2\text{H}_4-\text{C}_6\text{H}_4-\text{OH}$).

5.2.3 Synthesis of hyaluronic acid grafted with Dex-TA

Copolymers of hyaluronic acid grafted with Dex-TA (denoted as HA-g-Dex-TA) were synthesized by a coupling reaction of Dex-TA-NH₂ with hyaluronic acid using EDAC/NHS as coupling reagent. Sodium hyaluronate (1 g) was dissolved in 50 mL of MES (0.1 M, pH 6.0), to which EDAC (1.8 g, 9.4 mmol) and NHS (1.1 g, 9.4 mmol) were added. After 30 min, a Dex-TA-NH₂ solution (1.25 g, in 10 mL of MES buffer) was added and the mixture was stirred under nitrogen for 3 d. The solution was then neutralized with 1 M NaOH to pH 7. To remove uncoupled Dex-TA-NH₂, the solution was ultrafiltrated (MWCO 10000), first with an aqueous solution of 50 mM NaCl and then deionized water. HA-g-Dex-TA was obtained as a white foam after freeze-drying. Yield: 1.9 g (84 %). ¹H NMR (D₂O): δ 1.5-1.6 (-NH-CH₂-C₂H₄-CH₂-NHCO-), 2.0 (-NHCO-CH₃), 2.6 and 3.0 (-C₂H₄-C₆H₄-OH and -NH-CH₂-C₂H₄-CH₂-NHCO-), 3.2-4.1 (dextran and HA glucosidic protons), 4.4-4.6 (HA anomeric proton), 5.0 (dextran anomeric proton), 6.9 and 7.2 (-C₂H₄-C₆H₄-OH).

5.2.4 Polymer characterization

¹H NMR (300 MHz) spectra were recorded on a Varian Inova spectrometer (Varian, Palo Alto, USA). The signals of solvent residues were used as reference peaks for the ¹H NMR chemical shift and were set at δ 4.79 for water. The degree of substitution (DS) of Dex-TA, which is defined as the number of tyramine moieties per 100 anhydroglucose rings in dextran, was determined using ¹H NMR by comparing the integrals of signals at δ 5.0 (dextran anomeric proton) and δ 6.5-7.5 (tyramine aromatic protons). The number of grafted Dex-TA chains per HA molecule was determined using ¹H NMR by comparing integrals of signals at δ 2.0 (acetamide methyl protons of HA) and δ 5.0 (dextran anomeric proton).

The molecular weight and polydispersity of Dex-TA-NH₂, HA and HA-g-Dex-TA copolymers were determined by gel-permeation chromatography (GPC) relative to dextran standards (Fluka). GPC measurements were performed using a PL-GPC 120 Integrated GPC/SEC System (Polymer Labs) and two thermostated (30 degrees Celsius) PL-aquagel-OH columns (8 μ m, 3007.5 mm, Polymer Labs). Sodium acetate buffer (NaAc, 300 mM, pH 4.5) containing 30 % (v/v) methanol was used as eluent at a flow rate of 0.5 mL/min.

5.2.5 Hydrogel formation and gelation time

Hydrogel samples (~0.25 mL) were prepared in vials at 37 degrees Celsius. In a typical example, to a PBS solution of HA-g-Dex-TA DS 10 (200 μ L, 12.5 % wt), freshly prepared solutions of H₂O₂ (17.5 μ L of 0.2 % stock solution) and HRP (32.5 μ L of 11 unit/mL stock solution) in PBS were added and the mixture was gently vortexed. The final concentration of HA-g-Dex-TA was 10 % wt. In all experiments 0.25 mg HRP per mmol phenol groups and a H₂O₂/phenol molar ratio of 0.2 were applied. The time to form a gel (denoted as gelation time) was determined using the vial tilting method. No flow within 1 min upon inverting the vial was regarded as the gel state. The experiments were performed in triplicate.

5.2.6 Swelling and enzymatic degradation

For the swelling test, hydrogels (~ 0.25 mL) of HA-g-Dex-TA were prepared as described above and freeze-dried (Wd). Subsequently, 2 mL of PBS solutions were applied to the dried hydrogels, which were then incubated at 37 degrees Celsius for 72 h to reach the swelling equilibrium. The buffer solution was then removed from the samples and the hydrogels were weighed (Ws). The experiments were performed in triplicate and the degree of swelling was expressed as $(Ws-Wd)/Wd$.

In degradation experiments, 2 mL of PBS containing 100 U/mL hyaluronidase was placed on top of 0.25 mL of the prepared hydrogels and the samples were then incubated at 37 degrees Celsius. At regular time intervals, the buffer solution was removed from the samples and the hydrogels were weighed. The remaining gel (percentage) was calculated from the original gel weight after preparation (W_i) and remaining gel weight after exposure to the enzyme containing buffer (W_t), expressed as $W_t/W_i \times 100$ %. The buffer was replaced every 2-3 days and the experiments were performed in triplicate.

5.2.7 Rheological analysis

Rheological experiments were carried out with a MCR 301 rheometer (Anton Paar) using parallel plates (25 mm diameter, 0) configuration at 37 degrees Celsius in the oscillatory mode. In a typical example, 52.5 μ L of a H_2O_2 stock solution and 97.5 μ L of a HRP stock solution in PBS were mixed. The HRP/ H_2O_2 solution was then immediately mixed with 600 μ L of a solution of HA-g-Dex-TA (12.5 % wt, in PBS) using a double syringe (2.5 mL, 1:4 volume ratio) equipped with a mixing chamber (Mixpac). After the samples were applied to the rheometer, the upper plate was immediately lowered to a measuring gap size of 0.5 mm, and the measurement was started. To prevent evaporation, a layer of oil was introduced around the polymer sample. A frequency of 0.5 Hz and a strain of 0.1 % were applied in the analysis. The measurement was allowed to proceed until the storage moduli reached a plateau value.

5.2.8 Chondrocyte isolation and incorporation

Bovine chondrocytes were isolated as previously reported [23] and cultured in chondrocyte expansion medium (DMEM with 10 % heat inactivated fetal bovine serum, 1 % penicillin/streptomycin (Gibco), 0.5 mg/mL fungizone (Gibco), 0.01 M MEM nonessential amino acids (Gibco), 10 mM HEPES and 0.04 mM L-proline) at 37 degrees Celsius in a humidified atmosphere (95 % air/5 % CO_2). Hydrogels containing chondrocytes were prepared under sterile conditions by mixing a HA-g-Dex-TA /cell suspension with HRP/ H_2O_2 . Solutions of HA-g-Dex-TA were made using medium and HRP and H_2O_2 stock solutions were made using PBS. All the components were sterilized by filtration through filters with a pore size of 0.22 μ m. Chondrocytes (P1) were incorporated in the hydrogels using the same procedure as that in the absence of cells. The cell/gel constructs were prepared in vials. The final concentration of HA-g-Dex-TA was 10 % wt and the cell seeding density in the gels was 5 million/mL.

After gelation, 1 mL of chondrocyte differentiation medium (DMEM with 0.1 μ M dexamethasone (Sigma), 100 μ g/mL sodium pyruvate (Sigma), 0.2 mM ascorbic acid, 50 mg/mL insulin-transferrin-selenite (ITS+1, Sigma), 100 U/ml penicillin, 100 μ g/ml streptomycin, 10 ng/mL transforming growth factor β 3 (TGF- β 3, Invitrogen)) was added on top of the hydrogels and the constructs were incubated at 37 degrees Celsius in a humidified atmosphere containing 5 % CO₂. The medium was replaced every 3 or 4 days.

5.2.9 Cell viability and SEM

The effect of hydrogels on cell survival was studied using a Live-dead assay. At days 1, 7, 14 and 21, the hydrogel constructs were rinsed with PBS and stained with calcein AM/ethidium homodimer using the Live-dead assay Kit (Invitrogen), according to the manufactures instructions. Hydrogel/cell constructs were visualized using fluorescence microscopy (Zeiss). As a result living cells fluoresce green and the nuclei of dead cells red.

The morphology of the chondrocytes in the hydrogels was studied using a Philips XL 30 ESEM-FEG scanning electron microscope (SEM). After 21 days *in vitro* culturing in differentiation medium, the hydrogel/cell constructs were fixed with formalin followed by sequential dehydration and critical point drying. These samples were gold sputtered (Carrington) and analyzed with SEM.

Hydrogel degradation in the presence of chondrocytes. The gel/cell constructs (0.1 mL) were prepared in vials as described above and weighed (Wci). About 1 mL of chondrocyte differentiation medium was added on top of the gel and the constructs were incubated at 37 degrees Celsius in a humidified atmosphere containing 5 % CO₂. The medium was replaced every 3-4 days and the cell/gel constructs were weighed at regular time intervals (Wct). The swelling ratio of constructs was calculated from Wct/Wci. Afterwards, the constructs were washed extensively with water to remove the salts from the medium and then freeze-dried (Wcdt). The degradation profiles of the hydrogels with chondrocytes were based on the dry gel mass which was normalized to the original wet gel weight (Wci), expressed as Wcdt/Wci100 %. Dex-TA DS 15 hydrogels with chondrocytes were used as a control under the same conditions.

5.2.10 Matrix production

After 1, 7, 14 and 21 days, samples were washed with PBS and frozen at -80 degrees Celsius. After thawing, the constructs were digested with proteinase-K solution at 56 degrees Celsius (more than 16 h). Quantification of total DNA was done using the CyQuant dye kit (Molecular Probes) and a fluorescent plate reader (Perkin-Elmer). The amount of GAG was determined spectrophotometrically after reaction with dimethylmethylene blue dye (DMMB, Sigma-Aldrich). The intensity of the color was quantified immediately with a microplate reader (EL 312e Bio-TEK Instruments) by measuring the absorbance at 540 nm. The amount of GAG was calculated using a standard of chondroitin sulphate A or B (Sigma-Aldrich). The total collagen content was determined using the hydroxyproline assay in which hydroxyproline makes up

12.5 % of collagen [38]. The hydroxyproline content was determined via a colorimetric assay by reaction with chloramine T and dimethylaminobenzaldehyde. All values were corrected for the background staining of gels without cells and normalized to the dry gel mass (expressed as GAG or collagen (μg)/mg dry gel) or DNA content (expressed as GAG or collagen (μg)/DNA (μg)). Data ($n=3$, measured in triplicate) are expressed as mean \pm standard deviation (SD).

5.2.11 Statistical analysis

Statistical differences between two groups were analyzed using a Student's t-test. Those among three or more groups were analyzed using the One-way Analysis of Variance (ANOVA) with Turkey's post-hoc analysis. Statistical significance was set to a p value <0.05 . Results are presented as mean \pm standard deviation.

5.3 Results and discussion

5.3.1 Synthesis and characterization of HA-g-Dex-TA copolymer

Hyaluronic acid (HA) was grafted with a preformed dextran-tyramine (Dex-TA) conjugate via a four-step reaction, as shown in Figure 5.2. First, according to a previously described method, dextran ($M_r = 6,000$ g/mol) was functionalized with tyramine moieties to give the Dex-TA conjugate [20]. The degree of substitution (DS), defined as the number of conjugated tyramine moieties per 100 anhydroglucose rings in dextran, was determined using ^1H NMR by comparing the integrals of signals at δ 5.0 (anomeric protons, Figure 5.3a, peak 1) and δ 6.9-7.2 (aromatic protons, Figure 5.3a, peak 2). Different Dex-TA conjugates with DS values of 5, 10, 15 and 20 were prepared by changing the feed molar ratio of p-nitrophenyl chloroformate to hydroxyl groups in dextran from 0.05 to 0.25.

The conjugates were subsequently modified at their reducing terminal glucose residue with an excess of N-Boc-1,4-diaminobutane, followed by reductive amination using sodium cyanoborohydride for 3 days. After the deprotection of the Boc group using trifluoroacetic acid, conjugates with a terminal free primary amine group (denoted as Dex-TA-NH₂) were obtained. Complete deprotection of the Boc group was confirmed by ^1H NMR showing the disappearance of the t-butyl signal at δ 1.4 (Figure 5.3a, peak 3). The degree of end group conversion was over 90 % as determined from ^1H NMR by comparing the integrals of signals at δ 5.0 (anomeric protons, Figure 5.3a, peak 1) and δ 1.5-1.6 (methylene protons, Figure 5.3a, peak 3). Finally, a coupling reaction between the primary amine groups of these Dex-TA-NH₂ conjugates and the carboxylic acid groups of HA using an EDAC/NHS activation reaction at a feed molar ratio of HA to NH₂ of 1:6 yielded the HA-g-Dex-TA graft copolymers. The molecular weights of these polymers were determined by gel-permeation chromatography (GPC).

Typical elution profiles of Dex-TA-NH₂ DS 10, HA and HA-g-Dex-TA DS 10 are presented in Figure 5.4. The HA-g-Dex-TA DS 10 polymer was eluted earlier than HA and Dex-TA-NH₂ DS 10 in a unimodal GPC-trace. This indicated that the

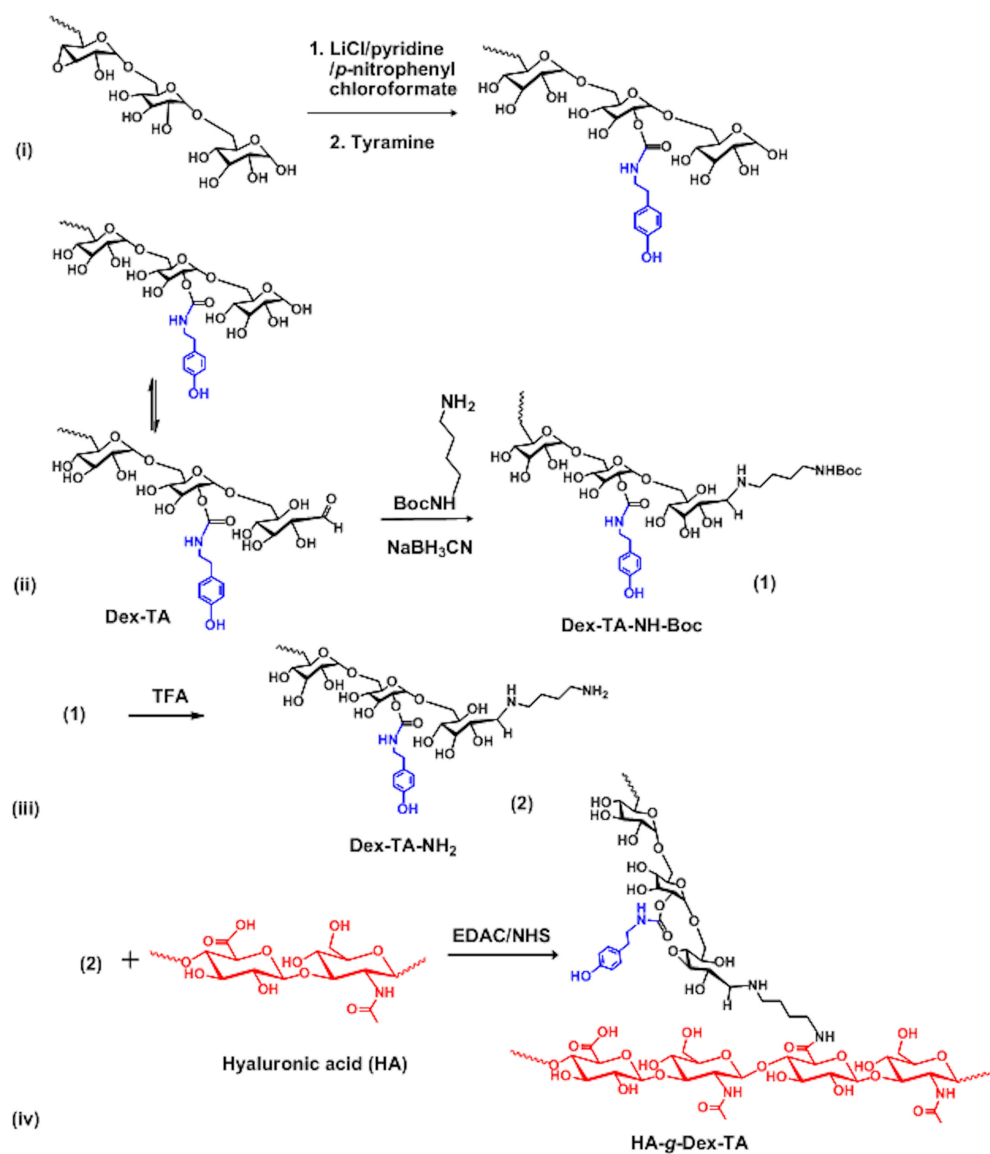


Figure 5.2: Synthesis of hyaluronic acid grafted with dextran-tyramine conjugates (HA-g-Dex-TA).

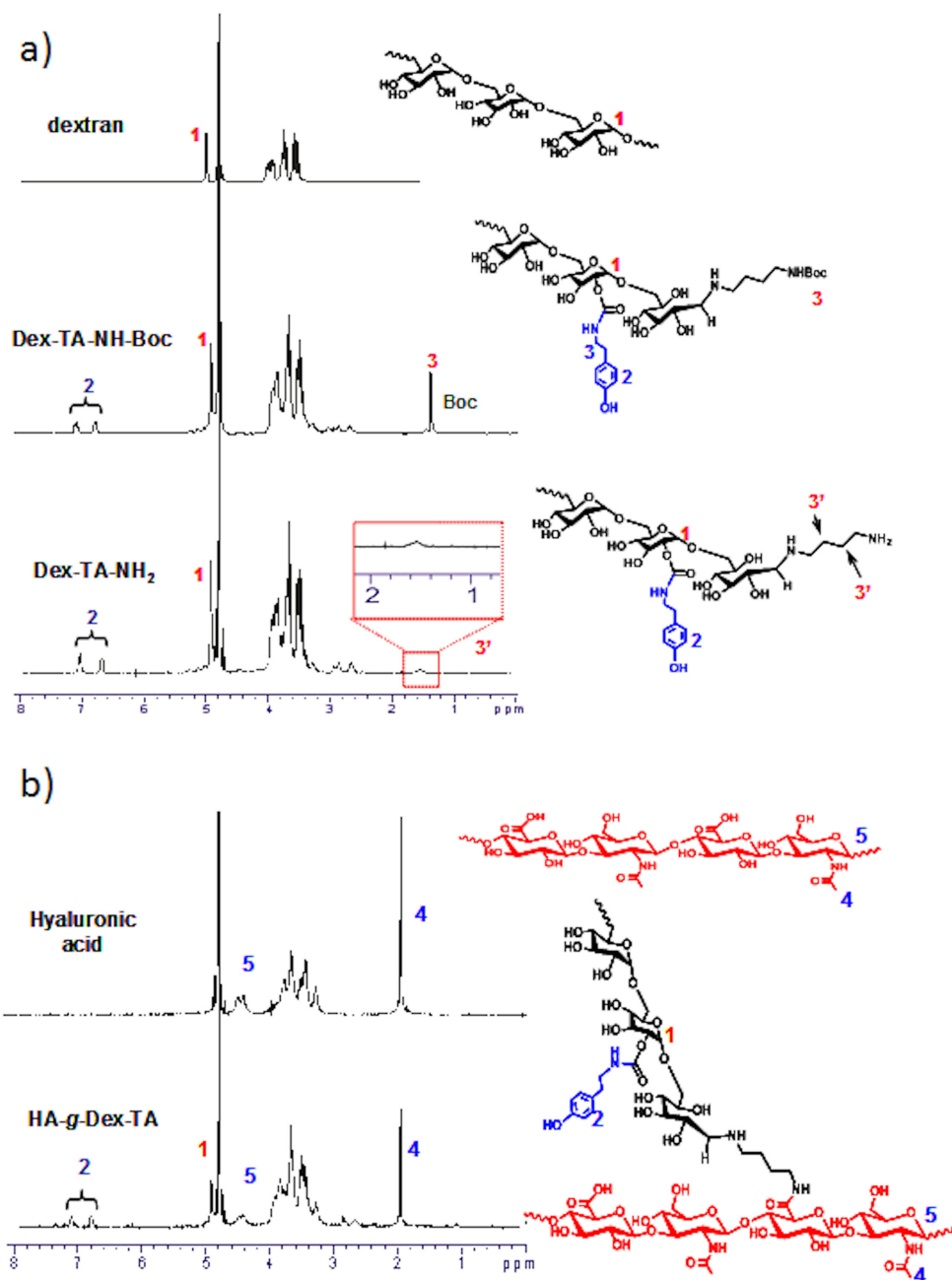


Figure 5.3: ¹H-NMR spectra of dextran, Dex-TA, Dex-TA-NH-Boc and Dex-TA-NH₂; (b) hyaluronic acid (HA) and HA grafted with dextran-tyramine conjugates (HA-g-Dex-TA) in D₂O.

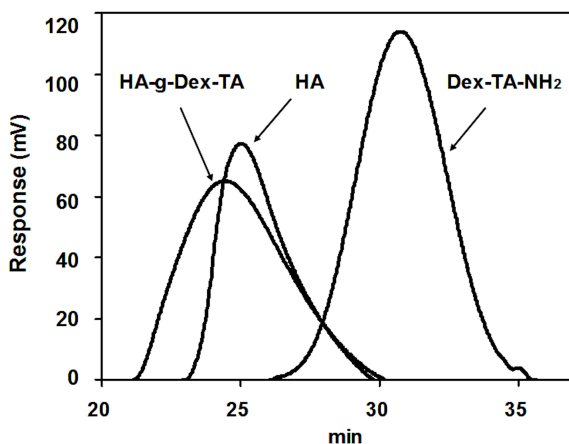


Figure 5.4: GPC chromatograms of Dex-TA-NH₂ DS 10, HA and the copolymer HA-g-Dex-TA DS 10. Eluent: NaAc buffer (300 Mm, pH 4.5, containing 30 % (v/v) methanol).

HA-g-Dex-TA polymer was successfully synthesized. The average number molecular weights of these polymers ranged from 38.4 to 40.0 kg/mol with a relatively low polydispersity index (PDI 1.3-1.7) (Table 5.1). The chemical structure of the HA-g-Dex-TA polymers was confirmed by ¹H NMR. In Figure 5.3b, it is shown that besides signals attributable to the anomeric and methyl protons of HA (peaks 4 and 5), new peaks at 5.0 (peak 1) and 6.9-7.2 (peaks 2) were present in the spectra. These peaks were attributable to the anomeric and aromatic protons from coupled Dex-TA. The number of grafted Dex-TA conjugates per HA molecule was approximately 4, as determined with ¹H NMR by comparing the integrals of signals at δ 2.0 (methyl protons of acetamide groups in HA) and δ 5.0 (dextran anomeric protons) (Table 5.I). It was found that the average number molecular weights of the HA-g-Dex-TA polymers calculated using ¹H NMR were in agreement with those determined by GPC measurements.

5.3.2 Hydrogel formation and gelation time

Hydrogels of HA-g-Dex-TA were conveniently prepared in PBS by the horseradish peroxidase (HRP)-mediated coupling reaction of phenol moieties. According to earlier research, 0.25 mg HRP per mmol phenol moieties and a molar ratio of H₂O₂/TA of 0.2 were applied in this study due to the good cytocompatibility of the resulting gels [39]. The gelation time was determined by the vial tilting method.

The enzymatic crosslinking of HA-g-Dex-TA led to fast gelation, i.e. the gelation times were within 2 min for all combinations tested (Figure 5.5). The longest gelation times were found for the HA-g-Dex-TA copolymers with a low DS, due to the decreased number of tyramine units per chain. Effects on gelation time were even

| Polymer (code) | M_n (kg/mol) | PDI | $M_{n,NMR}$ (kg/mol) | Number of grafted Dex-TA per HA chain (n) | Number of TA per HA chain |
|-------------------------|-------------------|-----|-------------------------|---|---------------------------------|
| Dextran | 3.3 | 1.7 | -- | -- | -- |
| Hyaluronic acid (HA) | 25.4 | 1.8 | -- | -- | -- |
| HA-g-Dex-TA DS 5 | 39.2 | 1.6 | 40.4 | 4.3 | 4.3 |
| HA-g-Dex-TA DS 10 | 38.4 | 1.3 | 38.2 | 4.0 | 8.0 |
| HA-g-Dex-TA DS 15 | 39.2 | 1.6 | 38.3 | 4.2 | 12.8 |
| HA-g-Dex-TA DS 20 | 40.0 | 1.7 | 40.9 | 4.5 | 18.8 |

a. Coupling reactions between HA and Dex-TA-NH₂ were performed in MES with a feed molar ratio of HA to NH₂ of 1:6.

Table 5.1: Composition, molecular weight and polydispersity of HA-g-Dex-TA copolymers (a)

more pronounced with decreasing polymer concentration. The fastest gelation, within 10 s, occurred using HA-g-Dex-TA DS 20 hydrogels at a polymer concentration of 10 % wt. Thus, an attractive feature of these HA-g-Dex-TA hydrogel systems is that the gelation occurred in a reasonably short time (10 s to 2 min) under mild conditions. Furthermore, gelation times of the HA-g-Dex-TA hydrogels can be easily tuned by adjusting the DS of tyramine units and polymer concentration, which makes the systems highly suitable as injectable scaffolds for various applications.

5.3.3 Hydrogel characterization

The degree of swelling of the HA-g-Dex-TA hydrogels in PBS was determined after 72 h (Figure 5.6). In general, all HA-g-Dex-TA hydrogels showed degrees of swelling ranging from 15 to 41. These values were in the same range of photocrosslinked HA-based hydrogels [40, 41]. Additionally, the values were lower at higher DS values of tyramine units and higher polymer concentration ($p < 0.05$). This can be explained by the increased crosslinking density of the hydrogels. Compared to previously reported Dex-TA hydrogels, HA-g-Dex-TA hydrogels showed improved swelling behavior [20], which can be explained by an increase in water uptake resulting from the electrostatic repulsion of negatively-charged HA chains at pH 7.4.

The storage moduli (G') of the HA-g-Dex-TA hydrogels after gelation were determined at 37 degrees Celsius by rheology. As shown in Figure 5.7, hydrogels prepared

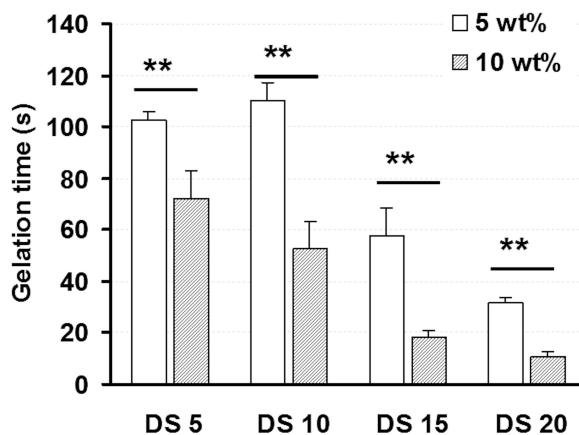


Figure 5.5: Gelation time of hydrogels based on HA-g-Dex-TA as a function of DS and concentration. (n=3, ** p<0.01)

at a concentration of 10 % wt showed a 2 to 3 fold higher storage modulus compared to 5 % wt hydrogels. Furthermore, by increasing the DS from 5 to 20, the corresponding G' values significantly increased. This is most likely due to the increased crosslinking density in DS 10 gels versus DS 5 gels. In general, the moduli of HA-g-Dex-TA hydrogels ranged from 370 to 18000 Pa. This is comparable to values previously reported for dextran-tyramine hydrogels [20]. They are, however, much higher than values reported for other enzymatically crosslinked hydrogels such as hyaluronic acid-tyramine DS 6 hydrogels (10-4000 Pa) [19].

5.3.4 Enzymatic degradation

HA is biodegradable via enzymatic hydrolysis using hyaluronidase (HAse) [42]. To determine the enzymatic degradation profiles of the HA-g-Dex-TA hydrogels, 2 mL of PBS containing 100 U/mL HAse was applied on top of 0.25 mL of the hydrogels. The hydrogels were kept at 37 degrees Celsius and their weights were monitored at regular time intervals. The remaining gel (%) was expressed as the remaining gel weight after exposure to enzyme buffer (Wt) divided by the original gel weight after preparation (Wi). In buffer without the enzyme present, the gels swelled and the weight increased during the first 3 days, which remained stable up to 21 days (data not shown). In the presence of hyaluronidase, the gel weight first increased because of water uptake during the degradation process, and then decreased when the increase in the swelling is overtaken by the gel weight loss due to the dissolution and release of small fragments. The degradation time was defined as the time required to completely dissolve at least one of 3 samples tested. It was found that the degradation of HA-g-Dex-TA hydrogels depended on the DS and polymer concentration (Figure 5.8). The HA-g-Dex-TA DS 5 hydrogels prepared at polymer concentrations of 5 and 10 % wt

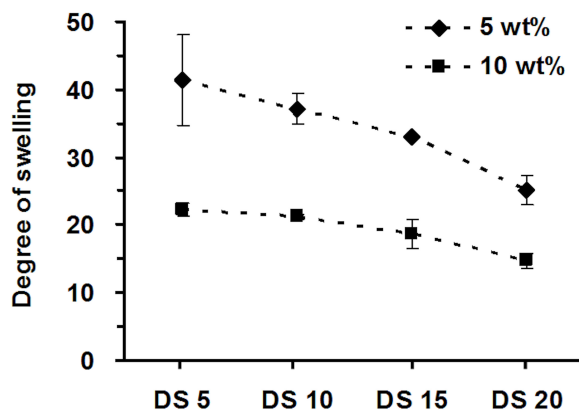


Figure 5.6: Degree of swelling of HA-g-Dex-TA hydrogels as a function of DS ($n=3$).

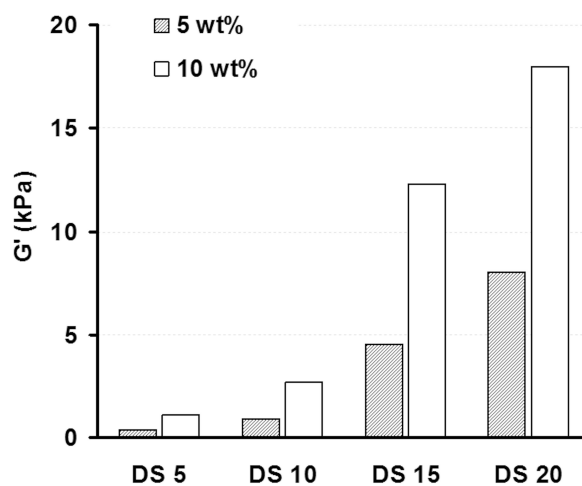


Figure 5.7: Storage modulus of HA-g-Dex-TA hydrogels as a function of DS ($n=1$).

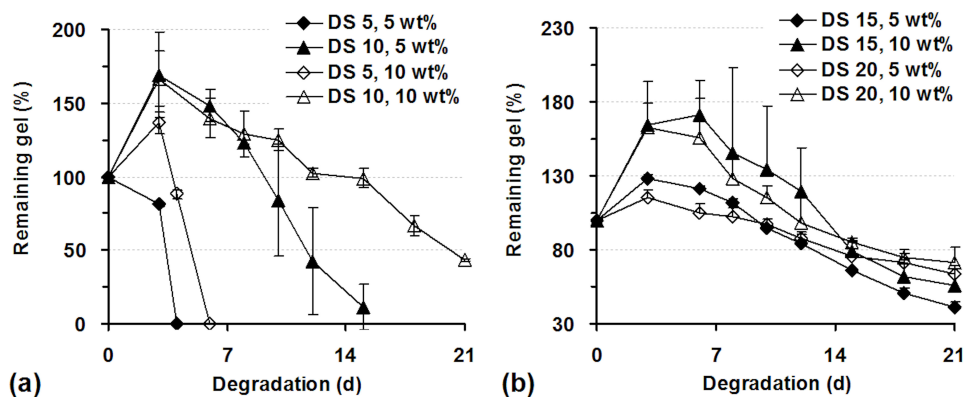


Figure 5.8: Enzymatic degradation of HA-g-Dex-TA hydrogels at DS 5, 10 (a) and DS 15, 20 (b) exposed to PBS containing 100 U/ml Hase at 37 degrees Celsius (n=3).

were completely degraded after 4 and 6 days, respectively, while the 5 % wt HA-g-Dex-TA DS 10 hydrogels showed a longer degradation time of 15 days. The hydrogels of HA-g-Dex-TA at a high DS of 15 and 20 were more stable with more than 30 % wt of gel remaining after 21 days of degradation. Even after 2 months, these gels were not completely degraded (data not shown). Compared to previously reported hyaluronic acid-tyramine (HA-TA) hydrogels which were completely degraded within 1 day in the presence of 25 U/mL of Hase in PBS [19], our gels were much more stable even in the presence of a 4-fold higher concentration of Hase (100U/mL). The increased stability can be attributed to the presence of dextran. The improved degradation characteristics compared to HA-TA gels makes HA-g-Dex-TA hydrogels more suitable for cartilage tissue engineering.

5.3.5 Cytotoxicity

In cell experiments, 10 % wt HA-g-Dex-TA DS 15 and 20 hydrogels, which showed the best stability, were selected for the preparation of gel/cell constructs for *in vitro* studies. The cytocompatibility of HA-g-Dex-TA DS 15 and 20 hydrogels was investigated by the incorporation of bovine chondrocytes in HA-g-Dex-TA hydrogels at a polymer concentration of 10 % wt. Cell survival of the chondrocytes was analyzed by a Live-dead assay (Figure 5.9), in which living cells fluoresce green and dead cells fluoresce red. In both HA-g-Dex-TA DS 15 and DS 20 hydrogels, over 95 % of chondrocytes stained green, indicating cytocompatible enzymatic crosslinking conditions.

5.3.6 Chondrocyte morphology

The cell/scaffold constructs were investigated by SEM (Figure 5.10). The chondrocytes encapsulated inside HA-g-Dex-TA DS15 and 20 hydrogels retained a round

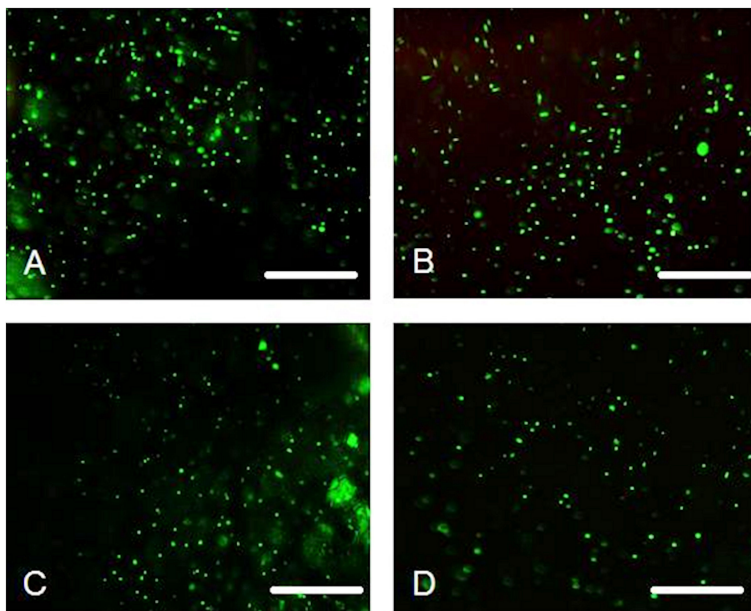


Figure 5.9: (a) Live-dead assay showing chondrocytes incorporated in HA-g-Dex-TA DS 15 (A and C) and DS 20 (B and D) hydrogels after 7 (A and B) and 14 (C and D) days in culture. Scale bar: 500 μm .

shape at 21 days in culture, which was also observed in Dex-TA DS 15 hydrogels [39]. High magnification of SEM images showed that the chondrocytes deposited an extracellular matrix.

5.3.7 Swelling and degradation of hydrogels in the presence of cells

To study the swelling and degradation behavior of the HA-g-Dex-TA hydrogels in the presence of chondrocytes, the constructs were incubated in a chondrocyte expansion medium and weighed at regular intervals. The swelling ratio of a Dex-TA DS 15 hydrogel remained almost constant during the total culturing time up to 21 days. In contrast, the swelling ratios of the HA-g-Dex-TA hydrogels increased from day 1 to day 7 and decreased slightly after day 14 (Figure 5.11a). The swelling behavior suggests a loss in crosslinking density with time as a result of degradation [19]. This is supported by the pronounced decrease in the swelling ratio for HA-g-Dex-TA DS 15 hydrogels at day 14 and day 21 compared to day 1. The degradation of HA-g-Dex-TA hydrogels was further studied by determining the dry gel mass, which is normalized to the initial wet gel weight after preparation (Figure 5.11b). Dex-TA DS 15 hydrogels had a dry gel mass of 8 % at day 1, which remained stable up to 21 days. In contrast, the values for HA-g-Dex-TA DS 15 and 20 hydrogels decreased from 8 % at day 1 to

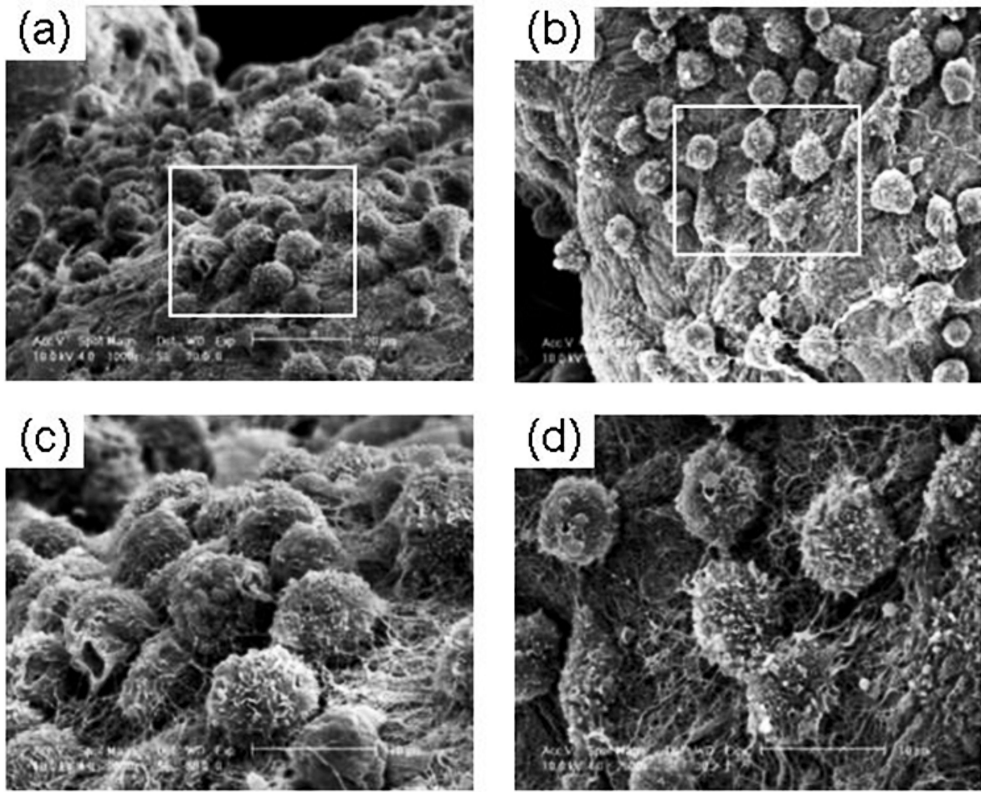


Figure 5.10: SEM images of chondrocytes incorporated in the (a) HA-g-Dex-TA DS 15 and (b) HA-g-Dex-TA DS 20 hydrogels at day 21. High magnification SEM images of the boxed regions of Figure 5.10a and 5.10b are shown in Figure 9c and 9d, respectively.

3 % and 6 % at day 21, respectively ($p < 0.05$). The significant differences ($p < 0.05$) in the swelling and degradation behavior in time between the Dex-TA and the HA-g-Dex-TA hydrogels are most likely explained by the presence of Hase produced by incorporated chondrocytes [43].

5.3.8 Cell proliferation and matrix production

Our earlier studies have shown that chondrocytes incorporated in Dex-TA hydrogels proliferated and maintained their phenotype without dedifferentiating to fibroblast-like cells [39]. Chondrocyte proliferation in HA-g-Dex-TA DS 15 and DS 20 hydrogels was assessed by a CyQuant DNA assay by measuring the DNA content of the hydrogels during the culturing period up to 21 days. The phenotype of chondrocytes incorporated was characterized in terms of their matrix production. The ECM ma-

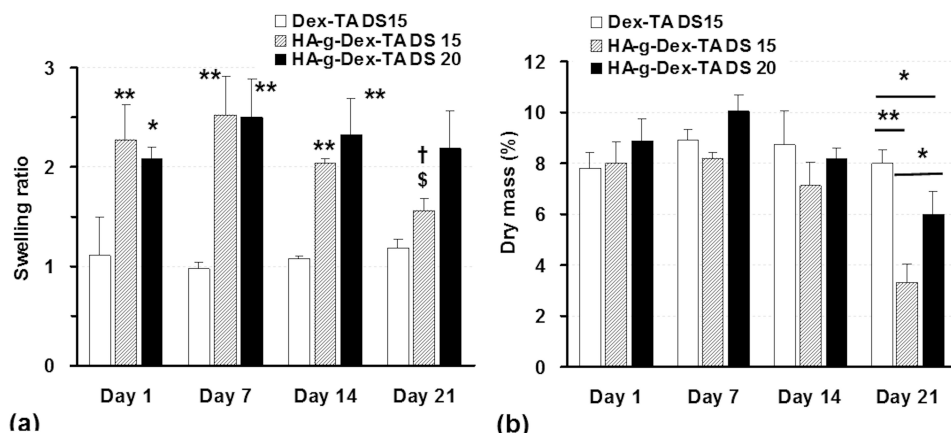


Figure 5.11: (a) Swelling and (b) degradation of Dex-TA and HA-g-Dex-TA hydrogels in the presence of chondrocytes as a function of culturing time. Figure 5.11a: * $p < 0.05$, ** $p < 0.01$, vs. Dex-TA DS 15; $p < 0.05$, vs. Day 1; $p < 0.01$, vs. Day 7). Figure 5.11b: the dry mass of the construct is normalized to the original wet gel weight after preparation. (* $p < 0.05$, ** $p < 0.01$)

trix produced was analyzed by a dimethylmethylene blue assay and a hydroxyproline assay for glycosaminoglycans (GAGs) and collagen, respectively, and the values were normalized to the dry gel weight of each sample.

In the CyQuant DNA assay, the DNA content was expressed as the DNA amount normalized to the dry gel weight. Results were compared to hydrogels prepared from a dextran-tyramine conjugate Dex-TA DS 15 (Mn, Dex=14.5 kg/mol) which served as a reference [20, 25]. In general, in all these hydrogels the DNA content increased with increasing culturing time. Interestingly, at day 21, the DNA content in the HA-g-Dex-TA DS 15 hydrogel was higher than that in the Dex-TA DS15 hydrogel (Figure 5.512a). These results demonstrated the benefit of the presence of HA in Dex-TA hydrogels.

In the control group of GAG assay, hydrogels prepared from Dex-TA DS15, the GAG content increased from day 1 to day 7, and then remained unchanged throughout the experimental period (Figure 5.12b). Similar trends were also observed for the HA-g-Dex-TA hydrogels. The HA-g-Dex-TA DS 15 hydrogels showed a statistically higher average GAG content per mg of dry gel weight than the Dex-TA DS 15 hydrogels at day 14 and 21 (4.8 vs 2.3 and 4.9 vs 1.7, respectively). The average GAG content in HA-g-Dex-TA DS 20 hydrogels was found to be 2.7 and 2.6 μg per mg of dry gel weight at day 14 and 21, respectively, which was close to that of Dex-TA DS 15 hydrogels. These results suggest that the DS of the Dex-TA conjugate in the HA-g-Dex-TA had a significant effect on the GAG production, indicating that appropriate design of the gel chemistry might lead to an optimal performance in ECM production.

The total collagen content, determined using a hydroxyproline assay, was normalized to the dry gel weight (Figure 5.12c). The results showed that the total collagen

| Polymer (code) | M_n (kg/mol) | PDI | $M_{n,NMR}$ (kg/mol) | Number of grafted Dex-TA per HA chain (n) | Number of TA per HA chain |
|-------------------------|-------------------|-----|-------------------------|---|---------------------------------|
| Dextran | 3.3 | 1.7 | -- | -- | -- |
| Hyaluronic acid (HA) | 25.4 | 1.8 | -- | -- | -- |
| HA-g-Dex-TA DS 5 | 39.2 | 1.6 | 40.4 | 4.3 | 4.3 |
| HA-g-Dex-TA DS 10 | 38.4 | 1.3 | 38.2 | 4.0 | 8.0 |
| HA-g-Dex-TA DS 15 | 39.2 | 1.6 | 38.3 | 4.2 | 12.8 |
| HA-g-Dex-TA DS 20 | 40.0 | 1.7 | 40.9 | 4.5 | 18.8 |

a. Coupling reactions between HA and Dex-TA-NH₂ were performed in MES with a feed molar ratio of HA to NH₂ of 1:6.

Figure 5.12: (a) DNA content normalized to dry gel weight of Dex-TA DS 15, HA-g-Dex-TA DS 15 and 20 hydrogels containing chondrocytes after *in vitro* culturing for 1, 7, 14 and 21 days. (* $p < 0.05$ at day 7; ** $p < 0.01$ vs. HA-g-Dex-TA DS 15 at day 14 and 21) (b) GAG and (c) total collagen accumulation (values were normalized to the dry gel weight per sample) in Dex-TA and HA-g-Dex-TA hydrogels containing chondrocytes after *in vitro* culturing for 1, 7, 14 and 21 days. (** $p < 0.01$ vs. Dex-TA DS 15 at each time point) (d) GAG and total collagen content normalized to DNA content in Dex-TA and HA-g-Dex-TA hydrogels containing chondrocytes after *in vitro* culturing for 21 days. (* $p < 0.05$ vs. Dex-TA DS 15).

accumulation increased in time and reached the highest value at day 21 for all groups. Interestingly, the average value of total collagen content was higher in HA-g-Dex-TA DS 15 and DS 20 hydrogels than in Dex-TA DS 15 hydrogels, irrespective of the culturing time. After 7 and 21 days in culture, significant higher collagen deposition was found in HA-g-Dex-TA DS 15 than in Dex-TA DS 15 hydrogels.

For comparative studies, the GAG and total collagen content were normalized to the DNA content, as shown in Figure 5.12d. In general, enhanced matrix deposition was observed for HA-g-Dex-TA compared to Dex-TA hydrogels. At day 21, the GAG/DNA ratio was 1.6 fold higher in the HA-g-Dex-TA DS 15 hydrogels than Dex-TA hydrogels. Further, significantly higher collagen/DNA ratios were observed for HA-g-Dex-TA DS 20 hydrogels than for Dex-TA DS 15 hydrogels. Previous studies have shown that GAGs play an important role in regulating the expression of the chondrocyte phenotype and support matrix formation [44, 45]. Therefore, the application of hyaluronic acid, one of the components of a native cartilaginous matrix, could be a reason for enhanced matrix production [46-48].

Taken together, HA-g-Dex-TA hybrids were designed which resemble the macro-structure of proteoglycans as can be found in native cartilage. Biomimetic hydrogels based on these materials showed a better stability than HA-TA hydrogels and an improved chondrocyte performance than Dex-TA hydrogels. Thus they hold great promise as injectable scaffolds for cartilage tissue engineering. Importantly, the concept for the design of proteoglycan analogs can be easily extended to other polysaccharides such as heparan sulfate and chondroitin sulfate or proteins such as collagen.

5.4 Conclusions

Novel injectable biomimetic hydrogels based on polysaccharide hybrids (HA-g-Dex-TA) were designed for cartilage tissue engineering. HA-g-Dex-TA copolymers were prepared by the conjugation of dextran-tyramine conjugates with different degrees of substitution of tyramine units (DS 5, 10, 15 and 20) to hyaluronic acid using EDAC/NHS activation. Hydrogels were obtained by enzymatic crosslinking of HA-g-Dex-TA under physiological conditions using HRP as a catalyst and H_2O_2 as an oxidant. The gelation is fast with gelation times lower than 2 min, which can be regulated by varying the DS and polymer concentration. Hydrogels are readily degraded in the presence of hyaluronidase. Hydrogels prepared at a higher DS and concentration had higher storage moduli and stability. The behavior of chondrocytes incorporated inside HA-g-Dex-TA hydrogels demonstrated that the gel systems had a good biocompatibility. Compared to Dex-TA hydrogels, these biomimetic HA-g-Dex-TA hydrogels induced an enhanced cell proliferation and matrix deposition (increased glycosaminoglycan and collagen production). In conclusion, we have demonstrated that these novel injectable biomimetic hydrogels based on polysaccharide hybrids are very promising for the development of scaffolds for cartilage tissue engineering.

References

1. Bryant SJ, Anseth KS. Hydrogel Properties Influence ECM Production by Chondrocytes Photoencapsulated in Poly(ethylene glycol) Hydrogels. *J. Biomed. Mater. Res.* 2002;59: 63-72.
2. Bryant SJ, Anseth KS. Controlling the Spatial Distribution of ECM Components in Degradable PEG Hydrogels for Tissue Engineering Cartilage. *J. Biomed. Mater. Res. A* 2003;64A: 70-79.
3. Bryant SJ, Anseth KS, Lee DA, Bader DL. Crosslinking Density Influences the Morphology of Chondrocytes Photoencapsulated in PEG Hydrogels During the Application of Compressive Strain. *J. Orthop. Res.* 2004;22: 1143-1149.
4. Bryant SJ, Arthur JA, Anseth KS. Incorporation of Tissue-Specific Molecules Alters Chondrocyte Metabolism and Gene Expression in Photocrosslinked Hydrogels. *Acta Biomater.* 2005;1: 243-252.
5. Bryant SJ, Bender RJ, Durand KL, Anseth KS. Encapsulating Chondrocytes in Degrading PEG Hydrogels with High Modulus: Engineering Gel Structural Changes to Facilitate Cartilaginous Tissue Production. *Biotech. Bioeng.* 2004;86: 747-755.
6. Bryant SJ, Durand KL, Anseth KS. Manipulations in Hydrogel Chemistry Control Photoencapsulated Chondrocyte Behavior and Their Extracellular Matrix Production. *J. Biomed. Mater. Res. A* 2003;67A: 1430-1436.
7. Elisseeff J, Anseth K, Sims D, McIntosh W, Randolph M, Langer R. Transdermal Photopolymerization for Minimally Invasive Implantation. *Proc. Natl. Acad. Sci. USA* 1999;96: 3104-3107.
8. Fedorovich NE, Oudshoorn MH, van Geemen D, Hennink WE, Alblas J, Dhert WJA. The Effect of Photopolymerization on Stem Cells Embedded in Hydrogels. *Biomaterials* 2009;30: 344-353.
9. Williams CG, Malik AN, Kim TK, Manson PN, Elisseeff JH. Variable Cytocompatibility of Six Cell Lines with Photoinitiators Used for Polymerizing Hydrogels and Cell Encapsulation. *Biomaterials* 2005;26: 1211-1218.
10. Jefferiss CD, Lee AJC, Ling RSM. Thermal Aspects of Self-Curing Polymethylmethacrylate. *J. Bone Joint Surg. Br.* 1975;57B: 511-518.
11. Hiemstra C, van der Aa LJ, Zhong Z, Dijkstra PJ, Feijen J. Rapidly *in situ*-Forming Degradable Hydrogels from Dextran Thiols through Michael Addition. *Biomacromolecules* 2007;8: 1548-1556.
12. Hiemstra C, van der Aa LJ, Zhong Z, Dijkstra PJ, Feijen J. Novel *in situ* Forming, Degradable Dextran Hydrogels by Michael Addition Chemistry: Synthesis, Rheology, and Degradation. *Macromolecules* 2007;40: 1165-1173.
13. Tortora M, Cavalieri F, Chiessi E, Paradossi G. Michael-Type Addition Reactions for the *in situ* Formation of Poly(vinyl alcohol)-Based Hydrogels. *Biomacromolecules* 2007;8: 209-214.
14. Zheng Shu X, Liu Y, Palumbo FS, Luo Y, Prestwich GD. *in situ* Crosslinkable Hyaluronan Hydrogels for Tissue Engineering. *Biomaterials* 2004;25: 1339-1348.
15. Lutolf MP, Lauer-Fields JL, Schmoekel HG, Metters AT, Weber FE, Fields GB, and Hubbell JA. Synthetic Matrix Metalloproteinase-Sensitive Hydrogels for the Conduction of Tissue Regeneration: Engineering Cell-Invasion Characteristics. *Proc.*

Natl. Acad. Sci. USA 2003;100: 5413-5418.

16. Lutolf MP, Raeber GP, Zisch AH, Tirelli N, Hubbell JA. Cell-Responsive Synthetic Hydrogels. *Adv. Mater.* 2003;15: 888-892.

17. Lutolf MP, Hubbell JA. Synthesis and Physicochemical Characterization of End-Linked Poly(ethylene glycol)-Co-Peptide Hydrogels Formed by Michael-Type Addition. *Biomacromolecules* 2003;4: 713-722.

18. Hahn SK, Oh EJ, Miyamoto H, Shimobouji T. Sustained Release Formulation of Erythropoietin Using Hyaluronic Acid Hydrogels Crosslinked by Michael Addition. *Int. J. Pharm.* 2006;322: 44-51.

19. Lee F, Chung JE, Kurisawa M. An Injectable Enzymatically Crosslinked Hyaluronic Acid-Tyramine Hydrogel System with Independent Tuning of Mechanical Strength and Gelation Rate. *Soft Matter.* 2008;4: 880-887.

20. Jin R, Hiemstra C, Zhong Z, Feijen J. Enzyme-Mediated Fast *in situ* Formation of Hydrogels from Dextran-Tyramine Conjugates. *Biomaterials* 2007;28: 2791-2800.

21. Ogushi Y, Sakai S, Kawakami K. Synthesis of Enzymatically-Gellable Carboxymethylcellulose for Biomedical Applications. *J. Biosci. Bioeng.* 2007;104: 30-33.

22. Sakai S, Kawakami K. Synthesis and Characterization of Both Ionically and Enzymatically Cross-Linkable Alginate. *Acta Biomater.* 2007;3: 495-501.

23. Jin R, Moreira Teixeira LS, Dijkstra PJ, Karperien M, van Blitterswijk CA, Zhong ZY, and Feijen J. Injectable Chitosan-Based Hydrogels for Cartilage Tissue Engineering. *Biomaterials* 2009;30: 2544-2551.

24. Sakai S, Hirose K, Taguchi K, Ogushi Y, Kawakami K. An Injectable, *in situ* Enzymatically Gellable, Gelatin Derivative for Drug Delivery and Tissue Engineering. *Biomaterials* 2009;30: 3371-3377.

25. Jin R, Moreira Teixeira LS, Dijkstra PJ, Karperien M, Zhong Z, Feijen J. Fast *in-Situ* Formation of Dextran-Tyramine Hydrogels for *in vitro* Chondrocyte Culturing. *J. Control. Release* 2008;132: e24-26.

26. Moreira Teixeira LS, Jin R, Dijkstra PJ, Feijen J, van Blitterswijk CA, Karperien M. Chitosan-Based Hydrogels as Extracellular Matrix for Cartilage Tissue Engineering: *in vitro* Biological Evaluation. *Tissue Eng. A* 2008;14: 711.

27. Yu L, Ding J. Injectable Hydrogels as Unique Biomedical Materials. *Chem. Soc. Rev.* 2008;37: 1473-1481.

28. Van Tomme SR, Storm G, Hennink WE. *in situ* Gelling Hydrogels for Pharmaceutical and Biomedical Applications. *Int. J. Pharm.* 2008;355: 1-18.

29. Kretlow JD, Klouda L, Mikos AG. Injectable Matrices and Scaffolds for Drug Delivery in Tissue Engineering. *Adv. Drug Deliver. Rev.* 2007;59: 263-273.

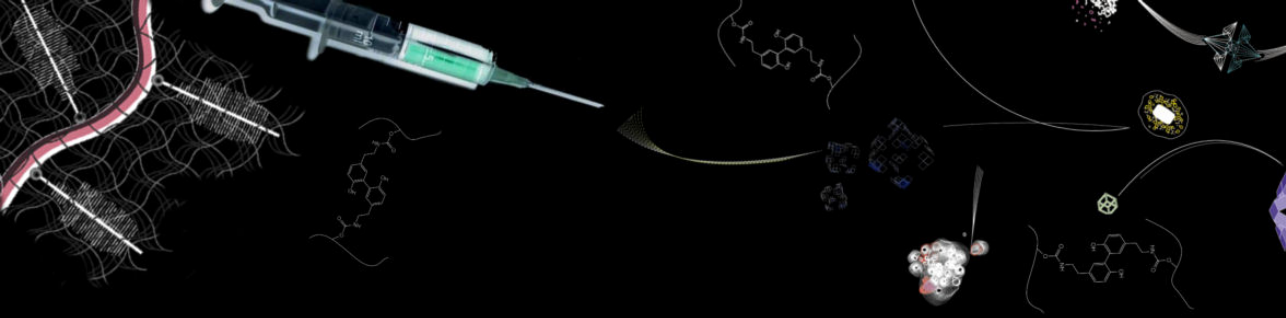
30. Malafaya PB, Silva GA, Reis RL. Natural-Origin Polymers as Carriers and Scaffolds for Biomolecules and Cell Delivery in Tissue Engineering Applications. *Adv. Drug Deliver. Rev.* 2007;59: 207-233.

31. Hong Y, Song H, Gong Y, Mao Z, Gao C, Shen J. Covalently Crosslinked Chitosan Hydrogel: Properties of *in vitro* Degradation and Chondrocyte Encapsulation. *Acta Biomater.* 2007;3: 23-31.

32. Hoemann CD, Sun J, Legare A, McKee MD, Buschmann MD. Tissue Engineering of Cartilage Using an Injectable and Adhesive Chitosan-Based Cell-Delivery Vehicle. *Osteoarthr. Cartilage* 2005;13: 318-329.

33. Rowley JA, Madlambayan G, Mooney DJ. Alginate Hydrogels as Synthetic Extracellular Matrix Materials. *Biomaterials* 1999;20: 45-53.
34. Park KM, Joung YK, Park KD, Lee SY, Lee MC. Rgd-Conjugated Chitosan-Pluronic Hydrogels as a Cell Supported Scaffold for Articular Cartilage Regeneration. *Macromol. Res.* 2008;16: 517-523.
35. Park KM, Lee SY, Joung YK, Na JS, Lee MC, Park KD. Thermosensitive Chitosan-Pluronic Hydrogel as an Injectable Cell Delivery Carrier for Cartilage Regeneration. *Acta Biomater.* 2009;5: 1956-1965.
36. Toole BP. Hyaluronan in Morphogenesis. *Seminars in Cell and Developmental Biology* 2001;12: 79-87.
37. Akmal M, Singh A, Anand A, Kesani A, Aslam N, Goodship A, and Bentley G. The Effects of Hyaluronic Acid on Articular Chondrocytes. *J. Bone Joint Surg. Br.* 2005;87-B: 1143-1149.
38. Edwards CA, O'Brien Jr WD. Modified Assay for Determination of Hydroxyproline in a Tissue Hydrolyzate. *Clin. Chim. Acta* 1980;104: 161-167.
39. Jin R, Moreira Teixeira LS, Dijkstra PJ, Karperien M, van Blitterswijk CA, Feijen J. Enzymatically Crosslinked Dextran-Tyramine Hydrogels as Injectable Scaffolds for Cartilage Tissue Engineering. Chapter 5.
40. Jia X, Burdick JA, Kobler J, Clifton RJ, Rosowski JJ, Zeitel SM, and Langer R. Synthesis and Characterization of *in situ* Cross-Linkable Hyaluronic Acid-Based Hydrogels with Potential Application for Vocal Fold Regeneration. *Macromolecules* 2004;37: 3239-3248.
41. Jennie Baier L, Kathryn AB, Charles WP, Jr., Christine ES. Photocrosslinked Hyaluronic Acid Hydrogels: Natural, Biodegradable Tissue Engineering Scaffolds. *Biotechnology and Bioengineering* 2003;82: 578-589.
42. Menzel EJ, Farr C. Hyaluronidase and Its Substrate Hyaluronan: Biochemistry, Biological Activities and Therapeutic Uses. *Cancer Letters* 1998;131: 3-11.
43. Tanimoto K, Suzuki A, Ohno S, Honda K, Tanaka N, Doi T, Nakahara-Ohno M, Yoneno K, Nakatani Y, Ueki M, Yanagida T, Kitamura R, and Tanne K. Hyaluronidase Expression in Cultured Growth Plate Chondrocytes During Differentiation. *Cell Tissue Res.* 2004;318: 335-342.
44. Sechriest VF, Miao YJ, Niyibizi C, Westerhausen-Larson A, Matthew HW, Evans CH, Fu FH, and Suh J-K. GAG-Augmented Polysaccharide Hydrogel: A Novel Biocompatible and Biodegradable Material to Support Chondrogenesis. *J. Biomed. Mater. Res.* 2000;49: 534-541.
45. Mouw JK, Case ND, Guldberg RE, Plaas AHK, Levenston ME. Variations in Matrix Composition and Gag Fine Structure among Scaffolds for Cartilage Tissue Engineering. *Osteoarthr. Cartilage* 2005;13: 828-836.
46. Abe M, Takahashi M, Nagano A. The Effect of Hyaluronic Acid with Different Molecular Weights on Collagen Crosslink Synthesis in Cultured Chondrocytes Embedded in Collagen Gels. *J. Biomed. Mater. Res. A* 2005;75A: 494-499.
47. Liao E, Yaszemski M, Krebsbach P, Hollister S. Tissue-Engineered Cartilage Constructs Using Composite Hyaluronic Acid/Collagen I Hydrogels and Designed Poly(propylene fumarate) Scaffolds. *Tissue Eng.* 2007;13: 537-550.
48. Chung C, Burdick JA. Influence of Three-Dimensional Hyaluronic Acid Microen-

vironments on Mesenchymal Stem Cell Chondrogenesis. Tissue Eng. A 2009;15: 243-254.



Chapter 6

Chondrogenesis in Injectable Enzymatically Crosslinked Heparin/Dextran Hydrogels

6

Liliana Moreira Teixeira*, Rong Jin*, Piet Dijkstra, Zhiyuan Zhong, Marcel Karperien, Clemens van Blitterswijk, Jan Feijen

* Shared first co-authorship

Abstract

In this study, injectable hydrogels were prepared by the horseradish peroxidase-mediated co-crosslinking of dextran-tyramine (Dex-TA) and heparin-tyramine (Hep-TA) conjugates and used as scaffolds for cartilage tissue engineering. The swelling and mechanical properties of these hydrogels can be easily controlled by the Dex-TA/Hep-TA weight ratio. When chondrocytes were incorporated in these gels, cell viability and proliferation were highest for gels with a 50/50 weight ratio of Dex-TA/Hep-TA. Moreover, these hydrogels induced an enhanced production of chondroitin sulfate and a more abundant presence of collagen as compared to Dex-TA hydrogels. The results indicate that injectable Dex-TA/Hep-TA hydrogels are promising scaffolds for cartilage regeneration.

6.1 Introduction

Tissue engineering is a promising method for the regeneration of degenerated or lost cartilage [1, 2]. This approach generally involves the use of cells placed in three-

dimensional scaffolds, the latter acting as a temporary artificial extracellular matrix (ECM). Injectable hydrogels may serve as temporary scaffolds to guide cell attachment and differentiation of chondrocytes and/or their progenitor cells, resulting in newly formed cartilage tissue. Compared to preformed hydrogels, injectable hydrogels have various advantages. They can be applied via a minimally invasive surgical procedure. They can fill irregular-shaped defects and allow easy incorporation of cells and bioactive molecules [3-5]. Therefore, in recent years injectable hydrogels have received much attention in cartilage tissue engineering.

Several chemical crosslinking methods, such as photopolymerization [6-8], Schiff-base formation [9], and Michael-type addition reactions [10, 11], have been employed to obtain injectable hydrogels that gel *in situ*. For example, Sontjens et al. reported on photocrosslinked methacrylated polyester-poly(ethylene glycol) hydrogels which can support the growth of chondrocytes *in vitro*, and their production of extracellular matrix components such as glycosaminoglycan and collagen type II [8]. In another study, Tan et al. reported on hydrogels prepared via Schiff base formation between water-soluble chitosan and oxidized hyaluronic acid and showed that chondrocytes were surviving in these hydrogels and retained their round morphology [9]. Recently, an efficient method, i.e. horseradish peroxidase (HRP)-mediated chemical crosslinking, has been developed to produce injectable hydrogels [12-19]. Using this approach, Lee et al. reported on hyaluronic acid-based injectable hydrogels for protein release [16, 17] and Sakai et al. prepared gelatin-based injectable hydrogels *in vitro* and indicated their potential application in tissue engineering *in vivo* [19]. We previously showed that fast *in situ* forming injectable hydrogels can be obtained via enzymatic crosslinking of dextran-tyramine conjugates (Dex-TA) or chitosan-phloretic acid conjugates in the presence of HRP and hydrogen peroxide [13, 14]. These hydrogels had good mechanical properties and low cytotoxicity [12, 14]. Importantly, chondrocytes incorporated in the gels remained viable, were capable of maintaining their phenotype and produced cartilaginous tissue [14, 20].

Heparin is a linear glycosaminoglycan composed of repeating units of 1,4-linked uronic acids (mainly D-glucuronic, L-iduronic or L-2-sulfated iduronic) and glucosamine residues (mainly D-N-acetyl glucosamine, D-di-N-6-sulfate glucosamine) [21]. It plays an important role in the interaction with bioactive proteins which are associated with cell adhesion, proliferation and differentiation [22, 23]. Over the past decades, heparin-containing hydrogels have been widely studied for biomedical applications such as controlled release of growth factors and tissue regeneration [24-28]. For example, heparin-containing hydrogels, prepared via a Michael addition reaction, were used for controlled release of growth factors. It was shown that incorporation of small amounts of heparin substantially influenced the release of basic fibroblast growth factors [26]. In recent studies, heparin has been shown to stimulate angiogenesis, adipogenesis and osteogenesis [25, 29, 30]. For example, photocrosslinked heparin-PEG hydrogels were shown to be capable of supporting the survival of human mesenchymal stem cells and inducing their osteogenic differentiation [25]. However, limited studies were reported on the use of heparin-containing hydrogels for chondrogenesis in cartilage tissue engineering [10, 31]. In this chapter, we describe biofunctional injectable hydrogels based on dextran and heparin for cartilage tissue engineering. We

hypothesized that the presence of heparin in the hydrogels may promote chondrocyte proliferation and differentiation as well as enhanced cartilage regeneration. Here we describe the preparation of injectable hydrogels from a mixture of a heparin-tyramine conjugate (Hep-TA) and a dextran-tyramine conjugate (Dex-TA) at different weight ratios. The properties of the hydrogels such as gelation time, swelling and mechanical properties were investigated. Moreover, bovine chondrocytes were incorporated in these hydrogels to evaluate their cytocompatibility, chondrocyte proliferation and matrix production.

6.2 Materials and methods

6.2.1 Materials

Heparin sodium (from porcine intestinal mucosa, molecular weight ranges from 3 to 30 kg/mol) was purchased from Celsus, Inc. N-ethyl-N-(3-dimethylaminopropyl) carbodiimide hydrochloride (EDAC) was purchased from Fluka. Tyramine (TA), hydrogen peroxide (H_2O_2), 4-morpholino ethanesulfonic acid (MES) and N-hydroxysuccinimide (NHS) were obtained from Aldrich-Sigma. Horseradish peroxidase (HRP, type VI, ~300 purpurogallin unit/mg solid) was purchased from Aldrich and used without further purification. All other solvents were used as received. Dextran-tyramine (denoted as Dex-TA) conjugates with a degree of substitution, defined as the number of tyramine units per 100 anhydroglucose rings in dextran, of 15 were prepared as previously reported [12].

6.2.2 Synthesis and characterization of heparin-tyramine conjugates

A heparin-tyramine conjugate (denoted as Hep-TA) was synthesized by the coupling reaction of tyramine amine groups to heparin carboxylic acid groups using EDAC/NHS activation. In a typical procedure, heparin sodium (2.0 g) was dissolved in 20 mL of MES (0.1 M, pH 6.0), to which EDAC (288 mg, 1.5 mmol) and NHS (227 mg, 1.5 mmol) were added. After 30 min, 6 mL of a DMF solution containing tyramine (69 mg, 0.5 mmol) was added and the mixture was stirred under nitrogen. After 3 days, the mixture was neutralized with 1 M NaOH and ultrafiltrated (MWCO 1000), first with 50 mM NaCl and then deionized water. The resultant Hep-TA conjugate was obtained in the form of a foam after freeze-drying (yield: 1.9 g, 95 %). The degree of substitution of tyramine residues in the Hep-TA conjugate, defined as the number of tyramine moieties per 100 repeating units of heparin, was 15, as determined by a UV measurement [15]. In brief, the Hep-TA conjugate was dissolved in PBS at a concentration of 2 mg/mL and the absorbance at 275 nm was measured using a Cary 300 Bio UV spectrophotometer (Varian). An unmodified heparin solution (2 mg/mL) was used as a blank. The absorbance was correlated to the concentration of tyramine in the conjugate using a calibration curve obtained from tyramine solutions in PBS.

6.2.3 Hydrogel formation and gelation time

Hydrogel samples (~ 0.25 mL) of Hep-TA or Hep-TA/Dex-TA mixtures at polymer concentrations of 10 or 20 % wt were prepared in vials at 37 degrees Celsius. In a typical procedure, to a PBS solution of Hep-TA (200 μ L, 25 % wt), a freshly prepared PBS solution of H_2O_2 (25 μ L of 0.3 % stock solution) and HRP (25 μ L of 150 unit/mL stock solution) were added and the mixture was gently vortexed. The final polymer and HRP concentrations were 20 % wt and 0.1 mg/mL (ca. 30 unit/mL), respectively. Hep-TA/Dex-TA hydrogels at Hep-TA/Dex-TA weight ratios of 75/25, 50/50 and 25/75 were prepared in the same manner starting from 25 % wt polymer solutions. The time to form a gel (denoted as gelation time) was determined using the vial tilting method. No flow within 1 min upon inverting the vial was regarded as the gel state. The experiment was preformed in triplicate.

6.2.4 Hydrogel characterization

The heparin content of the Dex-TA/Hep-TA hydrogels was determined by a colorimetric method based on the binding of toluidine blue, with some modifications [32, 33]. Briefly, the hydrogels prepared at Dex-TA/Hep-TA weight ratio of 75/25, 50/50 and 25/75 were extensively extracted with water and then freeze-dried. Samples (~ 1 mg, $n=3$) of dried gels were incubated overnight at room temperature in 2 ml of a 0.75 mg/ml toluidine blue solution. Subsequently, the solutions were diluted 10 times with H_2O and filtrated through 0.22 μ m filter. The absorbance of the filtrates was measured at 630 nm. A standard curve was prepared by mixing 1 ml of heparin solutions with known concentrations and 1 ml of 0.15 mg/ml toluidine blue solution in water at room temperature. After filtration through a 0.22 μ m filter, the absorbance of the solutions was measured at 630 nm. The heparin content in the hydrogels was calculated based on the heparin amount obtained from the toluidine blue assay and the dry gel weight after extraction. For swelling tests, hydrogel samples (~ 0.25 mL) were prepared as described above. Subsequently, 2 mL of PBS was applied on top of the hydrogels and then the samples were incubated at 37 degrees Celsius for 72 h to reach the swelling equilibrium. The buffer solution was then removed from the samples. The hydrogels were weighed (W_s) and then freeze-dried (W_d). The experiments were performed in triplicate and the degree of swelling of the hydrogels was expressed as $(W_s - W_d)/W_d$. Rheological experiments were carried out with a MCR 301 rheometer (Anton Paar) using parallel plates (25 mm diameter, 0) configuration at 37 degrees Celsius in the oscillatory mode. A stock solution of Hep-TA/Dex-TA (600 μ L, 25 % wt in PBS) at different weight ratios (100/0, 75/25, 50/50, 25/75 and 0/100) was mixed with 150 μ L of an HRP/ H_2O_2 mixture (75 μ L of 150 unit/mL HRP and 75 μ L of 0.3 % H_2O_2) using a double syringe (2.5 mL, 4:1 volume ratio) equipped with a mixing chamber (Mixpac). After the samples were applied to the rheometer, the upper plate was immediately lowered to a measuring gap size of 0.5 mm, and the measurement was started. To prevent evaporation of water, a layer of oil was introduced around the polymer sample. A frequency of 0.5 Hz and a strain of 0.1 % were applied in the analysis to maintain the linear viscoelastic regime. The measurement

was continued up to the time the storage moduli recorded reached a plateau value. A frequency sweep and a strain sweep were also performed on the hydrogels from 0.1 to 10 Hz at a strain of 0.1 %, and from 0.1 to 10 % at a frequency of 0.5 Hz, respectively.

6.2.5 Chondrocyte isolation and incorporation

Bovine chondrocytes were isolated as previously reported [14] and cultured in chondrocyte expansion medium (DMEM with 10 % heat inactivated fetal bovine serum, 1 % Penicillin/Streptomycin (Gibco), 0.5 mg/mL fungizone (Gibco), 0.01 M MEM nonessential amino acids (Gibco), 10 mM HEPES and 0.04 mM L-proline) at 37 degrees Celsius in a humidified atmosphere (95 % air/5 % CO₂). Hydrogels containing chondrocytes were prepared under sterile conditions by mixing a polymer/cell suspension with HRP/H₂O₂. Polymer solutions of Hep-TA/Dex-TA at different weight ratios (100/0, 75/25, 50/50, 25/75 or 0/100) were made in medium and HRP and H₂O₂ stock solutions were made in PBS. All the components were sterilized by filtration through filters with a pore size of 0.22 μ m. Chondrocytes (P1) were dispersed in the precursors of the hydrogels. The hydrogels were then formed using the same procedure as in the absence of cells. The final polymer concentration was 20 % wt and the cell seeding density in the gels was 510⁶ cells/mL. After gelation, the hydrogels (50 μ L of each) were transferred to a culture plate and 2 mL of chondrocyte differentiation medium (DMEM with 0.1 μ M dexamethasone (Sigma), 100 μ g/mL sodium pyruvate (Sigma), 0.2 mM ascorbic acid, 50 mg/mL insulin-transferrin-selenite (ITS+1, Sigma), 100 U/ml penicillin, 100 μ g/ml streptomycin, 10 ng/mL transforming growth factor β 3 (TGF- β 3, RD System) was added. The samples were incubated at 37 degrees Celsius in a humidified atmosphere containing 5 % CO₂. The medium was replaced every 3 or 4 days.

6.2.6 Cell viability and proliferation

A viability study on chondrocytes incorporated in the hydrogels was performed with a Live-dead assay. At day 3, 7 and 14, the hydrogel constructs were rinsed with PBS and stained with calcein AM/ethidium homodimer using the Live-dead assay Kit (Invitrogen), according to the manufacturers' instructions. Hydrogel/cell constructs were visualized using a fluorescence microscope (Zeiss). Living cells fluoresce green and the nuclei of dead cells red. Quantification of total DNA of the constructs cultured for 1, 7, 14 and 21 days was done using the CyQuant dye kit and a fluorescent plate reader (Perkin-Elmer) as previously reported [34].

6.2.7 Swelling in the presence of chondrocytes

To evaluate the swelling behavior of hydrogels with chondrocytes incorporated, 50 μ L of a gel/cell construct was incubated in medium at 37 degrees Celsius in a humidified atmosphere containing 5 % CO₂. After 3 days, samples (n=3) were taken out of the medium, weighed (W_{sc}) and then freeze-dried (W_{dc}). The degree of swelling was expressed as (W_{sc}-W_{dc})/W_{dc}.

| Primer | Direction | Sequence | Annealing Temp (°C) |
|----------------------------|-----------|----------------------------|---------------------|
| Bovine aggrecan | Forward | 5' GACCAGAAGCTGTGCGAGGA 3' | 60 |
| | Reverse | 5' GCCAGATCATCACCACACAG 3' | |
| Bovine collagen, type IIa1 | Forward | 5' ATCAACGGTGGCTT CCACT 3' | 60 |
| | Reverse | 5' TTCGTGCAGCCATCCTTCAG 3' | |
| Bovine collagen, type Ia1 | Forward | 5' GCGGCTACGACTTGAGCTTC 3' | 60 |
| | Reverse | 5' CACGGTCACGGACCACATTG 3' | |
| Bovine GAPDH | Forward | 5' GCCATCACTGCCACCCAGAA 3' | 60 |
| | Reverse | 5' GCGGCAGGTCAGATCCACAA 3' | |

Table 6.1: Polymerase Chain Reaction Primers

RNA extraction and reverse transcriptase polymerase chain reaction (RT-PCR). After culturing the hydrogel/cell constructs in differentiation medium for 21 days, the samples were collected and washed with PBS. After converting the gels into pieces by pipetting, Trizol reagent (Invitrogen, Carlsbad, CA) was added to lysate the cells. Total RNA was isolated using the Nucleospin RNA II kit (Bioke) according to manufacturers instructions. The RNA yields were determined based on the A260. Subsequently, the RNA (250 ng) was transcribed into single strand cDNA using the iScript Kit (BioRad) according to the manufacturers recommendations. One micro-liter of each normalized cDNA sample was analyzed using the SYBR Green PCR Core Kit (Applied Biosystems) and a real-time PCR Cyclor (BioRad). The expression of collagen type II and aggrecan (Table 6.1) was analyzed and normalized to the expression of the housekeeping gene glyceraldehyde-3-phosphate dehydrogenase (GAPDH). The efficiency of the single PCR reactions was determined and incorporated into the calculation.

6.2.8 Histological staining

Samples cultured for 21 days were fixed in 10 % formalin for 1 h. After embedding the samples in paraffin, 5 μ m sections were collected and rehydrated with xylene and a series of ethanol (from 100 % until 70 %). The slides were left in distilled water for 10 minutes. Afterwards, toluidine blue (Fluka, 0,1 % in deionized water) was added to the sections and left to incubate for 10 minutes. The slides were then washed with water and dehydrated. Sections were analyzed using a bright field microscope.

6.2.9 Matrix production

The secretion of chondroitin sulfate and collagen type II by chondrocytes was evaluated by immunofluorescent staining as previously reported [34]. For biochemical anal-

ysis, the constructs cultured for 1, 7, 14 and 21 days were digested using proteinase-K [20]. The total collagen content was determined using the hydroxyproline assay [35]. The hydroxyproline content was determined via a colorimetric assay by reaction with chloramine T and dimethylaminobenzaldehyde. All values were corrected for the background staining of gels without cells. Data (n=3, measured in triplicate) are expressed as mean \pm standard deviation (SD).

6.2.10 Statistical analysis

Statistical differences between two groups were analyzed using a Students t-test. Those among three or more groups were analyzed using the One-way Analysis of Variance (ANOVA) with Turkey's post-hoc analysis. Statistical significance was set to a p value <0.05. Results are presented as mean \pm standard deviation.

6.3 Results and discussion

6.3.1 Hydrogel formation and gelation time

The key material of this study, a heparin-tyramine (Hep-TA) conjugate, with a degree of substitution of tyramine residues of 15 (DS 15), was synthesized by the coupling reaction of the amino group of tyramine to the carboxylic acid groups of heparin using EDC/NHS activation. The, enzyme-mediated crosslinking of phenol moieties in the presence of HRP and H₂O₂, a method successfully used in the preparation of hydrogels from tyramine conjugated dextrans and phloretic acid conjugated chitosans [13, 14], was applied to form hydrogels from the Hep-TA conjugates at polymer concentrations of 10 and 20 % wt. In previous research it was shown that at concentrations of HRP of 0.2 mg/mL and concentrations of H₂O₂ of 0.01 M, biocompatible hydrogel/cell constructs were obtained [20]. These concentration ranges were also applied in the preparation of the hydrogels of Hep-TA, Dex-TA and mixtures thereof.

Because a short gelation time is a prerequisite for injectable gel/cell constructs, the gelation times of the Hep-TA hydrogels, as monitored at 37 degrees Celsius by the vial tilting method, were first optimized (Figure 6.2a). It was found that, by increasing the HRP concentration from 0.05 to 0.2 mg/mL, the gelation time decreased from about 340 s to 30 s (p<0.05). Moreover, shorter gelation times (less than 60 s) were observed for the 20 % wt hydrogels than for 10 % wt hydrogels, which can be explained by the presence of more crosslinkable moieties in the 20 % wt hydrogels. On the basis of these data, hydrogels from a mixture of Hep-TA (DS 15) and Dex-TA (DS 15) were prepared at a polymer concentration of 20 % wt (Figure 6.1b). The gelation times as a function of Dex-TA/Hep-TA weight ratio are presented in Figure 6.2b. Generally, these gels had shorter gelation times than the hydrogels based on Hep-TA. When the Dex-TA/Hep-TA ratio decreased from 75/25 to 25/75, the gelation times slightly increased from 30 to 50 s. The increase in the gelation time of heparin-containing hydrogels compared to Dex-TA hydrogels may be explained by the unfavorable interactions with the active site of the enzyme caused by the acid

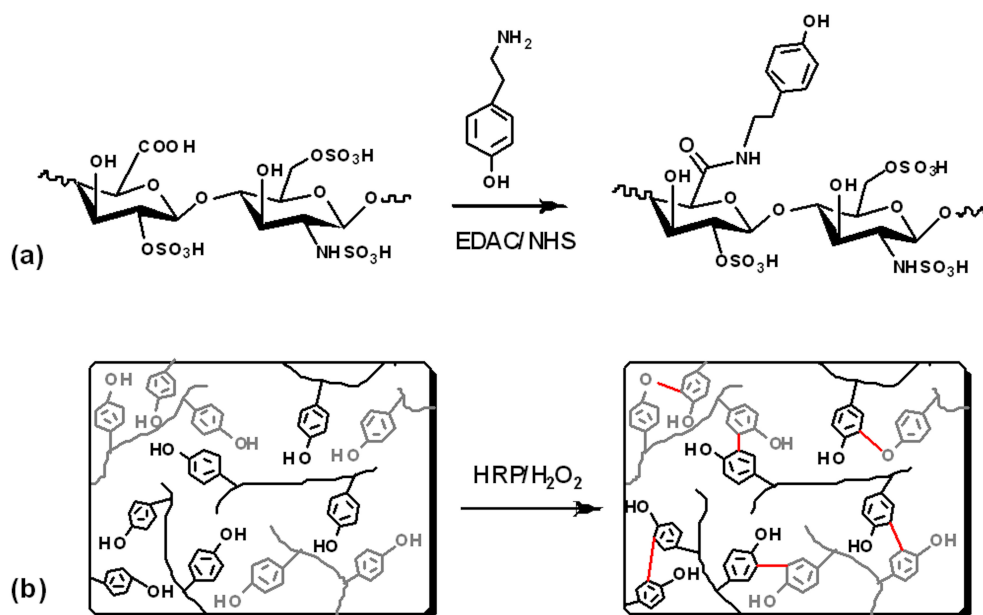


Figure 6.1: (a) Synthesis of heparin-tyramine conjugates (Hep-TA). (b) Hydrogel formation from dextran-tyramine (Dex-TA, black) and heparin-tyramine conjugates (Hep-TA, grey) via HRP-mediated crosslinking in the presence of H_2O_2 .

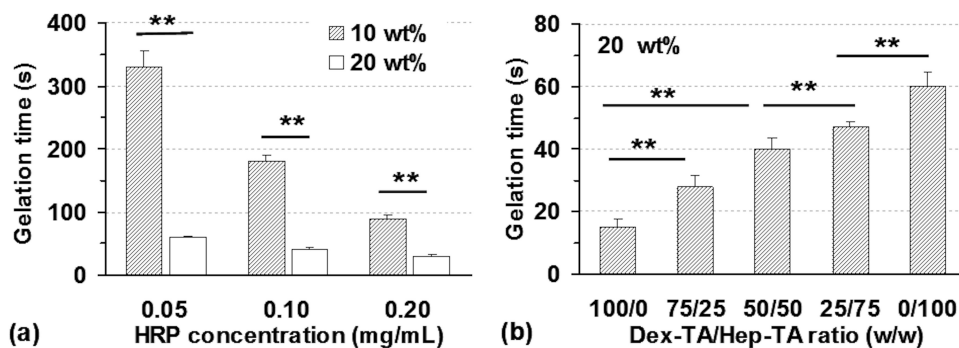


Figure 6.2: (a) Gelation times of Hep-TA hydrogels (10 and 20 % wt) as a function of HRP concentration. The molar ratio of $\text{H}_2\text{O}_2/\text{TA}$ was kept at 0.2. (b) Gelation times of Hep-TA/Dex-TA hydrogels (20 % wt) as a function of Hep-TA/Dex-TA ratio (w/w). The concentrations of HRP and H_2O_2 were kept at 0.05 mg/mL and 0.01 M, respectively. ($n=3$, ** $p<0.01$)

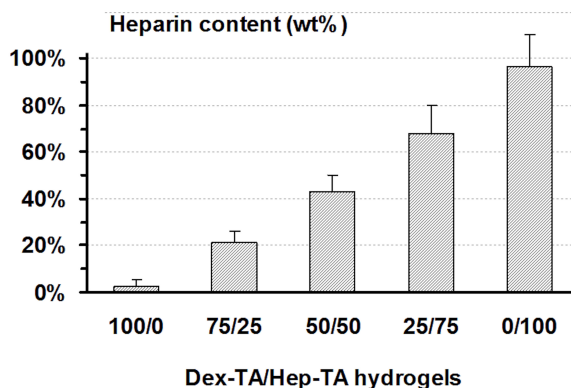


Figure 6.3: Heparin content (wt % in dry gel mass) of extracted 20 % wt Dex-TA/Hep-TA hydrogels.

groups in heparin chains (e.g. - NHSO_3^- , - OSO_3^- and - COO^-) either through steric hindrance or charge interactions [36].

6.3.2 Hydrogel characterization

The incorporation of heparin in Dex-TA hydrogels was confirmed by a toluidine blue assay. The values of heparin content were close to the theoretical values at which the gels were prepared (Figure 6.3b). This indicated that Hep-TA conjugates were successfully co-crosslinked with Dex-TA conjugates to form a hydrogel. The degrees of swelling of 20 % wt hydrogels at different Dex-TA/Hep-TA weight ratios are shown in Figure 6.4. The Hep-TA hydrogels had a higher degree of swelling than the Dex-TA hydrogel (16.7 vs. 4.9). Increasing the heparin content in Hep-TA in Dex-TA/Hep-TA hydrogels also showed an increase in the swelling values of the hydrogel ($p < 0.05$). It needs to be mentioned here that both Dex-TA and Hep-TA had a DS of 15. Because Hep-TA comprises disaccharide units, while Dex-TA comprises mono-saccharide repeating units, at the same polymer concentration, the TA concentration in Hep-TA solutions is always half of the TA concentration in Dex-TA solutions. This leads to a decreased crosslinking density of Hep-TA hydrogels as compared to Dex-TA gels at similar concentrations. Therefore, the high degree of swelling of Hep-TA containing hydrogels can be either due to the lower crosslinking density or due to the electrostatic repulsive force between negatively-charged carboxylic acid and sulfate groups in the heparin at the physiological pH of 7.4. Rheological measurements were performed to study the influence of the heparin content on the mechanical properties of the hydrogels. The hydrogel prepared from Hep-TA at a concentration of 20 % wt showed a low storage modulus of 3.6 kPa. The storage moduli of the Dex-TA/Hep-TA hydrogels increased from 3.6 to 48 kPa with decreasing ratio in the gels (Figure 6.5). This shows that heparin containing gels with an appropriate modulus can be obtained

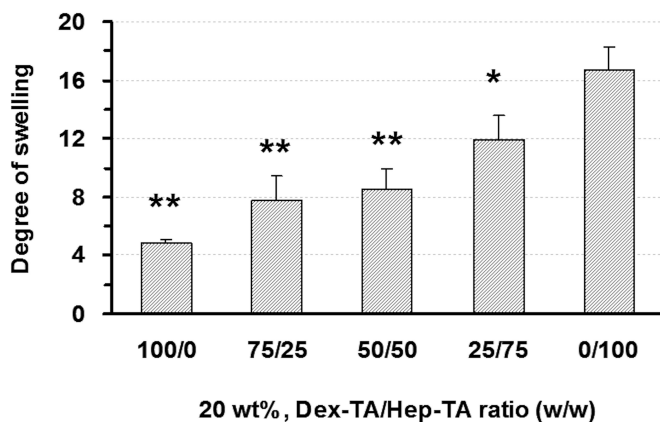


Figure 6.4: The degree of swelling of Dex-TA/Hep-TA hydrogels. (n=3, * $p < 0.05$; ** $p < 0.01$ vs. 0/100 gel)

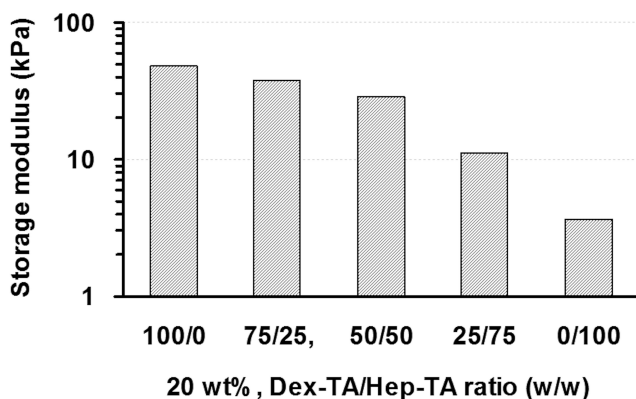


Figure 6.5: Storage moduli of Dex-TA/Hep-TA hydrogels. The concentrations of HRP and H_2O_2 were 0.05 mg/mL and 0.01 M, respectively (n=1).

by selecting the proper ratio of Dex-TA and Hep-TA to form the gels. The frequency and strain sweeps of 20 % wt Dex-TA/Hep-TA hydrogels are presented in Figure 6.6. From the frequency sweep experiments it is found that the hydrogels are elastic and the storage modulus is not dependent on the frequency (Figure 6.6a). The strain sweep tests show that the storage moduli of the hydrogels with a high Dex-TA/Hep-TA weight ratio (50/50 or 100/0) were strain independent within a strain range of 0.1-1 % (Figure 6.6b). As the strain increased to 2 % or even higher values, the storage moduli decreased, indicating a breakdown of the network. However, the moduli of

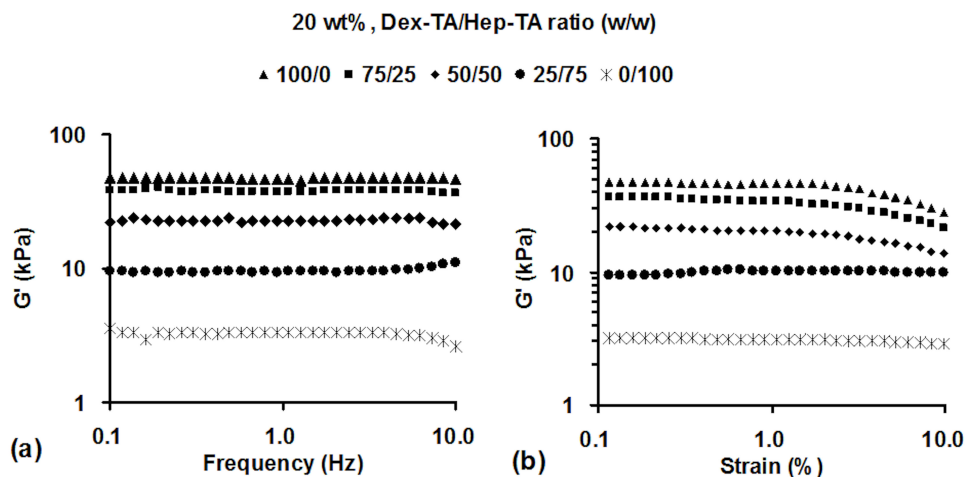


Figure 6.6: (a) Frequency sweep and (b) strain sweep of Dex-TA/Hep-TA hydrogels.

the hydrogels with a Dex-TA/Hep-TA weight ratio of 25/75 and 0/100 appeared independent of the strain up to 10%, suggesting that these hydrogels are quite robust. Moreover, the G decreased more rapidly with increasing strain at a higher Dex-TA content.

6.3.3 Cell viability and proliferation

Dex-TA and Dex-TA/Hep-TA hydrogels at Dex-TA/Hep-TA weight ratios of 100/0, 72/25, 50/50 and 25/75 were chosen for the biological studies. This selection was made because these gels have a shorter gelation time and a higher storage modulus compared to Hep-TA hydrogels. The biocompatibility of 20 % wt hydrogels was analyzed by a Live-dead assay after culturing for 3, 7 and 14 days, in which live cells fluoresce green and dead cells fluoresce red. At day 3, about 10-15 % dead cells were present in the Dex-TA hydrogels, while over 95 % chondrocytes remained viable in the Dex-TA/Hep-TA and Hep-TA hydrogels (Figure 6.7). The relatively low cell viability observed for the Dex-TA hydrogel may be attributed to the high crosslinking density of the hydrogels [37], and/or a limited nutrients supply resulting from the low degree of swelling in medium (Figure 6.8). A CyQuant DNA assay was used to determine the viability and proliferation of chondrocytes inside the Dex-TA/Hep-TA hydrogels up to 21 days (Figure 6.9). In general, the DNA content increased in time for the hydrogels at different Dex-TA/Hep-TA ratios from 100/0 to 25/75, indicative of cell proliferation. The chondrocytes in the hydrogels containing both Dex-TA and Hep-TA conjugates proliferated better than in Dex-TA hydrogels at all time intervals. This can be ascribed to both the enhancement of nutrient exchange in these highly

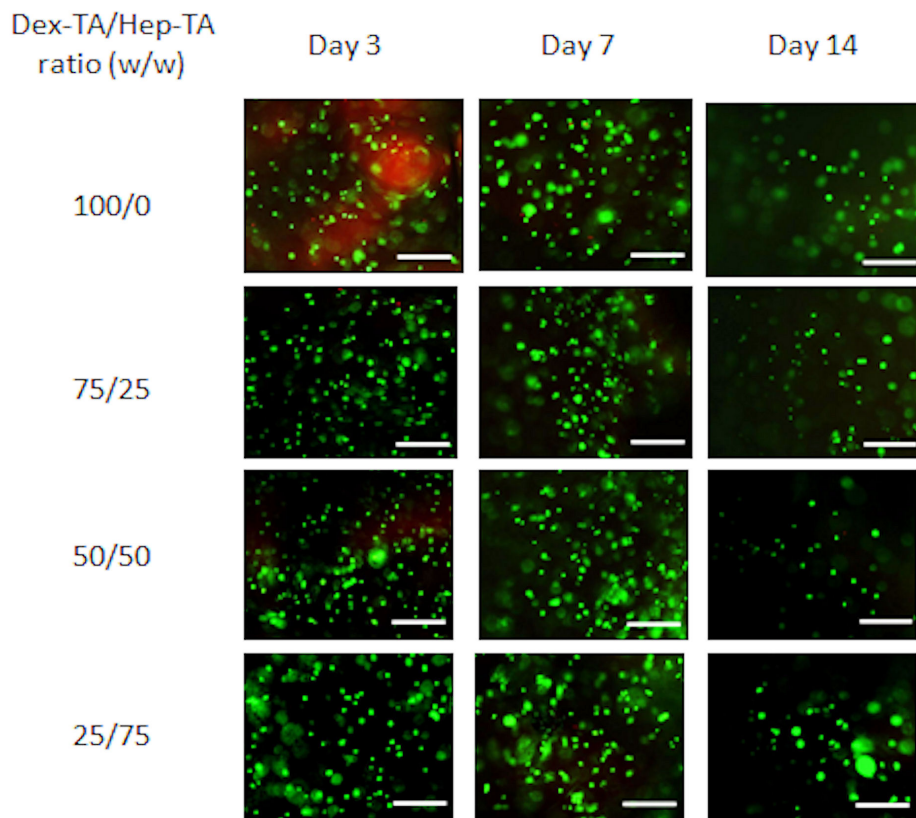


Figure 6.7: Live-dead assay showing the chondrocytes incorporated in Dex-TA/Hep-TA hydrogels after 3, 7 and 14 days in culture. Cell density is 5 million cells/mL gel. Scale bar: 200 μm .

swollen hydrogels and the potential biological role of heparin on the chondrocytes [9, 30, 39-41]. The 50/50 Dex-TA/Hep-TA hydrogel revealed the best proliferation of chondrocytes compared to the others (25/75 and 75/25), which suggested that there exists an optimal Dex-TA/Hep-TA ratio for cell proliferation.

6.3.4 Matrix production

The abilities of chondrocytes to maintain a chondrocytic phenotype and to form cartilaginous tissue *in vitro* were evaluated after culturing in differentiation medium up to 21 days. Gene expression of collagen type I and II and aggrecan were analyzed using RT-PCR. It is shown that the gene expression levels were dependent on the composi-

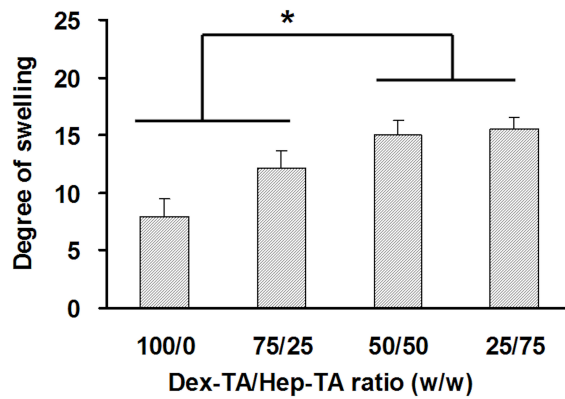


Figure 6.8: Degree of swelling of 20 % wt Dex-TA/Hep-TA hydrogels containing chondrocytes after incubating for 3 days *in vitro*. Cell seeding density: 5 million cells/mL. (n=3, * p<0.05).

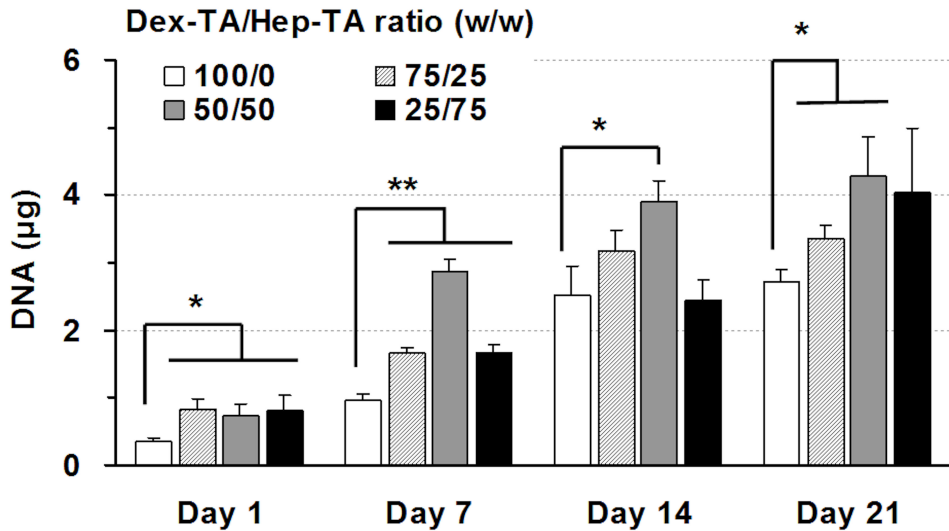


Figure 6.9: DNA content of 20 % wt Dex-TA/Hep-TA hydrogels containing chondrocytes after *in vitro* culturing for 1, 7, 14 and 21 days. Cell seeding density: 5 million cells/mL. (* p<0.05, ** p<0.01).

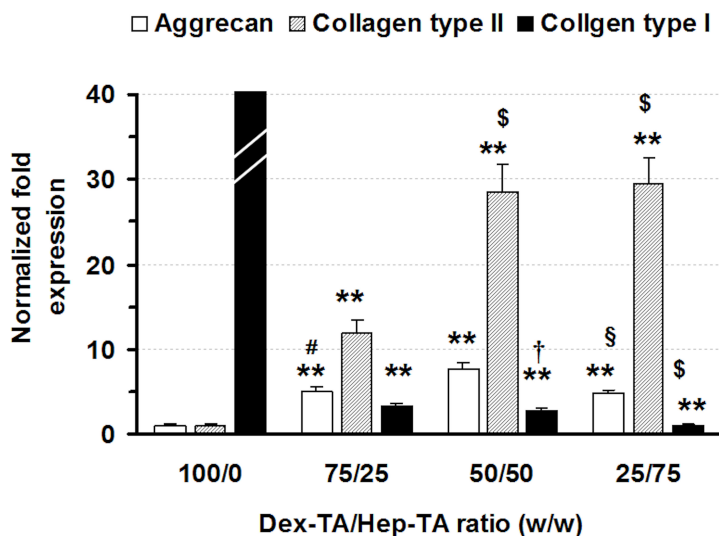


Figure 6.10: Real-time PCR of cartilage specific markers (aggrecan and collagen type I and II) by incorporated chondrocytes in 20 % wt Dex-TA/Hep-TA hydrogels after 21 days in culture. The expressions of collagen type I and II and aggrecan were normalized to the expression of the housekeeping gene GAPDH. (** $p < 0.01$ vs. 100/0 gel; $p < 0.05$ vs. 50/50 gel; $p < 0.01$ vs. 50/50 gel; $p < 0.01$ vs. 75/25 gel; $p < 0.05$ vs. 75/25 gel).

tion of the hydrogels (Figure 6.10). The chondrocytes in Dex-TA/Hep-TA hydrogels maintained significantly higher levels of aggrecan and type II collagen gene expressions compared to those in Dex-TA hydrogels ($p < 0.01$). In contrast, Dex-TA hydrogels expressed collagen transcripts mainly of type I instead of type II, suggesting a loss of chondrocyte phenotype. Additionally, the heparin present in the hydrogels was found to up-regulate aggrecan and collagen type II mRNA levels in a content-dependent manner. For example, it was observed that aggrecan gene expression was maximized when the Dex-TA/Hep-TA weight ratio was 50/50 while collagen type II gene expression was highest for hydrogels with Dex-TA/Hep-TA weight ratio of 50/50 and 25/75. Toluidine blue was used to stain deposited proteoglycans by chondrocytes in Dex-TA/Hep-TA hydrogels cultured for 21 days (Figure 6.11). Proteoglycans staining purple/blue were observed in Dex-TA hydrogels. Unfortunately, in Dex-TA/Hep-TA hydrogels, due to the presence of heparin, which is stained positive using toluidine blue, the gels showed intense background staining. Thus, immunofluorescence staining of chondroitin sulfate and collagen type II was used to detect the accumulation of newly formed cartilaginous matrix. The results confirmed the production of cartilaginous matrix in Dex-TA/Hep-TA hydrogels (Figure 6.12 and 6.13). The 50/50 and 25/75 Dex-TA/Hep-TA hydrogels showed a more intense staining of chondroitin

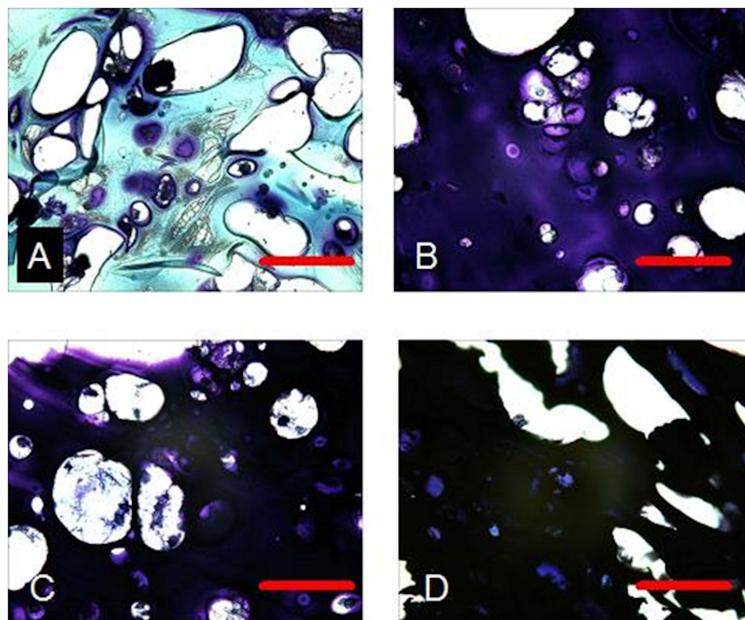


Figure 6.11: Toluidine blue staining of the hydrogels with Dex-TA/Hep-TA weight ratios of 100/0 (A), 75/25 (B), 50/50 (C) and 25/75 (D) after culturing for 21 days. Scale bar: 100 μm .

sulfate and collagen type II than the 100/0 and 75/25 gels. In addition, chondroitin sulfate in 100/0 and 75/25 hydrogels was only present in the pericellular region, while in 50/50 and 25/75 hydrogels, the chondroitin sulfate was evenly distributed over the pericellular and extracellular region. Since the 50/50 and 25/75 Dex-TA/Hep-TA hydrogels showed a degree of swelling of 16, statistically higher than 100/0 and 75/25 gels (9 and 13, respectively) (Figure 6.8), 50/50 and 25/75 hydrogels may induce more facilitated proteoglycan diffusion into the extracellular regions, thereby resulting in a more even distribution. This observation is similar to that observed for PEG-based hydrogels. These materials induced facilitated proteoglycan diffusion into the extracellular regions of the scaffolds at a degree of swelling higher than 9.3 [38].

The total collagen content was determined by a hydroxyproline assay, in which hydroxyproline makes up 12.5 % wt of collagen [35]. The total collagen accumulation increased in time and reached the highest value at day 21 at all gel compositions (Figure 6.14a). Hydrogels comprising both Dex-TA and Hep-TA showed significantly higher collagen production compared to Dex-TA hydrogels ($p < 0.05$). Moreover, the highest collagen production was obtained from the 50/50 and 25/75 Dex-TA/Hep-TA hydrogel. This is consistent with the results for collagen type II staining and the RT-PCR findings for collagen type II gene expression. When normalized to the DNA content, the total collagen content was statistically similar in all five systems at each

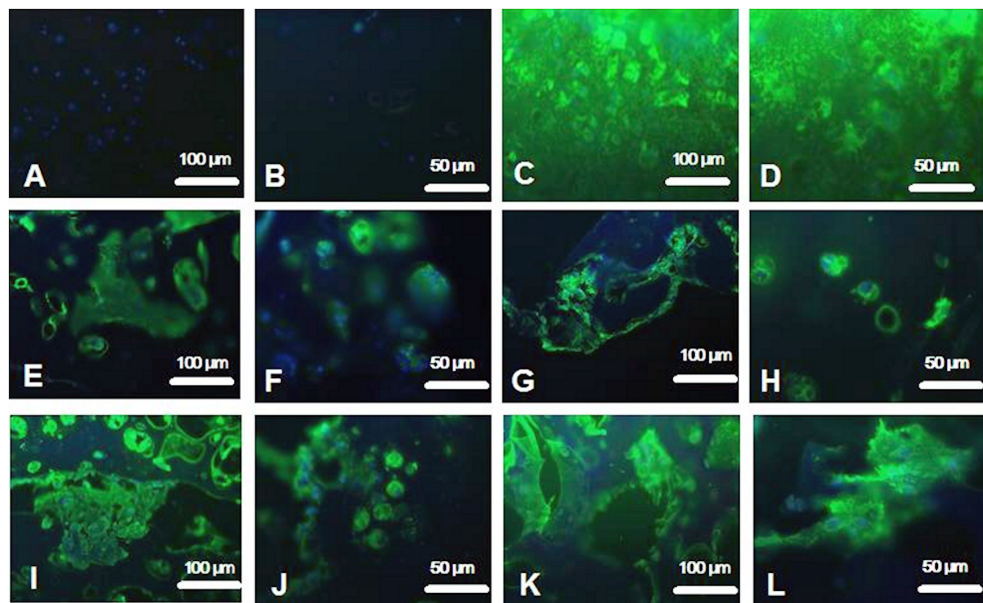


Figure 6.12: Chondroitin sulfate immunofluorescent staining of the Dex-TA/Hep-TA hydrogels containing chondrocytes after *in vitro* culturing for 21 days. Different Dex-TA/Hep-TA ratios: 100/0 (E and F), 75/25 (G and H), 50/50 (I and J) and 25/75 (K and L). The section of bovine cartilage without or with incubation with primary antibodies was used as a negative (A and B) and positive (C and D) control, respectively.

time point (Figure 6.14b).

The improvement of chondrocyte performance in the Dex-TA/Hep-TA hydrogels with respect to Dex-TA hydrogels may be due to several reasons. First, heparin can interact with ECM components such as fibronectin and collagen via either electrostatic or specific interactions. Through these interactions, heparin can modulate cell signaling, cellmatrix interactions and matrix assembly [30, 39, 40]. Second, the incorporation of negatively charged heparin moieties into Dex-TA hydrogels contributes to the increase in hydrogel swelling and the decrease of the storage modulus. This may result in a gel network with appropriate crosslinking density which allows good transportation of nutrients to the chondrocytes. Third, heparin can bind growth factors supplemented in medium or secreted by chondrocytes such as TGF- β 3. TGF- β 3 is a protein that regulates many aspects of cellular activity, including cell proliferation, differentiation, and ECM deposition in the process of cartilage regeneration [41, 42]. Thus, the hydrogel system serves as a reservoir for these crucial proteins, creating a biomimetic microenvironment favorable for chondrogenesis.

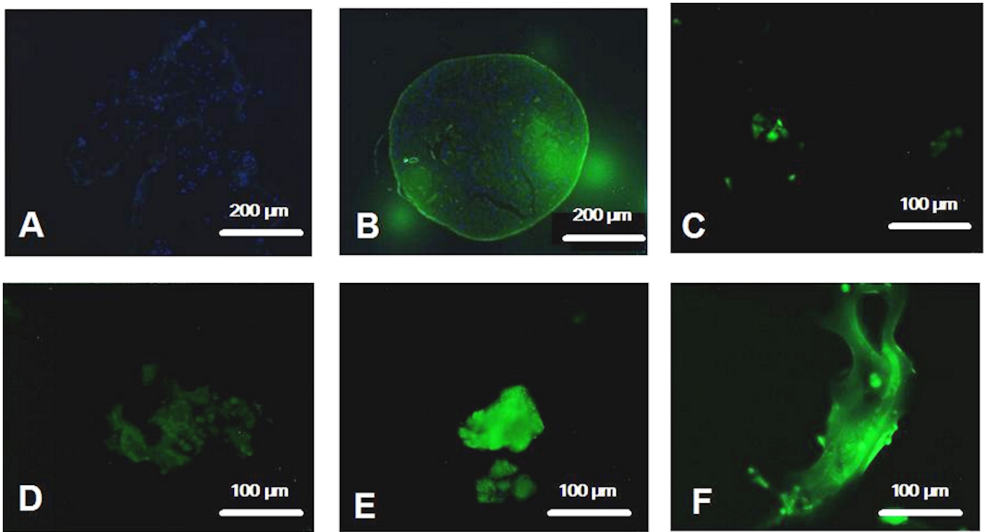


Figure 6.13: Collagen type II immunofluorescent staining of the Dex-TA/Hep-TA hydrogels containing chondrocytes after *in vitro* culturing for 21 days. Different Dex-TA/Hep-TA ratios: 100/0 (C), 75/25 (D), 50/50 (E) and 25/75 (F). The section of pellet human chondrocytes at 21 days without or with incubation with primary antibodies was used as a negative (A) and positive (B) control, respectively.

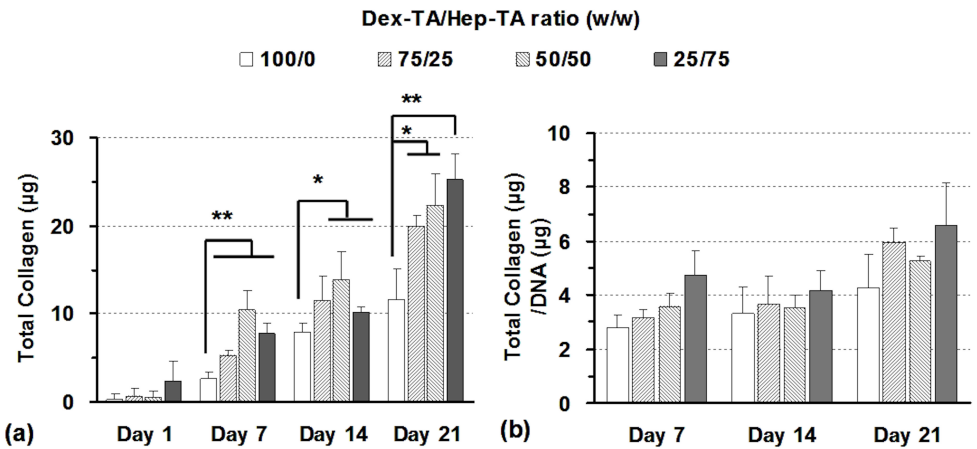


Figure 6.14: (a) Total collagen in Dex-TA/Hep-TA hydrogels containing chondrocytes after *in vitro* culturing for 1, 7, 14 and 21 days. Cell seeding density: 5 million cells/mL. (* $p < 0.05$, ** $p < 0.01$).

6.4 Conclusions

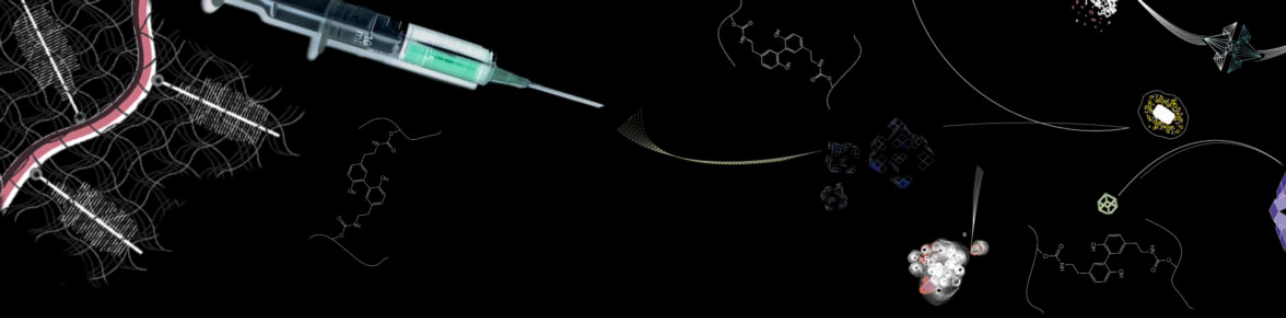
We have shown that injectable hydrogels containing a naturally occurring glycosaminoglycan, heparin, can be prepared via enzymatic crosslinking of Dex-TA and Hep-TA conjugates. The results showed that incorporation of heparin into the hydrogels greatly improved the hydrogel swelling properties, which is favorable for good nutrient transportation for cell culture. On the other hand, the combination of Dex-TA and Hep-TA afforded hydrogels with faster gelation and a higher storage modulus compared to Hep-TA hydrogels. Bovine chondrocytes were incorporated in these gels during gelation. The results showed that the hydrogel with a Dex-TA/Hep-TA weight ratio of 50/50 induced the best chondrocyte viability and proliferation, and an enhanced matrix production as compared to the hydrogels from Dex-TA conjugates. These results indicate that Dex-TA/Hep-TA hydrogels have a high potential as matrices for cartilage tissue engineering.

References

1. Chung C, Burdick JA. Engineering Cartilage Tissue. *Adv. Drug Deliver. Rev.* 2008;60: 243-262.
2. Tuli R, Li W-J, Tuan RS. Current State of Cartilage Tissue Engineering. *Arthritis. Res. Ther.* 2003;5: 235-238.
3. Kretlow JD, Klouda L, Mikos AG. Injectable Matrices and Scaffolds for Drug Delivery in Tissue Engineering. *Adv. Drug Deliver. Rev.* 2007;59: 263-273.
4. Van Tomme SR, Storm G, Hennink WE. *in situ* Gelling Hydrogels for Pharmaceutical and Biomedical Applications. *Int. J. Pharm.* 2008;355: 1-18.
5. Yu L, Ding J. Injectable Hydrogels as Unique Biomedical Materials. *Chem. Soc. Rev.* 2008;37: 1473-1481.
6. Wang D-A, Varghese S, Sharma B, Strehin I, Fermanian S, Gorham J, Fairbrother DH, Cascio B, and Elisseeff JH. Multifunctional Chondroitin Sulphate for Cartilage Tissue-Biomaterial Integration. *Nat. Mater.* 2007;6: 385-392.
7. Li Q, Wang J, Shahani S, Sun DDN, Sharma B, Elisseeff JH, and Leong KW. Biodegradable and Photocrosslinkable Polyphosphoester Hydrogel. *Biomaterials* 2006; 27: 1027-1034.
8. Sontjens SHM, Nettles DL, Carnahan MA, Setton LA, Grinstaff MW. Biodendrimer-Based Hydrogel Scaffolds for Cartilage Tissue Repair. *Biomacromolecules* 2006;7: 310-316.
9. Tan H, Chu CR, Payne KA, Marra KG. Injectable *in situ* Forming Biodegradable Chitosan-Hyaluronic Acid Based Hydrogels for Cartilage Tissue Engineering. *Biomaterials* 2009;30: 2499-2506.
10. Kim M, Shin Y, Hong B, Kim Y-J, Chun J-S, Tae G, and Kim YH. *in vitro* Chondrocyte Culture in a Heparin-Based Hydrogel for Cartilage Regeneration. *Tissue Eng. C* In press.
11. Park Y, Lutolf MP, Hubbell JA, Hunziker EB, Wong M. Bovine Primary Chondrocyte Culture in Synthetic Matrix Metalloproteinase-Sensitive Poly(ethylene glycol)-Based Hydrogels as a Scaffold for Cartilage Repair. *Tissue Eng.* 2004;10: 515-522.
12. Jin R, Moreira Teixeira LS, Dijkstra PJ, Karperien M, Zhong Z, Feijen J. Fast *in-Situ* Formation of Dextran-Tyramine Hydrogels for *in vitro* Chondrocyte Culturing. *J. Control. Release* 2008;132: e24-e26.
13. Jin R, Hiemstra C, Zhong Z, Feijen J. Enzyme-Mediated Fast *in situ* Formation of Hydrogels from Dextran-Tyramine Conjugates. *Biomaterials* 2007;28: 2791-2800.
14. Jin R, Moreira Teixeira LS, Dijkstra PJ, Karperien M, van Blitterswijk CA, Zhong ZY, and Feijen J. Injectable Chitosan-Based Hydrogels for Cartilage Tissue Engineering. *Biomaterials* 2009;30: 2544-2551.
15. Darr A, Calabro A. Synthesis and Characterization of Tyramine-Based Hyaluronan Hydrogels. *J. Mater. Sci.: Mater. M.* 2009;20: 33-44.
16. Lee F, Chung JE, Kurisawa M. An Injectable Enzymatically Crosslinked Hyaluronic Acid-Tyramine Hydrogel System with Independent Tuning of Mechanical Strength and Gelation Rate. *Soft Matter.* 2008;4: 880-887.
17. Lee F, Chung JE, Kurisawa M. An Injectable Hyaluronic Acid-Tyramine Hydrogel System for Protein Delivery. *J. Control. Release* 2009;134: 186-193.

18. Sakai S, Yamada Y, Zenke T, Kawakami K. Novel Chitosan Derivative Soluble at Neutral Ph and in-Situ Gellable Via Peroxidase-Catalyzed Enzymatic Reaction. *J. Mater. Chem.* 2009;19: 230-235.
19. Sakai S, Hirose K, Taguchi K, Ogushi Y, Kawakami K. An Injectable, *in situ* Enzymatically Gellable, Gelatin Derivative for Drug Delivery and Tissue Engineering. *Biomaterials* 2009;30: 3371-3377.
20. Jin R, Teixeira LSM, Dijkstra PJ, Zhong Z, Blitterswijk CA, Karperien M, and Feijen J. Enzymatically Crosslinked Dextran-Tyramine Hydrogels as Injectable Scaffolds for Cartilage Tissue Engineering. Chapter 5.
21. Casu B. Structure and Biological Activity of Heparin. *Adv. Carbohydr. Chem. Biochem.* 1985;43: 51-134.
22. Capila I, Linhardt RJ. Heparin-Protein Interactions. *Angew. Chem. Int. Edit.* 2002;41: 390-412.
23. Sasisekharan R, Venkataraman G. Heparin and Heparan Sulfate: Biosynthesis, Structure and Function. *Curr. Opin. Chem. Biol.* 2000;4: 626-631.
24. Benoit DSW, Anseth KS. Heparin Functionalized PEG Gels That Modulate Protein Adsorption for Hmsc Adhesion and Differentiation. *Acta Biomater.* 2005;1: 461-470.
25. Benoit DSW, Durney AR, Anseth KS. The Effect of Heparin-Functionalized PEG Hydrogels on Three-Dimensional Human Mesenchymal Stem Cell Osteogenic Differentiation. *Biomaterials* 2007;28: 66-77.
26. Cai S, Liu Y, Zheng Shu X, Prestwich GD. Injectable Glycosaminoglycan Hydrogels for Controlled Release of Human Basic Fibroblast Growth Factor. *Biomaterials* 2005;26: 6054-6067.
27. Nie T, Baldwin A, Yamaguchi N, Kiick KL. Production of Heparin-Functionalized Hydrogels for the Development of Responsive and Controlled Growth Factor Delivery Systems. *J. Control. Release* 2007;122: 287-296.
28. Lih E, Yoon Ki J, Jin Woo B, Ki Dong P. An *in situ* Gel-Forming Heparin-Conjugated PLGA-PEG-PLGA Copolymer. *J. Bioact. Compat. Pol.* 2008;23: 444-457.
29. Tyagi SC, Kumar S, Katwa L. Differential Regulation of Extracellular Matrix Metalloproteinase and Tissue Inhibitor by Heparin and Cholesterol in Fibroblast Cells. *J. Mol. Cell. Cardiol.* 1997;29: 391-404.
30. Luo W, Shitaye H, Friedman M, Bennett CN, Miller J, MacDougald OA, and Hankenson KD. Disruption of Cell-Matrix Interactions by Heparin Enhances Mesenchymal Progenitor Adipocyte Differentiation. *Exp. Cell Res.* 2008;314: 3382-3391.
31. Tan H, Lao L, Wu J, Gong Y, Gao C. Biomimetic Modification of Chitosan with Covalently Grafted Lactose and Blended Heparin for Improvement of *in vitro* Cellular Interaction. *Polym. Advan. Technol.* 2008;19: 15-23.
32. Hinrichs WLJ, ten Hoopen HWM, Wissink MJB, Engbers GHM, Feijen J. Design of a New Type of Coating for the Controlled Release of Heparin. *J. Control. Release* 1997;45: 163-176.
33. Wissink MJB, Beernink R, Pieper JS, Poot AA, Engbers GHM, Beugeling T, van Aken WG, and Feijen J. Immobilization of Heparin to EDC/NHS-Crosslinked Collagen. Characterization and *in vitro* Evaluation. *Biomaterials* 2001;22: 151-163.

34. Jin R, Teixeira LSM, Krouwels A, Dijkstra PJ, Blitterswijk CA, Karperien M, and Feijen J. Synthesis and Characterization of Hyaluronic Acid-PEG Hydrogels via Michael Addition: An Injectable Biomaterial for Cartilage Repair. *Acta Biomater.* Submitted.
35. Edwards CA, O'Brien Jr WD. Modified Assay for Determination of Hydroxyproline in a Tissue Hydrolyzate. *Clin. Chim. Acta* 1980;104: 161-167.
36. Sofia SJ, Singh A, Kaplan DL. Peroxidase-Catalyzed Crosslinking of Functionalized Polyaspartic Acid Polymers. *J. Macromol. Sci.* 2002;A39: 1151-1181.
37. Burdick JA, Anseth KS. Photoencapsulation of Osteoblasts in Injectable Rgd-Modified PEG Hydrogels for Bone Tissue Engineering. *Biomaterials* 2002;23: 4315-4323.
38. Bryant SJ, Anseth KS. Hydrogel Properties Influence ECM Production by Chondrocytes Photoencapsulated in Poly(Ethylene Glycol) Hydrogels. *J. Biomed. Mater. Res.* 2002;59: 63-72.
39. Woods A, Couchman JR. Syndecans: Synergistic Activators of Cell Adhesion. *Trends Cell Biol.* 1998;8: 189-192.
40. Beauvais D, Rapraeger A. Syndecans in Tumor Cell Adhesion and Signaling. *Reprod. Biol. Endocrin.* 2004;2: 3.
41. Yun K, Moon HT. Inducing Chondrogenic Differentiation in Injectable Hydrogels Embedded with Rabbit Chondrocytes and Growth Factor for Neocartilage Formation. *J. Biosci. Bioeng.* 2008;105: 122-126.
42. Tang QO, Shakib K, Heliotis M, Tsiridis E, Mantalaris A, Ripamonti U, and Tsiridis E. TGF- β 3: A Potential Biological Therapy for Enhancing Chondrogenesis. *Exp. Opin. Biol. Ther.* 2009;9: 689-701.



Chapter 7

Self-attaching and Cell-attracting *In-Situ* Forming Hydrogels of Natural Polymers for Cartilage Repair

Liliana Moreira Teixeira, Suzanne Bijl, Vishnu Pully, Cees Otto, Rong Jin, Jan Feijen, Clemens van Blitterswijk, Piet Dijkstra, Marcel Karperien

7

Abstract

Small cartilage defects are frequently encountered in arthroscopic procedures. The majority of these defects are treated with debridement or left untreated, predisposing to early onset osteoarthritis. Here, we propose to fill up these defects with a cell-free injectable, *in situ* gelating hydrogel comprising dextran-tyramine conjugates (Dex-TA) that can be readily applied during arthroscopic procedures. In this study, we report on the mechanism of adhesion between cartilage and Dex-TA hydrogels and enhancement of cell ingrowth by incorporation of Heparin-tyramine (Hep-TA) conjugates.

The crosslinking reaction of Dex-TA and Hep-TA hydrogels is based on the covalent binding of hydroxyphenyl residues catalyzed by horseradish-peroxidase (HRP). We hypothesized that the crosslinking reaction may result in covalent bonding of hydroxyphenyl residues, available in Dex-TA and Hep-TA conjugates to tyrosine residues in cartilage matrix proteins. The involvement of TA residues in the bonding was confirmed by modelling the enzymatic reaction occurring during hydrogel gelation. Inter-

estingly, the mechanical analysis indicated that when the tyramine content increased, stronger binding was achieved. Interfacial cartilage-hydrogel morphology and Raman spectroscopy demonstrated the reorganization of collagens and evidenced the coupling of tyramine residues to tyrosine residues in collagen. Moreover, Dex-TA allowed cell migration and the addition of Hep-TA induced cell recruitment.

Collectively, *in vitro* and *ex vivo* functional studies provided strong evidence for covalent bonding of hydrogels conjugated with tyramine to tyrosine residues in cartilage matrix proteins. The ability of these hydrogels to attract cells could be explored as a cell-free system to guide tissue repair in focal cartilage defects, preventing or delaying the onset of osteoarthritis.

7.1 Introduction

Articular cartilage degeneration is part of the clinical condition of osteoarthritis (OA). OA is the most common cause of chronic musculoskeletal pain and mobility disability. A diversity of treatments has the prospective to improve healing of articular surfaces, including micro-fracture of subchondral bone, mosaicplasty, autologous cell implantation (ACI), growth factors, and artificial matrices [1]. However, each of these methods exhibits disadvantages, for instance micro-fracture leads to fibro-cartilage, mosaicplasty results in poor integration and donor site morbidity and with ACI more hyaline cartilage is obtained, yet the long term outcome is still debated [2,3,4,5]. The use of an artificial matrix for filling up small focal defects is an attractive strategy for treatment of defects that are otherwise left untreated and may ultimately predispose to early onset osteoarthritis. We hypothesize that by applying a biocompatible and degradable hydrogel directly after the debridement, mechanical stability of cartilage can be improved while facilitating tissue regeneration. Such hydrogel may counteract mechanically induced cartilage erosion and, thus may effectively delay or even prevent the development of osteoarthritis. Ideally, the hydrogel should also be an adhesive material that can be applied in analogy to wound dressings [6].

To translate this to an approach that can be applied during an arthroscopic procedure, the following pre-requisites have to be fulfilled: i) the material should initially be fluid to fill up irregular defects, ii) should improve mechanical stability, iii) preferably mimic cartilaginous matrix properties, and finally iv) should be fully compatible with cell growth and tissue remodeling. More importantly, and in addition to these features, the biomaterial must bind strongly to the native tissue, preferably by covalent bonding. Hydrogels consisting of natural polymers are likely to fulfil these requirements, due to their resemblance to the cartilaginous matrix [7,8,9,10]. Injectable hydrogels are of particular interest for cartilage tissue engineering, since they can be applied in minimally invasive procedures [11]. Enzymatic crosslinking is an increasingly attractive method to induce *in situ* hydrogel formation due to the mildness of the process. Naturally occurring enzymes such as transglutaminases and peroxidases are commonly used as the catalysts [12,13,14,15]. Peroxidases are natural cross-linkers commonly used for enzyme-catalyzed polymerization and are involved in several catalytic processes within the human body. Examples of such enzymes are

eosinophil peroxidase, myeloperoxidase and lactoperoxidase [16,17]. We and others have previously reported the introduction of hydroxyphenyl groups in the backbone of naturally occurring polymers, such as dextran, hyaluronic acid and chitosan, which allow *in situ* gelation mediated by non-toxic concentrations of H_2O_2 and horseradish peroxidase. Using this system, covalent bonds between hydroxyphenyl groups are efficiently formed. Hydroxyphenyl residues are also present in tyrosine suggesting that during *in situ* gel formation the polymers may covalently bind to tyrosine-containing extracellular matrix proteins.

Commercially available tissue glues for surgical purposes based on fibrin are the current golden standard. Although biocompatible, these glues tend to rapidly degrade, in particular in the presence of increasing concentrations of chondrocytes [18]. Other injectable adhesive hydrogels based on chitosan show initial fixation, yet are slowly gelating and mechanically fragile [19]. An elegant multi-step system using chondroitin sulphate (CS)-based glue to covalently link cartilage to a hydrogel [20] has been reported. This approach improves the mechanical stability, however it requires an invasive procedure involving cartilage digestion followed by UV crosslinking. More recently, a scaffold adhesive based on CS and polyethylene glycol (PEG) has been described [21]. Although these CS-PEG gels were able to covalently crosslink to primary amines of collagens by the formation of amide bonds, they were not permissive for cell ingrowth and matrix remodelling. The ability of hydrogels to equally facilitate cell infiltration and matrix production is fundamental to develop a cell-free biomaterial to guide tissue repair. Cell-free systems demand less legislation for FDA approval; consequently, translation into clinical settings can occur more rapidly. Moreover, additional surgeries to collect autologous chondrocytes are avoided, as well as time and resource-consuming cell expansion steps.

Simultaneous positioning of a material at the diseased cartilage surface and cell-homing by one simple injection are keys for the success of cartilage repair strategies. Therefore, in this study, we explored the potential of covalent bond formation between the hydroxyphenyl groups present in both Dex-TA and cartilage matrix components, by evaluating whether Dex-TA based hydrogels promote self-attachment during the enzymatic crosslinking reaction. Additionally, we optimized the hydrogel features to enable cell invasion by incorporation of heparin components.

7.2 Materials and Methods

7.2.1 Synthesis of Dextran-Tyramine conjugates (Dex-TA)

Dextran from *leuconostoc* ssp. (Mn,dextran =14 k) and p-nitrophenyl chloroformate (PNC) were purchased from Fluka. Tyramine (TA), N,N-dimethylformamide (DMF) anhydrous 99,8 %, hydrogen peroxide (H_2O_2), pyridine anhydrous 99,8 %, lithium chloride (LiCl) and phosphorus pentoxide were obtained from Sigma-Aldrich. Heparin sodium (from porcine intestinal mucosa, molecular weight ranges from 3 to 30 kg/mol) was purchased from Celsus. Horseradish peroxidase (HRP, type VI, 256 purpurogallin unit/mg solid) was purchased from Sigma and used without further purification. Phosphate-buffered saline (PBS, 150mM, pH 7.4) was purchased from

B. Braun Co. LiCl was dried at 80 degrees Celsius under vacuum in the presence of phosphorus pentoxide. Dex-TA and Hep-TA were synthesized as previously described [22,23,24].

7.2.2 Cell culture

Bovine primary chondrocytes were isolated from bovine knee articular cartilage by collagenase digestion and cultured in chondrocyte expansion medium (DMEM containing FBS, non essential amino acids, ascorbic acid, proline, penicilline/streptomycin and fungizone) as previously described [14]. Cells were incorporated into the hydrogels with a cell density of 10×10^6 /mL (passage 0). The cell suspension was mixed with the polymer. The H_2O_2 and HRP solutions were added to the polymer/cell suspension and gelation occurred within one minute. The schematic representation of Dex-TA crosslinking is shown in figure 7.9-b. The amount of HRP used was fixed at 0.25mg per mmol of TA moieties and the molar ratio of H_2O_2 /TA was 0.20 (mol/mol). Constructs were cultured in chondrocyte expansion medium. The gelation reaction occurring in an artificially introduced bovine articular cartilage defect is depicted in figure 7.9-c.

7.2.3 Articular cartilage in contact with Dex-TA: SEM and histological analysis

Dex-TA hydrogels with primary chondrocytes were prepared on top of bovine knee articular cartilage explants (1x1x0.2 cm). After 15 days of culture, the centres of the constructs were visualized using wet mode Scanning Electron Microscopy (SEM) (100 % humidity, 10.0 kV, 3.7 Torr, XL 30 ESEM-FEG Philips). For high-resolution SEM (HR-SEM), Dex-TA hydrogels were prepared on top of bovine knee articular cartilage squares (0.5x0.5x0.2 cm) and cross-sections of these squares, to evaluate whether the hydrogels are able to bind equally to the cartilage surface and to deeper cartilage zones. Biopsies from rat muscle and fat pad were also analysed. After fixation in 10 % buffered formalin, the constructs were cut in half, dehydrated and lyophilized (CPD030 Balzers Critical Point Dryer). Dried constructs were then coated with gold (Cressington sputter coater) and sample centres were visualized using High Resolution (HR)-SEM. For histological analysis, hydrogel/cell constructs were formed on top of articular cartilage squares and collected after 21 days in culture. Samples of muscle and fat pad with Dex-TA were also processed for histology. Samples were embedded in paraffin and sections of 5 micron were used for the staining with Safranin O. After rehydration, the samples were counterstained with haematoxylin and fast green. After rinsing with acetic acid solution (1 %), the sections were stained with Safranin O solution (0.1 %) and dehydrated. Slides were assembled with resinous medium for visualization using light microscopy (Nikon Eclipse E-400).

7.2.4 Mechanical testing

Bovine articular cartilage explants were fixated in 4 % buffered formalin and immobilized in the Dynamic Mechanical Analyzer (DMA) sample holders. Hydrogel samples were directly crosslinked onto the cartilage. As control, previously crosslinked hydrogels were placed onto the cartilage. The DMA 8000 (PerkinElmer) was calibrated in shear setup. The storage modulus and damping factor were measured at room temperature. Average and standard deviations were calculated over similar time frames. Values were afterwards converted into percentages, with Dex-TA 14k-15 *in situ* crosslinked onto cartilage set to 100 %.

7.2.5 Micro-Raman spectroscopy

Fresh bovine articular cartilage pieces (1x3x3 mm) were collected. Dex-TA, dissolved in PBS, was directly crosslinked on top of the cartilage. The gel and cartilage pieces without gel were used as controls. Raman measurements were carried out on non-fixed freshly assembled samples. Raman measurements were performed using a custom-built confocal Raman spectrometer. A Kr-ion laser (Coherent, Innova 90-K, Santa Clara, CA) with an emission wavelength of 647.1 nm was used as an excitation source. Raman spectra of a 30x30 μm scan area were collected (Power: 35mW, 30xW objective, 50 ms/pixel accumulation time) as previously described [25,26]. A Raman calibration standard (toluene) with accurately known peak frequencies was used for wave number calibration of the spectra. All data manipulations were performed using routines written in MATLAB 7.4 (The Math Works Inc.). After hierarchical cluster analysis, a Raman cluster image and spectra for each cluster were obtained [25,27]. The peaks of interest were analysed using Origin software and Matlab.

7.2.6 Crosslinking of fluorescent labeled tyramide with components in the ECM of articular cartilage

Cy5-labeled tyramide (PerkinElmer) stock solution was prepared according to manufacturer's instructions and further dilutions were prepared in amplification diluent (PerkinElmer, USA). Articular cartilage explants (1x3x3 mm) were incubated for 1 hour at 37 degrees Celsius with Chondroitinase ABC (5,146 units/mL in 0,01 % BSA in PBS, Sigma). As a negative control, Chondroitinase ABC was replaced by PBS. Explants were washed with PBS and incubated with Cy5-labelled tyramide (1:50 or 1:100 dilutions of the stock solution, as supplied by the manufacturer), H_2O_2 and HRP for 10 minutes, under agitation. As a negative control, HRP was replaced by PBS. The volume ratio of HRP/ H_2O_2 used was 286/218 and the volume ratio of (HRP+ H_2O_2)/diluted tyramide was 1/4. Samples were visualized by fluorescence microscopy (Nikon E-400). All pictures were taken at the same exposure time. For quantification of fluorescence intensities, the mean colour of the pictures of the samples was determined using Corel Photo Paint 12 software. The colour scale ranges from 0 to 255, in which a value of 0 correlates with a pure black sample and a colour of 255 represents a pure red sample.

7.2.7 Cell adhesion and cell migration assay

Cell migration assays were performed using a transwell system. Dex-TA/Hep-TA hydrogels in ratios of 100/0, 75/25, 50/50 and 25/75 (final polymer content of 20 % (w/v)) were placed on the bottom of migration plates (Kit CytoSelect 24-well Cell Migration Assay 8 μm , Colorimetric format; CBA-100 Cell Biolabs, Inc.). Chondrocytes were isolated from human articular cartilage, obtained after total joint replacement surgery. Cartilage explants were kept in culture for two weeks to allow isolation of chondrocyte progenitor cells, as described elsewhere [28], or immediately digested using collagenase type II (Worthington), to isolate the chondrocytes. Isolated cells were seeded in a density of 3000 cells per cm^2 . Cells were expanded until use (passage 2). The insert was filled with 300 μL of a cell suspension containing 2 million human chondrocytes (hChond) or chondrocyte progenitor cells (hCPC)/ml in serum-free medium and cultured for 24 hours. Afterwards, the medium was carefully aspirated from the inside of the insert. The interior of the inserts was swabbed to remove all non-migratory cells. The inserts were transferred to a clean well containing 400 μL of Cell Stain Solution and were incubated for 10 minutes at room temperature. The stained inserts were washed several times and allowed to dry to air. Each insert was transferred to an empty well and 200 μL of Extraction Solution was added. After 10 minutes of incubation, each sample was transferred to a 96-well microtiter plate and the optical density (OD) at 560 nm was measured in a plate reader. The migration of cells within the hydrogels was also assessed. Dex-TA gels containing cells were prepared on top of Hep-TA gels without cells. Dex-TA gels contained 0.25×10^6 bovine primary chondrocytes (P2). Gels were removed from the wells and put upside down (Dex-TA on the bottom) in a cell culture plate, with chondrocyte expansion medium. Samples were fixated in 10 % buffered formalin at day 1, 3, 7 and 14. Cryosections (20 μm thickness) were stained for 10 minutes with 0.1 % toluidine blue solution (Fluka). After washing, samples were incubated with DAPI (100x diluted, Vector Laboratories) and analyzed by light and fluorescent microscopy.

7.3 Results

7.3.1 Higher number of hydroxyphenyl groups enabled stronger adhesion to the host tissue

Adhesion of a biomaterial to native cartilage is considered as a critical step in integrative cartilage tissue repair [29]. Figures 7.1-a and 7.1-b show a construct of bone-cartilage-hydrogel-cartilage-bone. Notably, Dex-TA with higher degree of substitution visually resembled cartilage and allowed the support of the whole construct. A dynamic mechanical analyzer (DMA) was used to measure the adhesion strength between cartilage and Dex-TA hydrogels. The shear setup was selected to determine the shear moduli of hydrogels with two different degrees of substitution: DS8 and DS15. In this way, the amount of hydroxyphenyl groups available for crosslinking within the polymeric network and onto the cartilage surface is almost doubled. The

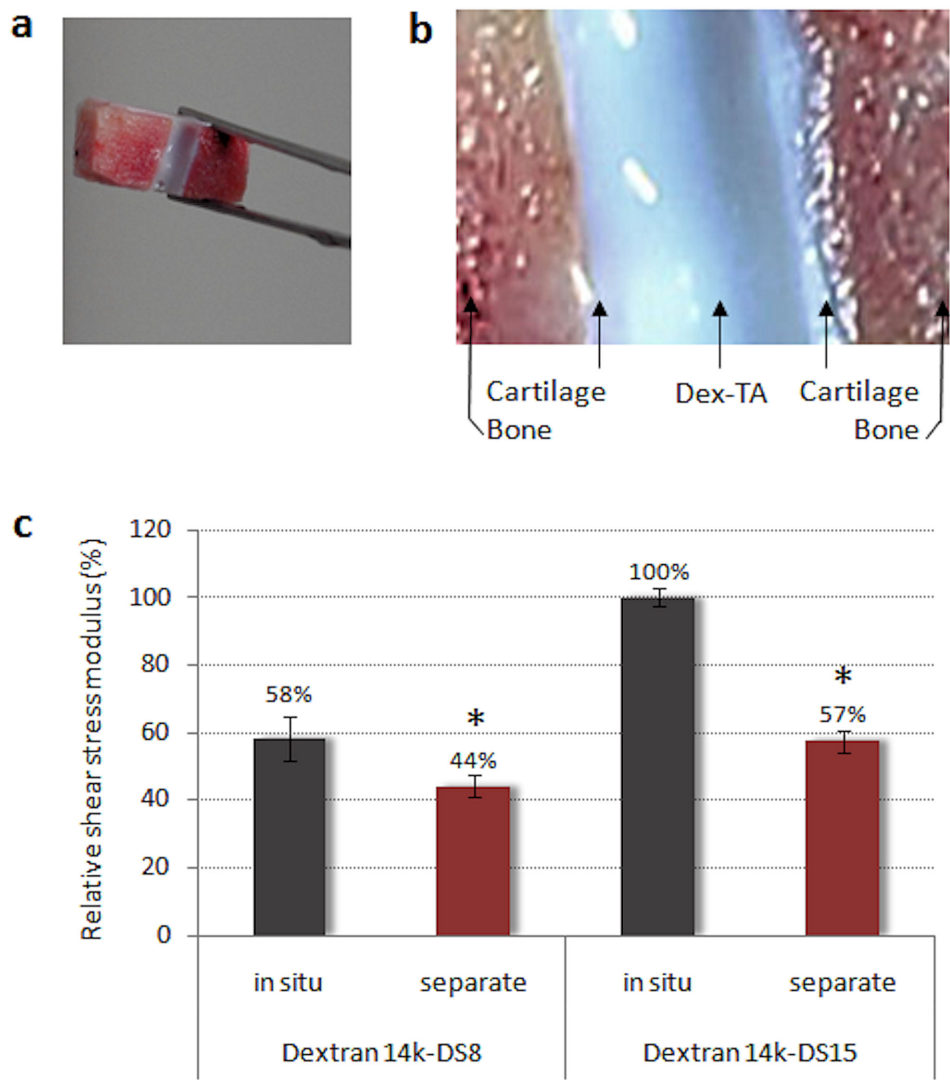


Figure 7.1: Hydrogel adhesion and maximal shear modulus. a. and b. Construct consisting of two bovine explants of sub-chondral bone covered with a layer of cartilage of 1 cm² with a layer of *in situ* formed Dex-TA hydrogel between the explants. The final construct shows high stability when held horizontally between tweezers. c, Maximal shear modulus (relative) of cartilage with 14k-DS8 and 14k-DS15 Dex-TA hydrogels formed *in situ* and for cartilage combined with pre-gelated 14k-DS8 and 14k-DS15 Dex-TA hydrogels.

maximal shear moduli were determined both for hydrogels crosslinked *in situ* on top of the cartilage and apart from the cartilage (Figure 7.1-c). In the latter case the gel and cartilage were joined together before measurements. Interestingly, the shear moduli of Dex-TA hydrogels *in situ* formed on cartilage were higher than for hydrogels combined with cartilage after gelation. In addition, the maximal shear moduli for the gels based on DS15 were higher than those based on DS8. Thus, higher degrees of substitution lead to both mechanically stronger gels [22] and to higher adhesion strength between the hydrogel and the native tissue, which lead us to investigate further the hypothesis of covalent bonding of the gels to tyrosine residues of the cartilage.

7.3.2 Analysis of the hydrogel - cartilage interface showed evidence for gel-tissue integration

When simulating *in situ* gelation of Dex-TA polymers together with 10×10^6 chondrocytes/ml in an articular cartilage defect created in the bovine patella, we observed smooth filling of the defect (figure 7.2-a). Consequently, we investigated the interface between the host tissue and the Dex-TA hydrogel in more detail. Representative histological analysis of sections showed the integration of Dex-TA hydrogels with articular cartilage, as shown in figures 7.2-b and c. The constructs of gel-cells/cartilage were cultured for 21 days with no further addition of growth factors. A gradient of proteoglycans in the hydrogel was visible, as evidenced by the increase in intensity of Safranin O staining (glycosaminoglycans stain red/pink). This staining decreased with increasing distance to the cartilage interface (figure 7.2-b), suggesting integrative interaction between the hydrogel and the cartilage. Intense safranin O staining was also observed surrounding the chondrocytes. Picrosirius red staining, which is used to visualize collagens under polarized light, showed a highly intense staining in the interface area and in the pericellular matrix surrounding chondrocytes embedded in the hydrogel, as shown in figure 7.2-c.

7.3.3 Bonding of the polymers to collagen fibrils in the cartilaginous matrix

To visualize the interface between *in situ* crosslinked Dex-TA hydrogels and articular cartilage at the micro and nanometre scale, two approaches were used: wet SEM and HR SEM imaging. In wet SEM, a smooth transition between Dex-TA hydrogel and articular cartilage was observed, as shown in figure 7.3-a. Due to the high pressure, water was extracted from the hydrogel but not from the cartilage, chondrocytes in the cartilage are visible as spheres allowing easy discrimination of the gel and native cartilage. Secondly, HR-SEM was performed to analyse the interface at the nanometre scale. The cross-sections shown in figures 7.3-b and 7.3-c clearly showed attachment of the hydrogels to articular cartilage through interconnections with cartilage ECM components. It is likely that these ECM components are collagen fibrils, since the D period in the observed fibrils was clearly visible at high magnifications (figure 7.3-c).

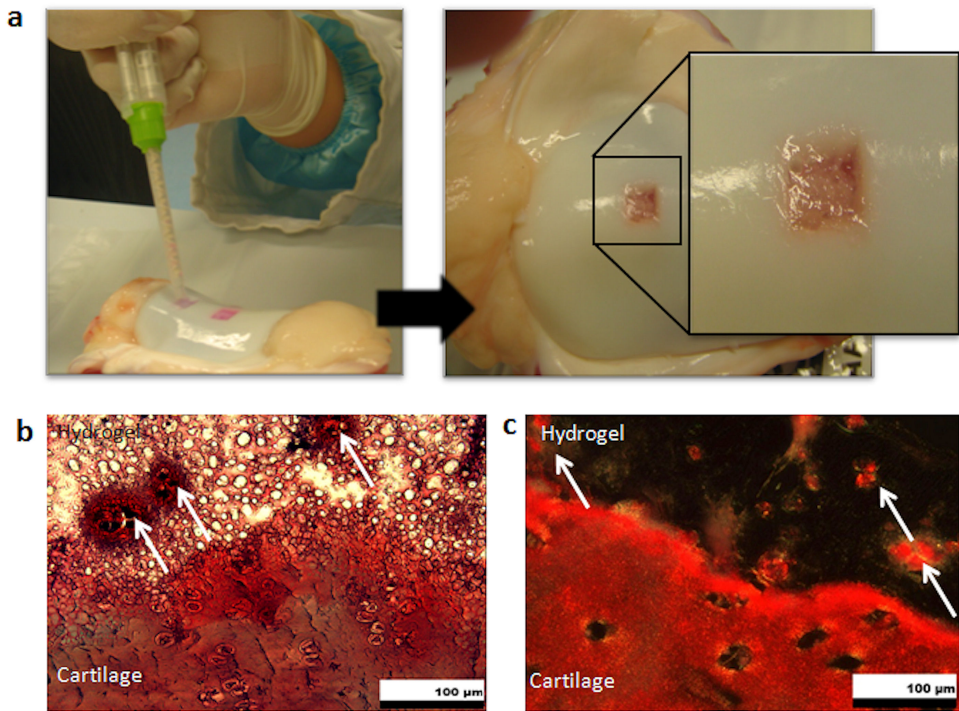


Figure 7.2: Overview and histological evaluation of cartilage defects filled up with Dex-TA hydrogel. a. A cartilage defect in the bovine patella is filled up with a Dex-TA hydrogel combined with bovine chondrocytes. The gel is applied using a dual syringe in which one chamber contains the cell suspension (10 million cells per mL) and the polymer (final volume of 10 % w/v) while the other chamber contains HRP and H_2O_2 . After mixing both chambers contents together along the circular final mixing compartment, gelation occurs within one minute which results in total filling of the defect, as shown in the detailed picture of the simulated defect site at the right. b. Safranin O staining indicating in pink/red the accumulation of glycosaminoglycans. The white arrows indicate the cells incorporated in the hydrogel. A decreasing gradient of glycosaminoglycans (GAGs), from cartilage to the hydrogel, indicating that diffusion of GAGs through the interface takes place. In addition, safranin O staining is surrounding the chondrocytes embedded in the hydrogel, indicating newly formed GAGs. c. Picrosirius red staining, visualized by polarized light, demonstrates the presence of collagen fibrils at the cartilage/hydrogel interface and surrounding the chondrocytes embedded in the hydrogel, indicated by the white arrows.

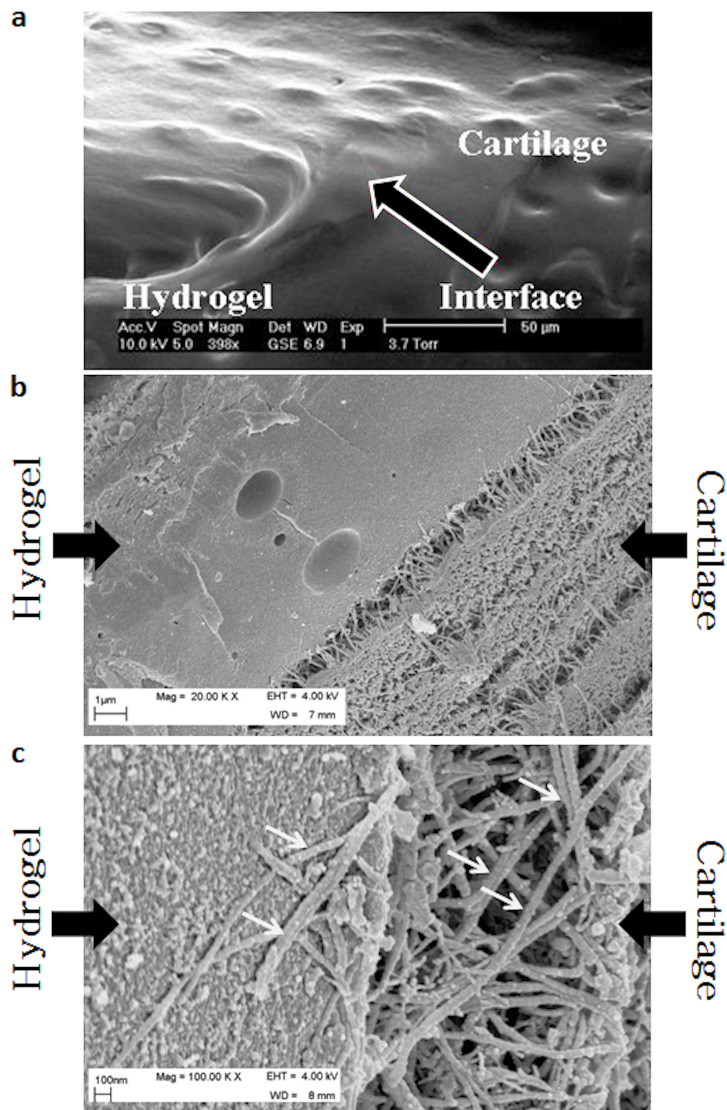


Figure 7.3: Morphological analysis of the cartilage-Dex-TA hydrogel interface. a, Representative wet mode SEM images showing a smooth transition between Dex-TA hydrogels and cartilage. The arrow indicates the cartilage-Dex-TA hydrogel interface. c and d, Representative HR-SEM pictures showing increasing magnifications of the hydrogel-cartilage interface. The images are suggestive for a direct interaction between the hydrogel and collagen fibrils of which the D period is clearly visible at higher magnifications (with arrows). The magnifications are indicated in the figures.

7.3.4 Formation of new C-C and C-O-C bonds suggestive of covalent bond formation

The intricate interaction of Dex-TA with collagen fibrils and the increase of adhesion strength when more hydroxyphenyl groups were present are strongly suggestive that the formation of covalent bonds with ECM proteins has taken place. We next used Raman micro-spectroscopy to identify the nature of the molecular interaction between the hydrogel and the cartilage. The interface of cartilage and the *in situ* formed Dex-TA was scanned and the spectra were analysed by hierarchical cluster analysis allowing discrimination of hydrogel only, cartilage only and interface spectra (figures 7.4-b to 7.4-d). The red spectrum represents the average spectra of pixels corresponding to the interface region between hydrogel and cartilage. This interfacial region spectrum showed different spectral properties compared to the spectra of hydrogel and cartilage only. Detailed analysis showed the presence of spectral features of both cartilage and hydrogel in the interface (figure 7.4-c and d). However, when enlarged also new features such as shifts in peaks, new peaks and reshaped peaks could clearly be identified as specific for this region (7.4-e to 7.4-i). These new peaks are listed in table 7.1, according to Movasaghi et al [30]. These peaks could be assigned to collagens, polysaccharides and aminoacids (especially tyrosine). Interestingly, new peaks could also be assigned to remodelling of C-C and C-O-C bonds which are formed during the peroxidase mediated crosslinking. An intricate interaction between cartilaginous ECM proteins and the hydrogel was furthermore supported by the resulting interface spectra with unique characteristics after subtraction of the hydrogel only spectrum (figure 7.5).

7.3.5 HRP enabled covalent crosslinking of tyramide residues to cartilage matrix

The enzymatic reaction occurring during crosslinking represented in figure 7.6-a on cartilaginous tissue was mimicked by fluorescent labelled tyramide to confirm whether the tyramine residues in Dex-TA were indeed involved in the adhesion reaction. Fluorescent-labelled tyramides (TyrCy5) were used to visualize tyramides retained on the cartilage surface after the peroxidase mediated crosslinking resulting in fluorescence. Unbound tyramides were washed off and did not result in fluorescence of cartilage explants. The effects of pre-digestion of articular cartilage by chondroitinase and various concentrations of the labelled tyramide in combination with H_2O_2 and HRP, were addressed. Figure 7.5-b shows a clear difference in the fluorescence level between the samples incubated with and without HRP. When no HRP was present the fluorescence level was lower. Moreover, a decrease in the fluorescence level could be detected when using 1:100 instead of 1:50 diluted tyramides.

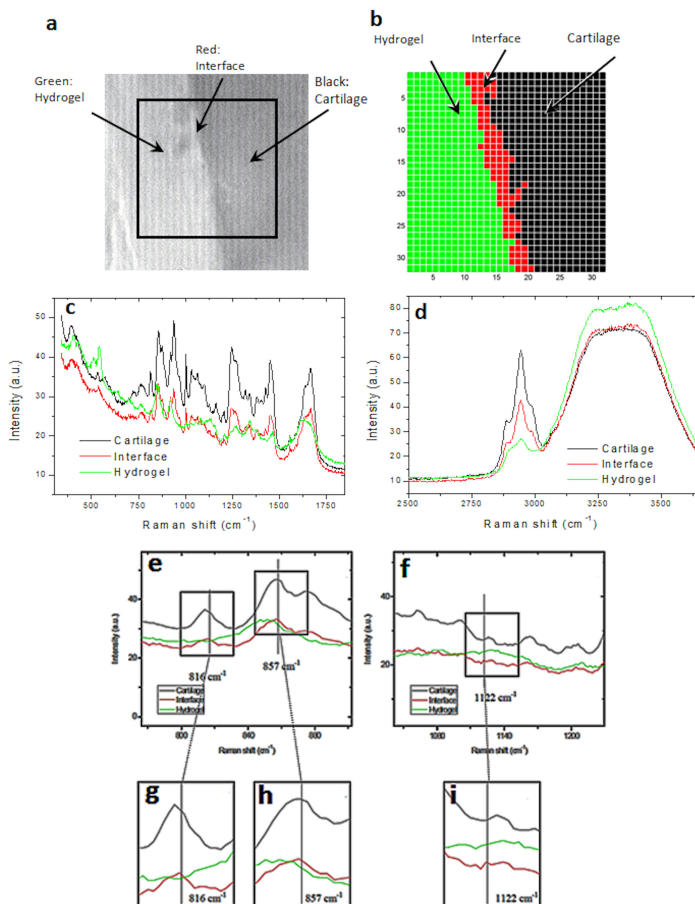


Figure 7.4: Raman micro-spectroscopy of the interface area. a, White light micrograph showing the scanned interface region of $30 \times 30 \mu\text{m}$ (boxed). In this area 1024 scans were taken. b, Hierarchical cluster analysis of 1024 Raman scans (Power: 35mW, objective: 40xW, accumulation time 50 ms/pix) identifies 3 different spectra corresponding to the hydrogel only (green), the cartilage only (black) or the interface (red). c, d, Raman spectra of the Dex-TA/cartilage interface with: the cartilage region (black cluster), the interface region (red cluster) and the Dex-TA 14k-DS10 hydrogel region (green). c, The most informative region of the spectrum; d, Spectrum showing the water bands (Power: 35 mW, objective: 40xW, accumulation time 50 ms/pix). e-f, Spectral range selections of figure c, of $\Delta=780\text{-}820 \text{ cm}^{-1}$ and of $\Delta=1050\text{-}1230 \text{ cm}^{-1}$, respectively, showing peaks of interest. g, Selected area of e, showing a change at 816 cm^{-1} . h, Selected area of e, showing a change at 857 cm^{-1} . i, Selected area of f, showing a change at 1122 cm^{-1} .

| Detected peak (cm ⁻¹) | Assignment |
|-----------------------------------|---|
| 728 | C-C stretching, proline (collagen assignment) |
| 816 | 815: Proline, hydroxyproline, tyrosine, ν_2 PO ₄ ²⁻ stretch of nucleic acids 817: C-C stretching (collagen assignment) |
| 857 | 855-856: Tyrosine C-C stretching 856: C-C vibration of the collagen backbone 859: Tyrosine, collagen |
| 1102 | 1100: C-C vibration mode of the gauche-bonded chain |
| 1122 | ν_s (C-C) skeletal, ν_{sym} (C-O-C) (polysaccharides, cellulose) |
| 1332 | -C stretch of phenyl (1) and C ₃ -C ₃ stretch and C ₅ -O ₅ stretch CH _α in-plane bend |

Table 7.1: Spectral interpretations of the Raman spectra. The detected peaks of interest in the interface spectra, showing a shift when compared to the spectra obtained from cartilage and hydrogel, are attributed to a specific assignment, according to Movasaghi et al [30].

7.3.6 Covalent bonding of hydrogels to collagen-rich tissues other than cartilage

We next examined whether *in situ* formed Dex-TA hydrogels could also covalently bind to other tissues than cartilage by evaluating their interaction between the hydrogels and muscle or fat pad. The ECM of these two tissues consists mainly of collagen type I with variations in quantity and structural organization. HR-SEM and histological evaluation was performed on constructs of tissue explants with an *in situ* formed layer of Dex-TA hydrogel. HR-SEM of the muscle-hydrogel interface showed interactions of the hydrogel with collagen fibrils (figure 7.7-a). The fat pad/Dex-TA interface observed by HR-SEM provided also evidence for an interaction between the hydrogel and collagen fibrils but in line with the lower quantity of collagen fibrils in fat tissue, the interactions were less abundant (figure 7.7-b). Histological analysis showed a smooth interface area without any gaps between muscle and Dex-TA hydrogels resembling the interface between cartilage and hydrogels (figure 7.7-a, right

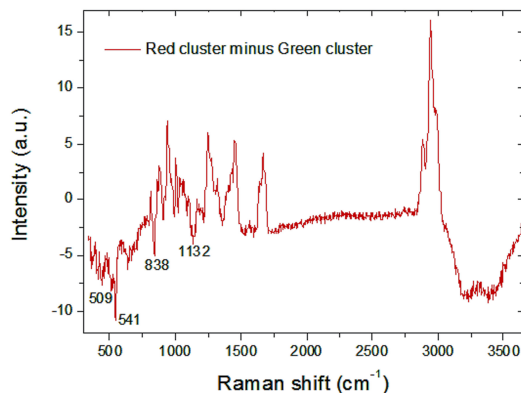


Figure 7.5: Average Raman spectra of average red cluster subtracted by average spectra of green cluster. Positive bands correspond to cartilage. Negative bands at 509, 541, 838 and 1132 cm^{-1} correspond to hydrogel. This shows the uptake of hydrogel by the cartilage, which occurs at the interface.

image showing a section stained with H and E). The interface morphology between the fat pad and Dex-TA showed areas with gaps (figure 7.7-b, right image showing a section stained with H and E), suggesting that the bonding of the *in situ* formed hydrogel to different tissues is dependent on the amount of collagen in the extracellular matrix of the respective tissue.

7.3.7 Incorporation of Hep-TA enabled cell adhesion and triggered cell homing in Dex-TA hydrogels

In addition to the characterization of the self-attachment properties of Dex-TA, the potential of this hydrogel to be used as a cell-free system was evaluated. Since the cell interaction potential of Dex-TA is limited, hydrogels were prepared with Dex-TA and Hep-TA hydrogels in different ratios to evaluate whether this strategy could induce cell recruitment. The cell migration potential of these hydrogels was determined by a trans-membrane migration assay. Two different cell types were used; human chondrocytes and chondrocyte progenitor cells, which are known to exhibit a higher migratory potential [28]. The results show that increasing contents of heparin induced higher cell homing towards the hydrogels, with no significant difference between the two cell types (Figure 7.8-a). In a dynamic cell seeding experiment, cells attached to the outer surface of a Dex-TA hydrogel were observed but these cells invaded the hydrogel only to a limited extent (figure 7.8-b). To test whether the Dex-TA hydrogels were compatible with cell migration Dex-TA hydrogels were incorporated with chondrocytes. Subsequently, a cell free Hep-TA hydrogel was prepared on top

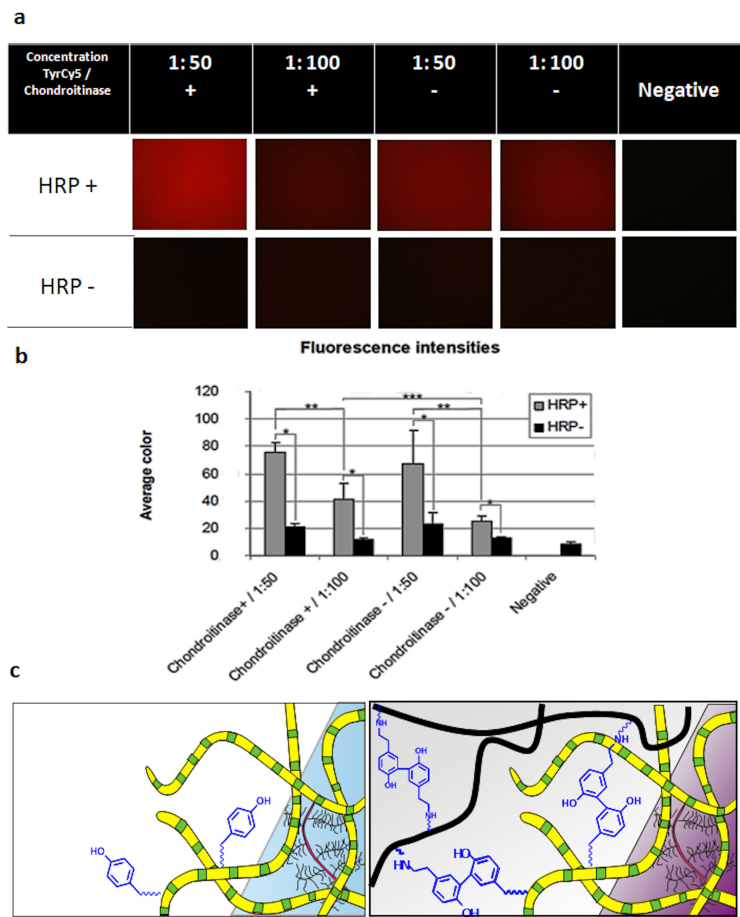


Figure 7.6: Enzymatic crosslinking of Cy5-labeled tyramide on bovine articular cartilage. a, Fluorescent microscopy images show representatives (n=4) of bovine articular cartilage incubated with or without chondroitinase, with and without HRP, with H₂O₂ and different concentrations of TyrCy5 (diluted 1:50 or 1:100). b, Fluorescence quantification of bovine articular cartilage incubated with and without chondroitinase, in the presence or absence of HRP and H₂O₂ with different concentrations of TyrCy5 (diluted 1:50 or 1:100). The mean color of the pictures was determined for quantification of fluorescence intensities (average of 3 spots within each sample, * P<0,05), average color: 0 = black, 255 = red. c, Schematic summary of the postulated enzymatic crosslinking between Dex-TA conjugates and collagen molecules present in the cartilage ECM via tyramine-tyrosine covalent bond formation.

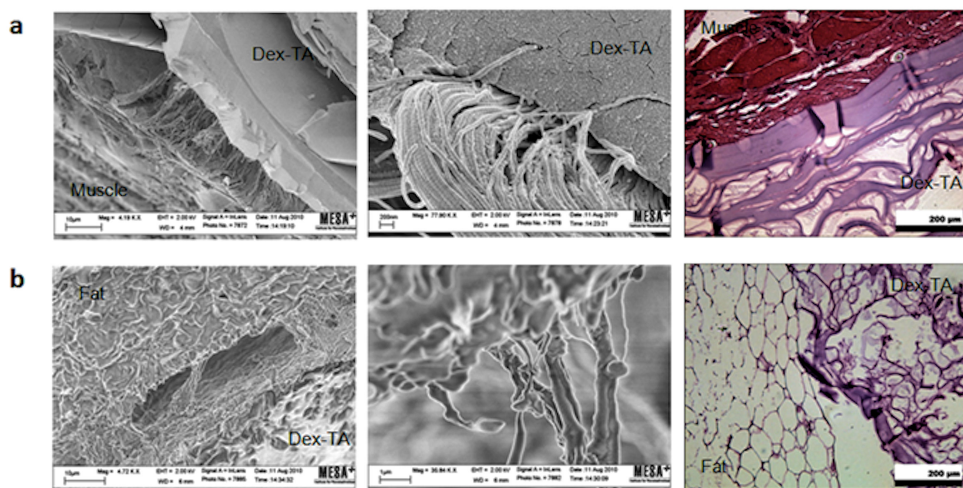


Figure 7.7: HR-SEM and histological images, showing the interface between other collagen-rich tissues and Dex-TA hydrogel. a, HR-SEM pictures showing the attachment of the hydrogels to muscle tissue via bonding to collagen fibrils (left and middle) and a representative histological section with H and E staining demonstrating the smooth transition without gaps at the muscle/hydrogel interface (right). b, HR-SEM pictures showing limited attachment of the hydrogels to fat tissue via bonding to collagen fibrils (left and middle) and a representative histological section with H and E staining, demonstrating the irregularities and poor attachment at the fat/hydrogel interface (right).

7

of these cell loaded Dex-TA hydrogels (Figure 7.8-c). Migration of cells through the Dex-TA into Hep-TA gels could be tracked as the two gel types could be distinguished by toluidine blue staining which stained heparin but not dextran. Interestingly, cell migration against gravity into Hep-TA hydrogels was observed indicating that Dex-TA hydrogels are compatible with cell migration and that the incorporation of Hep-TA renders hydrogels chemo-attractant properties (figure 7.8-d), likely due to the high affinity of heparin to bind with growth factors and chemokines.

7.4 Discussion

Hyaline cartilage regeneration remains challenging. Tissue engineering strategies may provide promising avenues for restoring function when the tissues self-renewal capacity cannot overcome the degeneration caused by disease, severe injury or age-related wear. Polymeric scaffolds that can be applied in minimally invasive procedures are of particular interest. These scaffolds can be designed to orchestrate ingrowth of tissue progenitor cells and facilitate the repair process. *in situ* gelating hydrogels of natural or synthetic polymers provide an excellent alignment with surrounding tissues, and both cells and bioactive molecules can easily and homogeneously be incorporated

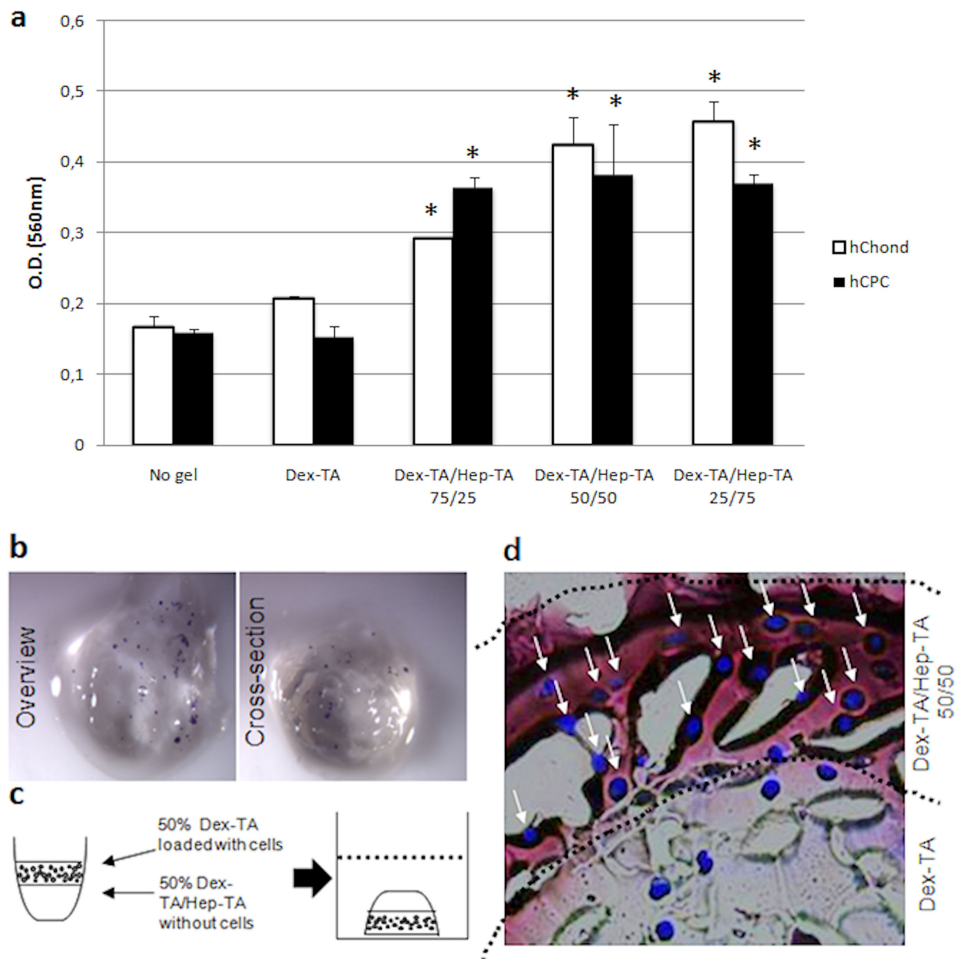


Figure 7.8: Evaluation of the cell migratory potential of Dex-TA-based hydrogels. **a.** Cell migration assay using human chondrocytes (hChond) and human chondrocyte progenitor cells (hCPCs). Dex-TA was mixed with Hep-TA in different ratios: 100/0, 75/25, 50/50 and 25/75 to prepare hydrogels and the migratory cells were quantified. Increasing contents of heparin induced higher cell homing towards the hydrogels, with no significant difference between cell types. **b.** Cell adhesion onto Dex-TA hydrogels was observed, after dynamic cell seeding. The hydrogels were kept in a spinner flask for 7 days and afterwards an MTT assay was performed. The metabolically active cells are stained in purple and can be visualized both at the surface and, to a lesser extent, within the hydrogel, as shown by the cross-section. **c.** Representation of the assembly of constructs of Dex-TA hydrogels containing cells, with Dex-TA/Hep-TA 50/50 gels, without cells, on top. **d.** Migration of cells through the Dex-TA into Dex-TA/Hep-TA 50/50 gels. Toluidine blue staining was used to stain the heparin fraction. Cells were stained with DAPI, which marks in blue the cell nuclei. Cell migration against gravity towards Dex-TA mixed with Hep-TA hydrogels was detected after 24 hours in culture, as cells were observed in the initial cell-free Dex-TA/Hep-TA 50/50 fraction.

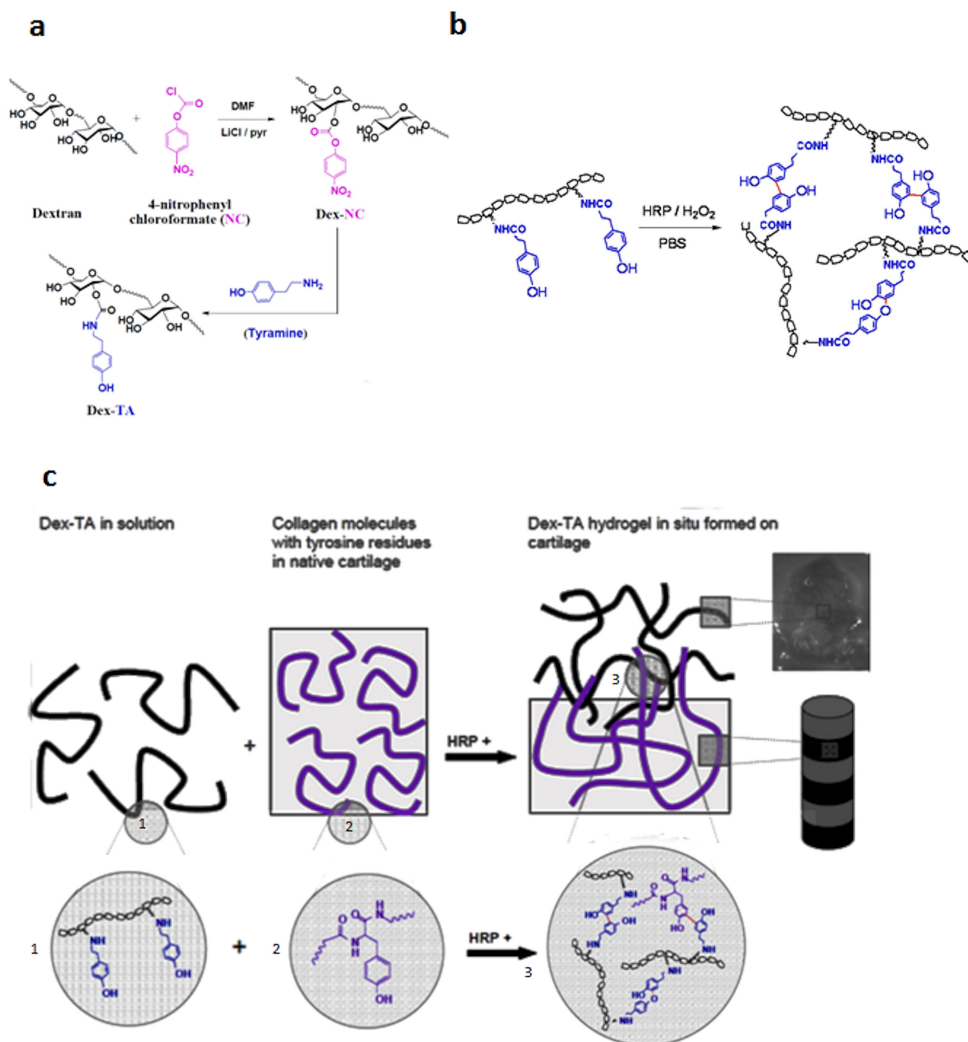


Figure 7.9: Synthesis and enzymatic crosslinking of Dex-TA conjugates and proposed mechanism involved in the adhesion onto cartilage. a, In the first step of the Dex-TA conjugates synthesis, p-nitrophenyl chloroformate is linked to the dextran backbone. This step is followed by substitution of the nitrophenyl group by tyramine through the formation of a urethane bond. b, Dex-TA hydrogels are formed by the HRP catalyzed oxidative coupling of the phenol groups of the tyramines present on the dextran backbone, via either carbon-carbon bonds or carbon-oxygen-carbon bond formation. c. Mechanism of enzymatic crosslinking between Dex-TA conjugates and collagen molecules present in the cartilage ECM via tyramine-tyrosine covalent bond formation.

[31]. However, despite all the advantages of such hydrogels, adequate integration of the hydrogel with native tissue, which is a prerequisite for long term integration of neo-tissue is still an unresolved challenge for most systems [32,33].

Previously, we and others have described hydrogels of natural polymers that gelate *in situ* by an enzymatic cross linking reaction [14,15,22,23,24,34]. Particularly Dex-TA and Hep-TA hydrogels have shown promising features for application in cartilage tissue engineering. These biodegradable hydrogels are formed by an enzymatic crosslinking reaction mediated by HRP (Figure 7.8-a and 7.8-b). The crosslinking reaction occurs under mild conditions and within one to two minutes and is compatible with incorporation of cells [22,23,24]. The integration and interaction between these hydrogels and native cartilage is of major importance, and, therefore, the main focus of this study. Initial adhesion is the key to fast formation of homogeneous tissue with sufficient mechanical stability and functionality [35]. Considering that the formation of di-tyramine, di-tyrosine and the oxidative coupling of other phenols occurs under the influence of HRP and H_2O_2 [36], we hypothesized that tyramine-tyrosine bonds could be formed during the *in situ* crosslinking of tyramine-containing hydrogels onto tyrosine-containing cartilaginous ECM proteins (figure 7.5-c and figure 7.8-c). A comparable mechanism has been described for poly(ethylene glycol)diacrylate (PEGDA) crosslinking on cartilage via tyrosyl radicals [35]. However, this hydrogel-cartilage crosslinking reaction is not based on phenol-phenol coupling and it demands a multi-step approach, involving aggressive oxidation methods with UV exposure and high H_2O_2 concentration (5 %). In contrast, mild oxidation methods with low H_2O_2 concentrations (less than 0,1 %) are used in the formation of Dex-TA hydrogels.

Here, we report the mechanism of adhesion between cartilage and peroxidase crosslinkable Dex-TA hydrogel. Mechanical analysis of the hydrogel using a rheometer has been previously described, providing information about the storage moduli of Dex-TA with various degrees of substitution and molecular weight [22]. Interestingly, our data showed that higher degrees of substitution do not only lead to stronger gels, but also to higher adhesion strength between the hydrogel and the native host tissue. This means that a higher number of tyramine groups are available in the polymer with higher degree of substitution, not only favoring the enzymatic crosslinking reaction between Dex-TA conjugates, but also between the conjugates and cartilage.

From the morphological analysis of the interfacial area between the host tissue and the hydrogel, we concluded that Dex-TA hydrogels do not only attached to the articular cartilage surface, but also to deeper zones of the cartilage, which can be a useful property in the treatment of full thickness or sub-chondral cartilage defects. Furthermore, three interesting phenomena were identified in the HR-SEM characterizations: first, a zone of approximately 2 micrometers wide was observed where the collagen fibrils in the articular cartilage could be identified; second, collagen fibrils were integrated into the hydrogel and finally, the collagen fibrils at the interface clearly reflected alignment towards the hydrogel. We addressed whether these adhesion events also take place when using other collagen-rich tissues. Similar results were obtained for muscle tissue but not for fat pad. These differences can be explained by the differences in collagen types, availability of collagen and, thus, by the availability of tyrosine motifs in these tissues. Taken together, these observations strongly in-

dicating the involvement of collagen fibrils in the immobilization of Dex-TA hydrogels onto articular cartilage and other collagen-rich tissues, during *in situ* gelation.

Covalent bond formation between PEGDA and cartilage analyzed by ATR-FTIR has been previously reported [35]. However, Raman spectroscopy performs better than ATR-FTIR in aqueous environments, therefore this technique is more adequate for the study of biological tissues and hydrogels [37,38]. This spectroscopic method is non-invasive, thus, does not demand any processing of the samples prior to use. Raman spectroscopy also allows for the identification of functional groups, bonding types and molecular conformations [30]. Previously, in our group, we have described the molecular finger-print of both dextran and cartilage tissue alone, using Raman Spectroscopy [27,39]. In the present study, we described the unique molecular finger-print of the interfacial area between the Dex-TA hydrogel and cartilage. Raman micro-spectroscopy analysis indicated the involvement and reorganization of collagen, polysaccharides and aminoacids, especially tyrosine, at the hydrogel/cartilage interface. Furthermore, and of great interest, is the fact that the cluster identified as being the interface between hydrogel and cartilage, when represented in a Raman cluster image, corresponded to a zone of 2-3 micrometers wide, comparable to the width of the region in which reorganized collagen fibrils were identified in the HR-SEM characterization.

The enzymatic reaction occurring during crosslinking on cartilage was mimicked by fluorescent labelled tyramide, to confirm whether the tyramine residues in Dex-TA were involved in the adhesion reaction. Labelled tyramides were found to be crosslinked on articular cartilage surfaces. The reaction was more efficient when more tyramine groups are present. Moreover, pre-treatment with chondroitinase, which degrades polysaccharides in cartilaginous ECM [40], induced a higher fluorescence intensity. This increase occurred because collagens were likely more accessible for the tyramines, HRP and H_2O_2 . Indeed the presence of HRP appeared to be essential to crosslink tyramine residues to cartilage matrix proteins. This mechanism is illustrated in supplementary figure 1-c. However, we cannot exclude that the obtained results could also be due to large tyramine complexes that were trapped in the extracellular matrix or due to deeper penetration of tyramines as a result of the digestion treatment.

Finally, an enhanced cell migratory effect in Dex-TA hydrogels was achieved by the incorporation of Hep-TA conjugates. Cells were likely attracted by the heparin, which might have performed as a driving force for migration of cells through the Dex-TA gel [41]. Heparin is a glycosaminoglycan, widely used as anticoagulant and antilipemic agent [42], which interacts with proteins involved in cell adhesion, migration, proliferation and differentiation [41,43]. Cell migration against gravity in Dex-TA hydrogels was possible and Hep-TA hydrogels were indeed able to induce cell recruitment. Attracting cells passively to the biomaterial/articular cartilage interface may lead to improved tissue integration. Moreover, because cells can be attracted from surrounding tissues, combinations of Hep-TA and Dex-TA may be used as a very effective cell-free system.

7.5 Conclusion

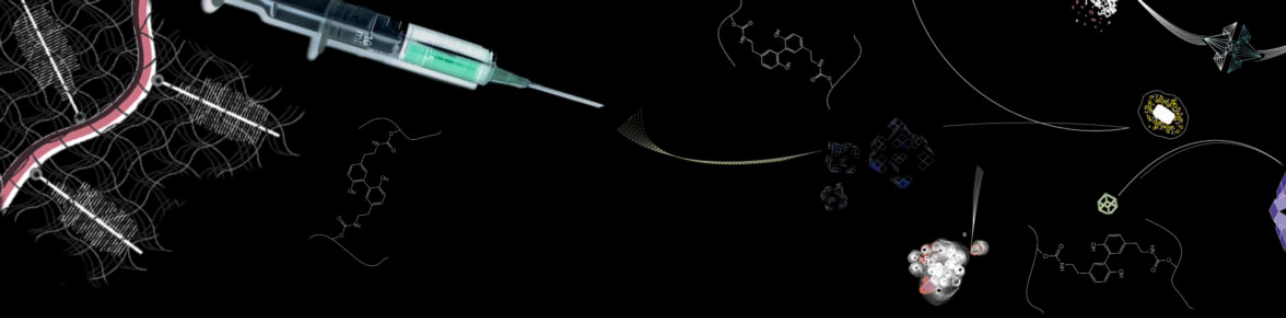
Taken together, our data clearly confirmed that it is feasible to fill up cartilage defects with an *in situ* gelating and mechanically stable hydrogel of natural polymers. During the crosslinking reaction, Dex-TA hydrogels firmly attached to the cartilage ECM by covalent bonding to tyrosine residues in collagen fibrils. In addition, by mixing combinations of natural polymers, for instance Dex-TA with Hep-TA, these hydrogels can be tailored to attract and facilitate cellular ingrowth of chondrocytes or chondrocyte progenitor cells. Thus, hydrogels containing mixtures of Dex-TA and Hep-TA conjugates are promising biomaterials for the development of a cell-free system that can repair tissue defects, not only in cartilage but also in other collagen rich tissues. To the best of our knowledge, this is the first system where cell migration and initial fixation is assured in a one-step minimally invasive procedure which will facilitate the translation of this strategy into clinical applications.

References

1. Buckwalter JA (1998) Articular cartilage: injuries and potential for healing. *J Orthop Sports Phys Ther* 28: 192-202.
2. Bedi A, Feeley BT, Williams RJ, 3rd (2010) Management of articular cartilage defects of the knee. *J Bone Joint Surg Am* 92: 994-1009.
3. Beris AE, Lykissas MG, Papageorgiou CD, Georgoulis AD (2005) Advances in articular cartilage repair. *Injury* 36 Suppl 4: S14-23.
4. Farr J, Cole B, Dhawan A, Kercher J, Sherman S (2011) Clinical Cartilage Restoration: Evolution and Overview. *Clin Orthop Relat Res*.
5. Kreuz PC, Muller S, Ossendorf C, Kaps C, Erggelet C (2009) Treatment of focal degenerative cartilage defects with polymer-based autologous chondrocyte grafts: four-year clinical results. *Arthritis Res Ther* 11: R33.
6. Zhong SP, Zhang YZ, Lim CT (2010) Tissue scaffolds for skin wound healing and dermal reconstruction. *Wiley Interdiscip Rev Nanomed Nanobiotechnol* 2: 510-525.
7. Elisseeff J, Puleo C, Yang F, Sharma B (2005) Advances in skeletal tissue engineering with hydrogels. *Orthod Craniofac Res* 8: 150-161.
8. Spiller KL, Maher SA, Lowman AM (2011) Hydrogels for the Repair of Articular Cartilage Defects. *Tissue Eng Part B Rev*.
9. Lutolf MP (2009) Biomaterials: Spotlight on hydrogels. *Nat Mater* 8: 451-453.
10. Nguyen MK, Lee DS (2010) Injectable biodegradable hydrogels. *Macromol Biosci* 10: 563-579.
11. Gutowska A, Jeong B, Jasionowski M (2001) Injectable gels for tissue engineering. *Anat Rec* 263: 342-349.
12. Aeschlimann D, Mosher D, Paulsson M (1996) Tissue transglutaminase and factor XIII in cartilage and bone remodeling. *Semin Thromb Hemost* 22: 437-443.
13. Greenberg CS, Birckbichler PJ, Rice RH (1991) Transglutaminases: multifunctional cross-linking enzymes that stabilize tissues. *FASEB J* 5: 3071-3077.
14. Jin R, Moreira Teixeira LS, Dijkstra PJ, Karperien M, van Blitterswijk CA, et al. (2009) Injectable chitosan-based hydrogels for cartilage tissue engineering. *Biomaterials* 30: 2544-2551.
15. Kim KS, Park SJ, Yang JA, Jeon JH, Bhang SH, et al. (2011) Injectable hyaluronic acid-tyramine hydrogels for the treatment of rheumatoid arthritis. *Acta Biomater* 7: 666-674.
16. Obinger C (2006) Chemistry and biology of human peroxidases. *Arch Biochem Biophys* 445: 197-198.
17. O'Brien PJ (2000) Peroxidases. *Chem Biol Interact* 129: 113-139.
18. Homminga GN, Buma P, Koot HW, van der Kraan PM, van den Berg WB (1993) Chondrocyte behavior in fibrin glue *in vitro*. *Acta Orthop Scand* 64: 441-445.
19. Hoemann CD, Sun J, Legare A, McKee MD, Buschmann MD (2005) Tissue engineering of cartilage using an injectable and adhesive chitosan-based cell-delivery vehicle. *Osteoarthritis Cartilage* 13: 318-329.
20. Wang DA, Varghese S, Sharma B, Strehin I, Fermanian S, et al. (2007) Multifunctional chondroitin sulphate for cartilage tissue-biomaterial integration. *Nat Mater* 6: 385-392.

21. Strehin I, Nahas Z, Arora K, Nguyen T, Elisseeff J (2010) A versatile pH sensitive chondroitin sulfate-PEG tissue adhesive and hydrogel. *Biomaterials* 31: 2788-2797.
22. Jin R, Hiemstra C, Zhong Z, Feijen J (2007) Enzyme-mediated fast *in situ* formation of hydrogels from dextran-tyramine conjugates. *Biomaterials* 28: 2791-2800.
23. Jin R, Moreira Teixeira LS, Dijkstra PJ, van Blitterswijk CA, Karperien M, et al. (2011) Chondrogenesis in injectable enzymatically crosslinked heparin/dextran hydrogels. *J Control Release*.
24. Jin R, Moreira Teixeira LS, Dijkstra PJ, Zhong Z, van Blitterswijk CA, et al. (2010) Enzymatically crosslinked dextran-tyramine hydrogels as injectable scaffolds for cartilage tissue engineering. *Tissue Eng Part A* 16: 2429-2440.
25. Pully VV, Lenferink ATM, Otto C (2011) Time-lapse Raman imaging of single live lymphocytes. *Journal of Raman Spectroscopy* 42: 167-173.
26. van Manen HJ, Lenferink A, Otto C (2008) Noninvasive imaging of protein metabolic labeling in single human cells using stable isotopes and Raman microscopy. *Anal Chem* 80: 9576-9582.
27. van Manen HJ, van Apeldoorn AA, Verrijck R, van Blitterswijk CA, Otto C (2007) Intracellular degradation of microspheres based on cross-linked dextran hydrogels or amphiphilic block copolymers: a comparative raman microscopy study. *Int J Nanomedicine* 2: 241-252.
28. Koelling S, Miosge N (2009) Stem cell therapy for cartilage regeneration in osteoarthritis. *Expert Opin Biol Ther* 9: 1399-1405.
29. Ahsan T, Sah RL (1999) Biomechanics of integrative cartilage repair. *Osteoarthritis Cartilage* 7: 29-40.
30. Movasaghi Z, Rehman S, Rehman IU (2007) Raman spectroscopy of biological tissues. *Applied Spectroscopy Reviews* 42: 493-541.
31. Elisseeff J (2004) Injectable cartilage tissue engineering. *Expert Opin Biol Ther* 4: 1849-1859.
32. Koutsopoulos S, Unsworth LD, Nagai Y, Zhang S (2009) Controlled release of functional proteins through designer self-assembling peptide nanofiber hydrogel scaffold. *Proc Natl Acad Sci U S A* 106: 4623-4628.
33. Khan IM, Gilbert SJ, Singhrao SK, Duance VC, Archer CW (2008) Cartilage integration: evaluation of the reasons for failure of integration during cartilage repair. A review. *Eur Cell Mater* 16: 26-39.
34. Darr A, Calabro A (2009) Synthesis and characterization of tyramine-based hyaluronan hydrogels. *J Mater Sci Mater Med* 20: 33-44.
35. Wang DA, Williams CG, Yang F, Elisseeff JH (2004) Enhancing the tissue-biomaterial interface: Tissue-initiated integration of biomaterials. *Advanced Functional Materials* 14: 1152-1159.
36. Gross AJ, Sizer IW (1959) Oxidation of Tyramine, Tyrosine, and Related Compounds by Peroxidase. *Journal of Biological Chemistry* 234: 1611-1614.
37. Krafft C, Dietzek B, Popp J (2009) Raman and CARS microspectroscopy of cells and tissues. *Analyst* 134: 1046-1057.
38. Krafft C, Sobottka SB, Schackert G, Salzer R (2006) Raman and infrared spectroscopic mapping of human primary intracranial tumors: a comparative study. *Journal of Raman Spectroscopy* 37: 367-375.

39. Kunstar A, Otto C, Karperien M, van Blitterswijk C, van Apeldoorn A (2011) Raman microspectroscopy: a noninvasive analysis tool for monitoring of collagen-containing extracellular matrix formation in a medium-throughput culture system. *Tissue Eng Part C Methods* 17: 737-744.
40. Koga H, Muneta T, Ju YJ, Nagase T, Nimura A, et al. (2007) Synovial stem cells are regionally specified according to local microenvironments after implantation for cartilage regeneration. *Stem Cells* 25: 689-696.
41. Capila I, Linhardt RJ (2002) Heparin-protein interactions. *Angew Chem Int Ed Engl* 41: 391-412.
42. Casu B (1985) Structure and biological activity of heparin. *Adv Carbohydr Chem Biochem* 43: 51-134.
43. Netelenbos T, van den Born J, Kessler FL, Zweegman S, Huijgens PC, et al. (2003) *in vitro* model for hematopoietic progenitor cell homing reveals endothelial heparan sulfate proteoglycans as direct adhesive ligands. *J Leukoc Biol* 74: 1035-1044.



Chapter 8

Chondrocyte cluster formation stimulates cartilage matrix deposition

Liliana Moreira Teixeira*, Jeroen Leijten*, Jorge Sobral, Rong Jin, Aart van Apeldoorn, Jan Feijen, Clemens van Blitterswijk, Piet Dijkstra, Marcel Karperien

* Shared first co-authorship

Abstract

Cell cluster formation in articular cartilage is a hallmark in Osteoarthritis (OA). These cell clusters have been associated with both cartilage catabolism and anabolism. We addressed this issue by investigating the effect of clustering chondrocytes in highly controlled micro-aggregates on their morphology, stability and chondrogenic potential.

We designed a micro-mold that enables controlled formation of micro-aggregates ranging from 20 to 200 cells in high throughput. Morphology, stability and chondrogenic potential of micro-aggregates was evaluated and compared to single-cells cultured in micro-wells and in 3D after encapsulation in a Dextran-Tyramine (Dex-TA) hydrogel *in vitro* and *in vivo* after subcutaneous implantation in mice. We successfully formed micro-aggregates with highly controlled size, morphology, cell density, stability and viability. Micro-aggregates of 100 cells presented a superior balance in Collagen type I and Collagen type II gene expression over micro-aggregates of 20 and 50 cells. Matrix metalloproteinase (1, 9 and 13) gene expression was decreased in micro-aggregates compared to single cells. Histological analysis of hydrogels cultured

in vitro and after implantation in mice demonstrated enhanced matrix deposition in constructs seeded with micro-aggregates, compared to single-cell seeded constructs.

Using a highly controlled model for high throughput formation of micro-aggregates, we demonstrated that clustering chondrocytes in micro-aggregates stimulated cartilage matrix formation. Consequently, the use of micro-aggregates, compared to single cells, resulted in greatly improved neo-cartilage formation. Furthermore, our data provided experimental evidence suggesting that cartilage clusters found in osteoarthritic cartilage are part of a regenerative response.

8.1 Introduction

Chondrocyte clusters are a histological hallmark of osteoarthritis (OA), the most prevalent form of degenerative joint diseases [1]. The formation of chondrocyte aggregates or clusters in OA can occur by proliferation or active movement of the chondrocytes. Indeed, chondrocyte clusters in OA show characteristics of increased cell proliferation [2]. Cell cluster formation by migration is supported by the abundant presence of filopodia and cilia observed in these chondrocytes [3,4]. Chondrocyte clusters can be composed by more than 20 cells and are localized in the proximity of fissures in the upper cartilage layers [1,5]. Whether they are part of a catabolic response contributing to cartilage degradation or are an attempt of the degenerating cartilage to repair itself is not yet clear.

The up-regulation of matrix turn-over in early OA lesions [1] and the secretory phenotype of chondrocytes [3] found in the affected areas, are indications that chondrocyte clusters are a self-reparative response of the cartilage [6]. During disease progression, this self-repair response of the cartilage is outweighed by a stronger catabolic response resulting in a net loss of cartilage. We hypothesize that the chondrocyte clusters found in OA lesions are an attempt to repair the injured cartilage.

To the best of our knowledge, the role of chondrocyte clusters as being part of a catabolic or anabolic response has not been studied experimentally. The technology to model chondrocyte cell clusters as found in OA is nowadays available. Precise control of single cells and multicellular arrangements is enabled by recently developed micro-engineered tools. The incorporation of small cell clusters of precise size in photo-polymerizable hydrogels showed the first evidence that tissue organization at the microscale modulates cartilage matrix deposition by articular chondrocytes [7]. Although previous studies using chondrocyte aggregation are highly valuable for the technical insight, they fail at providing information related to the pathogenesis of OA.

In this study, we show that clustering chondrocytes in micro-aggregates induces a strong anabolic response stimulating neo-cartilage formation *in vitro* and *in vivo*. Our experimental data suggest that chondrocyte clusters in OA are likely part of a regenerative response of the damaged cartilage. Furthermore, seeding constructs for cartilage repair with high throughput generated clusters of chondrocytes rather than with single cells may be an efficient strategy to boost neo-cartilage formation.

8.2 Materials and Methods

8.2.1 Tissue source and preparation

The use of human material was approved by a local medical ethical committee. OA cartilage was obtained from the knee joints of adult patients suffering from late stage OA undergoing an arthroplasty, after informed consent. Tissue samples were fixated, dehydrated and embedded in paraffin. Macroscopically OA cartilage was used to evaluate morphological features. Sections of 5 microns were collected and stained with H and E for further evaluation using light microscopy.

8.2.2 Mold design and micro-aggregate formation

Stainless steel molds were machined using a femto-second pulsed laser system to produce a negative replica of the micro-wells. The depth of the mold was designed to be 200 - 300 μm . The spacing between wells was 250 μm . To produce agarose micro-wells, autoclave-sterilized powder Ultrapure Agarose (Invitrogen) was dissolved via heating in sterilized PBS at 2 % w/v and added drop by drop into a previously sterilized O-Ring (with an area of 1.9 cm^2) placed on top of the micro-fabricated stainless steel mold. The procedure is outlined in figures 8.2-A and 8.2-B. After drying, the gels were separated from the mold and transferred into 24 well culture plates. Each well of the 24-well culture plate contained 4×10^3 micro-wells.

Bovine primary chondrocytes were isolated from knee articular cartilage by collagenase digestion and cultured in chondrocyte expansion medium composed of Dulbeccos modified Eagles medium high glucose (Invitrogen), 10 % fetal bovine serum (Cambrex), 100U/mL penicillin (Invitrogen), 100 mg/mL streptomycin (Invitrogen), 0.2mM ascorbic acid (ASAP; Sigma), 0.1mM non-essential amino acids (Sigma), and 0.4mM proline (Sigma). Different cell densities (20, 50, 100, 200, 300 and 500 cells per micro-well) were used to study the effect of cell number on the form and size of the micro-aggregates. Appropriate cell densities were seeded into each well of the 24-well plates containing 4×10^3 agarose micro-wells to obtain micro-aggregates of 50, 100 and 200 cells. Aggregation was induced by gravity in micro-wells. Both expansion and chondrocyte differentiation medium (DMEM with 0.1 μM dexamethasone (Sigma), 100 $\mu\text{g/mL}$ sodium pyruvate (Sigma), 0.2 mM ascorbic acid, 50 mg/mL insulintransferrinselenite (ITS+1, Sigma), 100 U/mL penicillin, 100 $\mu\text{g/mL}$ streptomycin, 10 ng/mL transforming growth factor $\beta 3$ (TGF- $\beta 3$, Invitrogen)) were used. The micro-aggregates were kept in culture in the micro-wells in a humidified atmosphere containing 5 % CO_2 at 37 degrees Celsius up to 7 days. Single cells were cultured in 2D on tissue culture plastic at the same cell density. Microscopic images were collected at several time points and morphometric analysis of the micro-aggregates was performed using ImageJ software.

8.2.3 Dextran-Tyramine hydrogels (Dex-TA)

Dex-TA with a degree of substitution of 15, defined as the number of tyramine (TA) moieties per 100 anhydroglucose (AHG) units in dextran, was prepared as described

previously [8,9]. Bovine chondrocytes (passage 2) either as micro-aggregates or as single cell suspension at a concentration of 10×10^6 cells per mL were mixed with the polymer solution. The hydrogel precursor/cell suspension was mixed with H_2O_2 (hydrogen peroxide, Sigma-Aldrich) and horseradish peroxidase (HRP type VI, 298 purpurogallin unit/mg solid, Aldrich) and gelation occurred within one minute (the final concentration of Dex-TA was 10 % wt). The amount of HRP used was fixed at 0.25mg per mmol of TA moieties and the molar ratio of H_2O_2 /TA was 0.20 (mol/mol).

8.2.4 Metabolic activity and chondrocyte viability

Quantification of glucose consumption, as well as lactate and ammonia production by chondrocyte micro-aggregates of 100 cells on micro-wells and single cells cultured for 7 days in differentiation medium, was determined using a Vitros DT60 II medium analyzer (Ortho-Clinical Diagnostics, Tilburg, The Netherlands). The viability of the chondrocytes incorporated in the hydrogels either as single cells or as micro aggregates was assessed by a Live-dead assay. At day 7 and 14, the hydrogel constructs were rinsed with PBS and stained with calcein AM/ethidium homodimer using the Live-dead assay Kit (Invitrogen), according to the manufacturers instructions and evaluated using fluorescence microscopy. Living cells fluoresce green and the nuclei of dead cells red.

8.2.5 *In vivo* implantation

Chondrocyte micro-aggregates of 100 cells were allowed to form for 24 hours in expansion medium. Afterwards, the aggregates were flushed out of the micro-wells and mixed with polymer precursor, as described above. Samples of each hydrogel type, containing either single cells or aggregates of 100 cells were cultured *in vitro* and at pre-determined time-points analyzed for cell viability, metabolic activity, matrix biosynthesis and gene expression analysis or were surgically implanted subcutaneously in 8-weeks-old nude male mice (NMRI-Nude, Harlan) for a period of 2 or 4 weeks. The operative procedure and the care of the mice were performed under the regulation of the Central Laboratory Animal Institute (GDL), Utrecht University (Netherlands). The study was approved by a local animal ethical committee.

8.2.6 Histological analysis

At 14 and 21 days, hydrogel constructs seeded with single cells or aggregates of 100 cells and cultured in differentiation medium were fixed in 10 % buffered formalin for 1 hour. For the *in vivo* experiments, the samples were explanted after 2 and 4 weeks and allowed to fixate in 10 % buffered formalin overnight at 4 degrees Celsius. After embedding the samples in cryomatrix (Cryomatrix, Shandon), a cryo-microtome (Leica) was used to collect 10 μ m sections onto gold-coated slides. The cryomatrix was washed off the slides by incubation in distilled water for 10 minutes. Afterwards, three histological stainings were performed: Picosirius Red staining for total collagen visualization (processed according to the manufacturers instructions (Polysciences) and

both Toluidine blue (Fluka, 0,1 % in deionized water, 10 minutes incubation) and Safranin O (Sigma, 0,1 % in deionized water, 5 minutes incubation) for glycosaminoglycans (GAGs) visualization. The slides were then washed, dehydrated, mounted and analyzed using a bright field microscope (Nikon Eclipse E400).

8.2.7 Gene expression analysis

Hydrogel/cell constructs cultured for 14 and 21 days in differentiation medium were washed with PBS and lysed using Trizol reagent (Invitrogen, Carlsbad, CA). Total RNA was isolated using the Nucleospin RNA II kit (Bioke) according to manufacturers instructions. The RNA yields were determined using the Nanodrop2000 (ND-1000 Spectrophotometer, Isogen LifeScience). Subsequently, cDNA was synthesized using the iScript Kit (BioRad) according to the manufacturers recommendations. Expression levels of individual genes were analyzed by quantitative PCR (MiQ, Bio-rad), using the following forward and reverse primers: Collagen type I 5-GCGGCTACGACTTGAGCTTC-3, 5-CACGGTCACGGACCACATTG-3; Collagen type II 5- ATCAACGGTGGCTTCCACT-3, 5-TTCGTGCAGCCATCCTTCAG-3; Collagen type X 5-CATGCTGCCACAAACAGC-3, 5-TGGATGGTGGGCCTTTTA-3; Aggrecan 5-GACCAGAAGCTGTGCGAGGA-3, 5'-GCCAGATCATCACCACACAG-3; Sox 9 5-CCATTCAGGCCCACTACAAG-3, 5-CAGGGTTTCCGTCTGACATC-3; glyceraldehyde-3- phosphate dehydrogenase (GAPDH) 5-GCCATCACTGCCACCCAGAA-3, 5-GCGGCAGGTCAGATCCACAA-3. Gene expression was normalized to the expression of GAPDH.

8.2.8 Statistical analysis

Statistical differences between two groups were analyzed using the Students t-test. Statistical significance was set to a p value <0.05 and indicated with an asterisk. Results are presented as mean \pm standard deviation.

8.3 Results

8.3.1 High-throughput generated chondrocyte micro-aggregates resemble chondrocyte clusters in OA

Chondrocyte clusters in OA cartilage were localized in close proximity to fissures at the cartilage surface. They usually have a circular appearance and can consist of a few up to 40 chondrocytes. Typical examples of chondrocyte clusters in OA cartilage are shown in figure 8.2-A. Micro-fabricated molds were used as a tool to generate chips of identically shaped micro-wells in agarose. These chips were placed in 24-well plates and subsequently used to generate micro-aggregates similar to the ones observed in OA cartilage for *in vitro* studies in high throughput. The procedure is outlined in Figures 8.1A. Figure 8.1-B and supplementary Figure 8.7-A I to IV correspond to light microscope and SEM images of the agarose chips visualizing the formed micro-wells. Shortly after seeding, gravitational force resulted in the concentration

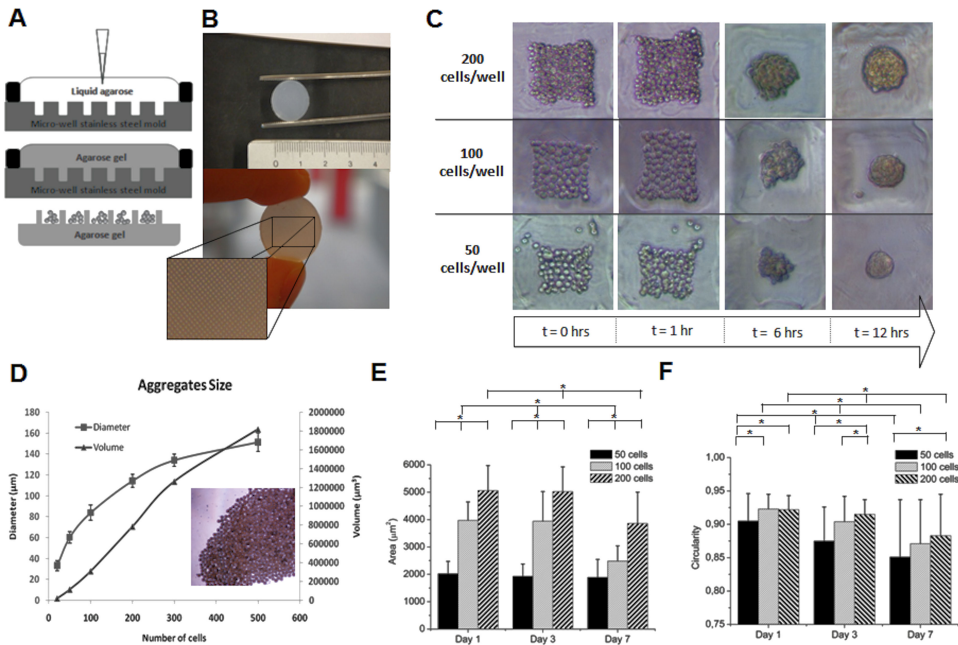


Figure 8.1: High-throughput formation of chondrocyte micro-aggregates. (A) Schematic representation of the micro-well technique for the formation of aggregates from single cell suspensions. A stainless steel mold was used to form micro-wells in agarose chips. (B) Each agarose chip contains 4×10^3 micro-wells. (C) Pictures at specific time points during aggregate formation. Each well of a 24 wells plate containing an agarose micro-well chip was seeded with the appropriate number of cells to obtain micro aggregates of 50, 100 or 200 cells. Aggregation started to occur approximately 6 hours after seeding. After 12 hours, the aggregates had acquired a spherical shape, independently of aggregate size. (D) Correlation between the number of cells per micro well and the diameter (μm) and the volume (μm^3) of the obtained aggregates after 12 hours. Each data point represents the measurement of minimally 50 micro aggregates. At the lower right side of the graphic, aggregates obtained after flushing off the agarose chips are shown. (E) Micro-aggregate area (μm^2) slightly decreased over time most notably in aggregates bigger than 100 cells. Each data point represents the measurement of minimally 50 aggregates (F) Measurement of circularity of micro-aggregates over time demonstrated a decrease in average circularity and an increase in spread. A perfect circle has a value of 1. Each data point represents the measurement of about 50 micro aggregates. Error bars were means \pm SD.

of chondrocytes at the bottom of the micro-wells. The chondrocytes contracted to a spherical aggregate thereby increasing intercellular contacts and minimizing free energy (Figure 8.1-C). To study the effect of cell number in aggregation speed and stability of the micro-aggregates, pictures of the aggregates in the micro-wells were collected at different time points after seeding. The number of cells affected the speed of aggregate formation. We observed that lower cell densities demanded longer aggregation time, most likely due to limited contact opportunities (Figure 8.1-C). After 24 hours, the aggregates were collected by flushing the non-adherent agarose chips with medium. The percentage of aggregate recovery was 96.6 %. The aggregates could withstand centrifugation and resuspension in medium, as shown in Figure 8.1-D. We next studied the correlation between cell seeding density, aggregate diameter and volume. We observed a linear correlation between seeding density and the aggregate volume assuming a spherical conformation (Figure 8.1-D).

To evaluate aggregate stability after formation, the area and circularity of aggregates composed of 50, 100 and 200 cells were analyzed, after 1, 3 and 7 days in culture. The area and circularity of the aggregates are represented in figures 8.2-E and F. As expected, the area of the aggregates decreased slightly over time due to condensation. The circularity of the aggregates provided information about stability and uniformity of the aggregates. Higher deviations in circularity were observed at later stages of culture and particularly in aggregates with lower cell densities. In subsequent experiments, aggregates were collected 24 hours after seeding, since extended culture did not show advantageous effects. Furthermore, after increased culture time, aggregates started to migrate to neighboring wells and merge, suggesting a chemotactic attraction between the aggregates (Figure 8.7-B).

8.3.2 Micro-aggregation stimulates cartilage matrix formation

Gene expression of Aggrecan and Collagen type II was evaluated. Aggregates with densities of 50, 100 and 200 cells were cultured in the micro-wells and compared with single cells cultured in 2D. Figure 8.3-A shows that aggregates cultured in expansion medium tended to slightly up-regulate the expression of both collagen type II and aggrecan, compared to single cells cultured in 2D. Figure 8.3-B shows that, when the aggregates were chondrogenically stimulated with TGF- β 3, the gene expression of collagen type II and aggrecan significantly increased in micro-aggregates of 50 and 100 cells, compared to single cells and to aggregates of 200 cells. Overall, gene expression analysis demonstrated that micro-aggregates behaved similarly to single cells when cultured without stimulation. However, when the micro-aggregates were exposed to chondrogenic conditions containing stimulatory molecules like found in cartilage, cartilage matrix formation was enhanced in aggregates of 50 and 100 cells with a less pronounced effect in aggregates of 200 cells. Given the higher stability of aggregates of 100 cells compared to aggregates of 50 cells, these cell clusters were selected for further experimentations.

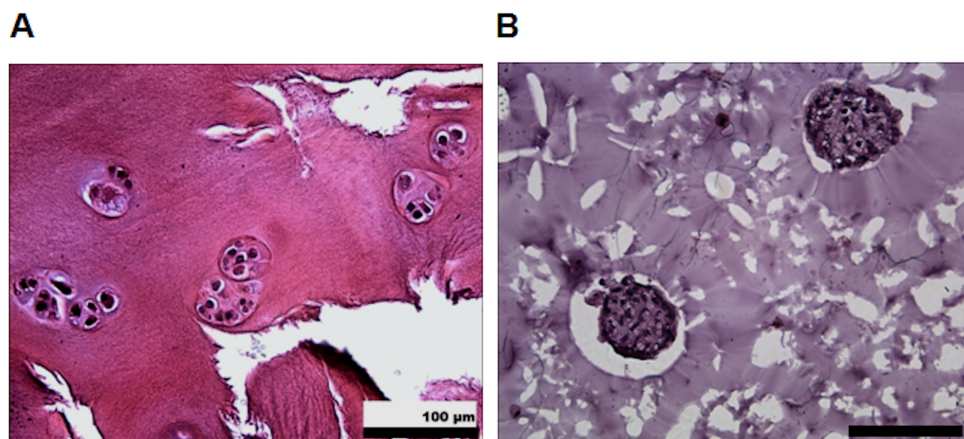


Figure 8.2: Cell clusters in OA cartilage. (A) OA tissue specimen stained with H and E, showing the presence of several chondrocyte clusters near fissures at the cartilage surface. (B) Detail of representative micro-aggregates of 100 cells embedded in an in situ gelating Dex-TA hydrogel, stained with H and E.

8.3.3 Micro-aggregated cell clusters remain viable after embedding in a hydrogel

We studied the effect of micro-aggregation on cell metabolism in comparison to equal numbers of single cells. Micro-aggregated cell clusters were metabolically more active than single cell seeded constructs (Figure 8.4-A). Micro-aggregates had a significantly higher consumption of glucose and production of both lactate and ammonia. This suggested that aggregation of chondrocytes stimulated cell metabolism presumably due to higher cell-cell contacts. During glycolysis, oxidation of one molecule of glucose leads to two molecules of pyruvate and, subsequently, by anaerobic respiration, to two molecules of lactate. This expected 2:1 ratio of lactate:glucose is obtained when single cells were cultured in the hydrogels. When cells were cultured in aggregates this ratio dropped to 1:1. This significant difference is suggestive for a metabolic shift in which part of the glucose may be used for biosynthesis of extracellular matrix molecules rather than energy consumption. Micro-aggregates of 100 cells were successfully incorporated into Dex-TA hydrogels and their viability was assessed after 7 and 14 days in culture. As shown in figure 8.4-B, both single cells and micro-aggregates were uniformly distributed in the hydrogel and remained viable. The integrity of the micro-aggregates did not change over culture time.

8.3.4 Cell cluster formation enhances cartilage matrix deposition

Micro-aggregates of 100 cells or single cells suspensions with equal cell numbers were incorporated in a Dex-TA hydrogel and cultured in chondrocyte differentia-

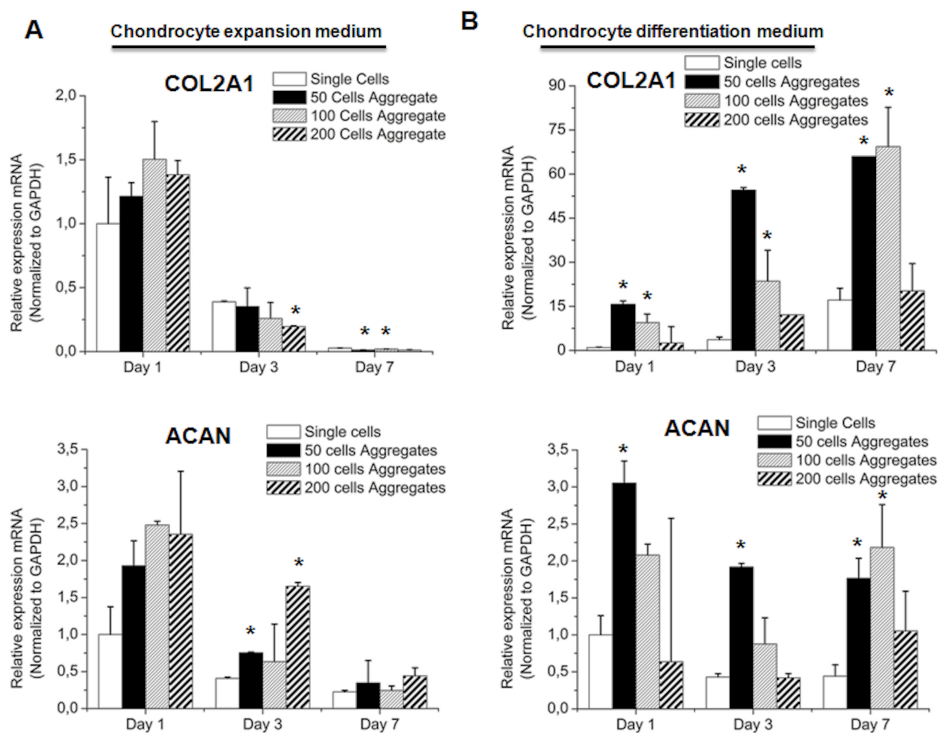


Figure 8.3: Micro-aggregation enhances COL2A1 and ACAN expression. (A) qPCR analysis of collagen type II and aggrecan gene expression at day 1, 3 and 7 of culture in chondrocyte expansion medium. Equal amounts of cells were cultured in micro-aggregates of 50, 100 and 200 cells and compared with single cells cultured in a 2D system. At day 7, no changes were observed between the different culture methods. (B) qPCR analysis of collagen type II and aggrecan gene expression was evaluated at day 1, 3 and 7 of culture in chondrogenic conditions. Micro-aggregated cell clusters of 50, 100 and 200 cells were compared with single cells cultured in a 2D system. COL2A1 and ACAN expression was potently stimulated by culturing the cells in micro-aggregates of 50 and 100 cells. Error bars were means \pm SD ($n=3$ /condition).

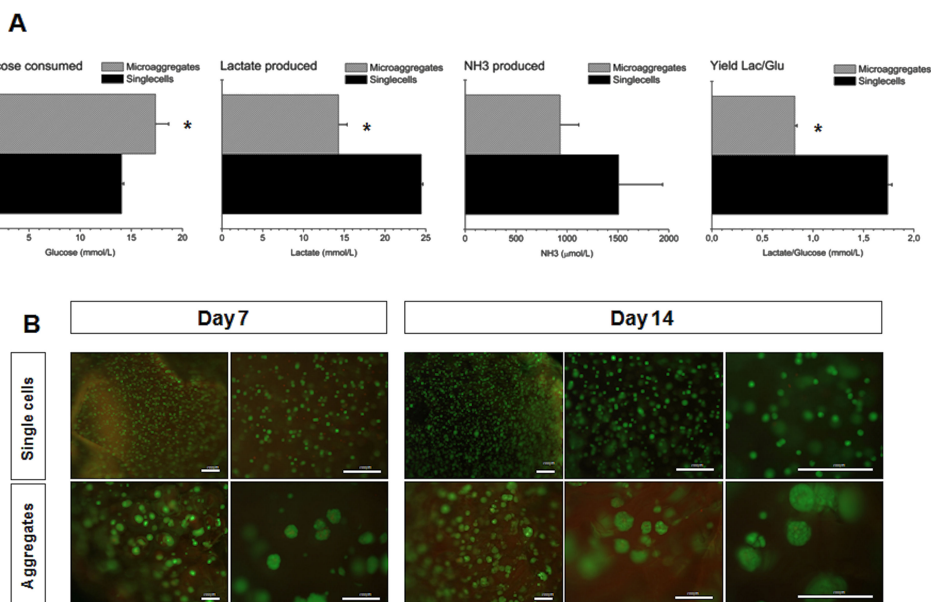


Figure 8.4: Micro-aggregation increases metabolic activity. (A) Glucose consumption and ammonia and lactate production were quantified after 7 days of culture of equal cell numbers of 100 cell micro-aggregates on agarose chips or as single cells in 2D. The ratio between lactate production and glucose consumption is represented in the lower right graphic. The clear difference between both culture systems was strongly suggestive for a shift in metabolic activity. Error bars represent means \pm SD ($n=3$ /condition). (B) Equal numbers of cells, either as micro-aggregates or as single cells, were embedded in an in situ gelating Dex-TA hydrogel. After 7 and 14 days of culture, a viability assay was performed in which living cells were shown in green and dead cells in red. Incorporation of cells in the hydrogels did not affect viability nor did micro-aggregation. Clusters retained their spherical shape over time.

tion medium for 14 and 21 days. The relative fold expressions of chondrogenic related genes such as aggrecan, collagen type II and Sox9 were up-regulated in hydrogels containing micro-aggregates compared to constructs seeded with equal number of single cells (Figure 8.5-A to C). Figure 8 shows that the ratio of collagen type II and collagen type I is improved in micro-aggregates. Over time, these differences became more pronounced. Importantly, no significant differences in expression of either collagen type I or X were observed when comparing hydrogel constructs seeded with single cells or with micro-aggregates, at any time point (Figure 8.5-D and E). The expression of several MMPs was analyzed after 21 days in culture to evaluate the effect of cell clustering. As shown in figure 8.5-F, a decrease in the expression of MMP-1, MMP-9 and MMP-13 was observed in hydrogels cultured with micro-aggregated cells. The expression of MMP-3 by the micro-aggregated cells was not detectable.

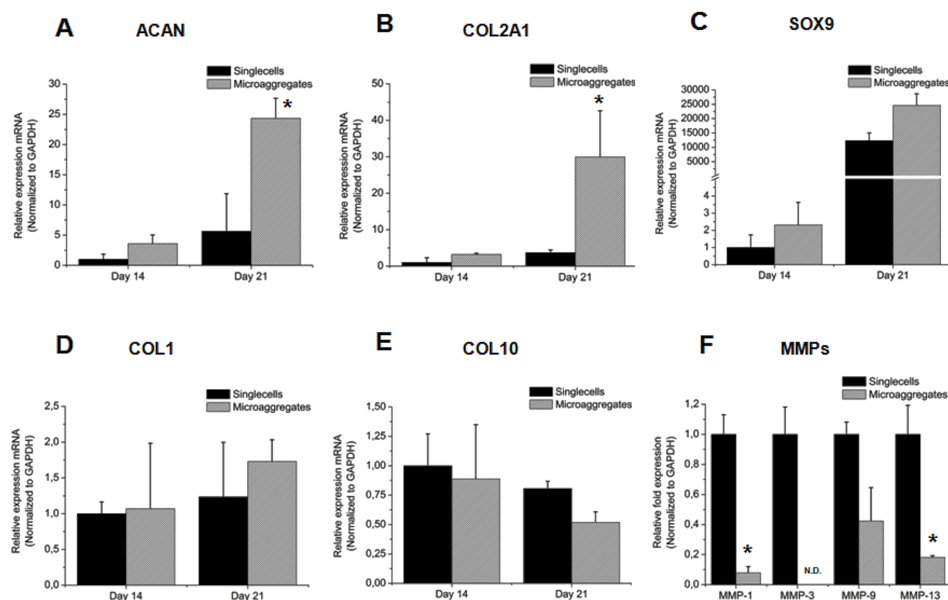


Figure 8.5: Micro-aggregation prior to seeding in hydrogels stimulates cartilage matrix gene expression. Relative mRNA levels for aggrecan (A), collagen type II (B), Sox9 (C), collagen type X (D) and Collagen type I (E), expressed by single cells or micro-aggregated cell clusters incorporated into Dex-TA hydrogels, after 14 and 21 days in culture. Similar cell numbers were seeded in each construct. Relative mRNA levels for MMPs 1, 3, 9 and 13 (F), expressed by single cells or micro-aggregated cell clusters incorporated into Dex-TA hydrogels, after 21 days in culture. Error bars were means \pm SD ($n=3$ /condition).

The gene expression analysis was corroborated by histology (Figure 8.6). Picrosirius red staining was more intense in hydrogels containing aggregated cells, suggesting the presence of more collagens, as shown in Figure 8.6-A. No clear distinction in intensity was observed between day 14 and day 21. The presence of GAGs was visualized by Toluidine blue and Safranin O staining (Figure 8.6-A). Both stainings were more intense in hydrogels seeded with micro-aggregates compared to single cell seeded constructs. This difference was more striking at day 21. Additionally, mainly at day 14, a gradient of GAGs diffusing out of the micro-aggregates and into the hydrogel was visible. Similar results, and even more pronounced, were obtained 2 and 4 weeks after subcutaneous implantation of the cell seeded hydrogel constructs in nude mice (Figure 8.6-B).

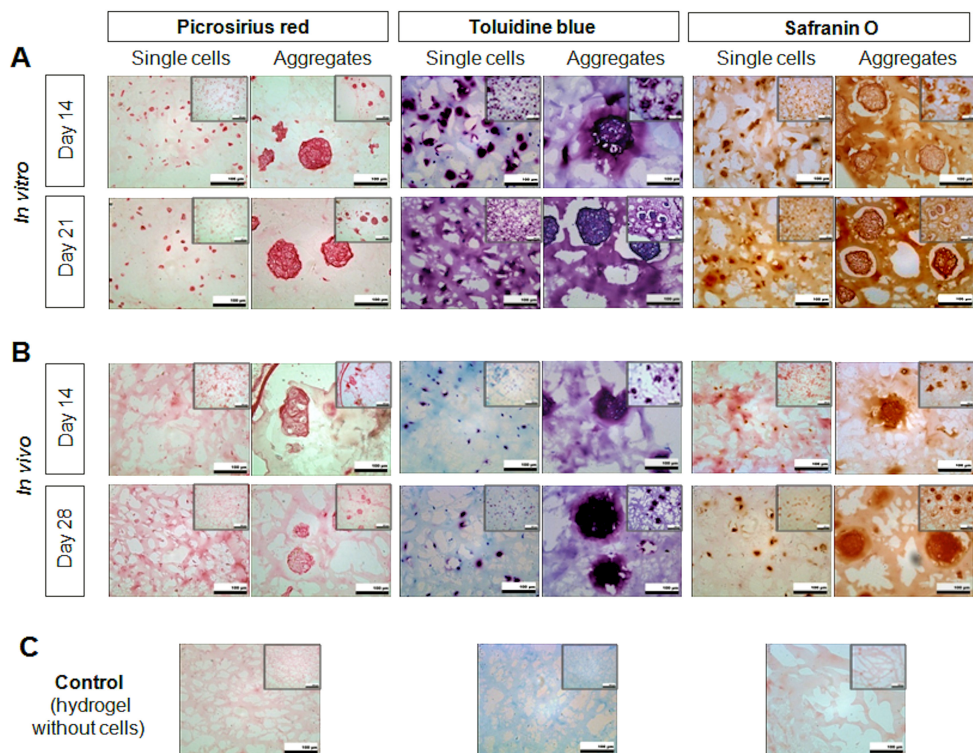


Figure 8.6: Micro-aggregation resulted in superior matrix production both *in vitro* and *in vivo*. (A) Histological evaluation of *in vitro* cultured hydrogels seeded with equal cell numbers either as single cells or as micro-aggregates of 100 cells, for 14 and 21 days. Picrosirius red staining was performed to visualize total collagen content (red/pink colour). Both Toluidine blue (purple colour) and Safranin O (red/orange colour) stainings were performed to visualize glycosaminoglycans deposition. A more intense staining was observed in constructs seeded with micro-aggregates indicative for higher matrix production. (B) Histological evaluation of hydrogel constructs with encapsulated single cells or micro-aggregates of 100 cells implanted subcutaneously in nude mice for 2 and 4 weeks ($n=6$ mice per time point). Hydrogels with encapsulated micro aggregates showed more cartilage matrix. (C) Histological stainings of a representative control sample, consisting of the hydrogel without cells.

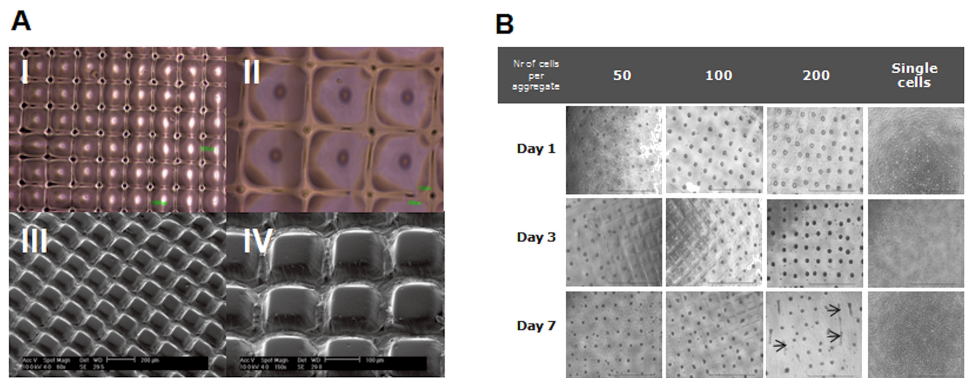


Figure 8.7: *In vitro* model for size specific cell cluster formation. (A) Light microscopic (A-I and II) and scanning electron-microscopic (SEM) (A-III and IV) images of agarose chips evidencing the presence of uniform micro-wells enabling high throughput formation of micro-aggregated cell clusters. (B) Pictures at specific time points (day 1, day 3 and day 7) of aggregates cultured on agarose chips seeded with different cell densities to obtain aggregates of 50, 100 or 200 cells. At day 7, the micro-aggregates, particularly the ones containing 200 cells, tended to merge, migrate and started to lose their round morphology (arrows). Single cells were used as a control.

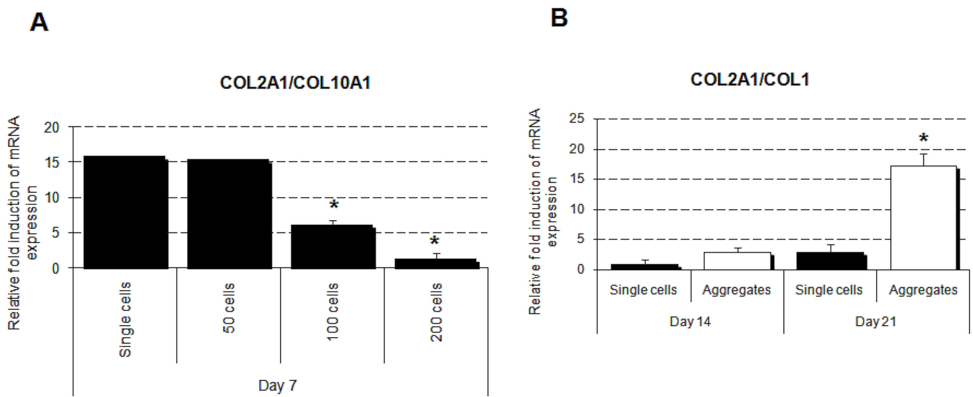


Figure 8.8: Micro-aggregation improved the ratio between collagen type II and both collagen type I and X expression. (A) Ratio between the relative mRNA levels of collagen type II and Collagen type X, after 7 days of culture of equal cell numbers of 100 cell micro-aggregates on agarose chips or as single cells in 2D, in chondrogenic medium. At day 14 no differences were detected. (B) Ratio between the relative mRNA levels of collagen type II and Collagen type I, in Dex- TA hydrogel constructs seeded with equal numbers of cells either as single cells or as micro-aggregated clusters of 100 cells, after 14 and 21 days in culture. Error bars were means \pm SD (n=3/condition).

8.4 Discussion

Cell clusters are a histological hallmark of OA cartilage [1,10]. It has been postulated that chondrocyte clusters in OA are likely to represent initial stages of cartilage regeneration but experimental evidence is lacking. Although previous studies have investigated the effect of chondrocyte clustering on cartilage formation, these aggregates were formed either in insufficient quantity, with improper or poorly controlled size ranges, or attached to scaffold sheets [11,12,13,14,15,16]. In our study, we developed an *in vitro* micro cell-cluster model that enabled the high throughput formation of highly controlled micro-aggregates that are able to be harvested without enzymatic digestion or mechanical shearing. This allowed us to study the effect of micro-aggregation of chondrocytes on cartilage matrix formation and their potential as therapeutic cell source when combined with an *in situ* gelating injectable biomaterial. We demonstrated that formation of micro-aggregates resulted in enhanced cartilage matrix production and decreased MMPs transcription.

Cartilage repair strategies based on autologous chondrocyte implantation still rely on *in vitro* expansion to obtain sufficient cells, with all inherent drawbacks such as chondrocyte dedifferentiation [17]. Studies focusing on chondrocyte self-aggregation potential and their effectiveness for elastic cartilage reconstruction have approached the problem of dedifferentiation and scarcity of starting material [11,12,18]. They have shown that by embedding aggregates in molded hydrogels, chondron-like clusters are formed and, thus, dedifferentiation of the chondrocytes is avoided, or at least delayed.

Due to the cartilages inherent low capacity to self repair, the retention of cells in cell-based cartilage repair strategies is of the highest importance. A myriad of biomaterials that provide an artificial extracellular matrix compatible with homogenous distribution of single cells or micro-aggregates are currently available for cartilage tissue regeneration strategies [19,20]. Among the classes of biomaterials, hydrogels of natural polymers show promising features as defect filling scaffolds due to their similarity to the native cartilaginous extracellular matrix. *In situ* gelating injectable hydrogels have deserved much attention since they can be applied in a minimally invasive procedure and allow the possibility of cell incorporation during the gelation reaction [17]. Recently, we have developed a novel injectable enzymatically crosslinkable Dextran-Tyramine hydrogel (Dex-TA, 14kDa, DS=15). This fast gelating hydrogel does not affect cell viability and has shown high potential for cartilage regeneration [8,9]. We have chosen these hydrogels to evaluate whether seeding constructs with micro-aggregated cells rather than single cells has a beneficial effect on cartilage formation.

Prior to incorporation of the micro-aggregates in the injectable Dex-TA hydrogels, different culture times and cell densities were evaluated to select the optimal micro-aggregate size. Interestingly we observed that larger micro-aggregates, such as 200 cells, were out performed by smaller micro-aggregates, composed of 50 and 100 cells. Additionally, higher micro-aggregates stability was achieved in shorter formation time with aggregates of 50 to 100 cells than 200 cells. After 3 days in culture, the micro-aggregates tended to merge due to cell migration, most likely facilitated by the increasing matrix that surrounded the aggregates. The merging of aggregates with

increasing culture time has been previously reported [11,13,21]. Most probably, this process is driven by chemotactic factors secreted by the chondrocytes [22,23]. Based on stability and formation characteristics, as well as expression of a chondrogenic gene profile, we selected aggregates of 100 cells as the optimal size for further experiments.

Micro-aggregates of 100 cells in Dex-TA hydrogels proved to be viable and retained their integrity. Moreover, the aggregates could be easily uniformly distributed in the gel. Interestingly, when the chondrocytes were cultured in the aggregated form within hydrogels, a change in cell metabolism appeared to be occurring. This might be due to a metabolic shift from a catabolic glycolysis pathway to a more anabolic pathway in aggregated cells. As cause or consequence of these events, glucose might have been directed to a greater extent for biosynthesis and, thus enhancing matrix production. Indeed this was supported by increased matrix deposition in hydrogels seeded with micro-aggregates. Likewise, the increase in biosynthesis in early cartilage lesions has been previously reported [10,24]. Comparable shifts from catabolic to the anabolic responses have been recently reported to occur by varying the exposure of chondrocytes to different oxygen percentages [18]. Lower oxygen percentages, similar to physiological concentrations, significantly enhanced the chondrogenic capacity of chondrocytes cultured in micromass pellets. The enhanced chondrogenic behavior of the micro-aggregates might be explained by a relatively lower exposure to oxygen of cells in micro-aggregates compared to single cells in 2D. However, other possibilities such as concentrating effects of both secreted soluble factors and extracellular matrix cannot be excluded. Regardless of the cause, micro-aggregates of 100 cells outperformed single cells and showed therefore a greater potential for cell-based cartilage repair strategies.

Interestingly, morphometric analysis and gene expression profiles suggested that without addition of chondrogenic stimuli, both single cells and micro-aggregates behaved similarly suggesting that aggregation itself does not change cell behavior. However, when stimulated with a chondrogenic stimulus, such as TGF- β 3, micro-aggregated cells showed a very distinct response from single cells. A strong additional effect on cartilage matrix formation was obtained when cells were cultured in a micro-aggregated form. This substantiates the hypothesis that micro-clusters of chondrocytes, such as observed in OA, may indeed be part of a regenerative response. To our knowledge, we are the first to address the function of micro-clusters by an experimental approach showing potent stimulation of cartilage matrix formation. Since we have not studied the function of micro-aggregates in an OA-like environment, e.g. in the presence of inflammatory cytokines, we cannot exclude that the OA-environment alters the behavior of the micro-aggregates. Using our model, the effect of various factors involved in OA can be easily addressed in a high-throughput approach.

Considering the difference in expression ratio of collagen type II and collagen type X between clusters, it might be worthwhile to explore differential seeding of constructs with micro-aggregates of various sizes to reconstruct the zonal organization of cartilage. The role of microscale organization in a cartilage model has previously been investigated using cell clusters obtained by photo-immobilization of single cells in a hydrogel as described by Albrecht et al. [7]. In contrast to our study, no effect on cartilage matrix formation was observed. This difference might be explained by

the cell-cell contact achieved with our approach of cell cluster formation, compared to the cell density approach in which cells are in close proximity, yet a couple of micrometers still apart. The two distinct outcomes suggest that close cell-cell contact and contraction forces during condensation of cell clusters strongly affect cell behavior [23,25]. Thus, the system reported by Albrecht et.al. resembled more a 2D cell system within a hydrogel support. Our approach has the advantage of first enabling aggregate condensation while still retaining the possibility of combining these aggregates with an injectable hydrogel.

8.5 Conclusion

Collectively, our data demonstrate that chondrocyte micro-aggregation prior to seeding of tissue engineered constructs has a beneficial effect on cartilage matrix formation compared to single cell cultures. Our experimental approach mimicking cell clusters, such as found in OA and other cartilage related diseases caused by chemical or mechanical injury, may indeed be part of an innate self-regenerative response of cartilage. Using our approach, it is possible to produce in high-throughput micro-aggregates with specific cell densities, using a simple and reproducible method. These micro-aggregates can be successfully incorporated into injectable in situ forming hydrogels, without affecting cell viability and the aggregates' spherical shape, while boosting cartilage formation compared to single cell-seeded constructs. Therefore, high-throughput formation of micro-aggregates prior to chondrocyte implantation, as occurs during current autologous chondrocyte implantation (ACI)-protocols, may improve and accelerate hyaline cartilage formation.

References

1. Lotz MK, Otsuki S, Grogan SP, Sah R, Terkeltaub R, et al. (2010) Cartilage cell clusters. *Arthritis Rheum.*
2. Pfander D, Kortje D, Weseloh G, Swoboda B (2001) [Cell proliferation in human arthrotic joint cartilage]. *Z Orthop Ihre Grenzgeb* 139: 375-381.
3. Kouri JB, Arguello C, Luna J, Mena R (1998) Use of microscopical techniques in the study of human chondrocytes from osteoarthritic cartilage: an overview. *Microsc Res Tech* 40: 22-36.
4. McGlashan SR, Cluett EC, Jensen CG, Poole CA (2008) Primary cilia in osteoarthritic chondrocytes: from chondrons to clusters. *Dev Dyn* 237: 2013-2020.
5. Schumacher BL, Su JL, Lindley KM, Kuettner KE, Cole AA (2002) Horizontally oriented clusters of multiple chondrons in the superficial zone of ankle, but not knee articular cartilage. *Anat Rec* 266: 241-248.
6. Lee GM, Paul TA, Slabaugh M, Kelley SS (2000) The incidence of enlarged chondrons in normal and osteoarthritic human cartilage and their relative matrix density. *Osteoarthritis Cartilage* 8: 44-52.
7. Albrecht DR, Underhill GH, Wassermann TB, Sah RL, Bhatia SN (2006) Probing the role of multicellular organization in three-dimensional microenvironments. *Nat Methods* 3: 369-375.
8. Jin R, Hiemstra C, Zhong Z, Feijen J (2007) Enzyme-mediated fast in situ formation of hydrogels from dextran-tyramine conjugates. *Biomaterials* 28: 2791-2800.
9. Jin R, Moreira Teixeira LS, Dijkstra PJ, Zhong Z, van Blitterswijk CA, et al. (2010) Enzymatically Crosslinked Dextran-Tyramine Hydrogels as Injectable Scaffolds for Cartilage Tissue Engineering. *Tissue Eng Part A* 16: 2429-2440.
10. Poole AR, Rizkalla G, Ionescu M, Reiner A, Brooks E, et al. (1993) Osteoarthritis in the human knee: a dynamic process of cartilage matrix degradation, synthesis and reorganization. *Agents Actions Suppl* 39: 3-13.
11. de Chalain T, Phillips JH, Hinek A (1999) Bioengineering of elastic cartilage with aggregated porcine and human auricular chondrocytes and hydrogels containing alginate, collagen, and kappa-elastin. *J Biomed Mater Res* 44: 280-288.
12. Fukuda J, Khademhosseini A, Yeo Y, Yang X, Yeh J, et al. (2006) Micromolding of photocrosslinkable chitosan hydrogel for spheroid microarray and co-cultures. *Biomaterials* 27: 5259-5267.
13. Hamilton DW, Riehle MO, Monaghan W, Curtis AS (2006) Chondrocyte aggregation on micrometric surface topography: a time-lapse study. *Tissue Eng* 12: 189-199.
14. Khademhosseini A, Langer R, Borenstein J, Vacanti JP (2006) Microscale technologies for tissue engineering and biology. *Proc Natl Acad Sci U S A* 103: 2480-2487.
15. Penick KJ, Solchaga LA, Welter JF (2005) High-throughput aggregate culture system to assess the chondrogenic potential of mesenchymal stem cells. *Biotechniques* 39: 687-691.
16. Kelm JM, Fussenegger M (2004) Microscale tissue engineering using gravity-enforced cell assembly. *Trends Biotechnol* 22: 195-202.
17. Kuo CK, Li WJ, Mauck RL, Tuan RS (2006) Cartilage tissue engineering: its

potential and uses. *Curr Opin Rheumatol* 18: 64-73.

18. Strobel S, Loparic M, Wendt D, Schenk AD, Candrian C, et al. (2010) Anabolic and catabolic responses of human articular chondrocytes to varying oxygen percentages. *Arthritis Res Ther* 12: R34.

19. Woodfield TB, Bezemer JM, Pieper JS, van Blitterswijk CA, Riesle J (2002) Scaffolds for tissue engineering of cartilage. *Crit Rev Eukaryot Gene Expr* 12: 209-236.

20. Wolf F, Candrian C, Wendt D, Farhadi J, Heberer M, et al. (2008) Cartilage tissue engineering using pre-aggregated human articular chondrocytes. *Eur Cell Mater* 16: 92-99.

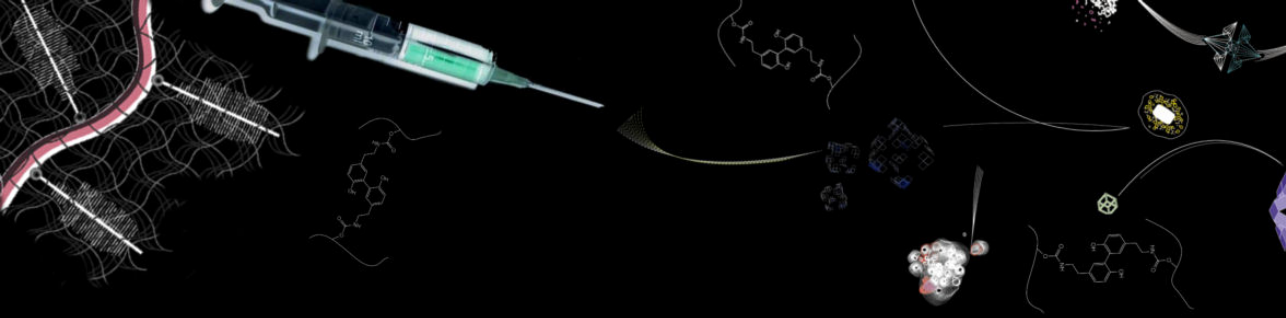
21. Furukawa KS, Suenaga H, Toita K, Numata A, Tanaka J, et al. (2003) Rapid and large-scale formation of chondrocyte aggregates by rotational culture. *Cell Transplant* 12: 475-479.

22. Martinez I, Polacek M, Bruun JA, Johansen O (2010) Differences in the Secretome of Cartilage Explants and Cultured Chondrocytes Unveiled by SILAC Technology. *Journal of Orthopaedic Research* 28: 1040-1049.

23. DeLise AM, Fischer L, Tuan RS (2000) Cellular interactions and signaling in cartilage development. *Osteoarthritis Cartilage* 8: 309-334.

24. Aurich M, Squires GR, Reiner A, Mollenhauer JA, Kuettner KE, et al. (2005) Differential matrix degradation and turnover in early cartilage lesions of human knee and ankle joints. *Arthritis Rheum* 52: 112-119.

25. Griffith LG, Swartz MA (2006) Capturing complex 3D tissue physiology *in vitro*. *Nat Rev Mol Cell Biol* 7: 211-224.



Chapter 9

Improved cartilage formation in a dextran-based hydrogel supplemented with an autologous growth factor source

Liliana Moreira Teixeira, Jeroen Leijten, Jos Wennink, Anindita Ganguli, Jan Feijen, Clemens van Blitterswijk, Piet Dijkstra, Marcel Karperien

Abstract

in situ gelating dextran-tyramine (Dex-TA) injectable hydrogels have previously shown promising features for cartilage repair. Yet, in spite of suitable mechanical properties, this system lacks intrinsic biological signals. Opposingly, platelet lysate-derived hydrogels are rich in growth factors and anti-inflammatory cytokines, but mechanically unstable. We hypothesised that the advantages of these systems may be combined in one hydrogel that can easily be translated into clinical settings.

Platelet lysate was successfully incorporated into Dex-TA polymer solution prior to gelation. After enzymatic crosslinking, rheological and morphological evaluations were performed, revealing that the addition of platelet lysate did not affect the mechanical properties and porosity of pure Dex-TA hydrogels. Subsequently, the effect of the platelet lysate on cell migration, adhesion, proliferation and multi-lineage differentiation was determined. Cell migration was induced and both cell adhesion along with proliferation were enhanced. Predominantly chondrogenic differentiation was stimulated by incorporation of platelet lysate, while no significant effects were ob-

served on osteogenic differentiation and adipogenic differentiation nor on blood vessel in growth. Finally, we evaluated the integration potential of this gel, which showed effective adhesion onto OA-affected cartilage.

The mechanical properties and covalent attachment of Dex-TA to cartilage tissue during *in situ* gel formation were successfully combined with the advantages of platelet lysate, revealing the potential of this enhanced hydrogel as a cell-free approach. Furthermore, released anabolic growth factors promoted proliferation and triggered chondrogenic differentiation of mesenchymal stromal cells. Thus, *in situ* gelating Dex-TA hydrogels with autologous platelet lysate shows high potential as an off-the-shelf cartilage repair strategy.

9.1 Introduction

Platelet-rich plasma is an autologous source of growth factors and cytokines paramount for local tissue homeostasis and repair of tissues after injury [1,2]. Recently, it has emerged as a potential substitute in cartilage tissue engineering and as treatment for osteoarthritis (OA) [3,4,5]. Cartilage damage caused by trauma or OA results in disability and, consequently, decreased quality of life. OA is one of the most prominent chronic joint diseases, with rising incidence in an ageing population. [6,7]. The current management of OA mainly aims at pain reduction and, at the end stage of the disease, total joint replacement. Total or partial prosthetic replacement of the joint, however, involves removing large parts of the joint and is usually limited to treatment of elderly patients [8]. In young patients, prosthetic replacement engage considerable problems mainly related to complications of revision surgery due to the limited life span of the current implants [9]. Regenerative medicine is an emerging promising therapeutic alternative for cartilage repair. Cartilage tissue engineering (TE) approaches require a suitable scaffold to promote mechanical support while providing the biochemical cues that assist the repair process. Although platelet-rich concentrates have shown significant potential for the treatment of cartilage pathologies, platelet-derived gels face two major limitations: i) rapid degradation and ii) poor mechanical properties [10], which severely limits their application as scaffolds for cartilage TE.

We have recently reported the promising features of injectable dextran-tyramine (Dex-TA) hydrogels for cartilage repair [11,12]. These gels form *in situ* by an enzymatic crosslinking reaction and possess considerable mechanical strength. Yet these hydrogels lack biological activity. This drawback can be partially overcome by mixing Dex-TA with other polymers such as heparin and hyaluronic acid [13,14]. Alternatively, biological performance of Dex-TA hydrogels can be improved by incorporation of different cell sources such as MSCs in combination with a limited population of chondrocytes. It has been shown that co-culture of MSCs with primary chondrocytes significantly improves cartilage matrix formation (ACI) [15,16,17,18,19]. Here we explored whether incorporation of platelet rich lysate could also improve the regenerative potential of Dex-TA hydrogels. This combination takes advantage of the platelet lysate richness in growth factors and anti-inflammatory cytokines that play a key role in cartilage repair, and of the mechanical stability and *in situ* immobilization

provided by a fast gelating injectable hydrogel. We hypothesized that the addition of platelet lysate to Dex-TA hydrogels will improve its biological properties by accelerating remodelling and matrix deposition. Our ultimate goal was to determine whether we can use this system as a cell-free approach for cartilage repair by adapting the hydrogel to attract MSCs or chondrocytes from the surrounding environment, and facilitating subsequent differentiation of these cells into the matrix producing chondrocytes, solely by addition of an autologous source of growth factors.

9.2 Materials and Methods

9.2.1 Platelet collection and cell sources

Human MSCs were isolated from fresh bone marrow aspirates, obtained after written consent, as previously described [20]. Briefly, aspirates were resuspended using a 20-gauge needle, plated at a density of 50×10^4 cells/cm² and cultured in MSC proliferation medium consisting of Alpha-MEM (α -MEM, Gibco), 10 % heat-inactivated fetal bovine serum (Biowhittaker), 0.2 mM ascorbic acid (Sigma), 2 mM L-glutamine (Gibco), 100 U/ml penicillin with 100 mg/ml streptomycin (Gibco) and 1 ng/ml basic Fibroblast Growth Factor (Instruchemie). Cells were expanded and used in passage 2. Chondrocytes were isolated from human articular cartilage, obtained after total joint replacement surgery. Cartilage pieces were digested using collagenase type II (Worthington), as previously described [21]. Isolated cells were seeded at 3000 per cm² and expanded in chondrocyte expansion medium containing DMEM (Gibco), 10 % heat-inactivated fetal bovine serum (Biowhittaker), 1x non-essential amino acids (100x, Sigma), 0.2 mM ascorbic acid, 0.4 mM proline (Sigma-Aldrich), 1 % penicillin and streptomycin. Cells were expanded and used in passage 2. Human blood was collected from healthy volunteers, after written consent, and directly passed through an aphaeresis unit, which separates the platelets, returning back the rest of the blood. The platelet-rich fraction was immediately frozen until further use. Two freeze-thawing cycles were used to lyse the platelets. Freezing and thawing have been reported to be the superior method to release growth factors from the platelet-rich fraction [2]. The study protocols were approved by a local medical ethical committee.

9.2.2 Mechanical properties

Dex-TA with a degree of substitution of 15, defined as the number of tyramine (TA) moieties grafted per 100 disaccharide units, was prepared as described previously [11,12]. Rheology experiments were performed on an Anton Paar Physica MCR 301 rheometer with flat plate geometry (20 mm diameter, 0.5 mm gap) in oscillating mode, at 37 degrees Celsius. 20 % (w/v) Dex-TA polymer solution was mixed with pure platelet lysate to obtain 10 (w/v) polymer solution. As a control, instead of platelet lysate, the polymer was mixed with culture medium to obtain 10 % (w/v) polymer solution. The crosslinking method was induced by mixing the polymer with horseradish peroxidase (HRP) and hydrogen peroxide (H₂O₂). The reaction conditions were 0,25 mg of HRP per mmol of phenol groups and the molar ratio of H₂O₂/TA was 0,2.

After the samples were applied to the rheometer, the upper plate was lowered to a measuring gap size of 0.5 mm. The measurement was started immediately after sample preparation. A layer of oil was added to prevent evaporation. A frequency of 0.5 Hz and a strain of 0.1 % were applied in the analysis. The measurement was allowed to proceed until the storage modulus reached a plateau value.

9.2.3 Cell migration assay

A cell migration assay based on a trans-well system was performed. 20 % (w/v) Dex-TA polymer solution was mixed with pure platelet lysate to obtain 10 % (w/v) polymer solution. As a control, instead of platelet lysate, the polymer was mixed with culture medium to obtain 10 % (w/v) polymer solution. The crosslinking was induced by mixing with a solution of HRP/H₂O₂. The hydrogels were added to the bottom of the migration plates (Kit CytoSelect 24-well Cell Migration Assay 8 μ m, Colorimetric format; CBA-100 Cell Biolabs, Inc.). A volume of 300 μ L of a cell suspension of human chondrocytes or human MSCs, containing 2 million cells/ml in serum-free media, was added to each insert and incubated for 24 hours. Afterwards, the media was carefully aspirated from the inside of the insert. The interior of the inserts was swabbed to remove all non-migratory cells. The inserts were transferred to a clean well containing 400 μ L of Cell Stain Solution and incubated for 10 minutes at room temperature. The stained inserts were washed several times and allowed to air dry. Each insert was transferred to an empty well and 200 μ L of Extraction Solution were added. After 10 minutes of incubation, each sample was transferred to a 96-well microtiter plate and the OD 560nm was measured in a plate reader. After the assay, the hydrogels were incubated with an MTT solution that allowed visualization of metabolically active cells. Briefly, the hydrogels were incubated with chondrocytes proliferation medium or MSC proliferation medium with the MTT solution (5 mg/mL, Gibco) for 2 hours at 37 degrees Celsius in a 5 % CO₂ atmosphere incubator. MTT is a pale yellow substrate that when reduced by living cells to formazan turns dark purple. This process requires active mitochondria. Images were captured using a colour camera (Nikon SMZ-10A).

9.2.4 DNA quantification

The bottom of 48 well plates was covered with 200 μ L of Dex-TA (10 % w/v) with or without platelet lysate. MSCs were seeded onto the pre-gelated hydrogels (25000 cells per cm²). The cells were cultured in MSC proliferation media. Quantification of total DNA was determined with the CyQuant DNA kit, according to the manufacturer's description (Molecular Probes, Eugene, Oregon, USA), using a fluorescent plate reader (emission: 520 nm; excitation: 480 nm) (Perkin-Elmer, Victor 3, USA). The standard curve for DNA analysis was generated with λ DNA included in the kit. The assays were performed after 2 and 8 days in culture.

9.2.5 Scanning Electron Microscopy analyses

MSC adhesion on scaffolds was analyzed by SEM (n=3). After 8 days in culture, Dex-TA hydrogels with and without platelet lysate were fixated in 10 % (v/v) buffered formalin overnight at 4 degrees Celsius. Specimens were then dehydrated using sequential ethanol series (from 70 %, until 100 % (v/v), 1 hour each, and critical point dried using a Balzers CPD 030 machine. The samples were gold-sputtered for further observation by SEM operated at 10 kV accelerating voltage.

9.2.6 Multi-lineage differentiation

Samples of 100 μ L Dex-TA (10 % w/v) with or without platelet lysate were prepared with 10 million cells/mL of passage 2 MSCs and gelation was induced by adding HRP and H₂O₂. The constructs were cultured for 21 days in expansion medium, chondrogenic, osteogenic or adipogenic media. For chondrogenic differentiation, MSCs were cultured in chondrogenic medium composed of DMEM supplemented with 0,1 μ M dexamethasone (Sigma), 50 mg/mL ascorbic acid, 100 μ g/mL sodium pyruvate (Sigma), 40 mg/mL L-proline, 1 % insulin-transferrin selenous acid-plus premix (BD Bioscience Pharmingen), 100U/mL penicillin, 100 mg/mL streptomycin, and 10 ng/mL Transforming Growth Factor (TGF)- β 3 (RD Systems). Osteogenic differentiation was induced by culturing constructs in medium composed of α -MEM with 10 nM dexamethasone, 5 mM β -glycerolphosphate (Sigma), and 50 mM ascorbic acid-2- phosphate. Adipogenic differentiation was induced by culturing constructs in α -MEM supplemented with 10 % fetal bovine serum, 100U/ mL penicillin, 100 mg/mL streptomycin, 1.6 μ M insulin, 0.25 μ M dexamethasone, 0.5mM 1-methyl-3-isobutylxanthine, 3,7-dihydro-1-methyl-3-(2-methylpropyl)-1H-purine-2,6-dione, 3-isobutyl-1-methyl-2,6(1H,3H)-purinedione (IBMX, Sigma-Aldrich) and 50 μ M indomethacin.

9.2.7 Histological evaluation

After 21 days in culture, the hydrogel constructs were fixed in 10 % buffered formalin for 1 hour. After washing with PBS, the samples were embedded in cryomatrix (Cryomatrix, Shandon). A cryo-microtome (Leica) was used to collect 10 μ m sections onto gold-coated slides. The cryomatrix was washed off the slides by incubation in distilled water for 10 minutes. Afterwards, histology and immunohistochemistry were performed. Toluidine blue (Fluka, 0,1 % in demi-water, 10 minutes incubation) was used to stain glycosaminoglycans (GAGs). For collagen type II immuno-staining, the samples were treated with 10 mM citric acid buffer for 10 minutes, and then were washed with PBS/BSA 1 %. Col2A1 monoclonal antibody (Purified mouse immunoglobulin IgG1, clone 3H1-F9, Abnova) was diluted at 1:100 in PBS/BSA 1 % and incubated overnight at room temperature. After the sections were washed twice for 5 min in PBS/BSA 1 %, an incubation step with Alexa Fluor 488-Goat anti-Mouse IgG1 (Invitrogen, Molecular Probes, 1:1000) followed, for 1 hour. After extensive washes, the sections were incubated with VECTASHIELD Mounting Medium with DAPI (Vector Laboratories, Burlingame, CA) for 1 minute and mounted. Alizarin

Red and von Kossa stainings were used for osteogenic differentiation, and Oil Red O was used to stain adipocytes. The slides were then washed, dehydrated, mounted and analyzed using bright field or fluorescence (FITC filter) microscopy (Nikon Eclipse).

9.2.8 Gene expression analysis

Hydrogel/cell constructs cultured for 21 days in expansion or differentiation media were washed with PBS and lysed using Trizol reagent (Invitrogen, Carlsbad, CA). Total RNA was isolated using the Nucleospin RNA II kit (Bioke) according to manufacturers instructions. The RNA yields were determined using the Nanodrop2000 (ND-1000 Spectrophotometer, Isogen LifeScience). Subsequently, cDNA was synthesized using the iScript Kit (BioRad) according to the manufacturers recommendations. Expression levels of individual genes were analyzed by quantitative PCR (MiQ, Bio-rad), using the following forward and reverse primers: Collagen type I (COL1A1) Forward 5' GTCACCCACCGACCAAGAAACC 3' Reverse 5' AAGTCCAGGCTGTCCAGGGATG 3'; Collagen type II (COL2A1) Forward 5' CGTCCAGATGACCTTCCTACG 3' Reverse 5' TGAGCAGGGCCTTCTTGAG 3'; Alkaline phosphatase (ALPL) Forward 5' ACAAGCACTCCCACTTCATC 3' Reverse 5' TTCAGCTCGTACTGCATGTC 3'; Osteocalcin (OC) Forward 5' GGCAGCGAGGTAGTGAAGAG 3' Reverse 5' GATGTGGTCAGCCAACTCGT 3'; Peroxisome proliferator-activated receptor gamma (PPARG) Forward 5' GATGTCTCATAATGCCATCAGGTT 3' Reverse 5' GGATTCAGCTGGTCGATATCACT 3'; Glyceraldehyde-3- phosphate dehydrogenase (GAPDH) Forward 5' CGCTCTCTGCTCCTCCTGTT 3' Reverse 5' CCATGGTGTCTGAGCGATGT 3'. Gene expression was normalized to the expression of GAPDH.

9.2.9 Chorioallantoic membrane (CAM) model

Fertilized eggs were purchased from a local farm (Enschede, The Netherlands) and placed horizontally in an incubator at a temperature of 37 degrees Celsius with 75 % humidity. After 3 days of incubation, the eggs were punctured and 3 mL of liquid was removed. A rectangle was sawed off the eggshell, the window covered with tape and the viable eggs with a developing membrane were placed back into the incubator. On day 7, 10 % (w/v) Dex-TA with platelet lysate gels were placed in contact with the CAM. Eggs without hydrogels were considered as controls. Four days after placing the hydrogels in contact with the membrane, images were collected to study vasculature development. Additionally, after sacrificing the embryos by ethanol injection, the CAM with the hydrogel was fixated in 10 % buffered formalin and processed for further visualization under the microscope.

9.2.10 Growth factor release profiles

Platelet lysate is a rich source of growth factors. To quantify the release of growth factors present in the platelet lysate incorporated into Dex-TA hydrogels, we collected the supernatant and quantified two growth factors involved in cartilage formation:

TGF- β 3 and BMP-6. The *in vitro* release of TGF- β 3 and BMP-6 from 10 % (w/v) Dex-TA with platelet lysate gel was monitored up to 14 days. Samples of 100 μ L of hydrogel were prepared. After gelation, 100 μ L PBS was added to each sample and incubated at 37 degrees Celsius, under agitation. The supernatant was collected and the PBS replaced by fresh PBS at every time point. The quantification of the released TGF- β 3 and BMP-6 was obtained by Enzyme-Linked Immunosorbent Assay (ELISA), according to manufacturer's instructions (human Duo ELISA sets, RD Systems). This quantification method only detects activated TGF- β 3. Cumulative release of both growth factors was obtained by quantification of TGF- β 3 and BMP-6 in the platelet lysate and normalizing to the total amount present in the lysate solution used. All release profiles were performed in triplicate.

9.2.11 Analysis of interface morphology

Samples of 100 μ L of 10 % Dex-TA hydrogels with and without platelet lysate were crosslinked onto standardized biopsies of human OA cartilage (0.5x0.5x0.1 mm). The use of human material was approved by a local medical ethical committee. OA cartilage was obtained from the knee joints of adult patients suffering from late stage OA undergoing an arthroplasty, after informed consent. After fixation in 10 % buffered formalin, the hydrogel-cartilage constructs were dehydrated and lyophilized (CPD030 Balzers Critical Point Dryer). Dried samples were sputtered with gold (Cressington sputter coater) and visualized using SEM, as described above. For histological analysis, the samples were dehydrated and embedded in paraffin. Sections of 5 μ m were used for Haematoxylin and Eosin staining (HE Sigma). Slides were assembled with resinous medium for visualization using light microscopy (Nikon Eclipse).

9.2.12 Statistical analysis

Each experiment was performed in triplicate unless otherwise specified. The results are presented as mean \pm standard deviation (SD). Experimental data were analyzed for statistical significance using a student t-test. Statistical significance was set to p-value <0.05 (*).

9.3 Results

9.3.1 Platelet lysate does not affect mechanical properties of Dex-TA hydrogels

Two approaches were taken to incorporate platelet lysate in Dex-TA hydrogels. In the first approach, a dual crosslinking was attempted by separating platelet plasma into thrombin and fibrinogen and adding one of these components to the Dex-TA polymer solution and the other to the solution of HRP and H₂O₂ (data not shown). This approach was not successful because either the gelation did not occur, likely due to inactivation of the enzyme or loss of oxidative properties of the H₂O₂, or hydrogels were obtained in which the platelet gel was heterogeneously distributed,

with part of the components remaining liquid. This strategy was not further pursued. In the second approach, experiments were performed with hydrogels in which the polymer was dissolved in platelet lysate prior to peroxidase mediated crosslinking. Using this approach, the platelet lysate was homogeneously dispersed and successfully incorporated into Dex-TA hydrogels. Moreover, the gelation occurred within 1 minute and was not affected by dissolving the polymer in platelet lysate instead of PBS or culture medium (data not shown).

The mechanical properties of 10 % (w/v) Dex-TA hydrogels with incorporated platelet lysate were analyzed by oscillatory rheology and compared with Dex-TA hydrogels dissolved in culture medium and with a platelet gel formed by mixing fibrinogen with thrombin in a 1:1 ratio. The kinetics of the gelation was evaluated by monitoring of storage and loss modulus throughout time. A gradual increase in the storage modulus was observed in all gel types, which reached a plateau within 5 minutes after starting the crosslinking reaction (Fig. 9.1-A). The plateau moduli values of the hydrogels were collected at 10 minutes and are presented in figure 9.1-B as the average of three measurements for each gel type. No significant differences were detected in the storage modulus of a Dex-TA hydrogel prepared in culture medium or in platelet lysate. The platelet gel showed very low mechanical properties, compared to the Dex-TA-based hydrogels, yet it showed higher visco-elasticity, as indicated by a high damping factor value (defined as damping modulus/storage modulus). No differences were detected in the porosity of Dex-TA dissolved in culture medium or dissolved in platelet lysate, as shown in figures 9.1-C and 9.1-D, respectively.

9.3.2 Platelet lysate induced cell migration into Dex-TA hydrogels

Next, we examined whether incorporation of platelet lysate would render 10 % (w/v) Dex-TA hydrogels chemo-attractant using a cell migration assay. The chemo-attractant properties of a 10 % Dex-TA hydrogel without platelet lysate are poor and lower compared to a pure platelet lysate hydrogel (Fig 9.2-A), irrespective of the cell source. Mixing platelet lysate into a 10 % Dex-TA hydrogel considerably improved the chemo-attractant properties which surpassed the chemo-attractant properties of a pure platelet lysate hydrogel when primary chondrocytes were used. When human MSCs were used, the highest value was observed using a pure platelet lysate hydrogel, which is likely due to faster dispersion of chemotactic factors, such as SDF-1 α , that are specific for MSCs. The metabolic activity of the cells that migrated and adhered onto the hydrogels was assessed by MTT staining (figure 9.2-B). Using this assay, the cells that crossed the membrane and entered the hydrogels were visualized. A limited amount of cells adhered onto Dex-TA hydrogels. In contrast, a considerably higher amount of cells could be detected in Dex-TA hydrogels mixed with platelet lysate, using both human chondrocytes and MSCs.

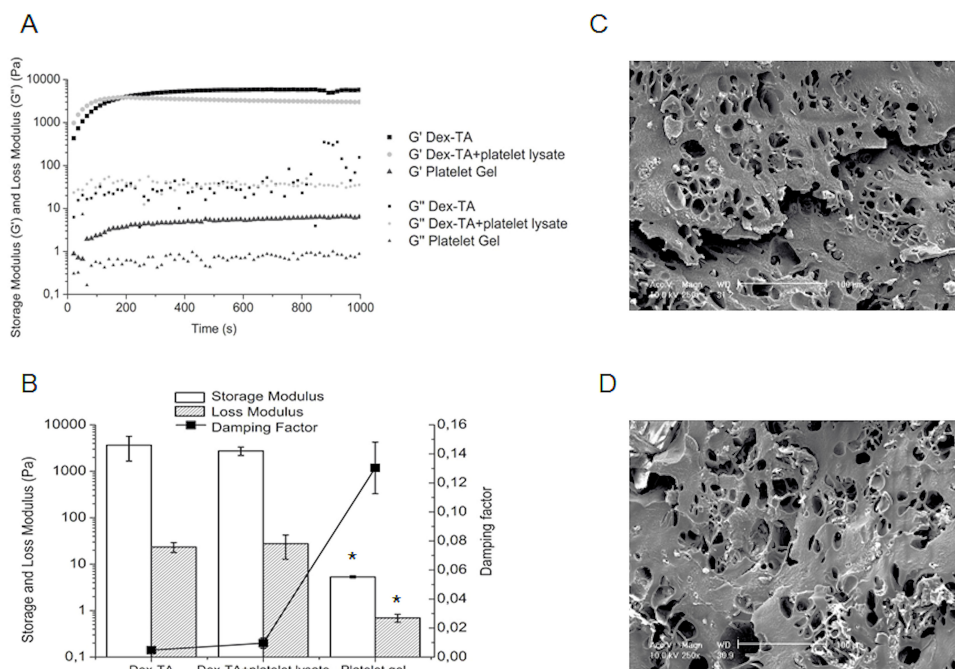


Figure 9.1: Rheological analysis and hydrogel morphology. A) Storage (G') and loss (G'') modulus of Dex-TA, Dex-TA with platelet lysate and platelet gel, as a function of time; B) Storage and loss modulus plateau values, as well as damping factors ($tg=G''/G'$) of Dex-TA, Dex-TA with platelet lysate and pure platelet gel; C) Representative SEM image of critical point dried Dex-TA hydrogel sample; D) Representative SEM image of critical point dried Dex-TA with platelet lysate hydrogel sample, showing no difference in porosity compared with Dex-TA only. Scale bars correspond to 100 μm .

9.3.3 Cell adhesion is enhanced by the addition of platelet lysate

The effects of the incorporation of platelet-lysate in a 10 % (w/v) Dex-TA hydrogel on cell adhesion and proliferation were evaluated. After gelation, MSCs were seeded onto the hydrogels. The adhered cells were quantified after 2 and 8 days in culture. As shown in figure 9.3-A, at day 2 the number of adhered cells was more than 4-fold higher for Dex-TA hydrogels with platelet lysate compared to pure Dex-TA hydrogels. Similar results were obtained at day 8. At this time point, samples of both gel types were stained for cell metabolic activity using the MTT assay. Higher number of adhered cells with uniform distribution was found in the presence of platelet lysate (figure 9.3-B). The uniform cell spreading and cell infiltration into the Dex-TA with platelet lysate could also be observed using SEM (Figure 9.3-C). The surface of the gel was covered with a uniform cell layer. In addition, upon cross-sectioning of the

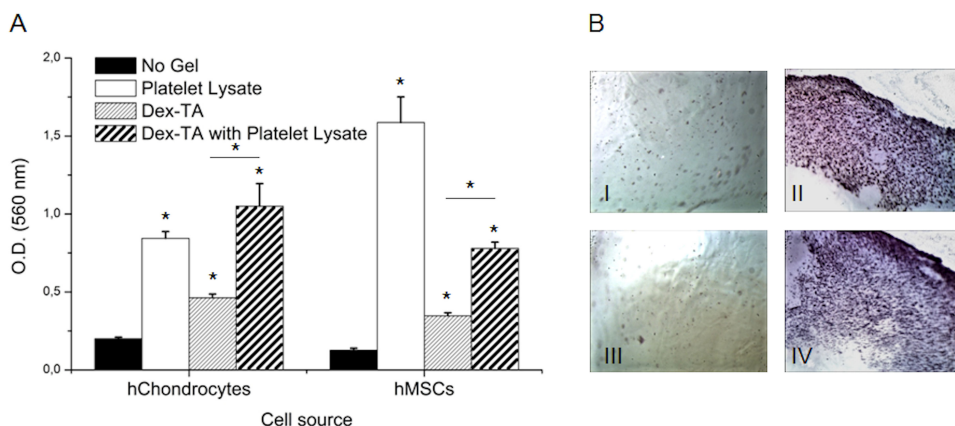


Figure 9.2: Platelet rich lysate renders Dex-TA hydrogels chemo-attractant.

A) Cell migration was assessed by a 24-hours trans-well cell migration assay using either human chondrocytes (hChondrocytes) or human bone marrow derived mesenchymal stromal cells (hMSCs). Platelet lysate mixed in the culture medium, Dex-TA and Dex-TA with platelet lysate hydrogels were prepared on the wells and the migratory cells that crossed the membrane were quantified. The platelet lysate as a medium component or incorporated in Dex-TA acted as a chemo-attractant. B) MTT assay performed in the hydrogels immediately after the collection of the membranes for quantification. The metabolically active cells that crossed the membrane and adhered onto the hydrogels are stained purple. I) Dex-TA with adhered hChondrocytes; II) Dex-TA with platelet lysate with adhered hChondrocytes; III) Dex-TA with adhered hMSCs; IV) Dex-TA with platelet lysate with adhered hMSCs.

gel, spindle shaped cells invading the hydrogel could be identified.

9

9.3.4 Platelet lysate induces chondrogenic but not osteogenic nor adipogenic differentiation

MSCs incorporated in Dex-TA hydrogels in the presence or absence of platelet lysate were cultured in chondrogenic, osteogenic and adipogenic differentiation inducing medium. Expansion medium, without growth factors, was used as control. Both histological evaluation and gene expression analyses were performed. Cells showed the potential to differentiate into the different mesodermal lineages. The potential to differentiate into chondrocytes is indicated by the Toluidine Blue and Collagen type II staining. Both staining were more intense when cells were incorporated into Dex-TA hydrogels with platelet lysate, as shown in figure 9.4-A. Platelet lysate did not have a beneficial effect on collagen type II mRNA expression when constructs were cultured in chondrogenic differentiation medium (Figure 9.4-C). In control medium, collagen type II mRNA expression was higher in the presence of platelet lysate. Interestingly,

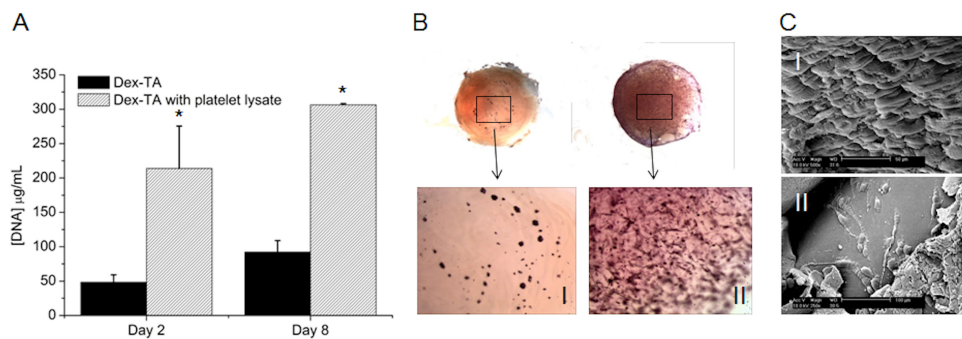


Figure 9.3: Adhesion and proliferation profile. A) DNA quantification of MSCs were seeded onto the pre-gelated Dex-TA hydrogels prepared with or without platelet lysate hydrogels (2.5×10^4 cells per cm^2). The assays were performed after 2 and 8 days in culture. B) MTT assay of the MSCs adhered onto the pre-gelated Dex-TA hydrogels prepared with or without platelet lysate hydrogels, after 8 days in culture. Metabolically active cells are stained purple. C) Representative SEM image of critical point dried Dex-TA hydrogel with platelet lysate with adhered MSCs, after 8 days in culture. I) Top view of the hydrogel sample; II) Cross-section of the hydrogel sample, showing cells that have migrated from the top into the interior of the gel.

the presence of platelet lysate potentially inhibited collagen type I mRNA expression (figure 9.4-D). Osteogenic differentiation can be detected using Alizarin Red staining, where calcium depositions stain red, and von Kossa staining, which stains mineralized areas dark brown. Both stainings appeared to be more intense when incorporating MSCs into Dex-TA with platelet lysate (figure 9.5-A). Yet no significant differences were found in ALP gene expression, which is an early osteogenic marker. The expression of OC, which is a late osteogenic marker, was decreased (figures 9.5-B and 9.5-D, respectively). This decrease was observed in control conditions and in osteogenic culture medium. No significant differences in adipogenic differentiation were observed between Dex-TA or Dex-TA-platelet lysate hydrogels using Oil Red O staining and PPAR γ mRNA expression (figures 9.6-A and 9.6-B, respectively). Finally, to study the effect of platelet lysate on attracting blood vessel in growth into Dex-TA hydrogels a CAM assay was performed. Visual inspection of the CAM, four days after placing the hydrogels in contact with the membrane, did not reveal an effect of platelet lysate on blood vessel growth towards the hydrogel construct (figure 9.7-B).

9.3.5 Chondro-inductive effect stimulated by addition of platelet lysate

Previously we and others have shown that combining MSC with primary human chondrocytes potentiates cartilage formation in micromass cultures [19,22,23]. The

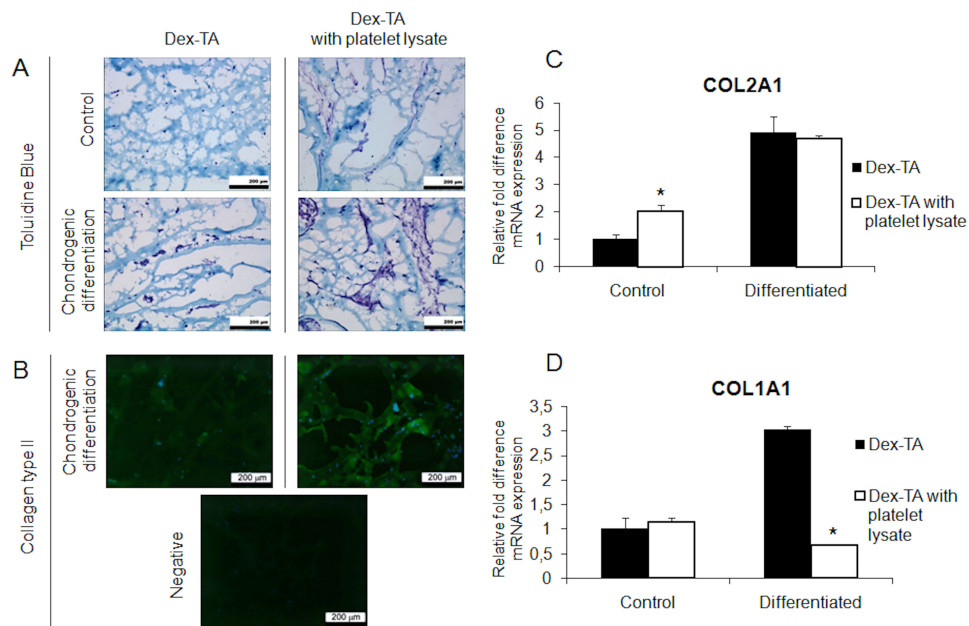


Figure 9.4: Chondrogenic differentiation. A) Histological evaluation of representative samples of Dex-TA with or without platelet lysate with incorporated MSCs, cultured for 21 days in expansion or chondrogenic media, stained with Toluidine blue (purple color indicates GAG deposition). B) Collagen type II immuno-fluorescence staining of representative samples of Dex-TA with or without platelet lysate with incorporated MSCs, cultured for 21 days in chondrogenic media (collagen type II is stained in green and cell nuclei are stained blue). The negative control sample was obtained by absence of incubation with primary anti-body. C) Expression levels of COL2A1 and COL1A1 genes analyzed by quantitative PCR of hydrogel/cell constructs of Dex-TA with or without platelet lysate with incorporated MSCs cultured for 21 days in expansion or differentiation media. Gene expression was normalized to the expression of GAPDH.

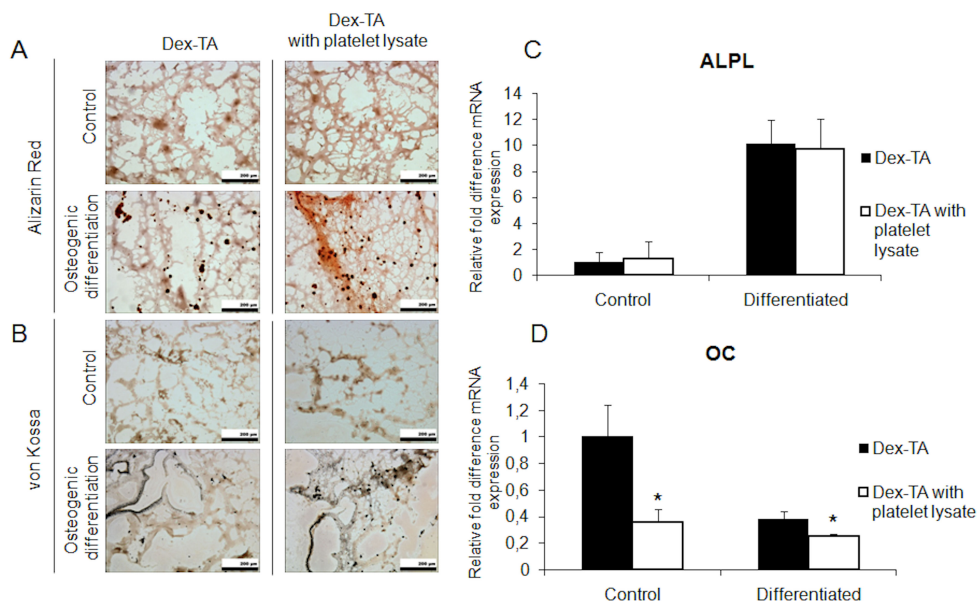


Figure 9.5: Osteogenic differentiation. A) Histological evaluation of representative samples of Dex-TA with or without platelet lysate with incorporated MSCs, cultured for 21 days in expansion or osteogenic media, stained with Alizarin Red (red colour indicates calcium deposition). B) Histological evaluation of representative samples of Dex-TA with or without platelet lysate with incorporated MSCs, cultured for 21 days in expansion or osteogenic media, stained with von Kossa (dark brown color indicates mineralization). C) Expression levels of ALP and OC genes analyzed by quantitative PCR of hydrogel/cell constructs of Dex-TA with or without platelet lysate with incorporated MSCs cultured for 21 days in expansion or differentiation media. Gene expression was normalized to the expression of GAPDH (n=3).

test whether this potentiating effect is retained in Dex-TA hydrogels, we cultured human chondrocytes or MSCs only or a combination of 80 % human MSCs mixed with 20 % human chondrocytes in Dex-TA dissolved in culture medium or in platelet lysate. The constructs were cultured in chondrogenic medium without TGF- β 3. Both Collagen type II gene expression and synthesis were significantly higher in presence of the platelet lysate in both culture systems, as shown in figures 9.8-A and 9.8-B. This increase was more dramatic, up to 9-fold, in a co-culture system in combination with platelet lysate.

To investigate whether improved chondrogenesis was due to the enrichment in growth factors typically associated with chondrogenic differentiation, such as TGF- β 3 and BMP-6, in platelet lysate containing gels, we studied their release profile. Dex-TA hydrogels with platelet lysate were prepared similarly to the cell-hydrogel constructs and the cumulative release was determined and expressed as percentage

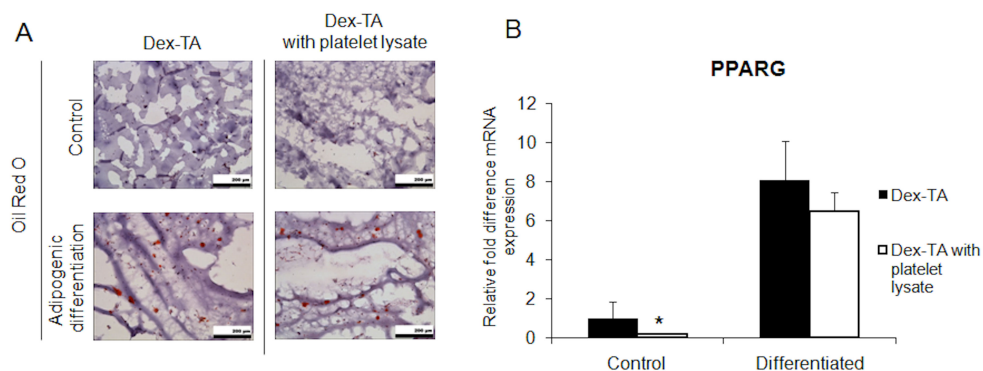


Figure 9.6: Adipogenic differentiation. A) Histological evaluation of representative samples of Dex-TA with or without platelet lysate with incorporated MSCs, cultured for 21 days in expansion or adipogenic media, stained with Oil Red O (red colour indicates fat deposition). B) Expression levels of PPARG mRNA analyzed by quantitative PCR of hydrogel/cell constructs of Dex-TA with or without platelet lysate with incorporated MSCs cultured for 21 days in expansion or differentiation media. Gene expression was normalized to the expression of GAPDH (n=3).

of the total initial content (figure 9.7-C). Notably, a burst release of both molecules from the hydrogel was detected in the first days; however, approximately 20 % of both growth factors remained entrapped within the hydrogel network up to 14 days. The release of BMP-6 showed a more sustained profile, whereas TGF- β 3 had a faster release, up to 70 % in 4 days. At day 14, both growth factors had been released to the same extent, approximately 80 %.

9.3.6 Effective adhesion onto OA-affected cartilage

The peroxidase crosslinking reaction results not only in crosslinking of tyramine residues resulting in hydrogel formation but also in tyramine-tyrosine cross links. The latter cross links enable direct fixation of the hydrogel at collagen rich tissues (Moreira *et al*, submitted). To test whether the incorporation of platelet lysate affected the fixation of Dex-TA hydrogels at the cartilage surface, we assessed the morphology of the hydrogel-cartilage interface. The hydrogel integration at the defect area was simulated by gelating Dex-TA dissolved in culture medium or in platelet lysate on top of human OA cartilage samples. The cartilage-hydrogel interface was evaluated by histology and SEM. As shown in figures 9.9-A and 9.9-B both hydrogels were properly integrated with the cartilage. They were in close proximity with the defective cartilage surface, with only minor gaps at the interfacial area due to the extreme roughness of the fissures in the cartilage which are typical for OA. Similar results were obtained using SEM by which the interfacial area of Dex-TA with platelet lysate hydrogels and

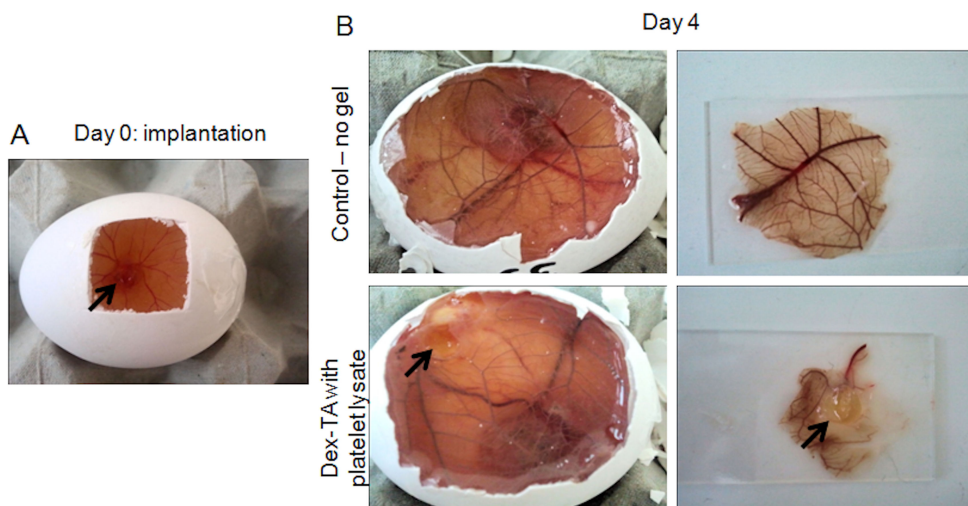


Figure 9.7: Vascularization potential using the chorioallantoic membrane (CAM) model. A) After 7 days of incubation at 37 C, Dex-TA with platelet lysate gels were placed in contact with the CAM, sealed and returned to the incubator. B) Four days after placing the hydrogels in contact with the membrane, images were collected to study vasculature development. After fixation, the hydrogels with the CAM were excised and transferred onto glass slides. The control corresponds to normal membrane development without hydrogel.

cartilage could be visualized in more detail (figure 9.9-C). The hydrogel showed close interaction with the cartilage specimen, most likely mediated by covalent bonds between the tyramine residues of the hydrogel and tyrosine residues present in collagen or other matrix proteins present in the cartilage tissue.

9.4 Discussion

Platelet lysate is an autologous source of a myriad of growth factors clinically relevant for the treatment of injuries in a number of tissues, such as skin, bone, cartilage and tendon. Recently, increasing attention has been focused on the high potential of platelet lysate as an enhancer of tissue repair by inducing cell recruitment and proliferation [24,25]. Indeed, previous studies have shown the efficiency of platelet gels for guided reconstructive surgery [26]. The poor mechanical properties of platelet-derived gels, however, hamper their application in mechanically demanding microenvironments, such as the joint. Additionally, platelet or fibrin gels without further crosslinking show rapid degradation [27,28], especially when cells are incorporated within [29]. This limits the time period in which the growth factors present in the lysate at the defect site can participate in tissue repair. Therefore, the challenge is

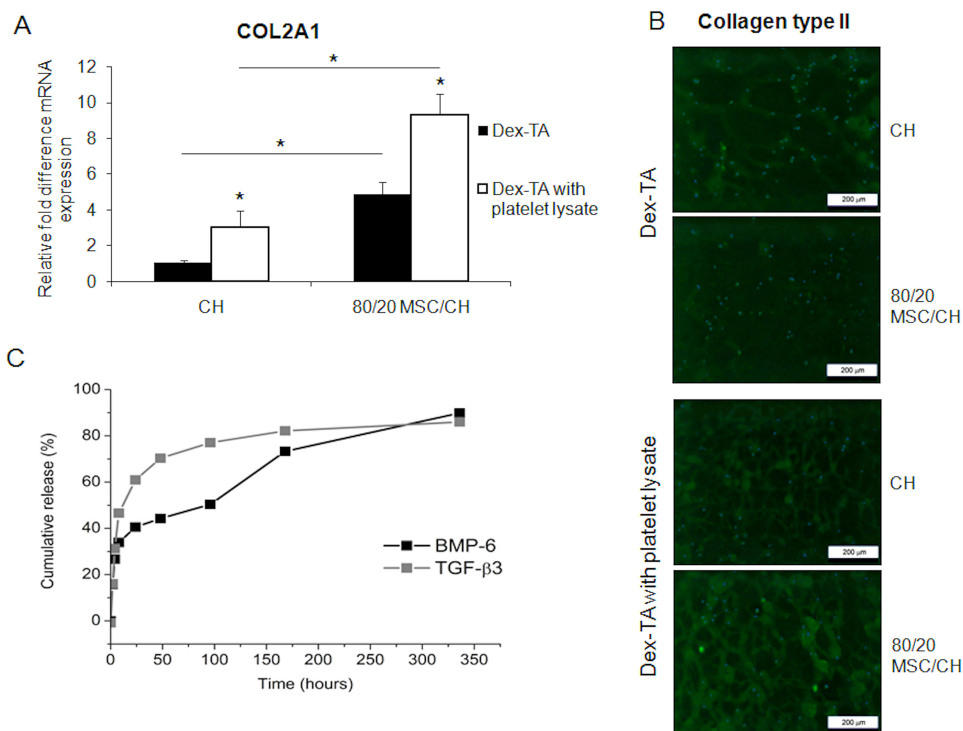


Figure 9.8: Platelet rich lysate enhances chondro-induction. A) Expression levels of COL2A1 gene analyzed by quantitative PCR of hydrogel/cell constructs of Dex-TA with or without platelet lysate with incorporated hChondrocytes or co-cultures of hMSCs with hChondrocytes (80/20 ratio), cultured for 21 days in chondrogenic medium without TGF- β 3 supplementation. Gene expression was normalized to the expression of GAPDH (n=3). B) Collagen type II immuno-fluorescent staining of representative samples of Dex-TA with or without platelet lysate with incorporated hChondrocytes or co-cultures of hMSCs with hChondrocytes (80/20 ratio), cultured for 21 days in chondrogenic medium without TGF- β 3 supplementation (collagen type II is stained in green and cell nuclei are stained blue). Scale bars correspond to 200 μ m. C) Release profile of the TGF- β 3 and BMP-6 present in the platelet lysate incorporated into Dex-TA hydrogels, up to 14 days. Cumulative release of both growth factors was obtained by quantification of TGF- β 3 and BMP-6 in the platelet lysate and was normalized to the total amount present in the lysate.

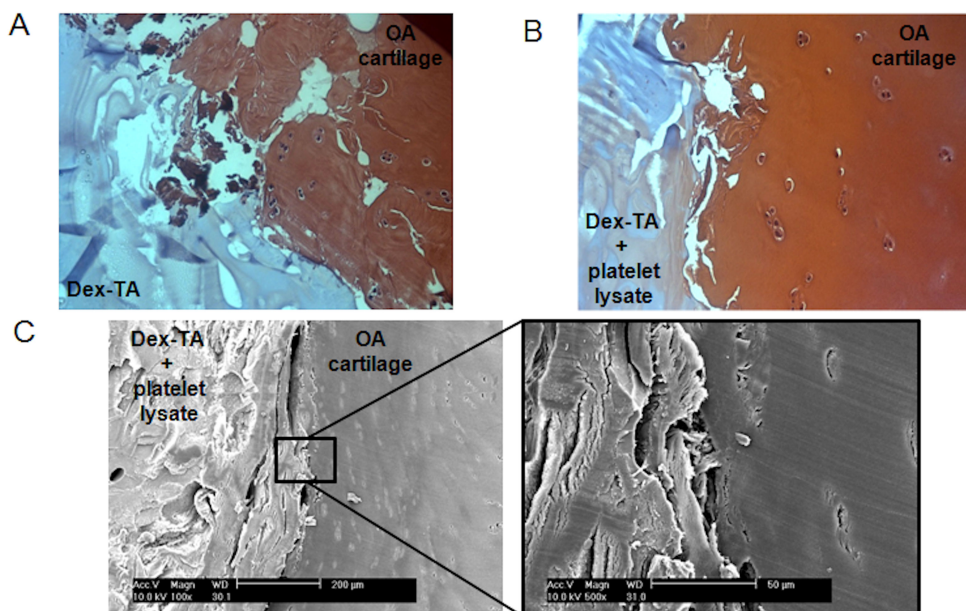


Figure 9.9: Interface hydrogel-OA cartilage. The integration and adhesion between the Dex-TA hydrogels with (A) and without platelet lysate (B) crosslinked onto standardized samples of human OA cartilage. Representative sections of the hydrogels were stained with H and E. C) Representative SEM image of the interface between Dex-TA hydrogel with platelet lysate and OA affected cartilage. The intricate interaction between the hydrogel and the host tissue is evidenced, highlighting the absence of gaps at the interfacial area.

to develop a method which can preserve the beneficial effects of platelet lysate over a longer period of time at the desired spot in the body. We have recently developed *in situ* gelating hydrogels of natural polymers, revealing promising features for cartilage repair [11,12]. Dex-TA injectable *in situ* forming hydrogels are biocompatible, biodegradable and hold mechanically suitable properties for cartilage repair strategies. These gels are formed by mixing the polymer with the enzyme peroxidase and non-toxic dilute amounts of hydrogen peroxide. In spite of these advantages, Dex-TA hydrogels lack biological activity. Thus, our premise was that Dex-TA and platelet lysate may complement each other, leading to one system with stable mechanical properties and enhanced biological features. A gel formed by combination of Dex-TA with platelet lysate is easy-to-apply and may be used to improve existing surgical techniques for cartilage repair, such as bone marrow-stimulation procedures.

In this study, we successfully incorporated platelet lysate as an autologous source of growth factors in Dex-TA hydrogels. The instructive signals provided by the release of growth factors from the platelet lysate incorporated in Dex-TA hydrogels provided the biological cues which eventually may lead to development of a cell-free system for

cartilage repair. Feasibility of such approach was shown by demonstrating that the incorporation platelet lysate resulted in a strong chemotactic signal enabling the recruitment and ingrowth of migratory stem or tissue progenitor cells. Additionally platelet lysate potentially triggered MSCs differentiation towards the chondrogenic lineage. The reduction in collagen type I expression may even suggest that the lysate directs the differentiating MSCs more into the hyaline cartilage lineage. The lysate components were easily entrapped within the polymer matrix. Incorporation of platelet lysate did not alter physical properties of Dex-TA hydrogels at least *in vitro*. It did not affect the mechanical properties, porosity or the gelation time of pure Dex-TA hydrogels. Moreover, the stiffness of Dex-TA with platelet lysate hydrogel is superior to pure platelet gels [11,12].

When in contact with platelet-derived plasma, dextran triggers platelet activation and the release of growth factors. Similarly, freeze thawing cycles lead to platelet lyses and subsequent release of growth factors and cytokines [2,30]. The possibility of turning an inert gel into a chemo-attracting cell-free system is one of the major advantages of the incorporation of platelet lysate in Dex-TA. In fact, our results showed that Dex-TA with platelet lysate induced cell migration of both chondrocytes and MSCs. Thus, this hydrogel can be used as a chemo-attractant when injected into cartilage defects. The gel may attract migratory cells from the synovial fluid, the synovium, the surrounding cartilage matrix such as highly migratory chondrogenic precursor cells [31] or from bone marrow (in case of osteochondral defects or micro-drilling) to invade the gel. The transmigration of crosswise matrix boundaries has been previously reported [32]. This process involved the presence of fibronectin and growth factors such as platelet-derived growth factor-BB (PDGF-BB) which induced the cells to express provisional matrix receptors [1,33]. These components are likely responsible for the enhancement of cell adhesion after incorporation of platelet lysate into Dex-TA. Furthermore, the "natural cocktail" of growth factors present in platelet lysate also stimulated cell proliferation. This enhancement of cell proliferation by platelet lysate and fibrin glues has previously been shown using both MSCs and chondrocytes [25,34].

Interestingly, our data showed that chondrogenic differentiation was induced by incorporation of platelet lysate into Dex-TA hydrogels complemented with human MSCs. In contrast, limited effects were observed on osteogenic or adipogenic differentiation. These effects were observed without addition of supplementary growth factors to the MSCs culture media. This allowed us to conclude that the growth factors present in the platelet lysate appeared to be sufficient to trigger preferentially the differentiation of MSCs into chondrocytes. The use of fibrin glue as inducer of chondrogenic differentiation of MSCs has been previously reported [5]. However, in the absence of protease inhibitors, these scaffolds degraded between 10 to 14 days. Dex-TA hydrogels are much more resistant to degradation facilitating much longer matrix-guided cartilage repair. Particularly relevant for cartilage repair is our observation that during chondrogenic differentiation of MSCs in Dex-TA hydrogels the presence of platelet lysate potentially repressed the expression of collagen type I while collagen type II expression was stimulated. Roussy *et al.* [35] have reported that activated platelet-rich plasma had no significant effect on *in vivo* bone formation,

which is in accordance to our *in vitro* results showing inhibitory effects on osteoblastic differentiation and repression of collagen type I expression. Previously, it has been shown that platelet lysate has a stimulatory effect on endothelial cell division [35]. As neo-vascularisation would be an undesired site effect of any cartilage repair strategy, we have evaluated the effect of the combined Dex-TA/platelet rich lysate gel on blood vessel formation and blood vessel ingrowth using the CAM-model also. Our gel did not appear to influence blood vessel formation. Yet additional experiments focusing on vessel development using our system are necessary for further conclusions. Taken together our data suggest that it may be attractive to combine Dex-TA hydrogels supplemented with platelet lysate with a bone marrow stimulation technique such as sub-chondral drilling. In such a combined approach, MSCs from the bone marrow are actively attracted by the chemo-attractant properties of the hydrogel. These cells are subsequently stimulated to differentiate into chondrocytes and considering the inhibitory effect of platelet lysate on COL1 mRNA expression, they may differentiate into hyaline cartilage rather than into non-permanent fibrous-like cartilage.

Previous reports have highlighted the trophic role of MSCs in stimulating chondrocyte proliferation and matrix deposition [19]. This effect is known as chondro-induction. To investigate whether the presence of the platelet lysate would have a stimulatory effect on chondro-inductivity, chondrocytes and co-cultures of chondrocytes with MSCs were cultured in Dex-TA with platelet lysate in the absence of growth factors. Gene expression and deposition of collagen type II by chondrocytes was enhanced by the presence of platelet lysate in the gel. Remarkably, the stimulatory effect was more pronounced in the co-culture system resulting in significantly higher deposition of extracellular matrix when Dex-TA hydrogels were combined with MSCs, chondrocytes and platelet lysate. This highly advantageous stimulatory effect of platelet lysate may possibly be combined with well-recognized cell based strategies such as autologous chondrocyte implantation (ACI) which may result in improved cartilage repair.

TGF- β 3 and BMP-6 are growth factors typically associated with chondrogenic differentiation of MSCs. These growth factors are abundantly present in platelet lysate and , therefore, we have examined their release from a Dex-TA/platelet rich lysate gel. The release profiles from Dex-TA with platelet lysate showed an overall sustained release. This is suggestive that the enhanced chondrogenic effect observed was at least partly mediated via the sustained release of these growth factors from the hydrogel. The use of autologous platelet rich lysate avoids the use of recombinant growth factors or products from animal origin avoiding the risk of an adverse immunological response. In addition, the use of platelet rich lysate is cost effective compared with the use of expensive recombinantly produced growth factors.

The adhesion and retention of the hydrogel at the cartilage defect site are of extreme importance for the tissue regeneration and integration of the neo-tissue with native cartilage. Previously, we have identified covalent binding of Dex-TA onto collagen fibrils present in cartilage via tyramine-tyrosine motifs during *in situ* gel formation (Moreira *et al*, submitted). The presence of platelet rich lysate did not interfere with this mechanism. Thus, the combination with Dex-TA allowed the retention of platelet rich lysate at the defect site. The initial fluidity of the gel allows

filling up irregularities at the cartilage surface as present in OA which may then provide mechanically support to the damaged cartilage. Moreover, platelet lysate has anti-inflammatory properties, which enhances its therapeutic potential of Dex-TA hydrogels for treatment of diseases caused by catabolic inflammatory cytokines, such as OA [36].

9.5 Conclusion

The present study described the use of autologous blood derived platelet rich plasma that can be efficiently incorporated into Dex-TA hydrogels. Dex-TA provided the mechanical strength and a resistance to enzymatic degradation which lack in platelet gels. In addition, the mild enzymatic crosslinking method allows retention of the platelet rich lysate at the defect site in the cartilage. The incorporation of platelet lysate provided biological cues that lack in Dex-TA hydrogels, such as chemo-attractant properties and anabolic growth factors. Taken together, our data shows that an *in situ* forming Dex-TA hydrogel complemented with platelet lysate can potentially be used as a cell-free approach to repair cartilage defects. Furthermore, we show that the bioactivity of the growth factors released by the gel promoted proliferation and triggered chondrogenic differentiation of MSCs. Therefore, this hydrogel system shows high potential as an out-of-the-shelf cell-free product for cartilage repair strategies either or not in combination with marrow stimulation by combining scaffold-guided regenerative medicine with an autologous source of growth factors.

References

1. Lu HH, Vo JM, Chin HS, Lin J, Cozin M, *et al.* (2008) Controlled delivery of platelet-rich plasma-derived growth factors for bone formation. *J Biomed Mater Res A* 86: 1128-1136.
2. Zimmermann R, Jakubietz R, Jakubietz M, Strasser E, Schlegel A, *et al.* (2001) Different preparation methods to obtain platelet components as a source of growth factors for local application. *Transfusion* 41: 1217-1224.
3. Saito M, Takahashi KA, Arai Y, Inoue A, Sakao K, *et al.* (2009) Intraarticular administration of platelet-rich plasma with biodegradable gelatin hydrogel microspheres prevents osteoarthritis progression in the rabbit knee. *Clin Exp Rheumatol* 27: 201-207.
4. Sampson S, Reed M, Silvers H, Meng M, Mandelbaum B (2010) Injection of platelet-rich plasma in patients with primary and secondary knee osteoarthritis: a pilot study. *Am J Phys Med Rehabil* 89: 961-969.
5. Ahmed TA, Giulivi A, Griffith M, Hincke M (2011) Fibrin glues in combination with mesenchymal stem cells to develop a tissue-engineered cartilage substitute. *Tissue Eng Part A* 17: 323-335.
6. Calich AL, Domiciano DS, Fuller R (2010) Osteoarthritis: can anti-cytokine therapy play a role in treatment? *Clin Rheumatol* 29: 451-455.
7. Iliopoulos D, Gkretsi V, Tsezou A (2010) Proteomics of osteoarthritic chondrocytes and cartilage. *Expert Rev Proteomics* 7: 749-760.
8. Mulhall KJ, Ghomrawi HM, Scully S, Callaghan JJ, Saleh KJ (2006) Current etiologies and modes of failure in total knee arthroplasty revision. *Clin Orthop Relat Res* 446: 45-50.
9. Klompmaker J, Jansen HW, Veth RP, Nielsen HK, de Groot JH, *et al.* (1992) Porous polymer implants for repair of full-thickness defects of articular cartilage: an experimental study in rabbit and dog. *Biomaterials* 13: 625-634.
10. Mehta S, Watson JT (2008) Platelet rich concentrate: basic science and current clinical applications. *J Orthop Trauma* 22: 432-438.
11. Jin R, Hiemstra C, Zhong Z, Feijen J (2007) Enzyme-mediated fast *in situ* formation of hydrogels from dextran-tyramine conjugates. *Biomaterials* 28: 2791-2800.
12. Jin R, Moreira Teixeira LS, Dijkstra PJ, Zhong Z, van Blitterswijk CA, *et al.* (2010) Enzymatically crosslinked dextran-tyramine hydrogels as injectable scaffolds for cartilage tissue engineering. *Tissue Eng Part A* 16: 2429-2440.
13. Jin R, Moreira Teixeira LS, Dijkstra PJ, van Blitterswijk CA, Karperien M, *et al.* (2011) Chondrogenesis in injectable enzymatically crosslinked heparin/dextran hydrogels. *J Control Release*.
14. Jin R, Teixeira LS, Dijkstra PJ, van Blitterswijk CA, Karperien M, *et al.* (2010) Enzymatically-crosslinked injectable hydrogels based on biomimetic dextran-hyaluronic acid conjugates for cartilage tissue engineering. *Biomaterials* 31: 3103-3113.
15. Hildner F, Albrecht C, Gabriel C, Redl H, van Griensven M (2011) State of the art and future perspectives of articular cartilage regeneration: a focus on adipose-derived stem cells and platelet-derived products. *J Tissue Eng Regen Med* 5: e36-51.

16. Doucet C, Ernou I, Zhang Y, Llense JR, Begot L, *et al.* (2005) Platelet lysates promote mesenchymal stem cell expansion: a safety substitute for animal serum in cell-based therapy applications. *J Cell Physiol* 205: 228-236.
17. Prockop DJ (1997) Marrow stromal cells as stem cells for nonhematopoietic tissues. *Science* 276: 71-74.
18. Yamada Y, Ueda M, Hibi H, Nagasaka T (2004) Translational research for injectable tissue-engineered bone regeneration using mesenchymal stem cells and platelet-rich plasma: from basic research to clinical case study. *Cell Transplant* 13: 343-355.
19. Wu L, Leijten JC, Georgi N, Post JN, van Blitterswijk CA, *et al.* (2011) Trophic Effects of Mesenchymal Stem Cells Increase Chondrocyte Proliferation and Matrix Formation. *Tissue Eng Part A*.
20. De Boer J, Jukes JM, Both SK, Leusink A, Sterk LMT, *et al.* (2008) Endochondral bone tissue engineering using embryonic stem cells. *Proceedings of the National Academy of Sciences of the United States of America* 105: 6840-6845.
21. Jin R, Moreira Teixeira LS, Dijkstra PJ, Karperien M, van Blitterswijk CA, *et al.* (2009) Injectable chitosan-based hydrogels for cartilage tissue engineering. *Biomaterials* 30: 2544-2551.
22. Hendriks J, Riesle J, van Blitterswijk CA (2007) Co-culture in cartilage tissue engineering. *Journal of Tissue Engineering and Regenerative Medicine* 1: 170-178.
23. Hendriks JAA, Miclea RL, Schotel R, de Bruijn E, Moroni L, *et al.* (2010) Primary chondrocytes enhance cartilage tissue formation upon co-culture with a range of cell types. *Soft Matter* 6: 5080-5088.
24. Chevallier N, Anagnostou F, Zilber S, Bodivit G, Maurin S, *et al.* (2010) Osteoblastic differentiation of human mesenchymal stem cells with platelet lysate. *Biomaterials* 31: 270-278.
25. Crespo-Diaz R, Behfar A, Butler GW, Padley DJ, Sarr MG, *et al.* (2010) Platelet lysate consisting of a natural repair proteome supports human mesenchymal stem cell proliferation and chromosomal stability. *Cell Transplant*.
26. Sanchez AR, Sheridan PJ, Kupp LI (2003) Is platelet-rich plasma the perfect enhancement factor? A current review. *Int J Oral Maxillofac Implants* 18: 93-103.
27. Ahmed TA, Dare EV, Hincke M (2008) Fibrin: A Versatile Scaffold for Tissue Engineering Applications. *Tissue Eng Part B Rev*.
28. Ahmed TA, Griffith M, Hincke M (2007) Characterization and inhibition of fibrin hydrogel-degrading enzymes during development of tissue engineering scaffolds. *Tissue Eng* 13: 1469-1477.
29. Pettersson S, Wettero J, Tengvall P, Kratz G (2009) Human articular chondrocytes on macroporous gelatin microcarriers form structurally stable constructs with blood-derived biological glues *in vitro*. *J Tissue Eng Regen Med* 3: 450-460.
30. Ts'ao CH, Krajewski DV (1982) Effect of dextran on platelet activation by polymerizing fibrin. *Am J Pathol* 106: 1-7.
31. Koelling S, Kruegel J, Irmer M, Path JR, Sadowski B, *et al.* (2009) Migratory chondrogenic progenitor cells from repair tissue during the later stages of human osteoarthritis. *Cell Stem Cell* 4: 324-335.
32. Greiling D, Clark RA (1997) Fibronectin provides a conduit for fibroblast transmigration from collagenous stroma into fibrin clot provisional matrix. *J Cell Sci* 110

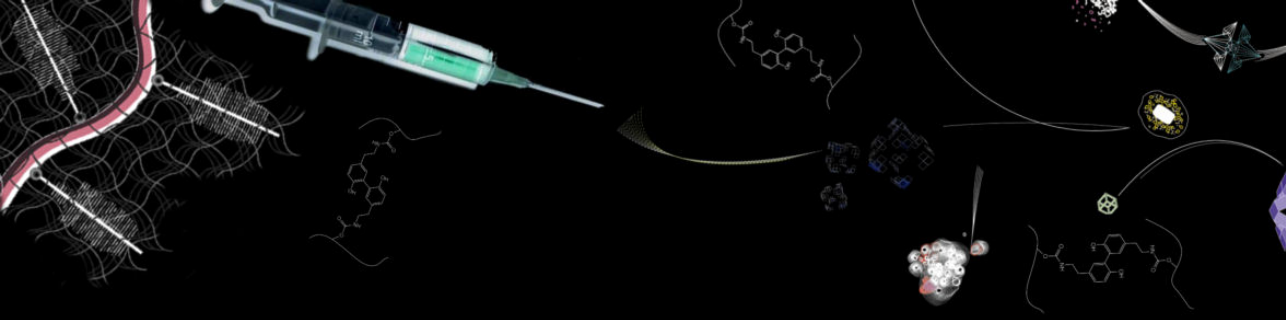
(Pt 7): 861-870.

33. Xu J, Clark RA (1996) Extracellular matrix alters PDGF regulation of fibroblast integrins. *J Cell Biol* 132: 239-249.

34. Akeda K, An HS, Okuma M, Attawia M, Miyamoto K, *et al.* (2006) Platelet-rich plasma stimulates porcine articular chondrocyte proliferation and matrix biosynthesis. *Osteoarthritis Cartilage* 14: 1272-1280.

35. Roussy Y, Bertrand Duchesne MP, Gagnon G (2007) Activation of human platelet-rich plasmas: effect on growth factors release, cell division and *in vivo* bone formation. *Clin Oral Implants Res* 18: 639-648.

36. Woodell-May J, Matuska A, Oyster M, Welch Z, O'Shaughnessey K, *et al.* (2011) Autologous protein solution inhibits MMP-13 production by IL-1beta and TNFalpha-stimulated human articular chondrocytes. *J Orthop Res*.



Chapter 10

General discussion

Stimulation of cartilage repair by nature mimicry

The current trend in tissue engineering strategies is to mimic what happens in nature [1]. On one hand, biomimetic biomaterials have proven their suitability and success as repair strategies for e.g. skin, bladder, bone and cartilage. On the other hand, the mimicry of the events occurring in native regenerative responses remains challenging, yet worth exploring to take tissue engineering one step further. One approach to harness the innate regenerative capacity is to design a scaffold with intrinsic regenerative signals that can activate local cell populations [2]. Induced regeneration is the fundamental nature of tissue engineering, thereby, the aim of this discipline is to persuade and encourage cells, tissues or organs (or their functions) to regenerate when this process does not occur spontaneously [3]. The challenge arises when tissues have a limited capacity of self-repair, such as cartilage. The progressive deeper understanding of cartilage biology is strengthening the link between engineering and functional tissue repair, as described in chapter 2, translating into the successful development of scaffolds that facilitate and accelerate tissue regeneration.

Generally, to ease clinical translation, cell-free products are favored. Clinicians typically try to minimize handling as well as try to simplify procedures. The drawbacks of using autologous cell-laden constructs are mainly related to time demanding cell isolation procedures and prolonged *in vitro* cell expansion prior to implantation. These practical issues highlight the magnitude of the intrinsic properties of scaffolds as key orchestrators of the repair mechanisms [4]. However, the importance of cells in

repair mechanisms cannot be disregarded. Overall, three approaches can be used to overcome the challenges inherent to the application of cell-laden scaffolds: i) design of instructive materials that can be loaded with (recombinant) proteins to enhance cell-mediated repair, ii) improve cell seeding procedures, either using co-culture systems or cell micro-aggregation, to ultimately achieve the best outcome with less cell numbers, or iii) the scaffold is implanted initially as a cell-free system that, once at the defect site, recruits local cells.

Overall, this thesis aimed at tailoring injectable hydrogel scaffolds for cartilage tissue engineering. *In situ* forming hydrogels were designed for the treatment of local cartilage defects and degenerative cartilage diseases, such as OA, acting as healing plasters. A recently developed technology platform of enzymatically crosslinkable hydrogels of natural polymers was the base of this study, in which we have focused on their *in vitro* biological evaluation. Several strategies described in this thesis were adopted to improve the biological properties of these hydrogels. *In situ* forming injectable hydrogels can be used for the delivery of chondrocytes or MSCs, immobilizing them at the defect site via an non-invasive procedure, or, alternatively, these hydrogels can attract cells from the sub-chondral bone or synovial fluid to restore joint homeostasis and stimulate cartilage regeneration. The incorporation of bioactive compounds in these hydrogels is a highly attractive approach to stimulate regeneration. The optimal microenvironment, which mimics the cartilaginous matrix in the hydrogel, will, in principle, allow direct contribution of the cells in new tissue formation.

10.1 Dextran-based *in situ* forming hydrogels as a potential off-the-shelf injectable system

The success of a repair strategy in the management of cartilage defects relies on the following requirements: i) It must be easy applicable, for example in a minimally invasive procedure, such as an arthroscopy or a single injection; ii) It must remain immobilized at the defect site; iii) be able to cope with normal wear of the joint; iv) be biodegradable and allow cartilaginous matrix deposition/remodelling; and v) be biocompatible and may not cause tissue irritation or an inflammatory response. Hydrogels consisting of natural polymers are likely to fulfil all these requirements due to their resemblance to the native cartilaginous matrix. Dextran was the polysaccharide of choice to form the backbone of the hydrogels described in this thesis, due to its stability, biocompatible properties and more interestingly, due to its structural resemblance to ECM components.

As described in chapter 3, enzymatic crosslinking is a mild and effective method to obtain injectable hydrogels of natural polymers, such as dextran. In chapter 4, we showed that enzymatic crosslinking is indeed a highly efficient method to prepare *in situ* forming dextran-based hydrogels [5,6]. Firstly, hydroxyphenyl groups were introduced on the polymer backbone by linking tyramine (TA) residues via an urethane bond to the polymer backbone, denoted as Dex-TA. Once hydroxyphenyl groups are introduced, *in situ* gelation rapidly induced. This mechanism is based on the covalent crosslinking of the hydroxyphenyl groups in the presence of the enzyme horseradish

peroxidase, as catalyst, and low, non-toxic concentrations of H_2O_2 . The reaction time is adjustable and occurs between several seconds and a couple of minutes. In comparison to Michael-type addition reactions and photo-polymerization [7], the gelation time in enzymatic crosslinking reactions are substantially shorter. After crosslinking, a highly porous 3D network is formed. The size of these pores can be tailored, as higher degree of substitution and polymer concentration resulted in smaller pore size. The pores created support cell encapsulation. The storage modulus of Dex-TA reached up to 60 kPa. The mechanical properties of Dex-TA can easily be customized by changing the polymer backbone properties. Chondrocytes incorporated within the hydrogels showed high cell viability and retained their typical round morphology. Moreover, the cells were capable of producing a cartilaginous matrix, which highlights the suitability of these hydrogels for cartilage repair.

10.2 Bioactivity and biomimicry to improve biological performance

The micro-environment sensed by cells consists of many different ECM molecules, such as GAGs and collagens each with tissue-specific functions. In spite of its excellent biocompatibility and stability, dextran has limited cell interaction capacities. Unlike other polysaccharides, such as hyaluronic acid, chondrocytes do not express specific receptors for dextran, which hampers cell attachment and migration of cells in the hydrogel. In addition, chondrocytes do not express enzymes that can degrade dextran, so the encapsulated cells are compromised in remodeling their extracellular environment once they are captured in a 3D-network of dextran.

We hypothesized that Dex-TA hydrogel biological performance could be improved by incorporation of different GAGs and/or (autologous sources of) growth factors. Three strategies were selected to improve the biological performance of Dex-TA: i) engraftment with hyaluronic acid, ii) mixing with heparin, and iii) incorporation of platelet lysate. The first two approaches are based on relatively simple chemistry to introduce tyramine residues in the selected model molecules: hyaluronic acid and heparin. In this thesis, we focused on these two model molecules, however, this method could also be used to obtain conjugates with other polysaccharides, such as chondroitin sulphate, or ECM proteins, like collagen type II, to tailor mechanical and biological properties. In this way a wide range of possible combinations of biofunctional scaffolds can be created each specifically adapted to modulate e.g. cell adhesion, migration, proliferation and differentiation as well as to direct new tissue formation [8,9]. The wide availability of functional groups such as hydroxyl groups, amino groups and/or carboxylic acid groups present in these polysaccharides are open to further chemical modifications and crosslinkable or bioactive moieties can easily be introduced into the polysaccharide precursors of these enzymatically cross linkable hydrogels.

Hyaluronic acid (HA) is one of the main components of the ECM in cartilage tissue and, for this reason, it was chosen as a biomimetic component of Dex-TA. HA interacts with chondrocytes through surface receptors, such as CD44, enabling modulation of cell activity by contributing significantly to cell proliferation and migration

[10,11,12]. Novel polysaccharide hybrids were designed, as described in chapter 5, in which Dex-TA was grafted onto HA (HA-g-Dex-TA) [13]. HA-g-Dex-TA copolymers were prepared with different degrees of substitution of tyramine units to HA using EDAC/NHS activation. Hybrid hydrogels could subsequently be obtained by enzymatic crosslinking. Overall, these biomimetic HA-g-Dex-TA hydrogels induced an enhanced cell proliferation and matrix deposition/remodeling as demonstrated by increased deposition of glycosaminoglycans and collagens, compared to Dex-TA hydrogels.

Preliminary *in vivo* evaluation of dextran-based hydrogels was performed by subcutaneous implantation in immunocompetent mice (unpublished data). Histological evaluation of representative samples, shown in Figure 10.1-a, indicates that a mild fibrous capsule was formed around the HA-g-Dex-TA hydrogel as a result of a foreign body response. The diameter of this capsule decreased throughout time of implantation, with almost no eosinophils or multinucleated cells being present in the hydrogel surroundings at day 28. No acute reaction seemed to be occurring, strongly suggesting that this hydrogel is biocompatible. Similar results were obtained with Dex-TA hydrogels (data not shown). This is furthermore supported by data showing that Dex-TA hydrogels could not elicit a respiratory burst when co-cultured with neutrophils *in vitro* (unpublished data). After verifying that HA-g-Dex-TA is biocompatible, the chondrogenic potential of this hydrogel was evaluated *in vivo*. HA-g-Dex-TA hydrogels were subcutaneously implanted in nude mice with and without chondrocytes. Samples were explanted after 28 days and representative sections were stained with Safranin O to determine the content in glycosaminoglycans. The strong red staining of HA-g-Dex-TA hydrogels with chondrocytes is indicative of the high amount of glycosaminoglycans being deposited (Figure 10.1b). Staining in these hydrogels was more intense than in implanted Dex-TA hydrogels (data not shown). The neo-cartilage formation within the hydrogels with chondrocytes appears to be replacing the HA-g-Dex-TA hydrogel, as this biomaterial slowly degrades. Overall, dextran-based hydrogels appear to be biocompatible and allow significant amounts of matrix deposition *in vivo*. Incorporation of HA in Dex-TA hydrogels increased cartilage matrix formation, confirming our hypothesis that HA incorporation increases biological performance of the Dex-TA presumably by matrix mimicry. Heparin was selected as model compound to further improve the bioactivity of dextran-based hydrogels, as described in chapter 6. Heparin is well known for its biocompatibility and resemblance to heparan sulphate, which is a natural component of the ECM. Heparin-containing hydrogels have previously been studied for biomedical applications such as controlled release of growth factors and tissue regeneration. To enable the enzymatic crosslinking of Dex-TA and heparin (Hep), tyramine residues were grafted on the free carboxylic groups of heparin also using EDAC/NHS chemistry to obtain Hep-TA [14]. The presence of Hep-TA increased cell survival 1 day after encapsulation of the cells in the gel from more than 95 percent to more than 99 percent. Moreover, cell proliferation and the de novo formation of a cartilaginous matrix were significantly improved by the incorporation Hep-TA. Interestingly, increasing ratios of Hep-TA in Dex-TA hydrogels also induce cell migration, as described in chapter 7. Thus, cells from the synovial fluid and/or bone marrow might be able to migrate into Dex-TA/Hep-TA

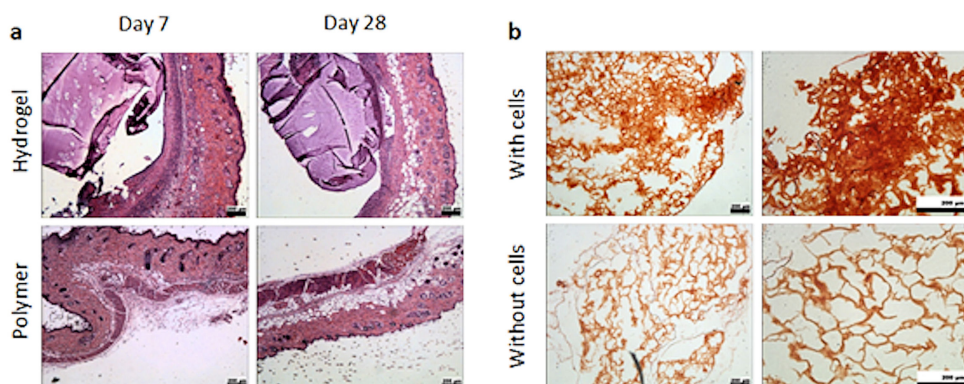


Figure 10.1: a) Subcutaneous implantation of *in situ* gelating HA-g-Dex-TA hydrogel in immuno-competent mice or injected with the polymer as a control. Samples were explanted after 7 and 28 days. Representative sections were stained with H and E. b) Subcutaneous implantation of HA-g-Dex-TA hydrogel in nude mice with incorporated chondrocytes with cell density of 10 million/mL or without cells. Samples were explanted after 28 days. Representative sections were stained with Safranin O. Glycosaminoglycans are stained red. Unpublished results.

hydrogels, allowing matrix to be produced within the hydrogel. The acquired data is indicative that this system can likely be developed and optimized as a cell-free system for cartilage repair.

As an alternative for the engraftment of hyaluronic acid or heparin, we explored whether incorporation of autologous platelet-rich lysate could also improve the regenerative potential of Dex-TA hydrogels. Platelet lysate is rich in growth factors and anti-inflammatory cytokines that play a key role in cartilage repair, yet platelet-derived gels are mechanically unstable [15,16]. Opposingly, Dex-TA is mechanical stable and can be immobilized *in situ* at the defect site, however, the biological performance of this hydrogel limited and could be improved. The advantages of both systems were successfully combined by incorporation of platelet lysate into Dex-TA. Interestingly, the bioactivity of the growth factors released by the gel promoted proliferation and triggered chondrogenic differentiation of MSCs. The Dex-TA/platelet-rich lysate hydrogels described in chapter 9 showed high potential as an out-of-the-shelf cell-free product for cartilage repair strategies by combining scaffold-guided regenerative medicine with an autologous source of growth factors.

10.3 Integrate to repair

Integration of TE constructs is of major importance for its function. Inappropriate tissue integration can ultimately result in failure, particularly at the interface between scaffolds and mechanically challenging tissues, such as joints [17,18]. Strategies

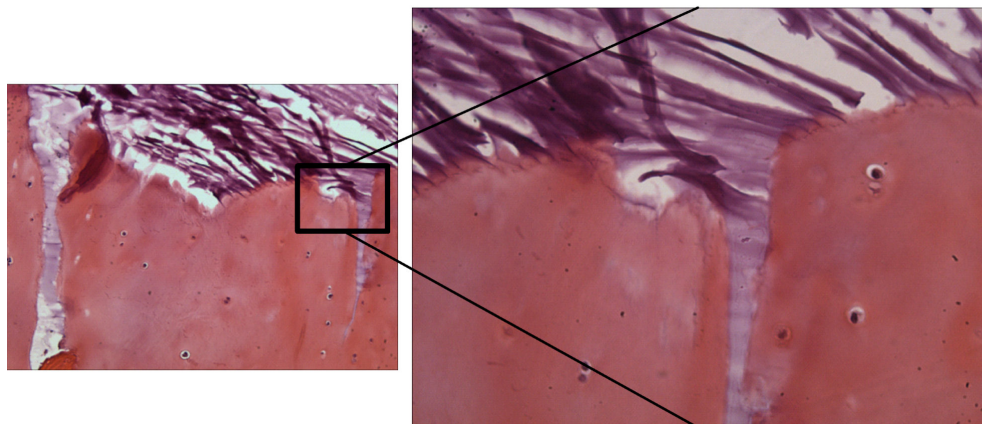


Figure 10.2: Representative histological section stained with H and E, demonstrating the smooth transition without gaps at the OA-affected cartilage/hydrogel interface. It should be noted that this hydrogel system has the initial fluidity that allows infiltration into cartilage gaps and cover uniformly irregular surfaces. This characteristic is strongly indicative of the high potential of dextran-based hydrogels as "healing plasters" for the repair of cartilage related diseases, such as OA. Unpublished results.

currently explored in cartilage resurfacing are based on attachment of the implanted material with sutures to the surrounding cartilage or involve a multistep glue-mediated procedure for the attachment of a synthetic hydrogel to the cartilage [19,20,21,22]. The polymers described in this thesis are designed to simultaneously form covalent bonds creating a 3D hydrogel network and firmly attach to the cartilage tissue by taking advantage of the hydroxyphenyl residues that are present in tyrosine-containing ECM proteins. We introduced hydroxyphenyl groups in the backbone of naturally occurring polymers, such as dextran, hyaluronic acid and heparin, which allow covalent bonding between tyramine groups of the hydrogels and tyrosine residues of cartilage collagens during *in situ* crosslinking reaction on articular cartilage. In chapter 7, we described the self-attachment of Dex-TA hydrogels during the enzymatic crosslinking reaction to predominantly collagen residues in the cartilaginous matrix. Similar results were obtained with other dextran-based hydrogels, such as Dex-TA/Hep-TA 50/50. Figure 10.2 shows that these hydrogels attach to not only healthy bovine cartilage, but also onto human OA-affected cartilage (unpublished data). Thus, hydrogels containing mixtures of Dex-TA and Hep-TA conjugates are promising biomaterials that can be used to repair tissue defects, not only in cartilage but also in other collagen rich tissues. This novel and simple, yet effective mechanism distinguishes itself from previously developed strategies, as it allows direct positioning and upholding of the hydrogel at the diseased cartilage surface by one simple injection. Therefore, the translation of this strategy into clinical applications is likely facilitated.

10.4 Boosting up cartilaginous ECM deposition

The native ECM composition and features were the base for the development of the repair strategies described in this thesis, mainly by structural mimicry. However, when using cell-laden constructs, cells play an equally important role as the carrier scaffolds. Current seeding methods could be improved to enhance cell performance and cell anabolic responses can also be mimicked from nature. Chondrocyte clusters have been associated with cartilage self-repair mechanisms. We explored this catabolic and anabolic cell response, hypothesizing that chondrocyte aggregation could stimulate both cartilaginous matrix deposition and remodeling thereby enhancing cartilage repair. In chapter 8, we provide evidence that seeding hydrogels with micro-aggregated chondrocytes rather than with single cells, which is the current golden standard, may be an effective strategy to boost neo-cartilage formation. We show that high-throughput formation of micro-aggregates prior to chondrocyte implantation may be an efficient approach to improve and accelerate hyaline cartilage formation during current autologous chondrocyte implantation procedures.

10.5 Concluding remarks and future perspectives

In this thesis we have described a recently developed technology platform of *in situ* gelating hydrogels of natural polymers that shows promising features for cartilage repair. These dextran-based hydrogels provide a protective environment and mechanical support to the eroded cartilage surface, while facilitating regeneration by attracting progenitor cells. Moreover, these hydrogels can be applied in a one-step minimal invasive procedure, such as an arthroscopy. Translation into a pre-clinical setting is the next step to further develop this injectable hydrogel system. This translation will involve the optimization of an injectable device, typically a syringe based on a double-jet system as is currently used for the application of fibrin glue, for application of dextran-based hydrogels in cartilage defects using minimally invasive procedures. Moreover, injection of these *in situ* forming hydrogels in simulated cartilage defects in medium and large animals, namely rabbits and horses, will pave the road for the initiation of clinical trials in man.

The sustained delivery of a myriad of compounds involved in cartilage repair and protection are worthwhile exploring in combination with dextran-based hydrogels. The high affinity of heparin [23,24,25] to bind to growth factors and the easy incorporation of drugs in HA [26] highlight the potential of Dex-TA/Hep-TA and HA-g-Dex-TA as possible mediators of sustained drug delivery. Further research may focus on sustained delivery of, for example, BMPs, DKK-1 or drugs for OA treatment. This would be valuable to further enhance the chondrogenic potential of these hydrogels and to assure the formation of hyaline neo-cartilage or explore anti-inflammatory OA treatments, respectively. Moreover, the influence of mechanical stimulation in matrix deposition in dextran-based hydrogels will be of great value in the development and selection of combinations other possible GAG-TA or collagen-TA fractions.

The features of the dextran-based hydrogels described in this thesis were focused on cartilage repair strategies. Cartilage is essentially an avascular and aneural tissue;

on the contrary, most of the other tissues such as bone, skin, cardiac tissue or muscle, are highly vascularized. TE strategies for these tissues rely on vascular development for efficient and functional repair. The biomimetic and bioactive properties of the dextran-based hydrogels described herein can potentially assist on vessel development. Other TE strategies might also explore the potential of these hydrogels to covalently bind to collagen-rich tissues, such as the development of skin replacements for wound healing or tendon reconstruction. Moreover, these hydrogels gels could potentially be optimized by mixing different combinations of various ECM compounds and evaluated in medium to high throughput to select the proper combinations for each specific desired function.

References

1. O'Brien FJ (2011) Biomaterials and scaffolds for tissue engineering. *Materials Today* 14: 88-95.
2. McCullen SD, Chow AG, Stevens MM (2011) *in vivo* tissue engineering of musculoskeletal tissues. *Curr Opin Biotechnol*.
3. Williams DF (2006) To engineer is to create: the link between engineering and regeneration. *Trends Biotechnol* 24: 4-8.
4. Woodfield TB, Bezemer JM, Pieper JS, van Blitterswijk CA, Riesle J (2002) Scaffolds for tissue engineering of cartilage. *Crit Rev Eukaryot Gene Expr* 12: 209-236.
5. Jin R, Hiemstra C, Zhong Z, Feijen J (2007) Enzyme-mediated fast *in situ* formation of hydrogels from dextran-tyramine conjugates. *Biomaterials* 28: 2791-2800.
6. Jin R, Moreira Teixeira LS, Dijkstra PJ, Zhong Z, van Blitterswijk CA, *et al.* (2010) Enzymatically crosslinked dextran-tyramine hydrogels as injectable scaffolds for cartilage tissue engineering. *Tissue Eng Part A* 16: 2429-2440.
7. Nicodemus GD, Bryant SJ (2008) Cell encapsulation in biodegradable hydrogels for tissue engineering applications. *Tissue Eng Part B Rev* 14: 149-165.
8. Rowley JA, Madlambayan G, Mooney DJ (1999) Alginate hydrogels as synthetic extracellular matrix materials. *Biomaterials* 20: 45-53.
9. Park KM, Joung YK, Park KD, Lee SY, Lee MC (2008) RGD-conjugated chitosan-pluronic hydrogels as a cell supported scaffold for articular cartilage regeneration. *Macromol Res* 16: 517-523.
10. Park KM, Lee SY, Joung YK, Na JS, Lee MC, *et al.* (2009) Thermosensitive chitosan-Pluronic hydrogel as an injectable cell delivery carrier for cartilage regeneration. *Acta Biomater* 5: 1956-1965.
11. Toole BP (2001) Hyaluronan in morphogenesis. *Seminars in Cell and Developmental Biology* 12: 79-87.
12. Akmal M, Singh A, Anand A, Kesani A, Aslam N, *et al.* (2005) The effects of hyaluronic acid on articular chondrocytes. *J Bone Joint Surg Br* 87-B: 1143-1149.
13. Jin R, Teixeira LS, Dijkstra PJ, van Blitterswijk CA, Karperien M, *et al.* (2010) Enzymatically-crosslinked injectable hydrogels based on biomimetic dextran-hyaluronic acid conjugates for cartilage tissue engineering. *Biomaterials* 31: 3103-3113.
14. Jin R, Moreira Teixeira LS, Dijkstra PJ, van Blitterswijk CA, Karperien M, *et al.* (2011) Chondrogenesis in injectable enzymatically crosslinked heparin/dextran hydrogels. *J Control Release*.
15. Ahmed TA, Dare EV, Hincke M (2008) Fibrin: A Versatile Scaffold for Tissue Engineering Applications. *Tissue Eng Part B Rev*.
16. Ahmed TA, Giulivi A, Griffith M, Hincke M (2011) Fibrin glues in combination with mesenchymal stem cells to develop a tissue-engineered cartilage substitute. *Tissue Eng Part A* 17: 323-335.
17. Ahsan T, Sah RL (1999) Biomechanics of integrative cartilage repair. *Osteoarthritis Cartilage* 7: 29-40.
18. Wang DA, Williams CG, Yang F, Elisseeff JH (2004) Enhancing the tissue-biomaterial interface: Tissue-initiated integration of biomaterials. *Advanced Func-*

tional Materials 14: 1152-1159.

19. Gerwin N, Hops C, Lucke A (2006) Intraarticular drug delivery in osteoarthritis. *Advanced Drug Delivery Reviews* 58: 226-242.

20. Martel-Pelletier J, Pelletier JP (2009) A single injection of anakinra for treating knee OA? *Nature Reviews Rheumatology* 5: 363-364.

21. Saito M, Takahashi KA, Arai Y, Inoue A, Sakao K, *et al.* (2009) Intraarticular administration of platelet-rich plasma with biodegradable gelatin hydrogel microspheres prevents osteoarthritis progression in the rabbit knee. *Clinical and Experimental Rheumatology* 27: 201-207.

22. Wang DA, Varghese S, Sharma B, Strehin I, Fermanian S, *et al.* (2007) Multifunctional chondroitin sulphate for cartilage tissue-biomaterial integration. *Nature Materials* 6: 385-392.

23. Capila I, Linhardt RJ (2002) Heparin-protein interactions. *Angew Chem Int Ed Engl* 41: 391-412.

24. Casu B (1985) Structure and biological activity of heparin. *Adv Carbohydr Chem Biochem* 43: 51-134.

25. Peattie RA, Fuegy PW, Riley CM, Cai SS, Yu BL, *et al.* (2007) Regulation of *in vivo* angiogenesis by heparin-controlled dual growth factor release from hyaluronan hydrogels. *Faseb Journal* 21: A479-A479.

26. Kim KS, Park SJ, Yang JA, Jeon JH, Bhang SH, *et al.* (2011) Injectable hyaluronic acid-tyramine hydrogels for the treatment of rheumatoid arthritis. *Acta Biomater* 7: 666-674.

Acknowledgements

I would like to express my sincere gratitude to all those whom have contributed to this finished journey, either scientifically or personally. After four years, I feel very pleased to look back and see how much I have learned, shared and grew. I really appreciated this journey and this thesis reflects a collective work of supervisors, colleagues, friends and family, who have contributed with scientific input, constant support, enthusiasm and/or love.

Firstly, I owe my deepest gratitude to my co-promotor, Marcel Karperien. Without your guidance, help and support, this thesis would not have been possible. I greatly appreciated your brilliant scientific input, valuable insights, encouragement and freedom explore new research topics.

It is also a great pleasure to acknowledge my promotor, Clemens van Blitterswijk, for providing me this opportunity to follow my dreams in research. The department of Tissue Regeneration (TR) is not only scientifically excellent but also provides a wonderful working atmosphere.

I would like to thank Dr. João Mano, Prof. Dr. L. Terstappen, Dr. Ir. P. Jonkheijm, Prof. Dr. P.R. van Weeren, Prof. Dr. F. Luyten, Prof. Dr. P.J. Dijkstra and Prof. Dr. J. Feijen for taking place in the graduation committee.

Thank you, my paranymphs, Jeroen and Belinha! Both of you are very special to me! Belinha, obrigada por estares do meu lado neste dia tão especial para mim. Prezo mesmo muito a nossa amizade e sei que, apesar da distancia, terei sempre o teu carinho, cumplicidade e incentivo! Espero que continuemos a crescer juntas!

The project entitled "Hybrid Hydrogels" enabled a close and enriching collaboration with the department of Polymer Chemistry and Biomaterials. I would like to express my gratitude to Piet Dijkstra and Jan Feijen for all the input provided, prompt and detailed corrections. A special thanks goes to Rong Jin, for all the patience in teaching me polymer chemistry. It was a pleasure and a true learning experience working with you! My thanks to Jos Wennink for continuing this process, your help was invaluable during all the polymer synthesis. I would also like to thank Mark Smithers for his help in acquiring beautiful HR-SEM images.

This learning process would not have been the same without the contribution of the Master students Suzanne and Teun. I was a great pleasure to work you! Minhas queridas Sara e Clarinha, como eu gostei de ser vossa "orientadeira"! A vossa alegria

e empenho são contagiantes. Estou mesmo muito contente por saber que em breve ambas estarão de volta ao TR!

A great institution is always the result of extraordinary people. Thus, I owe my sincere and earnest thankfulness to all my colleagues from TR with whom I had the pleasure to work with and helped me during this journey. Some of you are so much more than colleagues, you became my family here in Enschede. Sandrinha, amiga, obrigada por todo o apoio e sabios conselhos! Definitivamente estes quatro anos não seriam o mesmo sem ti. Os constantes e divertidos jantares, festas e viagens tornaram esta jornada aqui por Enschede (e ocasionalmente no Porto também) muito mais animada. Espero que tu e o Juan sejam felizes por muitos e longos anos! Ellie, Charlene and Alex, Ana e Hugo, and specially, Bernke, Andre, Karolina and Maciej, Nicole and Chris thank you for all the joyful moments and dinners shared. You made Enschede a happier place! A place I can call home!

Falta ainda expressar o meu profundo agradecimento a minha família. Papa, Mama, Paula e Bela, obrigada pelo constante apoio e incentivo incondicional durante esta minha aventura científica.

Lastly and most importantly, I wish to thank Jeroen, who has truly "enLeijtened" my life. This thesis is also yours. I am truly grateful for all your precious input, patience and above all, love. I admire your intelligence, humor, ambition and passion for science. Overall, almost every minute of these four years was shared with you, and how I cherished them! Happy to have shared this journey with you and hope for many more to come. I love you!

This has been a fascinating and extremely rewarding journey! Thank you all!

Curriculum Vitae

Liliana Moreira Teixeira was born on the 10th of April 1982 in Matosinhos, Portugal. She grew up in Porto until she graduated from Padrão da Legua high school. Afterwards, she went to Braga to study Applied Biology, at the University of Minho, Portugal, for which she received her Bachelor of Science degree, in 2005. The last part of her studies was conducted within the Erasmus program at the Department of Paediatric Immunology at the LUMC, Leiden, The Netherlands, (Dr. C.E.T. da Costa, Dr. N. E. Annels and Prof. Dr. R.M. Egeler). She then performed a traineeship at 3B's Research Group (Biomaterials, Biodegradables and Biomimetics), at the University of Minho, Portugal (Dr. I.B. Leonor, Dr. A.P. Marques and Prof. Dr. Rui Reis). In 2007, she obtained her Master of Science degree in Biomedical Engineering, at the Faculty of Engineering from the University of Porto, Portugal. Her master thesis was entitled "Bone remodeling: regulation by central nervous system". The research was performed at IBMC-INEB Associated Laboratory, Institute of Biomedical Engineering, NewTherapies Group, Biomaterials Division, Portugal (Dr. M. Lamghari). In July 2007, she started her PhD at the Department of Tissue Regeneration at the University of Twente, MIRA Institute for Biomedical Technology and Technical Medicine, The Netherlands, under the supervision of Prof. Dr. C.A. van Blitterswijk and Dr. M. Karperien. The subject of her research was the biological evaluation of injectable hydrogels for cartilage tissue engineering and the results are described in this thesis. This PhD project was performed in close collaboration with Prof. Dr. J. Feijen and Prof. Dr. P.J. Dijkstra, from the Department of Polymer Chemistry and Biomaterials, within the same institute. For part of the work described in this thesis, Liliana Moreira Teixeira has received travel grant, abstract and poster awards from the Curie Cutting Edge InVENTS, Biomedical Technology Institute of Twente University, TERMIS and NBTE. From July 2011, she will continue her scientific work as a Post-doc researcher at the Department of Tissue Regeneration, University of Twente.

List of Publications

Peer-reviewed papers

Jin R, Moreira Teixeira LS, Dijkstra PJ, Karperien M, van Blitterswijk CA, Zhong ZY, Feijen J. Injectable chitosan-based hydrogels for cartilage tissue engineering. *Biomaterials*. 2009 May;30(13):2544-51.

Jin R, Moreira Teixeira LS, Dijkstra PJ, Karperien M, van Blitterswijk CA, Feijen J. Enzymatically-Crosslinked Injectable Hydrogels Based on Biomimetic Dextran-Hyaluronic Acid Conjugates for Cartilage Tissue Engineering. *Biomaterials*. 2010 Apr;31(11):3103-13.

Jin R, Moreira Teixeira LS, Dijkstra PJ, Karperien M, van Blitterswijk CA, Feijen J. Synthesis and Characterization of Hyaluronic acid-PEG Hydrogels via Michael Addition: An Injectable Biomaterial for Cartilage Repair. *Acta Biomaterialia*. *Acta Biomater*. 2010 Jun;6(6):1968-77.

Moreira Teixeira LS*, Jin R*, Dijkstra PJ, Zhong ZY, van Blitterswijk CA, Karperien M, Feijen J. Enzymatically Crosslinked Dextran-Tyramine Hydrogels as Injectable Scaffolds for Cartilage Tissue Engineering. *Tissue Engineering: Part A*. 2010 Aug;16(8):2429-40. (* Shared first co-authorship)

Neves SC, Moreira Teixeira LS, Moroni L, Reis RL, van Blitterswijk CA, Alves NM, Karperien M, Mano JF. Chitosan/poly(-caprolactone) blend scaffolds for cartilage repair. *Biomaterials*. 2011 Feb;32(4):1068-79.

Moreira Teixeira LS*, Jin R*, Dijkstra PJ, Zhong ZY, van Blitterswijk CA, Karperien M, Feijen J. Chondrogenesis in Injectable Enzymatically Crosslinked Heparin/Dextran Hydrogels. *J Control Release*. 2011 May 30;152(1):186-95. (* Shared first co-authorship)

Correia C, Moreira Teixeira LS, Moroni L, Reis RL, van Blitterswijk CA, Alves NM, Karperien M, Mano JF. Chitosan scaffolds containing hyaluronic acid for cartilage tissue engineering. *Tissue Eng Part C Methods*. 2011 Jul;17(7):717-30.

Moreira Teixeira LS*, Georgi N*, Leijten JCH*, Wu L, Karperien M. Cartilage Tissue Engineering. Hormone research and paediatrics - Proceedings. Accepted. (* Shared first co-authorship)

Higuera GA, van Dalum J, Wu L, Moreira Teixeira LS, Leijten JCH, Karperien M, van Blitterswijk CA and Moroni L. High-throughput in 3D: Cell and tissue screening *In Vitro* and in vivo. Submitted.

Moreira Teixeira LS*, Leijten JCH*, Sobral J, Jin R, van Apeldoorn AA, Feijen J, van Blitterswijk CA, Dijkstra PJ, Karperien M. Chondrocyte cluster formation stimulates cartilage matrix deposition. Submitted. (* Shared first co-authorship)

Moreira Teixeira LS, Bijl S, Pully VV, Otto C, Jin R, Feijen J, van Blitterswijk CA, Dijkstra PJ, Karperien M. Self-attaching and Cell-attracting *In-Situ* Forming Hydrogels of Natural Polymers for Cartilage Repair. Submitted.

Moreira Teixeira LS, Leijten JCH, Wennink J, Ganguly A, de Boer J, Feijen J, van Blitterswijk CA, Dijkstra PJ, Karperien M. Cartilage repair enhancement by combination of an autologous growth factor source with a natural polymer-based injectable hydrogel. Submitted.

Moreira Teixeira LS, Feijen J, van Blitterswijk CA, Dijkstra PJ, Karperien M. Enzyme-catalyzed crosslinkable hydrogels: emerging strategies for tissue engineering. Accepted in Biomaterials.

Wennink JWH, Niederer K, Bochynska AI, Moreira Teixeira LS, Karperien M, Feijen J, Dijkstra PJ. Injectable hydrogels by enzymatic co-crosslinking of dextran and hyaluronic acid tyramine conjugates. Accepted in Macromolecular Symposia - Advanced Functional Polymers for Medicine.

Moreira Teixeira LS*, Janeczek-Portalska KK*, Leijten JCH, Feijen J, Dijkstra PJ, Boer J, van Blitterswijk CA, Boer J, Karperien M. *In situ* forming Dextran-Hyaluronic acid hydrogels promote endothelial cell branching. In preparation. (* Shared first co-authorship)

Abstracts selected for oral presentation

L.S. Moreira Teixeira, R. Jin, P.J. Dijkstra, J. Feijen, C.A. van Blitterswijk, M. Karperien. Chitosan-based hydrogels as extracellular matrix for cartilage tissue engineering: *In Vitro* biological evaluation. 3rd TERMIS-EU Conference. June 22-26, 2008, Porto, Portugal.

L.S. Moreira Teixeira, R. Jin, P.J. Dijkstra, J. Feijen, C.A. van Blitterswijk, M. Karperien. *In Vitro* biological evaluation of rapidly *In-Situ* forming dextran-tyramine hydrogels for cartilage tissue regeneration. 2nd Dutch Conference on Bio-Medical Engineering. January 22-23, 2009, Egmond aan Zee, The Netherlands.

L.S. Moreira Teixeira, R. Jin, P.J. Dijkstra, J. Feijen, C.A. van Blitterswijk, M. Karperien. *In Vitro* Biological Evaluation of Rapidly *In-Situ* Forming Dextran-Tyramine Hydrogels for Cartilage Tissue Regeneration. ESB Conference. September 7-11, 2009, Lausanne, Switzerland.

L.S. Moreira Teixeira, R. Jin, P.J. Dijkstra, J. Feijen, C.A. van Blitterswijk, M. Karperien. *In Vitro* Biological Evaluation of Rapidly *In-Situ* Forming Dextran-Tyramine Hydrogels for Cartilage Tissue Regeneration. 18th annual meeting of the NBTE. December 14-15, 2009, Lunteren, The Netherlands.

L.S. Moreira Teixeira, R. Jin, P.J. Dijkstra, J. Feijen, C.A. van Blitterswijk, M. Karperien. Dextran-tyramine Hydrogels for Cartilage Repair: enhanced chondrogenicity by engraftment with hyaluronic acid and heparin. TERMIS. June 13-17, 2010, Galway, Ireland. Best Abstract Award.

Abstracts selected for poster presentation

L.S. Moreira Teixeira, R. Jin, P.J. Dijkstra, C.A. van Blitterswijk, M. Karperien. Enzyme-catalyzed crosslinked hydrogels as synthetic extracellular matrixes for cartilage tissue engineering: biocompatibility and biological behaviour. 4th Marie Curie Cutting Edge InVENTS Conference on Biocompatibility evaluation and biological behaviour of polymeric biomaterials; 9-13 October, 2007, Alvor Algarve, Portugal. Travel Grant Award.

L.S. Moreira Teixeira, R. Jin, P.J. Dijkstra, J. Feijen, C.A. van Blitterswijk, M. Karperien. Chitosan-based hydrogels as extracellular matrix for cartilage tissue engineering: *In Vitro* biological evaluation. 9th Advanced Summer Course on Cell-Materials Interaction. June 16-20, 2008, Porto, Portugal.

L.S. Moreira Teixeira, R. Jin, P.J. Dijkstra, J. Feijen, C.A. van Blitterswijk, M. Karperien. Biological *In Vitro* evaluation of in situ forming chitosan-based hydrogels for cartilage regeneration. Symposium on Tissue Engineering. November 11-12, 2008, Noordwijkerhout, The Netherlands.

L.S. Moreira Teixeira, R. Jin, P.J. Dijkstra, J. Feijen, C.A. van Blitterswijk, M. Karperien. Biological *In Vitro* evaluation of in situ forming chitosan-based hydrogels for cartilage regeneration. Highlights in Biomedical Technology Symposium. Novem-

ber 20, 2008, Enschede, The Netherlands. Best poster award.

L.S. Moreira Teixeira, R. Jin, P.J. Dijkstra, J. Feijen, C.A. van Blitterswijk, M. Karperien. *In Vitro* biological evaluation of hyaluronic acid based hydrogels crosslinked via Michael's addition as injectable biomaterials for cartilage repair. Gordon Conference on Cartilage Biology and Pathology, June 7-12, 2009, Les Diablerets, Switzerland.

L.S. Moreira Teixeira, R. Jin, P.J. Dijkstra, J. Feijen, C.A. Van Blitterswijk, M. Karperien. Chondrocyte micro-aggregates enhances neo-cartilage formation. ICRS. September 26-29, 2010, Sitges, Spain.

L.S. Moreira Teixeira, R. Jin, P.J. Dijkstra, J. Feijen, C.A. Van Blitterswijk, M. Karperien. Chondrocyte micro-aggregates enhances neo-cartilage formation. NBTE. December 2-3, 2010, Lunteren, The Netherlands. Best Poster Award.

L.S. Moreira Teixeira, S. Bijl, R. Jin, V.V. Pully, C. Otto, J. Feijen, C. van Blitterswijk, P. Dijkstra, M. Karperien. Single step tissue-hydrogel integration using healing plasters of natural polymers for cartilage repair. Gordon Conference on Cartilage Biology and Pathology, March 6-11, 2011, Ventura, California, USA.

Patent applications

University of Twente, Karperien M, Jin R, Moreira Teixeira LS, Feijen J, Dijkstra PJ. Dextran-hyaluronic acid based hydrogels. PCT/NL2010/050751.

University of Twente, Karperien M, Jin R, Moreira Teixeira LS, Feijen J, Dijkstra PJ. Hydrogels based on polymers of dextran tyramine and tyramine conjugates of natural polymers. PCT/NL2010/050752.

List of Figures

| | | |
|-----|---|----|
| 1.1 | Osteoarthritic cartilage. A) Image of a focal cartilage defect. B) From left to right, healthy knee cartilage, partial arthritis and complete arthritis. C) Photo-micrographs of healthy cartilage, in the left, and arthritic cartilage, in the right. | 2 |
| 1.2 | Left: classical components of a tissue engineering approach: cells, scaffolds and biomolecules. Right: The total number of publications with 'tissue engineering' and hydrogel' or hydrogels' in the title. Reproduced from [4]. | 3 |
| 1.3 | Schematic representation of an injectable hydrogel for cartilage repair. . . | 4 |
| 1.4 | Cell incorporation by mixing with the hydrogel precursor. ECM synthesis must be synchronized with hydrogel degradation. Reproduced from [3]. . | 5 |
| 1.5 | Model of cell-ECM interactions. Several strategies have been developed for the incorporation of key ECM bio-functions, such as specific cell adhesion sites, proteolytic degradation domains, and growth factor binding domains. Reproduced from [20]. | 6 |
| 1.6 | Illustrative representation of a hydrogel designed to crosslink with the components of the host tissue. The figure in the right represents the typical irregular surface of OA affected cartilage. The middle figure represents the affected cartilage surface covered with an hydrogel. The hydrogel precursor should be initially fluid to allow the coverage of the irregular surface and after gelation the hydrogel must be retained at the defect site. The figure in the left illustrates the participation of the cells incorporated within the gel or invading the gel in the regenerative mechanism. These cells should be able to deposit hyaline cartilaginous ECM for fully functional repair. . | 8 |
| 2.1 | The tissue engineering approach. Adapted from: C.A. v Blitterswijk, Tissue Engineering. Academic Press Series in Biomedical Engineering [Elsevier / Academic press, Amsterdam; London, 2008] pp. xvi, 740 p. | 22 |
| 2.2 | Protein-based membranes and gels already available for autologous chondrocyte implantation. | 25 |
| 4.1 | Synthesis of dextran-tyramine conjugates (Dex-TA) and hydrogel formation via enzymatic crosslinking. | 60 |

| | | |
|------|---|----|
| 4.2 | Gelation times of Dex-TA conjugates (10 wt %) as a function of the H_2O_2 /TA molar ratio. Reaction conditions: 0.25 mg HRP per mmol phenol groups; 37 degrees Celsius, PBS. | 61 |
| 4.3 | SEM images of freeze dried hydrogel samples: (a) Dex31k-TA DS 10, (b) Dex14k-TA DS 10 and (c) Dex14k-TA DS 5. Reaction conditions: 0.25 mg HRP per mmol phenol groups; molar ratio of H_2O_2 /TA = 0.2. (Scale bar 500 μ m) | 61 |
| 4.4 | Typical graph of glucose (in water) diffusion from chamber A towards the chamber B using a Dex14k-TA DS 15 hydrogel as function of time at 37 degrees Celsius. | 62 |
| 4.5 | Live-dead assay of chondrocytes in Dex-TA hydrogels at day 14: (a) Dex14k-TA DS 15, (b) Dex14k-TA DS 10, (c) Dex14k-TA DS 5, (d) Dex31k-TA DS 10 and (e) Dex31k-TA DS 5. Agarose gels (0.5 wt %) were used as a control (f). Reaction conditions: 0.25 mg HRP per mmol phenol groups; molar ratio of H_2O_2 /TA = 0.2. Cells were stained with calcein-AM/ethidium Homodimer (living cells stained green and dead cells red). The chondrocyte seeding density was 5 million cells/mL. Scale bar: 200 μ m. | 64 |
| 4.6 | MTT staining of chondrocytes in Dex31k-TA DS 10, Dex14k-TA DS 15 and DS 10 hydrogels after 1, 7 and 14 days in culture. Metabolically active cells stained purple. Reaction conditions: H_2O_2 /TA molar ratio is 0.2; 0.25 mg HRP per mmol phenol groups. The chondrocyte seeding density was 5 million cells/mL. | 65 |
| 4.7 | (a) Quantitative determination of the metabolic activity of chondrocytes inside Dex-TA hydrogels (Students t-test, * $p < 0.05$). (b) Live-dead assay showing chondrocytes incorporated in a Dex14k-TA DS10 hydrogel after 14 days in culture (chondrocyte division is indicated by arrows, original amplification: 100x). Reaction conditions: the H_2O_2 /TA molar ratio is 0.2; 0.25 mg HRP per mmol phenol groups. The chondrocyte seeding density was 5 million cells/mL. | 66 |
| 4.8 | SEM images of chondrocytes in Dex-TA hydrogels after 14 days in culture. | 66 |
| 4.9 | SEM images of (a) a single chondrocyte in a Dex14k-TA DS 15 hydrogel (21 days) was surrounded by a fibrous matrix on the gel surface, (b) fibrous matrix at high magnification (c) Circles point to collagen fibrils with a visible D-period at high magnification. | 67 |
| 4.10 | Alcian blue staining of Dex-TA hydrogels with chondrocytes after culturing for 14 and 21 days in differentiation medium. GAGs were stained blue/green. The chondrocyte seeding density was 5 million cells/mL. | 67 |
| 4.11 | Collagen type II staining of Dex14k-TA DS 15 (A and D), Dex14k-TA DS 10 (B and E), and Dex31k-TA DS 10 (C and F) hydrogels after culturing for 14 (A-C) and 21 (D-F) days in differentiation medium; The chondrocyte seeding density was 5 million cells/mL. A pellet of human chondrocytes cultured for 21 days in chondrocyte differentiation medium was used as a positive control (G) and the section without incubation with primary antibodies was used as a negative control (H). Collagen type II fluoresced green and nuclei of the cells were stained with DAPI (blue). | 68 |

| | | |
|------|---|----|
| 4.12 | GAG accumulation in Dex-TA and agarose hydrogels containing chondrocytes after <i>in vitro</i> culturing for 14, 21 and 28 days in differentiation medium. (a) GAG and (b) DNA content per hydrogel sample; (c) GAG accumulation normalized to the DNA content per gel sample. (Cell seeding density: 5 million/mL, ANOVA: * $p < 0.05$). | 69 |
| 5.1 | Chemical structure of (a) polysaccharide hybrids based on hyaluronic acid and dextran-tyramine conjugates and (b) structure of a proteoglycan. . . | 77 |
| 5.2 | Synthesis of hyaluronic acid grafted with dextran-tyramine conjugates (HA-g-Dex-TA). | 83 |
| 5.3 | $^1\text{H-NMR}$ spectra of dextran, Dex-TA, Dex-TA-NH-Boc and Dex-TA-NH ₂ ; (b) hyaluronic acid (HA) and HA grafted with dextran-tyramine conjugates (HA-g-Dex-TA) in D ₂ O. | 84 |
| 5.4 | GPC chromatograms of Dex-TA-NH ₂ DS 10, HA and the copolymer HA-g-Dex-TA DS 10. Eluent: NaAc buffer (300 Mm, pH 4.5, containing 30 % (v/v) methanol). | 85 |
| 5.5 | Gelation time of hydrogels based on HA-g-Dex-TA as a function of DS and concentration. (n=3, ** $p < 0.01$) | 87 |
| 5.6 | Degree of swelling of HA-g-Dex-TA hydrogels as a function of DS (n=3). . . | 88 |
| 5.7 | Storage modulus of HA-g-Dex-TA hydrogels as a function of DS (n=1). . . | 88 |
| 5.8 | Enzymatic degradation of HA-g-Dex-TA hydrogels at DS 5, 10 (a) and DS 15, 20 (b) exposed to PBS containing 100 U/ml HASE at 37 degrees Celsius (n=3). | 89 |
| 5.9 | (a) Live-dead assay showing chondrocytes incorporated in HA-g-Dex-TA DS 15 (A and C) and DS 20 (B and D) hydrogels after 7 (A and B) and 14 (C and D) days in culture. Scale bar: 500 μm | 90 |
| 5.10 | SEM images of chondrocytes incorporated in the (a) HA-g-Dex-TA DS 15 and (b) HA-g-Dex-TA DS 20 hydrogels at day 21. High magnification SEM images of the boxed regions of Figure 5.10a and 5.10b are shown in Figure 9c and 9d, respectively. | 91 |
| 5.11 | (a) Swelling and (b) degradation of Dex-TA and HA-g-Dex-TA hydrogels in the presence of chondrocytes as a function of culturing time. Figure 5.11a: * $p < 0.05$, ** $p < 0.01$, vs. Dex-TA DS 15; $p < 0.05$, vs. Day 1; $p < 0.01$, vs. Day 7). Figure 5.11b: the dry mass of the construct is normalized to the original wet gel weight after preparation. (* $p < 0.05$, ** $p < 0.01$) | 92 |

| | | |
|------|---|-----|
| 5.12 | (a) DNA content normalized to dry gel weight of Dex-TA DS 15, HA-g-Dex-TA DS 15 and 20 hydrogels containing chondrocytes after <i>in vitro</i> culturing for 1, 7, 14 and 21 days. (* $p < 0.05$ at day 7; ** $p < 0.01$ vs. HA-g-Dex-TA DS 15 at day 14 and 21) (b) GAG and (c) total collagen accumulation (values were normalized to the dry gel weight per sample) in Dex-TA and HA-g-Dex-TA hydrogels containing chondrocytes after <i>in vitro</i> culturing for 1, 7, 14 and 21 days. (** $p < 0.01$ vs. Dex-TA DS 15 at each time point) (d) GAG and total collagen content normalized to DNA content in Dex-TA and HA-g-Dex-TA hydrogels containing chondrocytes after <i>in vitro</i> culturing for 21 days. (* $p < 0.05$ vs. Dex-TA DS 15). | 93 |
| 6.1 | (a) Synthesis of heparin-tyramine conjugates (Hep-TA). (b) Hydrogel formation from dextran-tyramine (Dex-TA, black) and heparin-tyramine conjugates (Hep-TA, grey) via HRP-mediated crosslinking in the presence of H_2O_2 | 106 |
| 6.2 | (a) Gelation times of Hep-TA hydrogels (10 and 20 % wt) as a function of HRP concentration. The molar ratio of H_2O_2 /TA was kept at 0.2. (b) Gelation times of Hep-TA/Dex-TA hydrogels (20 % wt) as a function of Hep-TA/Dex-TA ratio (w/w). The concentrations of HRP and H_2O_2 were kept at 0.05 mg/mL and 0.01 M, respectively. (n=3, ** $p < 0.01$) | 106 |
| 6.3 | Heparin content (wt % in dry gel mass) of extracted 20 % wt Dex-TA/Hep-TA hydrogels. | 107 |
| 6.4 | The degree of swelling of Dex-TA/Hep-TA hydrogels. (n=3, * $p < 0.05$; ** $p < 0.01$ vs. 0/100 gel) | 108 |
| 6.5 | Storage moduli of Dex-TA/Hep-TA hydrogels. The concentrations of HRP and H_2O_2 were 0.05 mg/mL and 0.01 M, respectively (n=1). | 108 |
| 6.6 | (a) Frequency sweep and (b) strain sweep of Dex-TA/Hep-TA hydrogels. . | 109 |
| 6.7 | Live-dead assay showing the chondrocytes incorporated in Dex-TA/Hep-TA hydrogels after 3, 7 and 14 days in culture. Cell density is 5 million cells/mL gel. Scale bar: 200 μ m. | 110 |
| 6.8 | Degree of swelling of 20 % wt Dex-TA/Hep-TA hydrogels containing chondrocytes after incubating for 3 days <i>in vitro</i> . Cell seeding density: 5 million cells/mL. (n=3, * $p < 0.05$). | 111 |
| 6.9 | DNA content of 20 % wt Dex-TA/Hep-TA hydrogels containing chondrocytes after <i>in vitro</i> culturing for 1, 7, 14 and 21 days. Cell seeding density: 5 million cells/mL. (* $p < 0.05$, ** $p < 0.01$). | 111 |
| 6.10 | Real-time PCR of cartilage specific markers (aggrecan and collagen type I and II) by incorporated chondrocytes in 20 % wt Dex-TA/Hep-TA hydrogels after 21 days in culture. The expressions of collagen type I and II and aggrecan were normalized to the expression of the housekeeping gene GAPDH. (** $p < 0.01$ vs. 100/0 gel; $p < 0.05$ vs. 50/50 gel; $p < 0.01$ vs. 50/50 gel; $p < 0.01$ vs. 75/25 gel; $p < 0.05$ vs. 75/25 gel). | 112 |
| 6.11 | Toluidine blue staining of the hydrogels with Dex-TA/Hep-TA weight ratios of 100/0 (A), 75/25 (B), 50/50 (C) and 25/75 (D) after culturing for 21 days. Scale bar: 100 μ m. | 113 |

| | | |
|------|--|-----|
| 6.12 | Chondroitin sulfate immunofluorescent staining of the Dex-TA/Hep-TA hydrogels containing chondrocytes after <i>in vitro</i> culturing for 21 days. Different Dex-TA/Hep-TA ratios: 100/0 (E and F), 75/25 (G and H), 50/50 (I and J) and 25/75 (K and L). The section of bovine cartilage without or with incubation with primary antibodies was used as a negative (A and B) and positive (C and D) control, respectively. | 114 |
| 6.13 | Collagen type II immunofluorescent staining of the Dex-TA/Hep-TA hydrogels containing chondrocytes after <i>in vitro</i> culturing for 21 days. Different Dex-TA/Hep-TA ratios: 100/0 (C), 75/25 (D), 50/50 (E) and 25/75 (F). The section of pellet human chondrocytes at 21 days without or with incubation with primary antibodies was used as a negative (A) and positive (B) control, respectively. | 115 |
| 6.14 | (a) Total collagen in Dex-TA/Hep-TA hydrogels containing chondrocytes after <i>in vitro</i> culturing for 1, 7, 14 and 21 days. Cell seeding density: 5 million cells/mL. (* $p < 0.05$, ** $p < 0.01$). | 115 |
| 7.1 | Hydrogel adhesion and maximal shear modulus. a. and b. Construct consisting of two bovine explants of sub-chondral bone covered with a layer of cartilage of 1 cm ² with a layer of <i>in situ</i> formed Dex-TA hydrogel between the explants. The final construct shows high stability when held horizontally between tweezers. c, Maximal shear modulus (relative) of cartilage with 14k-DS8 and 14k-DS15 Dex-TA hydrogels formed <i>in situ</i> and for cartilage combined with pre-gelated 14k-DS8 and 14k-DS15 Dex-TA hydrogels. | 127 |
| 7.2 | Overview and histological evaluation of cartilage defects filled up with Dex-TA hydrogel. a. A cartilage defect in the bovine patella is filled up with a Dex-TA hydrogel combined with bovine chondrocytes. The gel is applied using a dual syringe in which one chamber contains the cell suspension (10 million cells per mL) and the polymer (final volume of 10 % w/v) while the other chamber contains HRP and H ₂ O ₂ . After mixing both chambers contents together along the circular final mixing compartment, gelation occurs within one minute which results in total filling of the defect, as shown in the detailed picture of the simulated defect site at the right. b. Safranin O staining indicating in pink/red the accumulation of glycosaminoglycans. The white arrows indicate the cells incorporated in the hydrogel. A decreasing gradient of glycosaminoglycans (GAGs), from cartilage to the hydrogel, indicating that diffusion of GAGs through the interface takes place. In addition, safranin O staining is surrounding the chondrocytes embedded in the hydrogel, indicating newly formed GAGs. c. Picrosirius red staining, visualized by polarized light, demonstrates the presence of collagen fibrils at the cartilage/hydrogel interface and surrounding the chondrocytes embedded in the hydrogel, indicated by the white arrows. | 129 |

- 7.3 Morphological analysis of the cartilage-Dex-TA hydrogel interface. a, Representative wet mode SEM images showing a smooth transition between Dex-TA hydrogels and cartilage. The arrow indicates the cartilage-Dex-TA hydrogel interface. c and d, Representative HR-SEM pictures showing increasing magnifications of the hydrogel-cartilage interface. The images are suggestive for a direct interaction between the hydrogel and collagen fibrils of which the D period is clearly visible at higher magnifications (with arrows). The magnifications are indicated in the figures. 130
- 7.4 Raman micro-spectroscopy of the interface area. a, White light micrograph showing the scanned interface region of $30 \times 30 \mu\text{m}$ (boxed). In this area 1024 scans were taken. b, Hierarchical cluster analysis of 1024 Raman scans (Power: 35mW, objective: 40xW, accumulation time 50 ms/pix) identifies 3 different spectra corresponding to the hydrogel only (green), the cartilage only (black) or the interface (red). c, d, Raman spectra of the Dex-TA/cartilage interface with: the cartilage region (black cluster), the interface region (red cluster) and the Dex-TA 14k-DS10 hydrogel region (green). c, The most informative region of the spectrum; d, Spectrum showing the water bands (Power: 35 mW, objective: 40xW, accumulation time 50 ms/pix). e-f, Spectral range selections of figure c, of $\Delta=780\text{-}820 \text{ cm}^{-1}$ and of $\Delta=1050\text{-}1230 \text{ cm}^{-1}$, respectively, showing peaks of interest. g, Selected area of e, showing a change at 816 cm^{-1} . h, Selected area of e, showing a change at 857 cm^{-1} . i, Selected area of f, showing a change at 1122 cm^{-1} 132
- 7.5 Average Raman spectra of average red cluster subtracted by average spectra of green cluster. Positive bands correspond to cartilage. Negative bands at $509, 541, 838$ and 1132 cm^{-1} correspond to hydrogel. This shows the uptake of hydrogel by the cartilage, which occurs at the interface. . . 134
- 7.6 Enzymatic crosslinking of Cy5-labeled tyramide on bovine articular cartilage. a, Fluorescent microscopy images show representatives ($n=4$) of bovine articular cartilage incubated with or without chondroitinase, with and without HRP, with H_2O_2 and different concentrations of TyrCy5 (diluted 1:50 or 1:100). b, Fluorescence quantification of bovine articular cartilage incubated with and without chondroitinase, in the presence or absence of HRP and H_2O_2 with different concentrations of TyrCy5 (diluted 1:50 or 1:100). The mean color of the pictures was determined for quantification of fluorescence intensities (average of 3 spots within each sample, * $P<0,05$), average color: 0 = black, 255 = red. c, Schematic summary of the postulated enzymatic crosslinking between Dex-TA conjugates and collagen molecules present in the cartilage ECM via tyramine-tyrosine covalent bond formation. 135

- 7.7 HR-SEM and histological images, showing the interface between other collagen-rich tissues and Dex-TA hydrogel. a, HR-SEM pictures showing the attachment of the hydrogels to muscle tissue via bonding to collagen fibrils (left and middle) and a representative histological section with H and E staining demonstrating the smooth transition without gaps at the muscle/hydrogel interface (right). b, HR-SEM pictures showing limited attachment of the hydrogels to fat tissue via bonding to collagen fibrils (left and middle) and a representative histological section with H and E staining, demonstrating the irregularities and poor attachment at the fat/hydrogel interface (right). 136
- 7.8 Evaluation of the cell migratory potential of Dex-TA-based hydrogels. a. Cell migration assay using human chondrocytes (hChond) and human chondrocyte progenitor cells (hCPCs). Dex-TA was mixed with Hep-TA in different ratios: 100/0, 75/25, 50/50 and 25/75 to prepare hydrogels and the migratory cells were quantified. Increasing contents of heparin induced higher cell homing towards the hydrogels, with no significant difference between cell types. b. Cell adhesion onto Dex-TA hydrogels was observed, after dynamic cell seeding. The hydrogels were kept in a spinner flask for 7 days and afterwards an MTT assay was performed. The metabolically active cells are stained in purple and can be visualized both at the surface and, to a lesser extent, within the hydrogel, as shown by the cross-section. c. Representation of the assembly of constructs of Dex-TA hydrogels containing cells, with Dex-TA/Hep-TA 50/50 gels, without cells, on top. d. Migration of cells through the Dex-TA into Dex-TA/Hep-TA 50/50 gels. Toluidine blue staining was used to stain the heparin fraction. Cells were stained with DAPI, which marks in blue the cell nuclei. Cell migration against gravity towards Dex-TA mixed with Hep-TA hydrogels was detected after 24 hours in culture, as cells were observed in the initial cell-free Dex-TA/Hep-TA 50/50 fraction. 137
- 7.9 Synthesis and enzymatic crosslinking of Dex-TA conjugates and proposed mechanism involved in the adhesion onto cartilage. a, In the first step of the Dex-TA conjugates synthesis, p-nitrophenyl chloroformate is linked to the dextran backbone. This step is followed by substitution of the nitrophenyl group by tyramine through the formation of a urethane bond. b, Dex-TA hydrogels are formed by the HRP catalyzed oxidative coupling of the phenol groups of the tyramines present on the dextran backbone, via either carbon-carbon bonds or carbon-oxygen-carbon bond formation. c. Mechanism of enzymatic crosslinking between Dex-TA conjugates and collagen molecules present in the cartilage ECM via tyramine-tyrosine covalent bond formation. 138

- 8.1 High-throughput formation of chondrocyte micro-aggregates. (A) Schematic representation of the micro-well technique for the formation of aggregates from single cell suspensions. A stainless steel mold was used to form micro-wells in agarose chips. (B) Each agarose chip contains 4×10^3 micro-wells. (C) Pictures at specific time points during aggregate formation. Each well of a 24 wells plate containing an agarose micro-well chip was seeded with the appropriate number of cells to obtain micro aggregates of 50, 100 or 200 cells. Aggregation started to occur approximately 6 hours after seeding. After 12 hours, the aggregates had acquired a spherical shape, independently of aggregate size. (D) Correlation between the number of cells per micro well and the diameter (μm) and the volume (μm^3) of the obtained aggregates after 12 hours. Each data point represents the measurement of minimally 50 micro aggregates. At the lower right side of the graphic, aggregates obtained after flushing off the agarose chips are shown. (E) Micro-aggregate area (μm^2) slightly decreased over time most notably in aggregates bigger than 100 cells. Each data point represents the measurement of minimally 50 aggregates (F) Measurement of circularity of micro-aggregates over time demonstrated a decrease in average circularity and an increase in spread. A perfect circle has a value of 1. Each data point represents the measurement of about 50 micro aggregates. Error bars were means \pm SD. 150
- 8.2 Cell clusters in OA cartilage. (A) OA tissue specimen stained with H and E, showing the presence of several chondrocyte clusters near fissures at the cartilage surface. (B) Detail of representative micro-aggregates of 100 cells embedded in an in situ gelating Dex-TA hydrogel, stained with H and E. 152
- 8.3 Micro-aggregation enhances COL2A1 and ACAN expression. (A) qPCR analysis of collagen type II and aggrecan gene expression at day 1, 3 and 7 of culture in chondrocyte expansion medium. Equal amounts of cells were cultured in micro-aggregates of 50, 100 and 200 cells and compared with single cells cultured in a 2D system. At day 7, no changes were observed between the different culture methods. (B) qPCR analysis of collagen type II and aggrecan gene expression was evaluated at day 1, 3 and 7 of culture in chondrogenic conditions. Micro-aggregated cell clusters of 50, 100 and 200 cells were compared with single cells cultured in a 2D system. COL2A1 and ACAN expression was potently stimulated by culturing the cells in micro-aggregates of 50 and 100 cells. Error bars were means \pm SD (n=3/condition). 153

- 8.4 Micro-aggregation increases metabolic activity. (A) Glucose consumption and ammonia and lactate production were quantified after 7 days of culture of equal cell numbers of 100 cell micro-aggregates on agarose chips or as single cells in 2D. The ratio between lactate production and glucose consumption is represented in the lower right graphic. The clear difference between both culture systems was strongly suggestive for a shift in metabolic activity. Error bars represent means \pm SD (n=3/condition). (B) Equal numbers of cells, either as micro-aggregates or as single cells, were embedded in an in situ gelating Dex-TA hydrogel. After 7 and 14 days of culture, a viability assay was performed in which living cells were shown in green and dead cells in red. Incorporation of cells in the hydrogels did not affect viability nor did micro-aggregation. Clusters retained their spherical shape over time. 154
- 8.5 Micro-aggregation prior to seeding in hydrogels stimulates cartilage matrix gene expression. Relative mRNA levels for aggrecan (A), collagen type II (B), Sox9 (C), collagen type X (D) and Collagen type I (E), expressed by single cells or micro-aggregated cell clusters incorporated into Dex-TA hydrogels, after 14 and 21 days in culture. Similar cell numbers were seeded in each construct. Relative mRNA levels for MMPs 1, 3, 9 and 13 (F), expressed by single cells or micro-aggregated cell clusters incorporated into Dex-TA hydrogels, after 21 days in culture. Error bars were means \pm SD (n=3/condition). 155
- 8.6 Micro-aggregation resulted in superior matrix production both *in vitro* and *in vivo*. (A) Histological evaluation of *in vitro* cultured hydrogels seeded with equal cell numbers either as single cells or as micro-aggregates of 100 cells, for 14 and 21 days. Picrosirius red staining was performed to visualize total collagen content (red/pink colour). Both Toluidine blue (purple colour) and Safranin O (red/orange colour) stainings were performed to visualize glycosaminoglycans deposition. A more intense staining was observed in constructs seeded with micro-aggregates indicative for higher matrix production. (B) Histological evaluation of hydrogel constructs with encapsulated single cells or micro-aggregates of 100 cells implanted subcutaneously in nude mice for 2 and 4 weeks (n=6 mice per time point). Hydrogels with encapsulated micro aggregates showed more cartilage matrix. (C) Histological stainings of a representative control sample, consisting of the hydrogel without cells. 156
- 8.7 *In vitro* model for size specific cell cluster formation. (A) Light microscopic (A-I and II) and scanning electron-microscopic (SEM) (A-III and IV) images of agarose chips evidencing the presence of uniform micro-wells enabling high throughput formation of micro-aggregated cell clusters. (B) Pictures at specific time points (day 1, day 3 and day 7) of aggregates cultured on agarose chips seeded with different cell densities to obtain aggregates of 50, 100 or 200 cells. At day 7, the micro-aggregates, particularly the ones containing 200 cells, tended to merge, migrate and started to lose their round morphology (arrows). Single cells were used as a control. 157

- 8.8 Micro-aggregation improved the ratio between collagen type II and both collagen type I and X expression. (A) Ratio between the relative mRNA levels of collagen type II and Collagen type X, after 7 days of culture of equal cell numbers of 100 cell micro-aggregates on agarose chips or as single cells in 2D, in chondrogenic medium. At day 14 no differences were detected. (B) Ratio between the relative mRNA levels of collagen type II and Collagen type I, in Dex- TA hydrogel constructs seeded with equal numbers of cells either as single cells or as micro-aggregated clusters of 100 cells, after 14 and 21 days in culture. Error bars were means \pm SD (n=3/condition). 157
- 9.1 Rheological analysis and hydrogel morphology. A) Storage (G') and loss (G'') modulus of Dex-TA, Dex-TA with platelet lysate and platelet gel, as a function of time; B) Storage and loss modulus plateau values, as well as damping factors ($\tan\delta = G''/G'$) of Dex-TA, Dex-TA with platelet lysate and pure platelet gel; C) Representative SEM image of critical point dried Dex-TA hydrogel sample; D) Representative SEM image of critical point dried Dex-TA with platelet lysate hydrogel sample, showing no difference in porosity compared with Dex-TA only. Scale bars correspond to 100 μm . 171
- 9.2 Platelet rich lysate renders Dex-TA hydrogels chemo-attractant. A) Cell migration was assessed by a 24-hours trans-well cell migration assay using either human chondrocytes (hChondrocytes) or human bone marrow derived mesenchymal stromal cells (hMSCs). Platelet lysate mixed in the culture medium, Dex-TA and Dex-TA with platelet lysate hydrogels were prepared on the wells and the migratory cells that crossed the membrane were quantified. The platelet lysate as a medium component or incorporated in Dex-TA acted as a chemo-attractant. B) MTT assay performed in the hydrogels immediately after the collection of the membranes for quantification. The metabolically active cells that crossed the membrane and adhered onto the hydrogels are stained purple. I) Dex-TA with adhered hChondrocytes; II) Dex-TA with platelet lysate with adhered hChondrocytes; III) Dex-TA with adhered hMSCs; IV) Dex-TA with platelet lysate with adhered hMSCs. 172
- 9.3 Adhesion and proliferation profile. A) DNA quantification of MSCs were seeded onto the pre-gelated Dex-TA hydrogels prepared with or without platelet lysate hydrogels (2.5×10^4 cells per cm^2). The assays were performed after 2 and 8 days in culture. B) MTT assay of the MSCs adhered onto the pre-gelated Dex-TA hydrogels prepared with or without platelet lysate hydrogels, after 8 days in culture. Metabolically active cells are stained purple. C) Representative SEM image of critical point dried Dex-TA hydrogel with platelet lysate with adhered MSCs, after 8 days in culture. I) Top view of the hydrogel sample; II) Cross-section of the hydrogel sample, showing cells that have migrated from the top into the interior of the gel. 173

- 9.4 Chondrogenic differentiation. A) Histological evaluation of representative samples of Dex-TA with or without platelet lysate with incorporated MSCs, cultured for 21 days in expansion or chondrogenic media, stained with Toluidine blue (purple color indicates GAG deposition). B) Collagen type II immuno-fluorescence staining of representative samples of Dex-TA with or without platelet lysate with incorporated MSCs, cultured for 21 days in chondrogenic media (collagen type II is stained in green and cell nuclei are stained blue). The negative control sample was obtained by absence of incubation with primary anti-body. C) Expression levels of COL2A1 and COL1A1 genes analyzed by quantitative PCR of hydrogel/cell constructs of Dex-TA with or without platelet lysate with incorporated MSCs cultured for 21 days in expansion or differentiation media. Gene expression was normalized to the expression of GAPDH. . . 174
- 9.5 Osteogenic differentiation. A) Histological evaluation of representative samples of Dex-TA with or without platelet lysate with incorporated MSCs, cultured for 21 days in expansion or osteogenic media, stained with Alizarin Red (red colour indicates calcium deposition). B) Histological evaluation of representative samples of Dex-TA with or without platelet lysate with incorporated MSCs, cultured for 21 days in expansion or osteogenic media, stained with von Kossa (dark brown color indicates mineralization). C) Expression levels of ALP and OC genes analyzed by quantitative PCR of hydrogel/cell constructs of Dex-TA with or without platelet lysate with incorporated MSCs cultured for 21 days in expansion or differentiation media. Gene expression was normalized to the expression of GAPDH (n=3).175
- 9.6 Adipogenic differentiation. A) Histological evaluation of representative samples of Dex-TA with or without platelet lysate with incorporated MSCs, cultured for 21 days in expansion or adipogenic media, stained with Oil Red O (red colour indicates fat deposition). B) Expression levels of PPARG mRNA analyzed by quantitative PCR of hydrogel/cell constructs of Dex-TA with or without platelet lysate with incorporated MSCs cultured for 21 days in expansion or differentiation media. Gene expression was normalized to the expression of GAPDH (n=3). 176
- 9.7 Vascularization potential using the chorioallantoic membrane (CAM) model. A) After 7 days of incubation at 37 °C, Dex-TA with platelet lysate gels were placed in contact with the CAM, sealed and returned to the incubator. B) Four days after placing the hydrogels in contact with the membrane, images were collected to study vasculature development. After fixation, the hydrogels with the CAM were excised and transferred onto glass slides. The control corresponds to normal membrane development without hydrogel.177

| | | |
|------|---|-----|
| 9.8 | Platelet rich lysate enhances chondro-induction. A) Expression levels of COL2A1 gene analyzed by quantitative PCR of hydrogel/cell constructs of Dex-TA with or without platelet lysate with incorporated hChondrocytes or co-cultures of hMSCs with hChondrocytes (80/20 ratio), cultured for 21 days in chondrogenic medium without TGF- β 3 supplementation. Gene expression was normalized to the expression of GAPDH (n=3). B) Collagen type II immuno-fluorescent staining of representative samples of Dex-TA with or without platelet lysate with incorporated hChondrocytes or co-cultures of hMSCs with hChondrocytes (80/20 ratio), cultured for 21 days in chondrogenic medium without TGF- β 3 supplementation (collagen type II is stained in green and cell nuclei are stained blue). Scale bars correspond to 200 μ m. C) Release profile of the TGF- β 3 and BMP-6 present in the platelet lysate incorporated into Dex-TA hydrogels, up to 14 days. Cumulative release of both growth factors was obtained by quantification of TGF- β 3 and BMP-6 in the platelet lysate and was normalized to the total amount present in the lysate. | 178 |
| 9.9 | Interface hydrogel-OA cartilage. The integration and adhesion between the Dex-TA hydrogels with (A) and without platelet lysate (B) crosslinked onto standardized samples of human OA cartilage. Representative sections of the hydrogels were stained with H and E. C) Representative SEM image of the interface between Dex-TA hydrogel with platelet lysate and OA affected cartilage. The intricate interaction between the hydrogel and the host tissue is evidenced, highlighting the absence of gaps at the interfacial area. | 179 |
| 10.1 | a) Subcutaneous implantation of <i>in situ</i> gelating HA-g-Dex-TA hydrogel in immuno-competent mice or injected with the polymer as a control. Samples were explanted after 7 and 28 days. Representative sections were stained with H and E. b) Subcutaneous implantation of HA-g-Dex-TA hydrogel in nude mice with incorporated chondrocytes with cell density of 10 million/mL or without cells. Samples were explanted after 28 days. Representative sections were stained with Safranin O. Glycosaminoglycans are stained red. Unpublished results. | 191 |
| 10.2 | Representative histological section stained with H and E, demonstrating the smooth transition without gaps at the OA-affected cartilage/hydrogel interface. It should be noted that this hydrogel system has the initial fluidity that allows infiltration into cartilage gaps and cover uniformly irregular surfaces. This characteristic is strongly indicative of the high potential of dextran-based hydrogels as "healing plasters" for the repair of cartilage related diseases, such as OA. Unpublished results. | 192 |

List of Tables

| | | |
|-----|--|-----|
| 2.1 | Scaffold materials for cartilage repair. | 24 |
| 3.1 | Mechanism of the enzymatic reaction mediated by transglutaminases, advantages and drawbacks | 34 |
| 3.2 | Mechanism of the enzymatic reaction mediated by tyrosinases, advantages and drawbacks | 36 |
| 3.3 | Mechanism of the enzymatic reaction mediated by phosphopantetheinyl transferase, advantages and drawbacks | 37 |
| 3.4 | Mechanism of the enzymatic reaction mediated by lysyl oxidase and plasma amine oxidase, advantages and drawbacks | 39 |
| 3.5 | Mechanism of the enzymatic reaction mediated by phosphatases, thermolysin, β -lactamase and phosphatase/kinase, advantages and drawbacks | 40 |
| 3.6 | Mechanism of the enzymatic reaction mediated by peroxidases, advantages and drawbacks | 43 |
| 3.7 | Advantages and drawbacks the enzymatic reaction mediated by horseradish peroxidase mimetic enzymes | 44 |
| 3.8 | Enzyme-catalyzed crosslinkable hydrogels and potential applications | 45 |
| 3.9 | (Continuation of table 3.8) Enzyme-catalyzed crosslinkable hydrogels and potential applications | 46 |
| 4.1 | Gelation times, storage moduli and glucose diffusion for Dex-TA hydrogels (a). a: Reaction conditions: 10 % wt polymer concentration; molar ratio of $\text{H}_2\text{O}_2/\text{TA}$ is 0.2; 0.25 mg HRP per mmol phenol groups; 37 degrees Celsius, PBS. b: DS (Degree of substitution, defined as the number of tyramine units per 100 anhydroglucose rings in dextran) was determined using ^1H NMR. c: The percentage of glucose diffused after 72 h was expressed as the ratio of the glucose concentration in chamber B and the equilibrium conc. of 5 g/L, multiplied by 100 %. | 63 |
| 5.1 | Composition, molecular weight and polydispersity of HA-g-Dex-TA copolymers (a) | 86 |
| 6.1 | Polymerase Chain Reaction Primers | 104 |

| | | |
|-----|--|-----|
| 7.1 | Spectral interpretations of the Raman spectra. The detected peaks of interest in the interface spectra, showing a shift when compared to the spectra obtained from cartilage and hydrogel, are attributed to a specific assignment, according to Movasaghi et al [30]. | 133 |
|-----|--|-----|